Ana Cristina Figueiredo de Lemos Rial

METABOLIC MODIFICATIONS ASSOCIATED WITH MEMORY DEFICITS

Tese de doutoramento em Biociências, especialização em Neurociências,
orientada pelo Doutor Attila Köfalvi e pelo Doutor Rui A. Carvalho
e apresentada ao Departamento de Ciências da Vida da Faculdade de Ciências e Tecnologia da Universidade de Coimbra

Fevereiro 2016

· U C ·

UNIVERSIDADE DE COIMBRA

METABOLIC MODIFICATIONS ASSOCIATED WITH MEMORY DEFICITS

UNIVERSIDADE DE COIMBRA

Ana Cristina Figueiredo de Lemos, MSc
University of Coimbra
2016

Tese apresentada à Faculdade de Ciências e Tecnologia da Universidade de Coimbra, para prestação de provas conducentes ao grau de Doutor em Biociências – Ramo de especialização em Neurociências

Thesis submitted to the Faculty of Science and Technology of University of Coimbra as a requirement for the degree of PhD in Biosciences, Specialization in Neuroscience

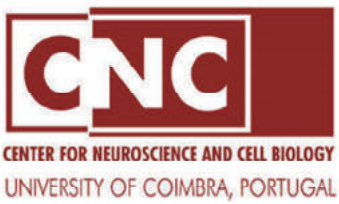

This work was conducted at the Center for Neurosciences and Cell Biology (CNC), University of Coimbra and at the Department of Life Sciences, Faculty of Sciences and Technology, University of Coimbra, Portugal,
Under the supervision of

Attila Köfalvi, PhD and **Rui A. Carvalho, PhD**.

The presented work was financially supported by: NARSAD, Santa Casa da Misercórdia, DARPA (09-68-ESR-FP-010), UID/NEU/04539/2013, CAPES-FCT and CNPq (Ciência sem Fronteiras) and co-funded by FEDER (QREN), through Programa Mais Centro under project CENTRO-07-ST24-FEDER-002006 and through Programa Operacional Factores de Competitividade (COMPETE) and National funds (PTDC/SAU-OSM/105663/2008, Pest-C/SAU/LA0001/2013-2014, PTDC/SAU-NMC/114810/2009, PTDC/EBB-EBI/115810/2009, UID/NEU/04539/2013 and RECI/BBB-BQB/0230/2012) via FCT – Fundação para a Ciência e a Tecnologia

Table of Contents

AGRADECIMENTOS/ACKNOWLEDGEMENTS

O percurso que levou à concretização desta tese foi extremamente enriquecedor tanto a nível científico como pessoal. Este foi um periodo de desafios constantes e de trocas de experiências. São várias as pessoas que diretamente contribuiram para que este trabalho fosse possível, que me ensinaram e me apoiaram imensamente e às quais gostaria de agradecer. Este é um trabalho de equipa.

Gostaria de agradecer aos meus orientadores, ao Doutor Attila Köfalvi e ao Doutor Rui de Carvalho pela oportunidade que me deram de realizar esta disseratação. Bem-haja Attila por teres acreditado em mim, pelo teu apoio, compreensão, empenho, esforço, disponibilidade e amizade. Bem-haja Rui por tudo, desde a vinda para a Universidade de Coimbra, pela partilha de ideais, pela atenção, apoio e amizade. Ao Doutor Rodrigo Cunha por me ter aceite no seu laboratório, como membro da sua equipa permitindo-me mergulhar no fabuloso mundo das neurociências. Bem-haja a todos pelo papel crucial no meu crescimento científico.

A todos os meus colaboradores, colegas e amigos do grupo “Purines at CNC” que partilharam parte desta aventura comigo. À Bárbara por todo o tempo passado juntas no laboratório por partilhar aquela felicidade de quando “dá certo”! A todo o grupo responsável pelas experiências de eletrofisiologia aqui apresentadas: aos Doutores Daniel Rial e Henrique Silva, e aos Mestres Francisco Gonçalves e António Carvalho, incansáveis e sempre com sentido de humor. Agradeço também à Doutora Ivana Jarak pela sua amizade e contribuição com as experiências de RMN juntamente com o meu orientador. Quero agradecer também ao grupo responsável pelas culturas celulares: Mestre Rui Beleza, e Doutores Joana Marques e Ricardo J. Rodrigues. Aos Doutores Stefania Zappettini, Joana Real, Samira Ferreira, Filipe Matheus, Catarina Gomes, Nélio Gonçalves, Patrícia Simões, Sílvia V. Silva, Pedro Garção, e aos Mestres Paula Silva, Caroline Veloso, João Amorim, Sofia Ferreira, Sofia Morais. Aos Doutores Paula Agostinho e Ângelo Tomé. Aos Doutores Frederico Pereira e Flávio Reis do IBILI pelas oportunidades de colaboração. Foi um prazer trabalhar com vocês! Gostaria de

agradecer também ao meu laboratório adotivo do Brasil, um grande obrigada ao Doutor Rui Prediger e a toda a sua equipa.

Ao meu marido, meu companheiro nesta viagem, para quem todas as palavras de agradecimento parecem poucas. Participaste activamente nesta aventura como parte do teu dia a dia, desde o input científico ao suporte emocional. Bem-haja.

À minha família, que é o meu porto de abrigo, pelo seu amor, carinho e apoio incondicional. Vocês tornaram possível a concretização desta etapa. Considero esta tese como Nossa e dedico-vos este trabalho.

LIST OF PUBLICATIONS

Part of the scientific work presented in this dissertation resulted in the publication in peer-reviewed international scientific journals:

Lemos, C., Pinheiro, B. S., Beleza, R. O., Marques, J. M., Rodrigues, R. J., Cunha, R. A., et al. (2015). Adenosine A_{2B} receptor activation stimulates glucose uptake in the mouse forebrain. *Purinergic Signal.*, 1–9. doi:10.1007/s11302-015-9474-3.

Lemos, C., Rial, D., Gonçalves, F. Q., Pires, J., Silva, H. B., Matheus, F. C., et al. (2015). High sucrose consumption induces memory impairment in rats associated with electrophysiological modifications but not with metabolic changes in the hippocampus. *Neuroscience*. doi:10.1016/j.neuroscience.2015.12.018.

Lemos, C., Valério-Fernandes, A., Ghisleni, G. C., Ferreira, S. G., Ledent, C., de Ceballos, M. L., et al. (2012). Impaired hippocampal glucoregulation in the cannabinoid CB_1 receptor knockout mice as revealed by an optimized in vitro experimental approach. *J. Neurosci. Methods* 204, 366–373. doi:10.1016/j.jneumeth.2011.11.028.

Gonçalves, F. Q., Pires, J., Pliassova, A., Beleza, R., **Lemos, C**., Marques, J. M., et al. (2015). Adenosine A_{2B} receptors control A_1 receptor-mediated inhibition of synaptic transmission in the mouse hippocampus. *Eur. J. Neurosci.* 41, 876–886. doi:10.1111/ejn.12851.

Active participation in work collaborations and other projects resulted in the publication in peer-reviewed international scientific journals

Rial, D., **Lemos, C**., Pinheiro, H., Duarte, J. M., Gonçalves, F. Q., Real, J. I., et al. (2016). Depression as a Glial-Based Synaptic Dysfunction. *Front. Cell. Neurosci.*, 521. doi:10.3389/fncel.2015.00521.

Bitencourt, R. M., Alpár, A., Cinquina, V., Ferreira, S. G., Pinheiro, B. S., **Lemos, C**., et al. (2015). Lack of presynaptic interaction between glucocorticoid and CB_1 cannabinoid receptors in GABA- and glutamatergic terminals in the frontal cortex of laboratory rodents. *Neurochem. Int.* doi:10.1016/j.neuint.2015.07.014.

Matheus, F. C., Rial, D., Real, J. I., **Lemos, C**., Ben, J., Guaita, G. O., et al. (2015). Decreased synaptic plasticity in the medial prefrontal cortex underlies short-term memory deficits in 6-OHDA-lesioned rats. *Behav. Brain Res.* doi:10.1016/j.bbr.2015.12.011.

Matheus, F. C., Rial, D., Real, J. I., **Lemos, C**., Takahashi, R. N., Bertoglio, L. J., et al. (2015). Temporal Dissociation of Striatum and Prefrontal Cortex Uncouples Anhedonia and Defense Behaviors Relevant to Depression in 6-OHDA-Lesioned Rats. *Mol. Neurobiol.* doi:10.1007/s12035-015-9330-z.

Pliássova, A., Lopes, J. P., **Lemos, C**., Oliveira, C. R., Cunha, R. A., and Agostinho, P. (2015). The association of amyloid-β protein precursor with α- and β-Secretases in mouse cerebral cortex synapses is altered in early Alzheimer's disease. *Mol. Neurobiol.* doi:10.1007/s12035-015-9491-9.

Valente-Silva, P., **Lemos, C**., Köfalvi, A., Cunha, R. A., and Jones, J. G. (2015). Ketone bodies effectively compete with glucose for neuronal acetyl-CoA generation in rat hippocampal slices. *NMR Biomed.* doi:10.1002/nbm.3355.

Soares, E., Prediger, R. D., Nunes, S., Castro, A. A., Viana, S. D., **Lemos, C**., et al. (2013). Spatial memory impairments in a prediabetic rat model. *Neuroscience* 250, 565–577. doi:10.1016/j.neuroscience.2013.07.055.

Other articles under preparation / submission:

Pinheiro, B. S., **Lemos, C**., Neutzling-Kaufmann, F., Marques, J. M., Silva-Santos, C. S., et al. Hierarchical glucocorticoid-endocannabinoid interplay regulates the activation of the nucleus accumbens by insulin. Response to Reviewers in preparation for Brain Research Bulletin

Köfalvi, A., **Lemos, C**., Martín-Moreno A. M., Bárbara S. Pinheiro, B. S., García-García, L., et al. Stimulation of brain glucose uptake by cannabinoid CB_2 receptors and its therapeutic potential in Alzheimer's disease. Response to Reviewers in preparation for Neuropharmacology

LISTA DE ABREVIATURAS / LIST OF ABBREVIATIONS

^{18}F-FDG	^{18}F-2-fluoro-2-deoxyglucose; fluorodeoxyglucose;
^{3}H/^{14}CDG	^{3}H/^{14}C-2-deoxy-D-glucose
^{3}HDG	2-^{3}H(N)-deoxy-D-glucose
^{3}HMG	^{3}H-oxygen-methyl-D-glucose
2-AG	*sn*-2-arachidonylglycerol
2-DG	2-deoxyglucose
4-AP	4-aminopyridine
2 or 6-NBDG	2 or 6-(N-(7-nitrobenz-2-oxa-1,3-diazol-4-yl)amino)-2-deoxyglucose)
Δ^9-THC	Δ^9-tetrahydrocannabinol
A_1R	adenosine A_1 receptor
A_{2A}R	adenosine A_{2A} receptor
A_{2B}R	adenosine A_{2B} receptor
A_3R	adenosine A_3 receptor
ACEA	arachidonyl-2'-chloroethylamide
ACSF	artificial cerebrospinal fluid
AD	Alzheimer's disease
ADA	adenosine deaminase
ADHD	attention deficit and hyperactivity disorder
ADP	adenosine 5'-diphosphate
ADK	adenosine kinase
Ala	alanine
AM251	1-(2,4-dichlorophenyl)-5-(4-iodophenyl)-4-methyl-N-(1-piperidyl)pyrazole-3-carboxamide
AMP	adenosine monophosphate
AMPA	α-amino-3-hydroxyl-5-methyl-4-isoxazole propionic acid
ANLS	astrocyte-to-neuron-lactate shuttle
ANOVA	analysis of variance
Asc	ascorbic acid
Asp	Aspartate
AR(s)	adenosine receptor(s)
ATP	adenosine 5'-triphosphate
BAY 60-6583	2-[[6-amino-3,5-dicyano-4-[4-(cyclopropylmethoxy)phenyl]-2-pyridinyl]thio]-acetamide
BBB	blood brain barrier
BCA	bicinchoninic acid
BSA	bovine serum albumin
CA1,3	*Cornu Ammonis* areas 1 and 3
cAMP	adenosine 3',5'-cyclic monophosphate
CB_1R	cannabinoid 1 receptor
CB_2R	cannabinoid 2 receptor
CD39	ecto-nucleoside triphosphate diphosphohydrolase 1,
CD73 (or 5'-NT)	ecto-5'-nucleotidase; ATP diphosphohydrolase
CGS 21680	3-[4-[2-[[6-amino-9-[(2R,3R,4S,5S)-5-(ethylcarbamoyl)-3,4-dihydroxy-oxolan-2-yl]purin-2-yl]amino]ethyl]phenyl]propanoic acid
ChAT	choline acetyltransferase
CHO	chinese hamster ovary
CNS	central nervous system
CNTs	concentrative nucleotide transporters
CoA	coenzyme A
CREB	cAMP response element-binding protein
CyB	cytochalasin B
DAG	*sn*-2-diacylglycerol
DAGLα	*sn*-2-DAG lipase α
DG	*dentate gyrus*
DIV 15	days *in vitro*
DL-TBOA	DL-threo-beta-benzyloxyaspartate

DMEM	Dulbecco's Modified Eagle's medium
DMSO	dimethyl sulfoxide
DPCPX	2-chloroadenosine and 8-cyclopentyl-1,3-dipropylxanthine
DPM	disintegrations per minute
DPCPX	8-cyclopentyl-1,3-dipropylxanthine
E17	day 17 of development
EC_{50}	half maximal effective concentration
E_{max}	maximal response (efficacy)
ENT(s)1/2	equilibrative nucleoside transporter(s) type 1, 2
EPM	elevated plus-maze test
FADH2	flavin adenine dinucleotide
fEPSP	field excitatory postsynaptic potentials
FOXO	forkhead box O
FR%	fractional release
FRET	fluorescence resonance energy transfer
FST	forced swimming test
G6P	glucose 6-phosphate
GABA	gamma-aminobutyric acid
$GABA_A$Rs	$GABA_A$ receptors
GDNF	glial cell line-derived neurotrophic factor
G_i	inhibitory regulative G protein
Gln	glutamine
Glu	glutamate
GLUT1/3/4	glutamate transporter 1, 3, 4
GLUTs	glucose facilitative transporters
GPCRs	G protein-coupled receptors
GS	glutamine synthetase
GSK3α/β	glycogen synthase kinase 3 α/β
GTP	guanosine-5'-triphosphate
HEPES	4-(2-hydroxyethyl)-1-piperazineethanesulfonic acid
HFS	high-frequency stimulation
HR-MAS	high-resolution magic angle spinning
Hsu	high sucrose diet
IC_{50}	concentration of half-maximal inhibition
icv	intracerebroventricular
IGF-1R	insulin-like growth factor-1 receptor
ip	Intraperitoneal
IR	insulin receptor
IRS	insulin receptor substrate
K_d	inverse of the affinity of 2-NBDG for its transporters
KO	Knockout
JNK	C-Jun N-terminal kinases
Lac	lactate
LTD	long-term depression
LTP	long-term potentiation
MCT1-4	monocarboxylate transporter
MG	3-O-methyl-D-glucose
MRS 1754	N-(4-cyanophenyl)-2-[4-(2,3,6,7-tetrahydro-2,6-dioxo-1,3-dipropyl-1*H*-purin-8-ylphenoxy]-acetamide
MWM	morris water maze
myo-ins	myo-inositol
Na^+/K^+-ATPase	sodium-potassium pump
NAA	N-acetylaspartate
NAD	nicotinamide adenine dinucleotide
NADPH	nicotinamide adenine dinucleotide phosphate
NALS	neuron-to-astrocyte lactate shunt
NAPE	*N*-arachidonyl-phosphatidylethanolamine
NESS0327	8-chloro-1-(2,4-dichlorophenyl)-N-piperidin-1-yl-5,6-dihydro-4H-benzo[2,3]cyclohepta[2,4-b]pyrazole-3-carboxamide

NMDA	N-methyl-D-aspartate
NMDAR	N-methyl-D-aspartate receptor
NMR	nuclear magnetic resonance
NORT	novel object recognition test
O-2050	(6ar,10ar)-3-(1-methanesulfonylamino-4-hexyn-6-yl)-6a,7,10,10a-tetrahydro-6,6,9-trimethyl-6H-dibenzo[b,d]pyran
ODT	object displacement test
OFT	open field test
PBS	phosphate buffered saline medium
PC	pyruvate carboxylase
PCho	phosphorylcholine
P-cre	phosphocreatinine
PDH	pyruvate dehydrogenase complex
PF514273	2-(2-chlorophenyl)-3-(4-chlorophenyl)-7-(2,2-difluoropropyl)-6,7-dihydro-2H-pyrazolo[3,4-f][1,4]oxazepin-8(5H)-one
PKA	protein kinase types A
PPF	paired pulse facilitation
PP-LFS	paired pulse-low frequency stimulation
PPP	pentose phosphate pathway
PPR	paired-pulse ratio
RI	recognition index
rpm	rotation per minute
S_2/S_1	treatment-induced changes ratio
SAH	S-adenosyl-homocystein
SCH 58261	5-amino-7-(2-phenylethyl)-2-(2-furyl)-pyrazolo[4,3-e]-1,2,4-triazolo-[1,5c]pyrimidine
SDS	sodium dodecyl sulfate
SDS-PAGE,	sodium dodecyl sulfate polyacrylamide gel electrophoresis
SEM	standard error of the mean
st-A_2AR KO	striatum-selective A_{2A}R KO mice
STZ	streptozotocin, *i.e.*, 2-deoxy-2-(3-(methyl-3-nitrosoureido)-D-glucopyranose
T	time (min)
τ_{50}	the time (min) necessary to reach the half of U_{max}
$\tau_{familiar}$	time of exploration of the familiar object/ location
τ_{novel}	time spent exploring the novel/displaced object
T1D	type 1 diabetes
T2D	type 2 diabetes
Tau	taurine
TBS-T	tris-buffered saline with Tween
TCA	tricarboxylic acid cycle
T_{max}	maximum number of transporters for 2-NBDG
U_{max}	theoretical maximum uptake
vGluT1	vesicular glutamate transporter type 1
VGCC	voltage gated calcium channel
WIN55212-2	(R)-(+)-[2,3-dihydro-5-methyl-3-(4-morpholinylmethyl)pyrrolo[1,2,3-de]-1,4-benzoxazin-6-yl]-1-napthalenylmethanone
WT	wild-type mice

RESUMO

Este trabalho foi iniciado partindo da premissa em como, no cérebro, a glucose disponível regula a memória e a cognição em humanos saudáveis e pacientes com demência.

Para além disso, a desregulação da glucose cerebral tem sido associada a doenças neuropsiquiátricas e as alterações na captação de glucose em áreas cerebrais específicas são considerados marcadores seletivos no diagnóstico de doenças neuropsiquiátricas. O trabalho experimental apresentado nesta tese de doutoramento teve como objetivo revelar como os neuromoduladores, incluindo a insulina, regulam o metabolismo da glicose no cérebro e quais as consequências dos danos ao nível do metabolismo da glicose cerebral em modelos animais.

Para concretizar este objectivo, efetuamos estudos bioquímicos e eletrofisiológicos em estruturas cerebrais que se correlacionam com a cognição e personalidade, que são, o hipocampo e o córtex frontal. Também procedemos a uma bateria de testes comportamentais em roedores. Primeiro, optimizamos vários métodos *in vitro* para medições espaço-temporais e quantitativas da captação e metabolismo da glucose em fatias de hipocampo, fatias do córtex frontal e em culturas celulares. Depois, exploramos as características básicas da captação de glucose e metabolismo em fatias de hipocampo, incluindo o papel das vias de sinalização da insulina e de duas outras importantes famílias de neuromoduladores. Aqui, reportamos que a administração sistémica de streptozotocina (induzindo diabetes tipo 1) afecta tanto o repouso como a despolarização induzida pela captação e metabolismo da glucose dependente do receptor de canabinóides CB_1 no hipocampo. Notavelmente, esta área cerebral é responsável pela formação e evocação da memória, que é regulada pela sinalização da insulina. Usando o mesmo composto diabetogénico mas agora administrado intracerebroventricularmente, obtivemos um modelo animal previamente caracterizado como diabetes cerebral, evitando a interferência de modificações periféricas. Além disso, os resultados apontaram para que a disfunção sináptica observada nas experiências de eletrofisiologia tenham ocorrido antes da perda sináptica e coincidiu com a disfunção metabólica.

Em seguida, outro modelo animal foi utilizado, associado com disfunção metabólica, um modelo pré-diabético induzido pelo consumo de uma dieta rica em

sacarose (Hsu). Este modelo tem a vantagem de ser menos invasivo do que a injeção cerebral de STZ e melhor mimetizar as doenças associadas ao estilo de vida humano, e para além disso permitir ainda o estudo da fase inicial da doença, a fase anterior à ocorrência da diabetes. De acordo com a análise de hipocampo por espectroscopia de elevada resolução por rotação em ângulo mágico (HRMAS) em tecidos de animais Hsu, a dieta Hsu induziu modificações metabólicas periféricas sem um impacto aparente no metabolismo cerebral, apesar destes animais exibirem danos na memória. Procuramos também modificações nos circuitos da via hipocampal Schaffer-CA1, que está conectada com tarefas dependentes de memória hipocampal e não foram detetadas alterações. Posteriormente, questionamos se a dieta Hsu afectaria outra via mediadora da consolidação da memória espacial e o processo de reconhecimento em ratos, nomeadamente a via temporomónica. Observamos que a dieta Hsu danifica a plasticidade sináptica na via temporomonica-CA1 das sinapses piramidais. Adicionalmente, testamos o papel do receptor adenosinérgico nestas vias e observamos que, no hipocampo, a dieta Hsu regula para cima o receptor A_1.

Seguidamente, investigamos a hipótese de que a ativação do receptor A_{2B} com baixa afinidade para a adenosina pudesse promover a captação de glucose em neurónios e astrócitos relacionando atividade cerebral com o metabolismo energético. Desenvolvemos um protocolo para a medição fluorescente em tempo real da captação de deoxiglucose em fatias de hipocampo, um complemento ideal das análises quantitativas. Verificamos que a ativação do receptor A_{2B} está associada com o aumento tónico e instantâneo do transporte de glucose para os neurónios e astrócitos no cérebro de ratinho, levantando a possibilidade de em futuras investigações se avaliar o potencial clínico deste novo mecanismo glucoregulador.

Em conclusão, este trabalho de tese contribuiu para elucidar os mecanismos pouco definidos que regulam o metabolismo da glucose cerebral. Encontramos novas provas que ligam a deficiência da plasticidade sináptica hipocampal e de memória às doenças metabólicas. Também identificamos o receptor A_{2B} como um possível novo alvo terapêutico para estimular o metabolismo da glucose cerebral com o objectivo de atenuar o aparecimento de doenças cerebrais.

Palavras-chave: memória, metabolismo, captação de glucose, 2-desoxiglucose, 3-O-metilglucose, 2-NBDG, sacarose, adenosina, hipocampo, estriado, córtex frontal, plasticidade sináptica, receptor de adenosina A_1, receptor de adenosina A_{2B}, receptor CB_1 canabinóide, lactato, glicogénio, insulina, diabetes.

ABSTRACT

This work started from the known premise that, in the brain, glucose availability regulates memory and cognition in both healthy humans and dementia patients. Furthermore, cerebral glucose deregulation has been associated with neuropsychiatric disorders, and alterations in glucose uptake in specific brain areas are selective hallmarks for the diagnosis of neuropsychiatric diseases. The experimental work presented in this doctoral thesis aimed at unveiling how neuromodulators including insulin regulate glucose metabolism in the brain and what are the consequences of impaired brain glucose metabolism in animal models.

To this aim, biochemical and electrophysiological studies were performed in brain structures that correlate with cognition and personality, that is, the hippocampus and the frontal cortex. Also a battery of behavioural studies was carried out in laboratory rodents. To begin with, various *in vitro* methods for both the spatiotemporal and the quantitative measurement of glucose uptake and metabolism in acute hippocampal and frontocortical slices and cell cultures were optimized. Then the basic characteristics of glucose uptake and metabolism in the hippocampal slice were explored, including the role of the insulin signalling pathway and the role of two other important neuromodulator families. We found and report for the first time that systemic streptozotocin-induced untreated type-1 diabetes affects both the resting and depolarization-induced glucose uptake and metabolism in a fashion dependent on the cannabinoid CB_1 receptor in the hippocampus. Notably, this brain area is responsible for the formation and recall of memory, which is regulated by insulin signalling. Using the same diabetogenic compound but now intracerebroventricularly administered, we achieved a previously characterized animal model of cerebral diabetes, thus avoiding confounding peripheral changes. This procedure led to the impairment of hippocampus-dependent memory. Furthermore, the results pointed out that synaptic dysfunction observed in the electrophysiological experiments occurred before the loss of synapses and coincided with metabolic dysfunction.

Next, we moved to another animal model associated with metabolic dysfunction, a prediabetic model induced through the consumption of a high sucrose diet (HSu). This model has the advantage of being less invasive than cerebral STZ-injection, and mimics

better human lifestyle-dependent disorders; furthermore it enables the study of the initial phase of the disease, prior to the occurrence of diabetes. According to the high-resolution magic angle spinning spectroscopic analysis of the hippocampal tissue, HSu-induced peripheric metabolic modifications did not cause an apparent impact on cerebral metabolism, albeit these HSu animals exhibited memory impairment. We looked for circuitry modifications in the hippocampal Schaffer-CA1 pathway, which is connected to hippocampal-dependent memory task, but none was found. Subsequently, we asked if HSu affected another pathway mediating spatial memory consolidation and recognition process of rats, namely, the temporoammonic branch of the perforant path. We observed that high sucrose consumption impairs synaptic plasticity at the temporoammonic pathway-CA1 pyramidal synapses. Additionally, we tested the role of adenosine receptors in those pathways and observed that high sucrose consumption upregulates adenosine A_1R in the hippocampus.

Next we investigated the hypothesis that the activation of the low-affinity adenosine A_{2B} receptor ($A_{2B}R$) could promote glucose uptake in neurons and astrocytes, thereby possibly linking brain activity with energy metabolism. We developed a protocol for real-time fluorescent measurement of deoxyglucose uptake in hippocampal slices, ideal to complement quantitative analyses. We found that $A_{2B}R$ activation is associated with an instant and tonic increase of glucose transport into neurons and astrocytes in the mouse brain. These prompt further investigations to evaluate the clinical potential of this novel glucoregulator mechanism.

In conclusion, the present thesis work has contributed to the elucidation the ill-defined mechanisms that regulate brain glucose metabolism. We have found additional proofs linking impaired hippocampal synaptic plasticity and memory with metabolic disorders. We also identified the $A_{2B}R$ as a possible novel therapeutic target to boost brain glucose metabolism with the objective of mitigating the outcome of brain disorders.

Keywords: memory, metabolism, glucose uptake, 2-deoxyglucose, 3-O-methylglucose, 2-NBDG, sucrose, adenosine, hippocampus, striatum .frontal cortex, synaptic plasticity, adenosine A_1 receptor, adenosine A_{2B} receptor, cannabinoid CB_1 receptor, lactate, glycogen, insulin, diabetes

Chapter 1

Introduction

1 INTRODUCTION

1.1 CEREBRAL ENERGY METABOLISM

1.1.1 Overview of brain metabolism

This thesis work, attempted to characterize the basic features of brain glucose use and its regulation by neuromodulators, with special attention to the alterations in brain metabolism and physiology under common systemic metabolic disorders. Therefore, it is the essential to provide an up-to-date overview of brain energy metabolism from the above vantage point.

The brain is a complex organ composed of a multiplicity of cell types including but not limited to neurons, astrocytes, oligodendrocytes, microglial cells, and capillary endothelial cells. Each has different metabolic requirements since they have different cellular functions (Hertz, 2008). At the cellular level, the distribution of energy consumption is still under debate. At a glance, neurons are predominantly oxidative while astrocytes are mostly glycolytic, whereas the neuroenergetic roles of oligodendrocytes and microglia are still ill-defined (Bélanger et al., 2011; Hyder et al., 2006).

1.1.2 The role of neurons and astrocytes

Neurons are communicating cells, organized into complex circuits, which use electric, gaseous and chemical synapses to process and transmit information, and these phenomena are called synaptic transmission. Neurons are divided into classes according to the neurotransmitter they use, hence can be GABAergic (inibitory), glutamatergic (excitatory) but also dopaminergic, cholinergic or serotoninergic neurons, as well as have "mixed" phenotype (Hof et al., 2004; Lodish et al., 2000).

The importance of astrocytes in neural transmission emerged with the concept of the "tripartite synapse" where astrocytes actively participate in the modulation of communication between the pre- and post-synaptic terminals (Araque et al., 1999; Perea et al., 2014). In fact, the synapse has at least one more component cell type, *i.e.*

microglia, but for sake of simplicity, the putative role of these immune cells in brain metabolism will be consistently overlooked in this Thesis.

Astrocytes outnumber neurons in the human brain (Nedergaard et al., 2003; Ransom et al., 2003). Beyond their crucial role in energy and metabolism (Brown and Ransom, 2007; Hertz et al., 2007; Magistretti, 2006; Magistretti and Pellerin, 1999), they are also involved in the maintenance of extracellular homeostasis, controlling ionic composition, pH and transmitter levels among others (Coulter and Eid, 2012; Hansson et al., 1985; Kressin et al., 1995). Astrocytes also participate in synaptic modulation (Perea et al., 2009; Santello et al., 2011), regulation of blood flow (Howarth, 2014), immune and inflammatory response (Aschner, 1998; Rossi, 2015), as well as in neuroprotection (Bélanger and Magistretti, 2009).

1.1.3 Glucose - a food for thoughts

Despite the brain being able to consume alternative substrates (Valente-Silva et al., 2015), brain energy metabolism in adults depends mainly on glucose (Sokoloff, 2004). The adult human brain uses ~25% of the total (resting) body glucose consumption and ~20% of the total oxygen consumed (Magistretti and Allaman, 2015). The majority of this energy is spent on the maintenance of membrane excitability, specifically, on the Na^+/K^+-ATPase (Alle et al., 2009; Attwell and Laughlin, 2001) as well as on neurotransmitter turnover (Pellerin et al., 2007). Since the brain is highly dependent on glucose supply, chronic maladaptive changes in the cerebral glucoregulation may compromise brain function and lead to neuropsychiatric disorders (Schubert, 2005; Shah et al., 2012). Brain disorders often involve specific early alterations in metabolism of glucose in the brain (Mosconi, 2005; Teune et al., 2010). The idea of alleviating symptoms of dementia by boosting cerebral energy metabolism has been toyed with for decades (Branconnier, 1983). Yet, there is still a lot to understand about healthy and pathological brain glucoregulation to define and market safe pharmacological agents with well characterized mechanism of action, with the objective of boosting the energy demands of the diseased or even the healthy brain.

Several experimental techniques, such as $^3H/^{14}C$-2-deoxy-D-glucose ($^3H/^{14}CDG$) autoradiographic methods, functional magnetic resonance imaging and positron emission tomography employing ^{18}F-fluorodeoxyglucose (^{18}FDG-PET), have shown a

correlation between the consumption of glucose and neuronal activity (Magistretti, 2006). In fact, the increase in neuronal activity boosts energy need, which is probably met mainly by an elevation in astrocytic glucose metabolism coupled with increased local blood flow (Giove et al., 2003; Magistretti, 2006; Pellerin et al., 2007; Sokoloff, 1977). The rate of glucose consumption depends on spatiotemporal variables: ^{3}HDG autoradiography and ^{18}FDG-PET studies revealed that the functionally active regions and especially, the grey matter are associated with greater signals (Raichle and Mintun, 2006). The rate of glucose use is different for each brain region and this variance is comparable between species. For example, rodents have higher metabolic rates than primates but the different brain areas consume proportionally similar amounts of glucose among mammalian species (McKenna et al., 2012; Sobrero et al., 2011).

The breakdown of energy consumption at the cellular level is still under debate. It is known that the oligodedendrocyte-dominated white matter tracts show a lower metabolic rate compared to synapse-laden regions rich in astrocytes and neurons (Clarke and Sokoloff, 1999). This higher energy need of synapses is likely the result of glutamatergic postsynaptic actions, which account for ~34% in rodents and ~74% in humans of the total energy expenditure of brain signalling, while glutamate uptake and glutamine synthesis demand only ~2% of energy expenditure in rodents and ~5% in humans (Attwell and Laughlin, 2001).

1.1.4 Brain glucose homeostasis at a glance

In brief, the energy homeostasis of the brain is tightly dependent on energetic glucose metabolism occurring either in oxidative or anaerobic pathways (Ivanov et al., 2014; Pellerin and Magistretti, 2012). The principal oxidative pathway is cytoplasmic glycolysis, producing two molecules of pyruvate, which can be further oxidized in the tricarboxylic acid cycle in mitochondria (Magistretti et al., 2004). The second oxidative pathway is NADPH generation from $NADP^{+}$ in the pentose phosphate shunt (Dringen et al., 2007) in order to reduce the major antioxidant molecule glutathion from its oxidized form (Kletzien et al., 1994). In astrocytes, glucose can be stored as glycogen – a reserve of glucose equivalents (Brown and Ransom, 2007; Gruetter, 2003). Under the activity of the circuitry, brain cells can rapidly mobilize phosphocreatinine and glycogen to support the increased energy need (Brown and Ransom, 2007; Gruetter, 2003). But

unlike the skeletal muscle, the brain rapidly uses up its energy reservoirs in a second to few minutes scale. Therefore, the brain is critically dependent on its continuous energy supply, which is tightly regulated by neurohumoral mechanisms (Stern and Filosa, 2013), and glucose entry is adjusted to demand (Castro et al., 2009; Leybaert et al., 2007). The underlying neurohumoral mechanisms are little understood at the cellular level, which allows us to advance our pioneering studies tackling these questions. In the following paragraphs, we overview the relevant features of brain glucoregulation.

1.1.5 Glucose transport into the brain

Circulating glucose enters the brain parenchima through specific facilitative glucose transporters (GLUT) located in the blood-brain barrier (BBB) (Castro et al., 2009; Leybaert et al., 2007). The first barrier is formed by endothelial cells, where the GLUT1 subtype allows the passage of glucose (Maher et al., 1994). The tight junctions of BBB endothelial cells serve as a seal to prevent the occurrence of paracellular diffusion (Leybaert et al., 2007). The transport across the BBB follows a classical Michaelis-Menten kinetics (Choi et al., 2001; Gruetter et al., 1998; Lund-Andersen, 1979; Vyska et al., 1985). This model proposes a linear correlation between brain and blood glucose levels (Gruetter et al., 1998).

The major GLUT subtypes in the mammalian brain are GLUT1 and GLUT3 present in astrocytes and neurons (Dwyer et al., 2002; Mueckler, 1992; Shah et al., 2012), as well as GLUT5, which is specific for microglia (Jurcovicova, 2014; Vannucci et al., 1997). The peripheral insulin-sensitive transporter, GLUT4 is also present in the brain, mostly co-localizing with GLUT3 (Apelt et al., 1999; Bakirtzi et al., 2009).

The BBB is endowed with the highly glycosylated 55 kDa isoform of GLUT1. The less glycosylated 45 kDa GLUT1 isoform is present in the parenchyma, specifically in the astrocytic end feet (around blood vessels), in astrocytic cell bodies but also in neurons (Vannucci et al., 1997). GLUT3 is present in neurons, in both dendrites and axons and enables glucose transport to neurons (Vannucci et al., 1997). It was observed in rodents that GLUT3 displays superior glucose transport capacity than GLUT1, which seems logical taken that glucose levels around neurons (1–2 mM) are smaller than in the serum (5–6 mM) (Cruz and Dienel, 2002a; Gruetter et al., 1998; Simpson et al., 2007, 2008). Although GLUT3 readily translocates to neuronal membranes upon combined

stimuli with high K^+ and insulin (Uemura and Greenlee, 2006), the importance of this process has been challenged by the appearance of the astrocyte-neuron lactate shuttle (ANLS) hypothesis (Magistretti and Pellerin, 1997, 1999; Pellerin et al., 2007; Pellerin and Magistretti, 2012), which is described in section **1.2.5** with more detail.

1.1.6 Glucose-6-phosphate and glycolysis

Once intracellular, glucose enters the glycolytic (Embden–Meyerhof) pathway of neurons and astrocytes. First, glucose is phosphorylated by hexokinases resulting in glucose-6-phosphate (G6P), which is the general intracellular representation of extracellular glucose in the *Animalia*. G6P can either enter glycolysis or be stored as glycogen (**Section 1.1.10**). In the late eighties, it was generally believed that G6P translocase isoforms were absent in neurons and astrocytes (Fishman and Karnovsky, 1986). Thus the phosphorylation by hexokinases of the hardly metabolizable 2-deoxyglucose (2-DG) into 2-DG6P virtually traps 2-DG inside the brain cells, because the G6 phosphatase-β enzyme (Ghosh et al., 2005) resides inside microsomes, having no direct access to cytoplasmic 2-DG6P (Schmidt et al., 1989). This makes radiolabeled 2-DG analogues a very attractive tool to measure the kinetics of brain glucose uptake in assays that do not last more than 45-60 min (Schmidt et al., 1989). The basis of this technique was pioneered by the recently deceased "godfather" of brain metabolism, Louis Sokoloff (Sokoloff et al., 1977). Refined techniques based on Sokoloff's method were also major research tools used in this thesis studies. Nevertheless, the past inference of the lack of microsomal membrane permeability for G6P was largely dismissed a few years later (Forsyth et al., 1993).

Through glycolysis, glucose is converted into two molecules of pyruvate with the concomitant formation of two molecules of both ATP and NADH. The key enzymes involved are hexokinase, phosphofructokinase, and pyruvate kinase (Lowry and Passonneau, 1964). Those enzyme activities are controlled by the levels of high-energy phosphates, and by citrate and acetyl-CoA (Magistretti, 2004). Pyruvate then can be transaminated to alanine or reduced to lactate or can enter into the mitochondria where it is oxidized in consecutive metabolic steps, through the TCA cycle, generating reducing equivalents for energy production in the oxidative respiratory chain (Hertz and Dienel, 2002) as well as substrates for biosynthetic processes (Gruetter, 2002). When

the glycolysis rate exceeds the rate of pyruvate entry into the TCA cycle, a dynamic equilibrium between pyruvate and lactate is created through the enzyme lactate dehydrogenase (Castro et al., 2009; Magistretti, 2004). In this situation, local lactate must be released to avoid influencing the reversible $NAD^+/NADH/H^+$-coupled redox reactions (Castro et al., 2009).

1.1.7 The tricarboxylic acid (TCA) cycle

In the mitochondria, pyruvate is decarboxylated to form acetyl-CoA, which is mediated by the pyruvate dehydrogenase complex and allows the production of $NADH/H^+$ and the release of CO_2 (Patel and Korotchkina, 2001). The tricarboxylic acid (TCA) (also known as Szentgyörgyi-Krebs) cycle starts with the condensation of acetyl-CoA with oxaloacetate to form citrate that subsequently isomerizes into isocitrate. Isocitrate is oxidized and decarboxylated to α-ketoglutarate, which is oxidized and decarboxilated to succinyl-CoA. Succinyl-CoA is then converted to succinate, forming GTP in the process. Succinate is further oxidized to fumarate. Afterward, the fusion of fumarate with a H_2O molecule creates malate, which is subsequently oxidized into oxaloacetate. From each acetyl-CoA, one turn of the TCA cycle directly generates three $NADH/H^+$, one $FADH_2$, one CO_2 and one GTP molecules. Taking into account that every $FADH_2$ yields 1.5 ATP and that each $NADH/H^+$ gives rise to 2.5 ATP molecules (when oxidized in the mitochondrial respiratory chain) the complete oxidation of one molecule of glucose is theoretically expected to produce 30 or 32 ATP molecules, depending on whether the $NADH/H^+$ generated in glycolysis is transported via the glycerol-3-phosphate or via the malate-aspartate mitochondrial shuttles, respectively (Voet and Voet, 1995).

1.1.8 Glutamate turnover and Na^+ pumps

The maintenance of the electrochemical gradient of excitable membranes with the help of Na^+/K^+-ATPases is the biggest consumer of glucose even under resting conditions in the brain (Astrup et al., 1981; Attwell and Laughlin, 2001). The Na^+/K^+-ATPase pump cotransports 3 Na^+ against 2 K^+ on the cost of an ATP molecule, and is an integral metabotropic receptor in the membranes of virtually most cell types of

vertebrate animals, and it possibly has an endogenous ligand called ouabain in mammals (Buckalew, 2015; Liu et al., 2007; Wu et al., 2013). While digitalis-like toxins such as ouabain act as agonists at the pump protein to induce metabotropic signalling, they block the ion exchanger activity of the pump. Thus, ouabain is a precious tool to dissect the roles of Na^+/K^+-ATPase pump in biological models (Juhaszova and Blaustein, 1997; Wu et al., 2013). An increase in extracellular glutamate levels has been shown to concomitantly augment glucose uptake in astrocytes, which can be blocked with ouabain, therefore it was concluded that the Na^+-glutamate electrogenic cotransport stimulates the Na^+/K^+-ATPase (Magistretti and Pellerin, 1997; Pellerin and Magistretti, 1994). This in turn leads to increased ATP consumption, adenosine release and augmented glucose uptake to replenish ATP stores. Nonetheless, ouabain is in fact a general Na^+ pump inhibitor; therefore, it also inhibits the Na^+/Ca^{2+} exchanger (Blaustein et al., 2002). A recent study unveiled that glutamate-uptake-induced sodium cotransport is necessary but not sufficient for the stimulation of glucose uptake: an additional intracellular Ca^{2+}-rise elicited by glutamate is necessary, too (Porras et al., 2008), albeit it remains to be elucidated how much - if any of the Na^+/Ca^{2+} exchanger is involved in the glutamate-induced glucose uptake.

Last but not least, it is worth to mention that the Na^+/K^+-ATPase pump is sensitive to neuromodulators, and three of them are relevant for this thesis. For instance, our group in collaboration with Dr. JF Chen (Boston) found that the adenosine A_{2A} receptor (**Section 1.5.4**) is negatively associated with the α_2 subunit of the Na^+/K^+-ATPase pump, thus $A_{2A}R$ agonists as well as phasic adenosine peaks are expected to decrease the activity of the pump, and consequently, the uptake of glutamate (Matos et al., 2013). Moreover, high concentrations of insulin were shown to decrease the activity of Na^+/K^+-ATPases in whole cortical membranes (Bojorge and de Lores Arnaiz, 1987), although insulin in general is a stimulator of Na^+/K^+-ATPases *e.g.* in myocites, kidney proximal tubule cells, corneal endothelium or hepatocytes (*e.g.* (Féraille et al., 1999). Finally, others found that the cannabinoid CB_1 receptor (**Section 1.4.3**) is positively associated with the Na^+/K^+-ATPase pump in nerve terminals (Araya et al., 2007).

1.1.9 The pros and cons of astrocyte-to-neuron lactate shuttle

The brain capillaries are surrounded by astrocytes (Kacem et al., 1998), contributing to the first cellular barriers for glucose to enter the brain parenchyma (Pappenheimer and Setchell, 1973). Their contact with microvessels well positions astrocytes to play a pivotal role in cerebral metabolism. However, the role of astrocytes in brain metabolism is currently viewed in strikingly opposite manner by two major schools.

One school believes that during intense activity, neurons obtain energy mainly from burning lactate produced for them by astrocytes (Bélanger et al., 2011; Hertz and Dienel, 2002; Pellerin et al., 2007; Pellerin and Magistretti, 1994; Wyss et al., 2011). This hypothesis is termed as astrocyte-to-neuron-lactate shuttle hypothesis (ANLS), and holds that during the activity of the neural tissue, astrocytic glucose uptake surpasses neuronal glucose use, and a metabolic link is formed between the two cell types: active principal neurons release glutamate which in part is taken up by astrocytes via the process of glutamate/Na^+ cotransport. As above stated in detail, the rise in intracellular Na^+ concomitantly triggers the Na^+/K^+-ATPase of the astrocytes resulting in an increased demand for ATP, thus stimulating glycogenolysis as well as the uptake of glucose. Astrocytes break down glucose via glycolysis into pyruvate to form lactate, and with this process, gain 2 ATP molecules to spend on the activity of the Na^+/K^+-ATPase. Lactate is then exported to neurons through monocarboxylate transporters. Once taken up by neurons, lactate is reverted into pyruvate to be used in the TCA cycle, each contributing to the generation of 15 ATP molecules (Barros and Deitmer, 2010; Pellerin and Magistretti, 1994). This way, astrocytes and neurons are linked through activity-dependent metabolic trafficking (Magistretti, 2006; Tsacopoulos and Magistretti, 1996). Of course, neurons can also use glucose besides lactate for both fuel (Brown and Ransom, 2007b; Dringen et al., 2007) and the generation of lipids, proteins and certain neurotransmitters such as acetylcholine, GABA and glutamate (Magistretti et al., 2002).

The other school provides experimental evidence that increased neuronal glucose uptake is necessary and sufficient to supply amplified energy demand of the circuitry (Gjedde and Marrett, 2001; Nehlig et al., 2004; Patel et al., 2014). Unfortunately, the gap between the two schools is not only widening when high-impact high-tech

publications show that glucose is the source of energy in neurons under activity (Lundgaard et al., 2015) contrasting clear molecular evidence of lactate gradient flowing down from astrocytes to neurons (Machler et al., 2016), but the scientific atmosphere has even become turbulent when others served *in vivo* support for the hypothetical neuron-to-astrocyte lactate shunt (NALS), which - contrasting to ANLS - suggests that neurons are the ones which supply astrocytes with lactate (Mangia et al., 2009, 2011). These latter authors claim that their model eventually does not prohibit ANLS to occur, *i.e.* that lactate flows from astrocytes to neurons, but that would require at least 12-times more lactate production by astrocytes and the lack of glycolysis in neurons, which they do not think to hold up against scientific evidence (Mangia et al., 2011). Nevertheless, Castro and colleagues assert that the release of ascorbic acid from astrocytes can be triggered by glutamate, which when taken up by neurons, switches glucose burning to lactate use, and this mechanism may help to resolve some of the discrepancies in the literature. Finally, some found that neurons also can rely on the oxidation of recycled glutamate, too, to support energy demands under heavy load (Torres et al., 2013).

1.1.10 Glycogen

Glycogen is the main energy reserve of the brain and mostly localized in astrocytes (Brown, 2004; Magistretti et al., 1993; Vilchez et al., 2007). Its levels in the healthy rat brain are around 3-8 μmol/g tissue (Cruz and Dienel, 2002a; Morgenthaler et al., 2008). Glycogen (like other glucans) is toxic to neurons (Brown, 2004; Duran et al., 2012; Magistretti and Allaman, 2007; Vilchez et al., 2007). The astrocytic glycogen reserve can sustain increased energy demand for a few minutes (Castro et al., 2009) and can extend white matter axon function for 20 min or longer (Brown and Ransom, 2007b). Some even claim that astrocytes have sufficient glycogen stores to supply the circuitry for more that 100 min of hypoglycemia (Gruetter 2003). Obviously, understanding what factors (receptors?) trigger the replenishment of the glycogen stores would represent a major breakthrough in the treatment of cerebral infarct, stroke and other hypoglycemic conditions.

Astrocytic filopodes in the synapse are often too slight to accommodate sufficient amount of mitochondria, thus increasing the importance of glycolytic energy production

(Hertz, 2008; Wiesinger et al., 1997). By the breakdown of glycogen into glucose-1-phosphate by glycogen phosphorylase, and its subsequent conversion into G6P by phosphoglucomutase, glycogen derived glucose enters the glycolysis pathway (Brown and Ransom, 2007b) to be further metabolized to lactate, as described above with the ANLS. Synaptic lactate has important neurophysiological functions as being indispensable for synaptic plasticity and memory formation (Suzuki et al., 2011). Consequently, deficits in cerebral glucose metabolism contribute to cognitive impairment.

1.1.11 Insulin

Cognition and plasticity are tightly connected to cerebral glucose (Messier, 2004) and insulin homeostasis (McNay and Recknagel, 2011). McNay and Recknagel (2011) described glucose transporters GLUT4 and GLUT8 in the brain as insulin-sensitive and fettered to the insulin effect in cognition and synaptic plasticity. Brain insulin is originated from both peripheral and central sources (Raizada, 1983). It is estimated that, independently from its origin, insulin acts through its own receptors present in the brain to perform its neurophysiological functions, such as the regulation of food intake, weight control, reproduction, cognition and memory formation and also, neuroprotection (Duarte et al., 2012a; Ghasemi et al., 2013).

It is suggested that insulin is *de novo* synthesised in the brain (Duarte et al., 2012a). Although there was previous data suggesting that insulin synthesis takes place mainly in pyramidal neurons (Duarte et al., 2012a), it is more likely now that insulin is released by neurogliaform cells (Molnár et al., 2014), which is a unique GABAergic cell type using volume transmission. Insulin from the periphery can be also transported to the brain through the BBB by specific concentrative transporters.

The insulin receptor (IR) and the insulin-like growth factor-1 receptor (IGF-1R) - the two major insulin-sensing receptors in the brain - are heterotetrameric protein complexes, composed of two extracellular α subunits (insulin-binding domain) and two transmembrane spanning β subunits. When the β subunits bind insulin, they undergo autophosphorylation through the stimulation of their tyrosine kinase domain, and consequently, they activate the signalling cascade. The cerebral insulin signalling cascade shares similarities with that in the periphery (Grillo et al., 2009), comprising the

phosphoinositide 3 kinase (PI_3K)–Akt and the MAPK/ERK kinase pathways, as well as G protein-mediated pathways (Biessels and Reagan, 2015; Duarte et al., 2012a; Grillo et al., 2015; Nelson et al., 2008).

We cannot talk about glucose and insulin without mentioning diabetes. There are four major types of diabetes currently distinguished. If it is of peripheral origin and involves insulinopenia, we call it type-1 diabetes (T1D) or insulin-dependent diabetes. Conversely, when insulin's action is ineffective at its receptors in peripheral tissues, the outcome is called type-2 diabetes (T2D). Insulin-resistant diabetes can also occur in the brain, and this is called type-3 diabetes, referring to the situation when insulin is unable to exert its cerebral roles (independently from the presence or absence of peripheral resistance (Lester-Coll et al., 2006; de la Monte and Wands, 2008). It is more and more prevailing to assume that Alzheimer's disease (AD) is a metabolic disease and that AD represents a form of diabetes that selectively involves the brain (de la Monte and Wands, 2008). Finally, hyperglycemia of variable severity and with onset during pregnancy is termed gestational or type-4 diabetes (Baz et al., 2015).

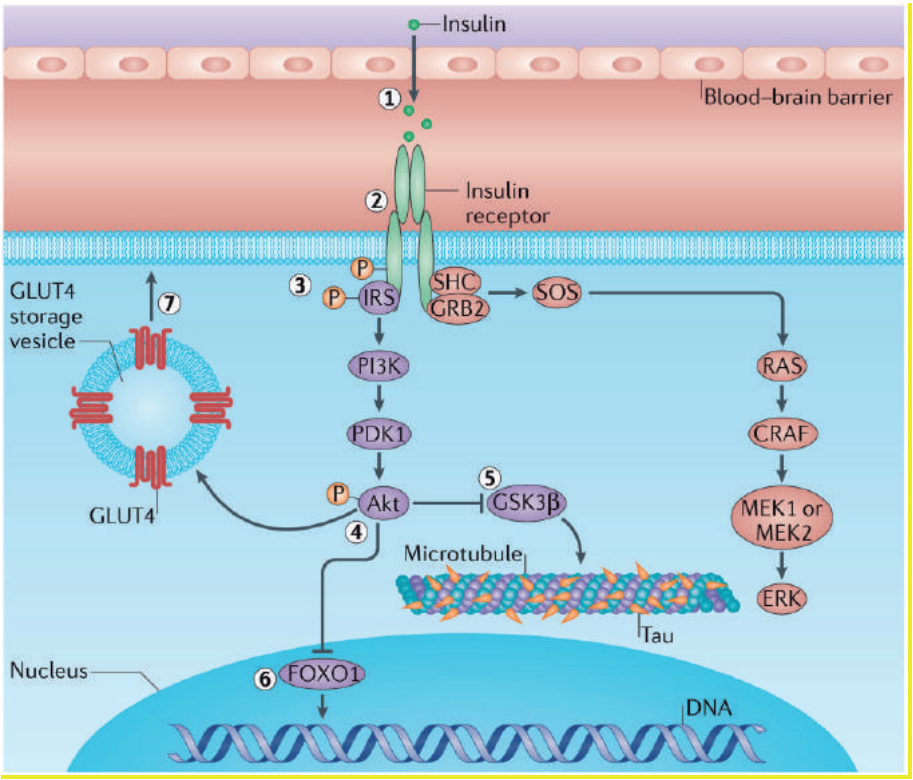

Figure 1.1 – Insulin receptor signalling in the hippocampus (reproduced from Biessels and Reagan, 2015).

In diseases conditions such as AD and T2D featuring hippocampal insulin resistance, the impairment in the insulin signalling cascade can occur at different levels, *i.e.* at the level of: 1) BBB insulin transport (Banks et al., 2012); 2) insulin receptors (*i.e.* expression/activity); 3) phosphorylation state of insulin receptor substrate (IRS); 4) Akt phosphorylation; 5) glycogen synthase kinase 3β (GSK3β), which is responsible for the phosphorylation state of the microtubule-associated proteins, tau; 6) forkhead box O (FOXO) family of transcription factors; 7) trafficking through GLUT4 to the plasma membrane (Biessels and Reagan, 2015) (**Figure 1.1**).

1.2 GLUCOSE METABOLISM AND BRAIN PHYSIOLOGY

Glucose metabolism is the main source of energy in the adult brain and is related to cognitive performance. For instance, hippocampus-dependent memory tasks may consume up to 32% of extracellular glucose (McNay et al., 2010). Interestingly, these authors also observed a positive correlation between the degree of difficulty of the behavioural paradigm and hippocampal glucose consumption. Systemic glucose administration replenished extracellular glucose levels and allowed improvement in the task performance. Indeed, optimal glucose doses administered either centrally or systemically improve learning tasks (Flint and Riccio, 1997; Hughes, 2002, 2003; Kopf and Baratti, 1995; Lee et al., 1988, 1988; Messier et al., 1998; Ragozzino et al., 1996; Winocur and Gagnon, 1998). More specifically, glucose administration right before or right after the behavioural training session increased the efficiency in learning and memory consolidation (Lee et al., 1988; Messier et al., 1998). Regarding humans, studies also linked bolus glucose with enhancement of kinesthetic learning (Scholey and Fowles, 2002), facial recognition (Metzger, 2000), long-term verbal and spatial (Sünram-Lea et al., 2001) memories as well as with more effective mental capacity (Benton, 1990). Contrariwise, poor glucose tolerance was associated with decreased general cognitive performance and atrophy of the hippocampus (Convit et al., 2003). Additionally, glycogenolysis is also enrolled in cognitive functions, taken that the blockade of glucose transporters or other interferences with astrocytic glucose metabolism abolished memory consolidation and learning in chicks (Gibbs et al., 2008).

1.2.1 Synaptic metabolism and plasticity

Memory is divided into four different phases: 1) encoding, 2) storage, 3) consolidation and 4) retrieval (Izquierdo et al., 1999). It is generally accepted that hippocampal dependent memory is mediated (or partially mediated) by hippocampal synaptic plasticity (Neves et al, 2008). Synaptic plasticity consists in modifications of the synaptic strength as response of changes of synaptic activity (Neves et al, 2008) and is critical for the encoding and intermediate storage of memory (Morris et al., 2003). The interdependence between synaptic plasticity and the storage of memory is known as the neurobiological theory of the hippocampus. Understandably, studying synaptic plasticity opens a window on the mechanisms of information processing of the brain. The hippocampus is organized in simple neural pathways including but not limited to the Schaffer collaterals-CA1 pathway and the temporoammonic pathway (see **Figure 1.2**). Extracellular recordings of synaptic events in acute slices permit studying the phenomena of synaptic plasticity, including but not limited to long-term potentiation (LTP) and long-term depression (LTD) (Bliss and Lomo, 1973). Albeit memory formation is generally thought to involve LTP, there are also LTD-dependent memory processes involved (Nabavi et al., 2014). LTP denotes the persistent increase of synaptic strength between two neurons connected via chemical synapses, while LTD refers to it persistent decrease.

The acquisition of new information through learning triggers a cascade of events and the formation of short and long-term memories. It is accepted that long-term memory formation has high metabolic demands (Suzuki et al., 2011). Suzuki et al. (2011) described that the learning process is associated with an increase in extracellular lactate levels. This lactate is originated from glycogenolysis – a brain metabolic process specific to astrocytes (Magistretti, 2004). Astrocytic glycogenolysis and consequent lactate release are fundamental for long-term memory formation, although not prerequisite of short-term memory formation as it depends predominantly on posttranslational modifications. On the other hand, the formation of long-term memories requires the phases of consolidation and stabilization, involving the activation of a gene cascade and the synthesis of proteins to modify the synaptic dynamics in neurons that store and acquired information (Dudai, 2004; Kandel, 2001; Klann and Sweatt, 2008). The breakdown of astrocytic glycogen and consequent lactate release is

fundamental for the maintenance of LTP. Interestingly, impaired lactate transport causes amnesia. If the amnesia is due to the impairment of astrocytic transporters, MCT1 and MCT4, it may be rescued by L-lactate but not equicaloric glucose (this same pattern is also observed under LTP impairment). If amnesia is due to the dysfunction of neuronal MCT2 transporters, neither L-lactate nor glucose are able to prevent it, stressing the importance of astrocyte-neuron lactate transport in the formation of long-term memory.

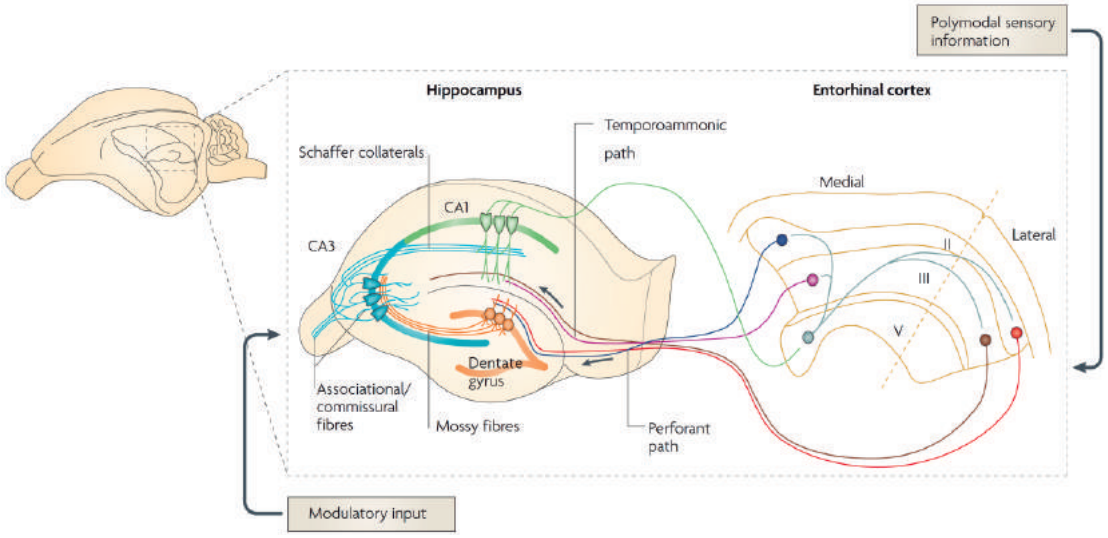

Figure 1.2 – Basic anatomy of the hippocampus (reproduced from Neves et al., 2008).

Furthermore, we also need to address the vital role of mitochondria in LTP and synaptic transmission (Calabresi et al., 2001; Li et al., 2010; Williams et al., 1998). Mitochondria control essential processes in synaptic plasticity through the production of energy (ATP and $NADH/H^{+}$) for maintenance and restoration of ion gradients, regulation of subcellular Ca^{2+} homoeostasis and Ca^{2+} signalling (Duchen, 2000; Nicholls and Budd, 2000; Toescu, 2000) and redox homoeostasis (Cheng et al., 2010). Mitochondria move within and between the subcellular compartments involved in synaptic plasticity (*e.g.* synaptic terminals, dendrites, cell body and the axon) (Sheehan et al., 1997) and redistribute to optimize neural activity (Miller and Sheetz, 2004). Impairment of mitochondrial functions may result in the disruption of synaptic plasticity and the appearance of neurodegeneration and diseases, including but not limited to AD, Parkinson's disease (PD) and psychiatric disorders (Cavallucci et al., 2013; Cheng et al., 2010; Moreira et al., 2006).

1.3 METABOLIC DYSFUNCTION AND BRAIN DISEASES

Over the years, an increasing number of studies in animals and humans pointed out a link between metabolic dysfunction and cognitive deficits (Strachan et al. 1997; Moreira et al. 2006), taken that brain energy metabolism is in part dependent on the activity of excitatory synapses (Viswanathan and Freeman, 2007). Synaptic dysfunction is the earliest morphological modification in neurodegenerative diseases and is also a phenomenon that well correlates with memory impairment (Selkoe, 2002a).

Obesity, hypertension, dyslipidemia, and insulin resistance are risks factors for metabolic syndrome and have been related with cognitive decline and vascular dementia (Bloemer et al., 2014; Crichton et al., 2012; Panza et al., 2010; Winocur et al., 2005; Winocur and Greenwood, 2005). The relation between metabolic dysfunction and dementia is reinforced by the tight association of AD with diabetes (Alexander and Moeller, 1994; Exalto et al., 2012a; Xu et al., 2010a). Indeed, epidemiological studies revealed that T2D confers susceptibility to AD (Akter et al., 2011b). T2D gradually develops from a metabolic impairment named prediabetic state (Tabák et al., 2012). T2D then leads to a progressive brain damage and increases the risk for cognitive decline and dementia (Carvalho et al., 2012a; Luchsinger et al., 2007; Ravona-Springer et al., 2012; Roriz-Filho et al., 2009; Xu et al., 2010a) at an early onset (Bélanger et al., 2004; Strachan et al., 1997). ^{18}FDG-PET allows detecting reductions in cerebral glucose metabolism in patients with prediabetes or T2D, and helps both in the early discovery and the monitoring of the evolution of AD (Baker et al., 2011; Cerami et al., 2015; de Leon et al., 2007). The technique "spatial covariance mapping combined with ^{18}FDG-PET" is also used to unveil aberrant metabolic patterns present in other neurodegenerative diseases (Alexander and Moeller, 1994; Eckert et al., 2007; Eidelberg, 2009; Patro et al., 2015), including PD (Poston and Eidelberg, 2010), progressive supranuclear palsy, multiple system atrophy (Habeck et al., 2008) and Huntington's disease (Feigin et al., 2007).

In Portugal, more than 8% of the adult population suffers from mood disorders and comorbid weight changes, often because of antidepressants (Correia and Ravasco, 2014). Depression is frequently combined with metabolic disturbances, as a result of interdependent insulin and serotonin signalling (Kim et al., 2015). Diabetes is also associated with mood disorders: 71% of diabetic patients suffer from depression, and

70% of them from anxiety – another disorder that is associated with impaired serotonin signalling (Detka et al., 2013; Palizgir et al., 2013). Importantly, impaired insulin signalling is implicated in the pathogenesis of most neuropsychiatric disorders besides depression (Aviles-Olmos et al., 2013; Lang and Borgwardt, 2013), which is in part mediated by serotonergic dysfunction (Broderick and Jacoby, 1989; Miyata et al., 2007). Hippocampal serotonin has been documented in the antidepressant action of insulin via the Akt/GSK3 axis. This axis also links obesity with mood disorders (Papazoglou et al., 2015) with 99% comorbidity in the Portuguese population (Correia and Ravasco, 2014). Both depression and cerebral insulin resistance are associated with decreased glucose uptake and brain activity in the limbic regions in adults (Baker et al., 2011; Detka et al., 2013; Su et al., 2014). Thus, the principal region of interest of our study will be the hippocampus.

1.4 THE ENDOCANNABINOID SYSTEM

The history of scientific research on cannabis stretches back over 150 years, which has been reviewed elsewhere (Mechoulam et al., 2014). The curiosity about the cellular targets of Δ^9-tetrahydrocannabinol (Δ^9-THC; the major psychoactive molecule of marijuana) and related phytocannabinoids has led to the discovery of a great number of proteins and lipid molecules that can be abridged as the "endocannabinoid system *sensu lato*". The term "endocannabinoid" (Di Marzo et al., 1994; Di Marzo and Fontana, 1995) was coined to distinguish cannabinoid molecules endogenously produced by the body from those of exogenous origin such as Δ^9-THC. Strictly speaking, the term "endocannabinoid system" refers to the endocannabinoid molecules - among them the most studied ones are *N*-arachidonylethanolamine (anandamide) and *sn*-2-arachidonylglycerol (2-AG); their synthesizing and metabolizing enzymes and the cannabinoid CB_1 and CB_2 receptors (CB_1Rs and CB_2Rs) (Katona and Freund, 2012; Pertwee et al., 2010).

Precursors for both anandamide and 2-AG are believed to be stored in the cell membranes where the synthesis and the release of the two endocannabinoids occur (Katona and Freund, 2012; Piomelli, 2003). Multiple synthetic routes have been identified for anandamide (Katona and Freund, 2012; Placzek et al., 2008). Its principal

precursor is *N*-arachidonyl-phosphatidylethanolamine (NAPE) (Katona and Freund, 2012; Placzek et al., 2008; Sugiura, 2008). Different enzymatic steps can lead to "on demand" anandamide cleavage from NAPE, which can involve the Ca^{2+}-dependent activation of specific phospholipases A_2, C, D and α,β domain serine hydrolase 4 (ABDH4) (Katona and Freund, 2012; Placzek et al., 2008; Sugiura, 2008). The chief biosynthetic pathway for 2-AG (when participating in endocannabinoid signalling) starts with the phospholipase-Cβ (PLCβ)-mediated hydrolysis of phosphatidylinositol 4,5-bisphosphate (PIP_2) resulting in the intermediate *sn*-2-diacylglycerol (DAG), from which 2-AG is cleaved by the enzyme *sn*-2-DAG lipase α (DAGLα) (Bisogno et al., 1999; Gao et al., 2010; Tanimura et al., 2010). In the nervous tissue, 2-AG – when participating in endocannabinoid signalling – is also thought to be released "on-demand" (Di Marzo et al., 1998). This means that typically in dendrites, a depolarization-induced Ca^{2+} entry and/or the stimulation of $G_{q/11}$ protein-coupled metabotropic receptors activate DAGLα to produce 2-AG in a millisecond to second scale (Castillo et al., 2012; Katona and Freund, 2012; Maejima et al., 2005).

The cloning and initial characterizations of the central cannabinoid receptor, CB_1R, were reported in the beginning of the nineties (Gérard et al., 1990, 1991; Matsuda et al., 1990, 1993). Only a few years later, another cannabinoid receptor type, the human and the rat CB_2R was discovered (Brown et al., 2002; Munro et al., 1993; Slipetz et al., 1995), with almost exclusive expression in the immune tissues (Galiègue et al., 1995). Both of these two receptors belong to the rhodopsin-like G protein-coupled receptor (GPCR) superfamily, and contain 7 α helical transmembrane domains. The high similarity in amino acid sequence of the 473 amino acid-long rat CB_1R (Matsuda et al., 1990) and the 472 amino acid-long human CB_1R (hCB_1R) (Gérard et al., 1991) represents evolutionary conservation (Irving et al., 2008). The first cloned hCB_2R has only 360 amino acids, sharing only 44% overall homology with the hCB_1R, and 68% identical amino acid identity considering only the 7 transmembrane domains (Munro et al., 1993). The CB_2R also couples predominantly to $G_{i/o}$ proteins (Howlett, 1995; Howlett et al., 2004) to inhibit adenylyl cyclase activity, which is thought to be the underlying mechanism of CB_2R-mediated downregulation of immune functions (Bayewitch et al., 1995; Howlett and Mukhopadhyay, 2000; Kaminski et al., 1994; Slipetz et al., 1995).

Both the CB_1R and the CB_2R receptors couple to multiple intracellular effectors, including adenylyl cyclase, extracellular regulated kinase 1/2 (ERK1/2) p38 kinase, c-Jun N-terminal kinase (JNK), and PI_3K/Akt (Bouaboula et al., 1996, 1997; Galve-Roperh et al., 2002; Gómez del Pulgar et al., 2000; Latini et al., 2014; Molina-Holgado et al., 2002, 2005; Rueda et al., 2000; Sánchez et al., 1998; Viscomi et al., 2009). The graphical visualization of the key intracellular signalosomes can be found elsewhere (Guzmán et al., 2001; Harkany et al., 2007). Nevertheless, cannabinoid receptor-mediated signalling cannot be viewed mechanistically, because context-dependent decisions are made at signalling crossroads. For example, CB_1R activation converging onto PI_3K and ERK activation promotes survival against ceramide-induced apoptosis (Galve-Roperh et al., 2002), but chronic CB_1R and CB_2R activation itself stimulates the generation of ceramide, which causes sustained ERK activation via Raf-1, leading to apoptosis (Guzmán et al., 2001; Herrera et al., 2006; Sánchez et al., 2001).

CB_1Rs and CB_2Rs can modulate intracellular cation levels. CB_1Rs are negatively coupled to N-, L-, P- and Q-types of voltage-gated Ca^{2+} channels (VGCCs) via the βγ subunit of the G protein, and positively associated with inwardly rectifying K^+ channels (GIRKs), probably via direct physical complexing (Felder et al., 1995; Lozovaya et al., 2009; Mackie et al., 1995; Mackie and Hille, 1992; McAllister et al., 1999; Roche et al., 1999). As discussed above, under special circumstances, CB_1Rs can trigger intracellular Ca^{2+} transients, too (Lauckner et al., 2005; Calandra et al., 1999). The stimulation of CB_2Rs may also produce transient increases in $[Ca^{2+}]_i$ via PLCβ (Shoemaker et al., 2005; Sugiura et al., 2000), at least in transfected cells.

1.4.1 The cellular and tissue distribution of cannabinoid receptors

The CB_1R has high expression (mRNA levels) and high density (protein levels) in the brain, while at lower levels, it is also expressed in adrenal gland, heart, lung, prostate, uterus, ovary, testes, bone marrow, thymus and tonsils (Galiègue et al., 1995). In the brain, CB_1R expression and protein densities are highest in the cerebellar molecular layer, substantia nigra pars reticulata (containing the CB_1R-laden terminals of the striatonigral pathway), globus pallidus externa and interna, inner granule cell layer of the olfactory bulb, anterior olfactory nucleus, layers II–III, Va and VI of the cerebral cortex (in humans, the highest levels were found in the cingulate gyrus, frontal,

secondary somatosensory and motor cortices), hippocampus, as well as in the dorsolateral striatum, while moderate levels of CB_1R expression is found in the hypothalamus and ventral striatum/nucleus accumbens, and finally, low CB_1R levels can be found in the brainstem with a lack of CB_1Rs in the respiratory control centers (Egertová and Elphick, 2000; Herkenham et al., 1990; Katona and Freund, 2012; Mackie, 2005; Mailleux and Vanderhaeghen, 1992; Marsicano and Lutz, 1999; Matsuda et al., 1993; Tsou et al., 1998). These explain why cannabis has mild effects on cardiovascular and respiratory functions (Hollister, 1986).

The CB_2R was originally identified as a protein with no expression in the brain and high density in the immune cells and tissues (Munro et al., 1993). An emerging body of evidence supports now physiological and pathological roles for neuronal CB_2Rs in the brain. For instance, a recent paper clearly argues that cerebral CB_2 proteins are mostly neuronal in the healthy brain, while inducible CB_2Rs become predominant in glia or microglia under disease conditions (Savonenko et al., 2015). In line with this evidence, an ultrasensitive and specific *in situ* hybridization method called the RNAscope revealed the CB_2R mRNA predominantly in excitatory and inhibitory neurons throughout the hippocampus with rare expression in microglia (Li and Kim, 2015). Although the vast majority of presynaptic cannabinoid receptors in the brain can be identified with the CB_1R, there is also pharmacological evidence for presynaptic inhibitory CB_2Rs in GABAergic terminals of the hippocampus (Andó et al., 2012) and in its relative vicinity, in the medial entorhinal area (Morgan et al., 2009). There are also intracellular CB_2Rs in layer II/III pyramidal cells of the medial prefrontal cortex where their activation results in IP_3R-dependent opening of Ca^{2+}-activated Cl^- channels, and a consequent inhibition of neuronal firing (den Boon et al., 2012, 2014).

1.4.2 The endocannabinoid system in systemic energy metabolism

It has been half a century that scientist have recognized that marihuana extracts and preparations modulate carbohydrate metabolism in animal models (Mahfouz et al., 1975; de Pasquale et al., 1978; el-Sourogy et al., 1966) and man (Benowitz et al., 1976).

CB_1R activation increases blood glucose levels via several potential mechanisms, including the inhibition of insulin release and of glucose utilization by peripheral tissue. It also stimulates appetite and ingestive behaviour through central mechanisms

concerning primarily the hypothalamus. Furthermore, CB_1R activation facilitates the growth of fat deposits rather than burning fat as a fuel for cells (Kunos et al., 2008; Matias et al., 2008a; Topol et al., 2010). Accordingly, genetic deletion of the CB_1R in laboratory rodents leads to a lean phenotype and resistance to diet-induced obesity and better insulin sensitivity (Harrold et al., 2002; Ravinet Trillou et al., 2004). Moreover, a silent intragenic biallelic polymorphism (1359G/A) of the human CB_1R gene is significantly associated with a lower body mass index (Gazzerro et al., 2007).

As a result of decade-long investigations, the CB_1R-selective inverse agonist, rimonabant was marketed in 2006 as it performed very well to reduce cardiometabolic risk factors in human patients (Matias et al., 2008a; Romero-Zerbo and Bermúdez-Silva, 2014). Unfortunately, rimonabant may trigger serious psychiatric side effects including depression and suicidality, which was already known during the clinical trials but those findings remained hidden from the authorities. Thus, rimonabant (Acomplia®) was banned from the European market for good (Rimonabant: depression and suicide, 2009; Romero-Zerbo and Bermúdez-Silva, 2014; Topol et al., 2010).

In the meantime, it became clear that central inverse agonism was the principal and only cause of psychiatric untoward effects, because neutral CB_1R agonists such as NESS0327 and O-2050 as well as less lipophilic CB_1R antagonists which do not cross the blood-brain barrier cause no central side effects but are still equally good to reduce food intake and combat cardiometabolic risk factors – at least in animals until CB_1R antagonists are again allowed to be tested in humans (Meye et al., 2014; Tam et al., 2010). At this point, the reader deserves more explanation about this dual form of CB_1R blockade.

Many GPCRs exhibit a so-called constitutive activity, meaning that they dissociate from GDP-bound G proteins at a low rate either because of the presence of residual levels of endogenous ligands or by a thermodynamically allowed low-probability reversal of association, in the absence of agonists (Makita and Iiri, 2014; Mukhopadhyay and Howlett, 2005). Theoretically, antagonists are not supposed to affect the constitutive auto-uncoupling. An antagonist is called silent or neutral when it only prevents an agonist from activating the receptor, but itself does not disturb the conformational state of the receptor, hence producing no effect *per se* (Pertwee, 2005). The classical cannabinoid O-2050 (Wiley et al., 2011) and the diarylpyrazole

NESS0327 (Ruiu et al., 2003) fall under this category as both prevent CB_1R activation when agonists are present, but *per se* they do not produce effect (Meye et al., 2013).

In special cases, a GPCR can assume an inactive structure, which would sequester surrounding G proteins rather than allowing their spontaneous dissociation. The probability of this to happen is greatly facilitated by certain ligands, which are called inverse agonists. The fist prototypic CB_1R antagonist, the 1,5-diarylpyrazole rimonabant (Rinaldi-Carmona 1994) is in fact an CB_1R inverse agonist (Bouaboula et al., 1997; Mukhopadhyay and Howlett, 2005; Pertwee, 2005), signifying that it triggers responses on its own via the blockade of constitutive (aka basal) CB_1R signalling, and the consequent disruption of active intracellular coupling. As a result, the direction of those responses will be perceived as reversed compared to the responses triggered by a true agonist, hence the name inverse agonist.

1.4.3 The endocannabinoid system in central energy metabolism

At the neuronal and astrocytic level, several *in vivo* studies have addressed the impact of systemic cannabinoid ligand treatment on local cerebral glucose utilization. One of the early studies investigated the effects of low to high doses of Δ^9-THC on radiolabelled 2-DG uptake using autoradiography in male rats. Interestingly, a low (0.2 mg/kg) dose of Δ^9-THC increased 2-DG uptake in all examined cortical and limbic structures, but not in the examined diencephalic and brainstem areas. In contrast, Δ^9-THC at 2.0 and 10.0 mg/kg inhibited 2-DG uptake in most of these regions (Margulies and Hammer, 1991), revealing different sensitivity of brains structures to cannabimimetics. The anatomic localization of Δ^9-THC effects is therefore consistent with the distribution of CB_1Rs in the brain.

Another early study utilizing positron emission tomography in eight normal human subjects reported that Δ^9-THC increases ^{18}FDG-PET signal (Volkow et al., 1991). This increase was only observed in the cerebellum, whereas global cerebral glucose metabolism in response to Δ^9-THC was variable. In this study, a relatively low amount (2 mg) of Δ^9-THC was injected intravenously to the subjects, and furthermore, during a PET scan, the majority of CB_1R-positive forebrain neurons (those regulating motor functions and cognition) are expected to be idle using glucose at baseline level. Glucose uptake in an idle neuronal network is not likely subject to modulation by CB_1R

receptors, questioning the usefulness of a PET scan in this type of research. Returning to the rat model, Pontieri and colleagues (1999) have reported that intravenously injected low doses of the synthetic cannabimimetic, WIN55212-2 modulated 2-DG uptake in selected brain areas of awake rats, and yet failed to affect behaviour. At 0.15 mg/kg, WIN55212-2 elevated 2-DG uptake in the shell of the nucleus accumbens by 23%, which was interestingly not observed at the 0.3 mg/kg dose. This bell-shaped dose-response curve can be interpreted as a possible outcome of the interaction at the network level between CB_1R-positive and -negative neurons. At the 0.3 mg/kg dose, however, WIN55212-2 decreased 2-DG uptake in the range of 19-33% in the ventromedial thalamus and in all subareas of the hippocampus, whereas other brain areas were still unaffected (Pontieri et al., 1999). In contrast to the findings of Margulies and Hammer (1991) and Pontieri and colleagues (1999), Freedland and colleagues (2002) reported that the low (0.25 mg/kg) dose of Δ^9-THC failed to affect 2-DG uptake in the rat brain. They found that only moderate (1.0 - 2.5 mg/kg) doses of Δ^9-THC (*ip*) inhibited dose-dependently 2-DG uptake in the rat brain 15 min after the injection of the tracer. At the highest Δ^9-THC dose tested, most (28 out of 38) brain areas were affected (in the range of -25 – -42%), and all effects were prevented by pre-treatment with the rimonabant. Brain areas of the limbic and sensory systems were affected to the highest extent. The same laboratory also reported that a single *ip* injection of Δ^9-THC (2.5 and 10 mg/kg) caused an inhibition of 2-DG uptake – an effect lasting for hours depending on the brain area (Whitlow et al., 2002).

In conclusion, it is difficult to conclude anything solid from *in vivo* studies. The works listed above certainly carry several limitations: 1) systemic injection with cannabinoid agonists decreases cerebral blood flow (Bloom et al., 1997; Goldman et al., 1975) and concomitantly, the level of available cerebral glucose. 2) Cannabinoids via several target organs and receptors also change systemic levels of glucose and different types of hormones, as well as core body temperature, in other words, systemic energy expenditure, at higher concentrations. 3) Last but not least, cannabinoid ligands may affect behaviour and neurotransmission and consequently neuronal activity. These inconsistencies therefore prompted us to test the effect of CB_1R ligands on brain glucose metabolism *in vitro*, in slice preparations free from systemic influences.

Of note, one interesting feature of the CB_1R is that it decreases both the release of the adenosine precursor, ATP (*e.g.* in the striatum; Ferreira et al., 2015) and it likely physically interacts with the adenosine A_1 (Sousa et al., 2011) and the A_{2A} receptors (Ferreira et al., 2015).

1.5 THE ADENOSINERGIC SYSTEM

Adenosine is a purine ribonucleoside that exists in all cells with the ability to regulate the central nervous system (CNS) in physiological and pathological situations (Cunha, 2008). In the CNS, adenosine acts as neuromodulator and as homeostatic regulator (Cunha, 2001a; de Mendonça and Ribeiro, 2001; Sebastião and Ribeiro, 2000) as will be described in **Section 1.5.3.1**. Furthermore, adenosine is a crucial intermediary metabolite functioning as a building block of nucleic acids and also functioning as part of the biological energy currency that is ATP (Chen et al., 2013). It is present under different forms in the cell and each form has a unique role in the cellular processes (Cunha, 2008). Adenosine is present freely, or bound to high energy phosphate forming AMP, ADP, ATP or cyclic AMP (cAMP) (Cunha, 2001a) .The cellular adenosine levels reflect the cell energy state, e.g., the cell metabolic demand and nutrient supply (Newby et al., 1985).

1.5.1 Generation, metabolism and transport of adenosine

Under normal physiological conditions adenosine is continuously produced in the intra and extracellular space (Cunha, 2005, 2008; Fredholm et al., 2005), and it is estimated that its intra- and extracellular levels are dynamically balanced (Alanko et al., 2006; Boison et al., 2013; Peng et al., 2005). Physiological extracellular adenosine levels in the resting brain are estimated around 25-300 nM (Ballarín et al., 1991; Dunwiddie and Diao, 1994; Rudolphi and Schubert, 1997), depending on the balance of the release and removal of adenosine by equilibrative nucleoside transporters (ENTs) and on the rate of ATP release and conversion into adenosine by ecto-nucleotidases and pyrophosphatases (Dunwiddie et al., 1997; Dunwiddie and Masino, 2001). When an energy imbalance occurs (stressful conditions) the adenosine levels increase, resetting the energy balance and acting as a retaliatory metabolite. Hence, adenosine act also as

an endogenous distress signal (Fredholm, 2007), since it accumulates rapidly in response to acute stressful conditions such as hypoxia (e.g. oxygen deprivation during stroke), ischemia, tissue damage and repair, immune functions of the brain (Cunha, 2008), increased neural activity and under extreme energy consumption (*e.g.* seizures) (Newby, 1991).

1.5.1.1 Extracellular adenosine formation

In theory, all the different cell types of the CNS grant extracellular adenosine. Nevertheless, the source depends upon the stimulus that provoked the release (Haskó et al., 2005). There are three known mechanisms responsible for the appearance of adenosine in the extracellular milieu: 1) adenosine release, as well as extracellular conversion of both; 2) ATP and 3) cAMP. Adenosine release by nucleoside transporters (Geiger and Fyda, 1991) follows a rise of the intracellular levels or a change in the sodium gradient. This mechanism implies that adenosine is released into the extracellular milieu through the brain-type ENTs (ENT1 and ENT2) (Anderson et al., 1996; Baldwin et al., 1999; Thorn and Jarvis, 1996). As for the extracellular conversion by the ectonucleotidase pathway of adenine nucleotides (ATP, ADP and AMP) released from the intracellular milieu, Cunha (1997) described this mechanism as the main source of phasic adenosine levels in the active synapse. Briefly, the breakdown of ATP, released by exocytose (Cunha et al., 1996; Dunwiddie et al., 1997), is called the ecto-nucleotidase pathway and consists of the hydrolyses of ATP into AMP by ATPases and/or by an ATP diphosphohydrolase (CD39) or pyrophosphatases, and the subsequent conversion of AMP into adenosine by an ecto-5'-nucleotidase activity (CD73) (Cunha, 2001b; Zimmermann, 1996). Additionally, adenosine may also be originated from the release of the cyclic AMP (cAMP) (Dunwiddie and Masino, 2001; Latini and Pedata, 2001) via a non-specific energy-dependent transport (Henderson and Strauss, 1991).

Recent studies suggest that, under physiological conditions, the "ATP-adenosine cycle" (adenosine formation from ATP catabolism and *vice versa*) is mainly responsible for the regulation of extracellular adenosine levels in astrocytes (Halassa et al., 2009; Inoue et al., 2010; Pascual et al., 2005). Furthermore, when cells or tissues are

metabolically stressed, the main source of extracellular adenosine is its release from the intracellular milieu (Cunha, 2001a).

1.5.1.2 Intracellular adenosine formation

Intracellular adenosine is formed from the degradation of adenosine monophosphate nucleotides (AMP) by an endo-5'-nucleotidase enzyme (5-ribonucleotide phosphohydrolase) (Phillips and Newsholme, 1979).

The second intracellular pathway (but with lower prominence) to form adenosine is through the hydrolysis of S-adenosyl homocysteine (Broch and Ueland, 1980), a reversible reaction catalyzed by S-adenosyl homocysteine (Hack and Christie, 2003; Reddington and Pusch, 1983).

1.5.1.3 Adenosine fate/clearance

When adenosine is present in the intracellular milieu, adenosine kinase (ADK; ATP: adenosine 5'-phosphotransferase) and adenosine deaminase (ADA) are the enzymes responsible for the removal. When present in low levels, adenosine may be phosphorylated back into AMP by ADK (*i.e.*, adenosine + ATP $\rightarrow$ AMP + ADP). When present in high levels, adenosine may be deaminated into inosine by ADA (Fox and Kelley, 1978). Under physiological conditions, it is estimated that ADK is the main responsible in the regulation of adenosine levels, because the K_m of ADK is $\approx$ 1 mM (De Jong, 1977; Drabikowska et al., 1985) while the K_m of ADA is 25–150 mM (Ford et al., 2000; Singh and Sharma, 2000). Furthermore, intracellular adenosine may also be integrated back in S-adenosyl homocysteine or released to the extracellular space by bi-directional ENTs (Crawford et al., 1998; Yao et al., 2002).

When present in the extracellular milieu, adenosine may be taken up by neurons and astrocytes through ENTs and concentrative nucleotide transporters (CNTs) (Latini and Pedata, 2001). CNTs displays both higher affinity and selectivity for nucleoside substrate then ENTs (Gray et al., 2004).

1.5.2 Adenosine receptors

Extracellular adenosine exerts its effect through four adenosine receptor (AR) subtypes, namely the A_1, A_{2A}, A_{2B} and A_3 adenosine receptors - all of which are commonly expressed in the CNS (Chen et al., 2013). All ARs are metabotropic and members of the superfamily of G protein-coupled-receptors (GPCRs) and classified as P1 receptor according to molecular, biochemical and pharmacological data. However, they show different distribution in the brain, different signal transduction pathways, and different responses to agonists/antagonists. Furthermore, these receptors exhibit different affinities for adenosine, suggesting a divergence in their role: A_1 (EC_{50}, 70 nM - high-affinity), A_{2A} (EC_{50}, 150 nM), A_{2B} (rat EC_{50}, 5100 nM, human EC_{50}, 15000 nM - low affinity), and A_3 (in the rat, EC_{50}, 6500 nM - low-abundance/low affinity, human EC_{50}, 290 nM) adenosine receptors (Dunwiddie and Masino, 2001; Fredholm et al., 2005, 2011). Therefore, the A_1R and A_{2A}R may be activated by adenosine under basal conditions, while for the activation of rat and human A_{2B}Rs, the concentration of adenosine should be way much higher, which is the case under pathological conditions (**Figure 1.3**). ARs are conventionally classified according to their differential coupling to adenylyl cyclase to regulate cAMP levels. So, ARs act firstly through the enzyme adenyl cyclase. This enzyme can be either stimulated or inhibited according to the receptor subtype triggered (van Calker et al., 1979; Londos et al., 1980). The most evident effect of adenosine in neuronal circuits of adult mammals is the selective depression of excitatory transmission (Dunwiddie et al, 1995), conveyed by the activation of A_1Rs and A_3Rs. A_1Rs and A_3Rs are coupled to $G_{i/o}$ and G_{i3}/G_q proteins to inhibit adenyl cyclase and consequently, reduce cAMP levels, resulting in decreased PKA activity and cyclic AMP response element binding protein (CREB) phosphorylation (van Calker et al., 1978; Kull et al., 2000; Londos et al., 1980; Olah, 1997). On the other hand, A_{2A}Rs and A_{2B}Rs are related to facilitatory events. The stimulation of adenyl cyclase, through the coupling to $G_{s/olf}$ proteins respectively, leads to the consequent increase in cAMP levels, PKA activation and CREB phosphorylation (Abbracchio et al., 1995; Akbar et al., 1994; Fredholm et al., 2005; Jockers et al., 1994; Kull et al., 2000; Schulte and Fredholm, 2003).

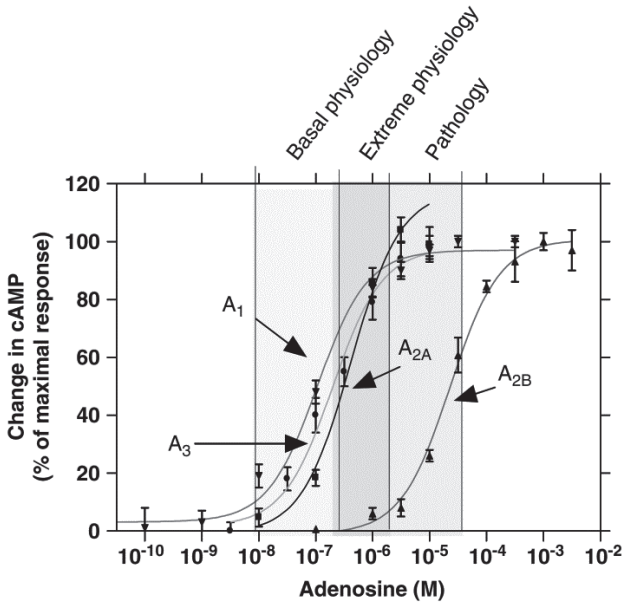

Figure 1.3 – Adenosine has different affinity for its four receptor subtypes. Under the blockade of adenosine transport, the experimental endpoint was the stimulation or inhibition of cAMP formation by human adenosine receptors expressed in Chinese hamster ovary cells. The increasing adenosine levels correspond to those observed under basal and extreme physiological conditions (heavy work, mild hypoxia, etc.) as well as pathophysiological conditions (e.g. severe hypoxia/hypoglycemia or cell lysis) (reproduced from Fredholm, 2007).

1.5.3 The function of adenosine in the CNS

1.5.3.1 Dual role of adenosine in the CNS

Adenosine has a dual role in the nervous system working as a homeostatic regulator and also as a neuromodulator. Adenosine is an important upstream regulator, having a direct role in the fine tuning of the integration between excitatory and inhibitory neurotransmission (Boison, 2008). The duality of adenosine functions are tangled according to the coupling between neural activity and glucose metabolism (Sebastião and Ribeiro, 1996). Adenosine also regulates how neurons process information (Sebastião and Ribeiro, 1996; Wei et al., 2011).

The *homeostatic regulator* role of adenosine occurs as transcellular messenger through paracrine signalling aiming for the coordination of the cells metabolic activity (Cunha, 2001a). Studies showed that this possible role of adenosine occurs through A_1R activation since a similar effect was observed when using A_1R agonists (Boison and Aronica, 2015; Meghji and Newby, 1990).

In parallel, adenosine also behaves as *neuromodulator* by controlling neurotransmitters release and neuronal excitability, and consequently, synaptic plasticity, establishing the balance needed between inhibition and excitation that leads to homeostasis (Cunha, 2001a, 2008; Gonçalves et al., 2015). Adenosine controls neuronal excitability, through cAMP levels and the opening of voltage gate calcium channels and potassium channels, affecting the release of neurotransmitters, including glutamate, γ-aminobutyric acid (GABA), acetylcholine, and dopamine, and consequently modulating synaptic plasticity, neuroinflammation and cell death (Sebastião and Ribeiro, 1996). Furthermore, ARs control the purported basic cellular mechanisms involved in memory formation, such as LTP and LTD in the hippocampus (Costenla et al., 2010). Additionally it enables a mechanism called adenosine-mediated metaplasticity (Dias et al., 2013).

It is commonly accepted that it is the A_1R subtype among ARs that inhibits synaptic transmission in the hippocampus (Gonçalves et al., 2015; Sebastião et al., 1990; Zhang et al., 2015), whereas $A_{2A}R$ activation exhibits opposite effect, since it is expected to increase the excitability of neuronal networks, though further investigations are necessary to better understand the physiological roles of this receptor (Boison, 2008; Cunha, 2001a; Rombo et al., 2015). In the hippocampus, the activation of A_3R modulates synaptic plasticity. Costenla et al., (2001) showed that A_3R activation increases LTP and decreases LTD. Nevertheless A_3R may also be involved in LTP impairment (Maggi et al., 2009).

1.5.4 Adenosine receptors in cognitive function and diseases

Adenosine and its receptors are in the spotlight as therapeutic targets to enhance cognitive functions. It has become clear that the homeostatic regulator and neuromodulator action of adenosine results in the regulation of cognition under normal and also diseases conditions (Chen, 2014).

The impact of adenosine receptors in cognitive functions was first suspected by the psychoactive effects of the caffeine – a non-selective antagonist of adenosine receptors (with affinities for A_1R, $A_{2A}R$ and $A_{2B}R$ in the micromolar order) (Fredholm et al., 2001; Stephenson, 1977). Caffeine is the most widely consumed psychoactive drug in the world (Fredholm et al., 1999) and is related with the enhancement of

alertness and mood, the attenuation of fatigue (Fredholm et al., 1999; Rogers and Dernoncourt, 1998) as well as the improvement of cognition (Ribeiro and Sebastião, 2010). Preclinical studies have shown the ability of caffeine to mitigate impairments in learning and memory, through the antagonism of adenosine receptors (Cunha and Agostinho, 2010; Takahashi et al., 2008). Notably, these are the impairments associated with a wide diversity of conditions such as AD (Arendash et al., 2006; Canas et al., 2009; Li et al., 2015; Orr et al., 2015a), PD (Gevaerd et al., 2001), sporadic dementia (Espinosa et al., 2013a) and neuropsychiatric conditions such as schizophrenia (Rial et al., 2014), attention deficit and hyperactivity disorder (ADHD) (Pandolfo et al., 2013; Prediger et al., 2005c), sleep deprivation (Snel and Lorist, 2011), depression, anxiety, bipolar and panic disorders (Lara, 2010), as well as drug addiction (Lopes et al., 2011). Over the years, human and animal studies were dedicated to the herculean task to pinpoint the role of each AR and brain region to cognition and cognitive disorders. Most of these studies have been focusing on the A_1R and $A_{2A}R$. Curiously, regarding the A_1R, pharmacological studies showed "effect inversion" upon the chronic *vs.* acute administration of A_1R ligands (agonists or antagonists), *i.e.*, they present diametrically opposite effects when administrated chronically and acutely (Jacobson et al., 1996). Pharmacological studies showed that hippocampal A_1Rs influence the impairment of both working (Ohno and Watanabe, 1996) and spatial memories triggered by chronic exposure to opiates (Lu et al., 2010). Nevertheless, studies involving two different A_1R-KO mouse lines did not show alterations in Morris water maze (MWM) tasks performance (Giménez-Llort et al., 2005, 2005; Lang et al., 2003). In fact, the genetic deletion of the A_1R mainly affects emotional behaviour among major behavioural paradigms (Giménez-Llort et al., 2002, 2005; Johansson et al., 2001; Lang et al., 2003).

Regarding the $A_{2A}R$, this receptor is known to contribute to the modulation of learning and memory (Cognato et al., 2010; Cunha and Agostinho, 2010; Li et al., 2015; Orr et al., 2015b; Pagnussat et al., 2015). In animal models of common human neuropsychiatric illnesses, $A_{2A}R$ blockade (*e.g.* by caffeine) has pro-cognitive and neuroprotective roles (Dall'Igna et al., 2007; Prediger et al., 2005a, 2005b, 2005c). Through pharmacological techniques, it was observed that $A_{2A}R$ blockade reversed memory impairment by reestablishing the functioning of glutamatergic synapses (Batalha et al., 2013; Canas et al., 2009; Duarte et al., 2009b; Rebola et al., 2003b). Furthermore, the ability of astrocytic $A_{2A}Rs$ to physically complex with and inhibit the

α2 isoform of Na^+/K^+-ATPases (Matos et al., 2012) provides a molecular basis for the metabolic and pro-cognitive effects of caffeine and other more selective $A_{2A}R$ antagonists. Indeed, as we discussed above, the activity of this pump is crucial for glucose and lactate transport across the astrocytic membrane (Gladden, 2004) to link neuronal activity with energy metabolism.

Regarding the $A_{2B}Rs$, most of the studies have been carried out outside the brain; therefore, little is known about the role of these receptors in the CNS. In the brain, the $A_{2B}R$ has a widespread distribution but low expression levels (Dixon et al., 1996). $A_{2B}Rs$ have been previously documented in the hippocampus (among other structures) of rodents (Dixon et al., 1996; Zhou et al., 2004) and humans (Perez-Buira et al., 2007). At the cellular level, this receptor is present mainly in astrocytes, but is also present in neurons (Allaman et al., 2003; Fredholm et al., 2005). $A_{2B}Rs$ can also couple with G_q, which regulates Ca^{2+} signalling and vesicular release in astrocytes (Jiménez et al., 1999; Peakman and Hill, 1994; Pilitsis and Kimelberg, 1998). Furthermore, $A_{2B}R$ activation is associated with the release of leukemia inhibitory factor (Moidunny et al., 2012) and glial cell line-derived neurotrophic factor (Yamagata et al., 2007) from astrocytes. Additionally, the $A_{2B}R$ knockout (KO) mice may present increased body weight, decreased insulin sensitivity and worse glucose clearance when compared to WT littermates (Peleli et al., 2015)

As for the A_3R, this receptor is related with neuroprotection, involving both neurons and glial cells, when the A_3R-selective agonist, IB-MECA is given chronically (Von Lubitz et al., 1999). Once again, an inversion of effect was seen by the acute administration of IB-MECA, which increased neuronal damage and mortality following ischemia (Von Lubitz et al., 1994). Moreover, studies propose that A_3R related neuroprotection might also result from its modulation of the immune system of the brain (Borea et al., 2009; Daré et al., 2007; Haskó et al., 2005)

1.6 OBJECTIVES

A major hallmark of neurological and psychiatric disorders is a region-specific dysmetabolism of glucose, which often precedes other symptoms by years, and thus bears diagnostic value. If we could understand what signalling systems are responsible for cerebral glucose homeostasis we might be able to identify novel pathomechanisms for brain diseases. Glucose is the principal source of energy for the brain cells, and impaired energy production may render them more susceptible to misfolded proteins, excitotoxicity or pathogens. Consequently, impaired glucose metabolism may not only be a passive consequence of disease onset but it may actively contribute to disease progression. If so, newly identified glucoregulator signals may offer therapeutic potential to mitigate the outcome or even halt disease progression.

Insulin is a widely known stimulator of peripheral glucose uptake. Does insulin exert similar roles in the brain? The release of adenosine and endocannabinoids are associated with neural activity, which is fuelled by glucose. Do these neuromodulators act as feed-forward signals onto glucose uptake? In the following studies, we aimed to probe the role of these neuromodulators – insulin, cannabinoids and adenosine – in the physiology of cerebral glucose metabolism *in vitro*. Since these neuromodulators are affected in systemic and cerebral illnesses involving glucose dysmetabolism, we were interested in the neurophysiological and behavioural consequences of metabolic modifications.

Our specific aims are the following:

-The characterization of *in vitro* and *ex vivo* glucose uptake and metabolism in neuronal and astrocytic cultures as well as in brain slices, with regard to absolute values, spatiotemporal kinetics, sensitivity to neuromodulators and metabolic disorders.

-The exploration of the consequences of type-1 and type-3 diabetes as well as pre-diabetes of type-2 (that is, metabolic syndrome) on cerebral metabolism, synaptic plasticity as well as behaviour including short- and long-term memory, in rodent models. Additionally, we aimed at investigating as much as possible the involvement of the above neuromodulators in the observed impairments in any of the outcomes. We hope that by identifying one or more neuromodulator receptors, we can pave the way toward novel therapeutic strategies to mitigate the outcome of certain brain diseases.

Chapter 2

Material and Methods

2 MATERIAL AND METHODS

2.1 ANIMALS AND TREATMENTS

2.1.1 Animals

All studies were conducted according to the principles and procedures outlined in the EU directive (2010/63/EU) for the care and use of laboratory animals and by the Reporting Guidelines Working Group (2010). Every procedure was performed in laboratory rodents and was approved by the local Animal Care Committee of the University (License Number 025781) and Portuguese Ministry of Agriculture. All animal studies were carried out according to the guidelines of "3Rs" (replacement, reduction, refinement) in the guidelines of EU (86/609/EEC) and FELASA. Particular care was taken to minimize both animal suffering and the animal number used in each study.

All the animals were housed in a conventional animal facility under controlled temperature (23 ± 2 ºC), with a scheduled 12 h dark/light cycles and *ad libitum* access to water and food. To perform the *in vitro* and *ex vivo* studies, the animals were deeply anesthetized with 2-bromo-2-chloro-1,1,1-trifluoroethane (halothane) or 2-chloro-2-(difluoromethoxy)-1,1,1-trifluoro-ethan (isoflurane), both at 0.015% v/v in air. The animals did not react to handling or tail pinch while still breathing, before decapitation.

Most studies were carried out or treatments were initiated in adult male Wistar rats (7-12 weeks old) and C57/BL6 mice (10-12 weeks old) from Charles Rivers (Barcelona, Spain), except where noted. Adenosine A_{2B} receptor global null-mutant (knockout, KO) animals (A_{2B}R KO; Belikoff et al., 2011) were kindly donated by Drs Akio Ohta and Michael Sitkovsky (New England Inflammation and Tissue Protection Institute, Northeastern University, Boston, MA, USA). The procedures involving A_{2B}R KO animals were performed with 10 to 12 weeks old animals. CB_1R KO male mice (Ledent et al., 1999) and their wild-type littermates on CD-1 background were raised at the laboratory of Dr. Catherine Ledent (IRIBHM, Université Libre de Bruxelles, Brussels B-1070), and genotyped from the tail before shipping. The mice arrived with 6 weeks of age and were kept at the animal facility until use, at least for a week.

2.1.2 Intraperitoneal STZ administration – animal models of type-1 diabetes

The experimental model of T1D was induced with 2-deoxy-2-(3-(methyl-3-nitrosoureido)-D-glucopyranose (streptozotocin or STZ) (Calbiochem, Merck Biosciences, Germany) – a broad-spectrum antibiotic with oncolytic, oncogenic, and diabetogenic properties (Rossini et al., 1977). STZ induces diabetes within 3 days. STZ is taken up by the glucose transporter GLUT 2, particularly abundant in pancreatic β-cells (Junod et al. 1969), causing the destruction of those cells (Akbarzadeh et al., 2007; Rees and Alcolado, 2005; Szkudelski, 2001). Rats were treated with STZ as follows: after four hours of food deprivation, an STZ dose of 60 mg/kg (prepared in 10 mM citrate buffer, pH 4.5) was administered by intraperitoneal (ip) injection. CD-1 mice were rendered diabetic following published protocol for CD-1 mice (Ventura-Sobrevilla et al., 2011). In short, nonfasted CD-1 mice were injected five times in five consecutive days with 40 mg/kg STZ dissolved in the above citrate buffer – each mouse receiving 100 μL/10 g body weight of STZ solution. Control rats and mice were injected with the vehicle and maintained in the same conditions as the treated ones. The studies with this experimental model of T1D are presented in **Section 3.2** of this thesis.

Blood glucose levels were monitored through the glucose oxidase method from tail vein blood, using a glucometer and reactive test stripes (Elite-Bayer SA, Portugal). For rats, this test was performed both before and three days after the injection as well as on the last day. The glycemia of the mice was measured both before and 2 weeks after the first injection, and repeated five times more thereafter. The first post-injection blood glucose analysis revealed that almost all STZ-injected animals became diabetic, as they had at least 3 g/L blood glucose. All mice and all but one rats became hyperglycaemic.

2.1.3 Intracerebroventricular STZ administration – a sporadic Alzheimer's disease (AD) model

The experimental model of AD employed here is described as a model of type-3 diabetes. This model enables us to recapitulate many features of sporadic AD (de la Monte and Wands, 2008). The studies with this model are presented in **Section 3.3** of this thesis. The animals were anaesthetised with an ip injection of a mixture composed of 90 mg/kg ketamine (Bayer Healthcare) and 10 mg/kg of xylazine (Rompun, Bayer

Healthcare) and supplemented throughout the surgical procedure as necessary. The animals were immobilized in a stereotaxic frame (Stoelting, US). A single bilateral intracerebroventricular (icv) injection was performed with the administration of a STZ solution, 3 mg/kg (in 0.05 mM citrate buffer, pH 4.5), 5 µL per ventricle (Espinosa et al., 2013a; Ponce-Lopez et al., 2011; Tiwari et al., 2009) using a 0.5 mL Hamilton syringe at a rate of 0.5 µL/min. The coordinates for the stereotaxic administration were -0.8 mm anterio-posterior to Bregma, and + and - 1.5 mm lateral to sagital suture, as well as -4.5 mm deep at the dorsoventral axis from the skull surface, according to Paxinos e Watson (2004). The same procedure was applied to the control rats to inject the same volume of vehicle icv.

2.1.4 High sucrose diet – a prediabetic animal model

The animals were treated for 9 weeks with a diet rich in sucrose consisting in a drinking solution of sucrose 35% (S0389; Sigma–Aldrich) and water for the control animals. Food and beverage consumption as well as body weight were monitored for both groups. These studies with this animal model are presented in **Section 3.4** of this thesis.

2.2 *IN VIVO* STUDIES

2.2.1 Behaviour protocols

The different batteries of behavioural tests were designed according to the literature and our previous experience and publications. The tests were organized in a gradient of awareness to conduct the most stressful tasks last. The sequence of testing and intervals between tests were chosen specifically for the purpose of each study to minimize the interference between the tests (McIlwain et al., 2001; Paylor et al., 2006).

All rat behavioural tests were performed during the night phase of the circadian cycle (between 8:30 PM to 3:00 AM), while the mouse behaviour assays were performed during the light phase of the cycle (between 8:30 AM to 2:00 PM), all under red/low light (DeFries et al., 1966).

Between each trial, the apparatus were cleaned with a 10% ethanol solution (except the water maze) to avoid odour cues. At the end of the training trial, the animals were removed from the mazes and kept in an individual cage in an adjacent room during the intertrial intervals.

All the experimental data was collected and analyzed with the help of the ANY-maze® video tracking system (Stoelting, US).

The behavioural experiments described next were the ones used to derive the results presented in **Sections 3.3.1**, **3.4.2** and **3.5.1**.

2.2.2 Open field test

The rat spontaneous locomotor activity was accessed in an open field arena of dimensions 100 × 100 × 90.cm. The exploratory behaviour of the animals was evaluated over a 5 min period, by counting the total distance travelled. This test also allowed screening for anxiety-like behaviour through the analysis of the time spent in the centre of the maze *vs.* the periphery (Matheus et al., 2015). The open field test protocol for rats was applied to obtain the results shown in **Sections 3.3.1** and **3.4.2**.

2.2.3 Object displacement test

The object displacement test (ODT) was designed to assess long term spatial recognition memory (Broadbent et al., 2004; Lee et al., 2005; Murai et al., 2007). The test was adapted from a previous protocol (Griffin et al., 2009a) and consisted of 3 phases: habituation, sample and test phases, all carried out sequentially with a 24 h interval after one another. In the habituation phase, the animals were placed in the centre of an open field apparatus (100 × 100 × 90 cm) and allowed to explore for 5 min. The sample phase consisted of 3 trials (with 5 min inter-trial interval) where the rats were placed in the same open field arena containing 2 objects and were allowed to explore the arena for 5 min in each trial. In the test phase, one of the same two objects was re-arranged in a different spatial combination and the rats were allowed again to explore the arena during 5 min. The spatial memory is determined by the localization index, corresponding to the ratio of the time spent exploring the displaced object (τ_{novel}) and the time spent with sniffing/exploring (*i.e.* being physically within 1 cm distance of

all objects, including the objects in the familiar location - $\tau_{familiar}$), was calculated using the following equation ($\tau_{novel} \times 100$) / ($\tau_{novel} + \tau_{familiar}$) (Assini et al., 2009). The exploration time was recorded using a stopwatch. Results obtained using this method are presented in **Section 3.4.2** and displayed in **Figure 3.26A**.

2.2.4 Novel object recognition test

The novel object recognition test (NORT) is based on the spontaneous tendency of rodents to spend more time exploring a novel object than a familiar one (Akkerman et al., 2012; Antunes and Biala, 2012a; Ennaceur et al., 2005). The NORT is composed of a sample and a test phase. The sample phase consists of placing the rats in the open field arena (100 × 100 × 90 cm) with 2 similar (familiar) objects (but different from the ones used in the object displacement) for 5 min. The test was performed after an inter trial interval of 90 min, with one object replaced by a new one and the rat was allowed to explore the objects for 5 min. The test phase was performed after 90 min, where one of the objects was replaced by an object with a different shape (novel), which the rats explored again for 5 min, as previously described (Espinosa et al., 2013). The results were analysed as follows and expressed as a recognition index (RI) = ($\tau_{novel} - \tau_{familiar}$) / ($\tau_{novel} + \tau_{familiar}$) where $\tau_{familiar}$ is the time spent with the familiar object and T_{novel} is the time spent with the novel object (Antunes and Biala, 2012a). The exploration time was recorded using a stopwatch. This method was used to obtain the results presented in **Sections 3.3.1** and **3.4.2,** and displayed in **Figure 3.20B** and **Figure 3.26B.**

2.2.5 Forced swimming test

Helpless behaviour – a measure of depression-like phenotype - was evaluated in a forced swimming test (FST), scoring the total duration of immobility during a 5 min test session in glass cylinders containing water, as previously described (Matheus et al., 2015) and adapted from (Porsolt et al., 1977).

Briefly, the animals were placed individually in 50 cm tall plastic swimming cylinders of 20 cm diameter, filled with prewarmed (24±1°C) tap water up to 30 cm of height for 15 min (pre-test). Twenty-four hours after the pre-test, the animals were

submitted to a session of 5-min forced swim (test session), which was recorded for the subsequent evaluation of the immobility time. Small movements required for floating was permitted during the immobility phase. Between two animals, the cylinder was cleaned properly and the water was changed. After each session (pre-test and test), the animals were removed and subjected to drying with clean and dry cloths in a separate box before returning to their home cages. During the test phase, the time the animal spent immobile (floating motionless) was manually scored by a trained observer. Decrease in immobility time is an indicator of a reduced helpless behaviour. This method was used to obtain the results presented in **Section 3.4.2** and displayed in **Figure 3.26D**.

2.2.6 Morris water maze test

The Morris water maze (MWM) consists of a circular swimming pool of the following dimensions: 1.7 m in diameter and 0.8 m in height, and containing 25 °C tap water of 60 cm depth. Inside the water, a target Plexiglas platform of the size of 10 × 10 cm was hidden 1.5 cm beneath the water surface. There were also 4 marked starting points on the inner wall of the pool, and also, there were distant visual cues on the walls. The training session consisted of 4 consecutive trials in which the animals were placed in the maze starting from the four cardinal positions (North, South, East and West) and then were allowed to freely swim for 60 s or until finding the submerged platform. If they failed to find the platform within this period, they were gently guided to it. The animals were allowed to remain on the platform for 10 s after escape and were removed from the tank for 30 s before being placed at the next starting point to re-start their searching for the platform. This procedure was repeated for 4 consecutive days. The test session was carried out 24 h later and consisted of a single probe trial where the platform was removed from the maze and each rat was allowed to swim for 60 s. The time spent in the correct quadrant of the removed platform and the number of crossings of the original place of the platform counted in the analysis (Soares et al., 2013). All trials were video-recorded to accurately score the latency of escape from the starting point to the platform and swimming pathway, using an image analyser (ANY-maze®, Stoelting, US).

This method was used to obtain the results presented in **Section 3.3.1** and displayed in **Figure 3.21** and **Figure** 3.22.

2.2.7 Elevated plus-maze test

The elevated plus-maze test (EPM) is an ethological test that was developed to evaluate anxiety-like behaviour (Walf and Frye, 2007) and to screen for anxioselective effects of drugs (Dawson and Tricklebank, 1995; Lister, 1987). The time the animal spends in the unprotected open arms is an experimental index of anxiety like behaviour (Walf and Frye, 2007).

An EPM apparatus suitable for mice was made of wood and covered with impermeable Formica. Elevated 60 cm above the floor, it was composed of four arms of 18 cm in length and 6 cm in width. Two opposite arms do not have walls at the sides or at the end, and these are called open arms where the mice can feel the cliff. The other two arms are enclosed by walls of 6 cm height and thus are termed as closed arms. The four arms are radially connected to a 6 × 6 cm platform called the centre of the EPM. At the beginning of the experiment, the mice were placed in the centre facing a closed arm and were allowed to explore the apparatus for 5 min (Gonçalves et al., 2015). This method was used to obtain the results presented in **Section 3.5.1** and displayed in **Figure 3.31**.

The EPM test paradigm relies on the animal tendency for thigmotaxis and to avoid threatening situations (such as the open area and the height of the runway) *vs*. the animal tendency to explore novel environments (Walf and Frye, 2007).

2.2.8 Y-maze: spontaneous alternation protocol test

The Y-maze is a gross test to assess working memory (Lalonde, 2002; Myhrer, 2003). This test relies on the innate preference of rodents to explore new environments, *i.e.*, if there is memory formation, the animal will investigate a new arm instead of returning to the previously investigated one.

The apparatus consists of three equal arms of 20 cm in length, 15 cm in height and 6 cm in width). The mice were placed at the end of one arm and were allowed to freely explore the maze for 5 min. The number of alternations, *i.e.*, consecutive entries in all

three arms, were quantified as previously described (Dall'Igna et al., 2007). This method was used to obtain the results presented in **Section 3.5.1** and displayed **in Figure 3.30**.

2.3 *IN VITRO*/*EX VIVO* STUDIES

2.3.1 Kinetics of the uptake and metabolism of radiolabelled glucose analogues

2.3.1.1 Recovery period

These methods correspond to the results presented under **Section 3.1**. Right after cutting 400 μm-thick transversal hippocampal and coronal frontocortical slices of the rat brain with the help of a McIllvain tissue chopper (the Mickle Laboratory Engineering Co. Ltd), the slices were collected in a 50 mL pregassed (5% CO_2, 95% O_2) and preheated (37ºC) bath. Each chamber contained six submerged baskets, which are 15 mm tall and 10 mm wide, and have a 80 μm nylon mesh bottom. This setup allows freely moving or batch incubating slices from up to 6 animals at the same time. Usually the baskets were not fully occupied to avoid the putative accumulation of biomolecules in the bath during the usually 90 min assay. Hence, normally we used ~5 mg protein in a 50 mL bath), allowing slices from 3 rats or 4 mice to be incubated simultaneously.

In the first steps of optimization, the recovery of glucose uptake and metabolism were tested every 15 min. Thus, starting from zero min (*i.e.* right after the slice preparation, then at min 15, 30… till 135 min after slice preparation), 3 randomly chosen hippocampal and 2 cortical slices (~0.5-0.7 mg protein) were transferred to another chamber containing 50 mL assay medium supplied with 2-^{3}H(N)-deoxy-D-glucose (^{3}HDG; 1 nM; specific activity; 60 Ci/ mM; American Radiolabeled Chemicals [ARC], USA) and $^{14}C_6$-glucose (50 nM; 360 mCi/mM; Perkin Elmer, USA). The idea behind this is that ^{3}HDG is a glucose analogue generally thought to represent only the net uptake process, as once it enters the cell it stays phosphorylated. On the contrary, $^{14}C_6$-glucose is subject to metabolism, thus a difference between the final ^{3}H and the ^{14}C

contents in the same slice may give a hint about the metabolic activity that affects glucose in the slices. The slices were left to incubate for 15 min, and replaced with new slices for additional 15 min. The incubated slices were washed 4-times in large quantities of ice-cold Krebs solution, transferred to polypropylene 2 mL Eppendorf tubes (that have conic bottom allowing the removal of excess liquid with a pipette without hurting the slices), and dissolved in 1 mL NaOH (0.5 M). Non-specific labels were also measured as detailed in **Section 2.3.1.3**.

2.3.1.2 The steady-state period

As soon as it was established that 60 min resting was sufficient for the slices to reach steady-state ^{14}C-loss from $^{14}C_6$-glucose (see **Section 3.1.1**), the uptake kinetics of $^{14}C_6$-glucose alone or in combination with ^{3}HDG (1 nM) or ^{3}H-3-O-methyl-D-glucose (^{3}HMG; 1 nM; 60 Ci/mM; ARC, USA) in the metabolically recovered slices was tested. The idea of involving the non-metabolizable analogue ^{3}HMG in the study was that it is hardly or not at all phosphorylated once intracellular (Randle and Morgan, 1964; Rodríguez-Enríquez et al., 2009), contrasting with ^{3}HDG which is phosphorylated. Accordingly, after 60 min of recovery, the medium was supplied with radiolabelled glucose analogues for maximum 60 min. We did not surpass 60 min because it was previously published that in the brain, DG uptake remains fairly linear within 45-60 min (Schmidt et al., 1989). We also did not believe that hours-long uptake periods would be relevant for the study of dynamic glucoregulation in the brain. Three cortical and 5 hippocampal slices were then removed after 15, 30, 45 and finally, 60 min of incubation, and washed and dissolved as detailed above. Non-specific labels were also measured as detailed in **Section 2.3.1.3**.

2.3.1.3 The bulk assay in brain slices

As detailed under **Section 2.3.1.1**, we observed that the best experimental layout is to incubate the slices with ^{3}HDG (with or without $^{14}C_6$-glucose) for the period of 30 min. This became a major neurochemical approach that was used to study *in vitro* glucose uptake and metabolism in slices and with some modifications, in cell cultures.

At the end of the total 90 min period of incubation that was the sum of the 60 min recovery and the 30 min uptake assay, the slices were washed and dissolved in NaOH as stated above. Each time, a few slices were kept in ice-cold assay solution but otherwise treated in the same manner as the slices in the main experiment. Slices on ice do not transport glucose across their membranes, and thus they only accumulate residual radioactivity, representing external (non-specific) labelling. The nonspecific value for the different radioligands varied among ~8-15 nmol/mg protein, independently of the species used.

2.3.1.4 Calculations for glucose uptake and metabolism

After administering the radioactive glucose analogues and allowing their dispersion, 181.8 µL of bath of each chamber was sampled and assayed for ^{14}C and ^{3}H counts. 181.8 µL volume of Krebs solution contains 1 µmol amount of glucose molecules if the total D-glucose concentration is 5.5 mM. Hence, the ^{3}H counts (X) and the ^{14}C counts (Y) of a 181.8 µL volume both can be associated with 1 micromol D-glucose quantity. Upon completion of the assays, the slices were washed gently but extensively and sequentially in 4 bathes of ice-cold Krebs solution. Then the slices were transferred to 2 mL Eppendorf tubes and dissolved in 1 mL NaOH (0.5 M). 800 µL of these samples were counted for the ^{3}H (χ) and ^{14}C (υ) by a dual-label protocol with the help of a 2900TR Tricarb β-counter (PerkinElmer). The χ/X and the υ/Y ratios revealed the ^{3}H and the ^{14}C contents of the slices, which we then normalized to protein (see end of this section). After subtracting the nonspecific "uptake" or more likely, external binding of ^{3}H and ^{14}C labels measured on ice (normally varying between 8 and 15 nmol/mg protein) we obtained the net glucose uptake value, based on the ^{3}HDG uptake.

^{14}C can readily leave the slice once metabolized from the parent molecule $^{14}C_6$-D-glucose. The loss of glucose-derived carbon atoms can be simply calculate based on the difference between total glucose uptake measured with ^{3}HDG and with ^{14}C-glucose, which is to be multiplied by 6 - the number of carbon atoms to be oxidized: dissipative glucose metabolism $\approx 6 \times (\chi/X - \upsilon/Y)$ where the values in the parenthesis are already the specific uptake values. This approximation is a robust estimation of glucose-derived carbon atom dissipation. This method slightly underestimates the actual metabolic

activity, meaning that once metabolized, not all glucose-derived carbon atoms would leave the slice.

Protein amounts were determined from the remaining 200 µL by the bicinchoninic acid assay (BCA, Smith-assay) method (Smith et al., 1985). It is not necessary to prepare fresh bovine serum albumin (BSA) standards each time, as they can be prepared as 0.25, 0.5… up to 6 mg/ mL concentration in milliQ water, and kept at 4ºC during weeks without losing activity. However, the day-to-day samples were prepared in 0.5 M NaOH, which substantially alters the colour of the BCA product. One alternative could be the preparation of the BSA standards also in 0.5 M NaOH, but the biological samples slowly lose their protein content in NaOH. This NaOH-mediated degradation of protein content is notable already after an overnight incubation. Instead, it was only used 25 µL of BSA standards made in H_2O MQ, in duplicate, which were freshly mixed with 25 µL of NaOH (1 M) in the wells. These standards were paralleled with 50 µL of fresh brain slice samples in 0.5 M NaOH, after a short, 20 min heating at 70 ºC.

2.3.1.5 Fluorescent glucose uptake in hippocampal slices

Experiments were essentially the same as for radioactive glucose uptake, but with 300 µm-thick hippocampal slices so that they remain translucid enough for fluorescent microscopy. Experiments were performed essentially in two different modes: 1) batch endpoint incubation and later assessment under the microscope; and 2) realtime monitoring of fluorescent glucose uptake.

For the batch endpoint assay, slices were divided in thee chambers, and left to recover at 37ºC under gentle gassing with CO_2 (5%) and O_2 (95%). At min 50 of the recovery period, AM251 (500 nM) was added to one chamber, and at min 55 of the recovery period, WIN55212-2 (500 nM) or their vehicle DMSO were bath applied for the rest of the chambers, and 5 min later, 6-(N-(7-nitrobenz-2-oxa-1,3-diazol-4-yl)amino)-6-deoxyglucose (6-NBDG) was added to the bath with the final concentration optimized to 30 µM/L, and then the system was protected from light. Half an hour later, the slices were removed and gently washed in ice-cold Krebs solution. Three slices from each treatment/animal were photographed using a 5× Fluar-objective (NA 0,25, Axiovert 200M microscope, Carl Zeiss, Germany) and band-pass filters for excitation (BP470/40) and emission (BP525/50), with identical parameters for each set of the

slices from one animal. The time of exposure of the digital camera (Axiocam HRm, Carl Zeiss, Germany) was set to avoid pixel saturation. The intensity scale embraced the scale of 2^0-2^{14} arbitrary intensity units. Average pixel intensities inside the contour of the slice or occasionally, in quadrants of hippocampus subregions were measured with ImageJ (NIH, USA), and averaged as 3 slices/treatment/animal. Representative control and treatment images were transferred to Jasc Paintshop Pro and their intensity was diminished until one of the slices lost its signal, revealing the subregions affected by the treatment described in **Section 3.1.2.2**.

For the real-time fluorescent measurement of deoxyglucose uptake study, the brains were mounted on an iron block in ice-cold Krebs solution, and 300 μm-thick coronal slices at the level of the dorsal hippocampi were cut with a Vibratome (Leica, Germany). After recovering for one hour at room temperature (under continuous gassing 95% O_2 and 5% CO_2) the slices containing the hippocampus were mounted in the center of 16 mm coverslips attached to an RC-20 superfusion chamber (specific for fluorescence microscopy) supported by PH3 platform (Warner Instruments, Harvard, UK) placed in an inverted Axiovert 200M fluorescence microscope (Carl Zeiss, Germany) coupled to a Lambda DG-4 integrated 175 Watt light source and wavelength switching excitation system and a 5× Plan Neofluar objective (Sutter Instrument Company, Novato, CA, USA). The data were band-pass filtered for excitation (470/40) and emission (525/50) and a photography of the slice was taken every 30 s over 30 min. A closed superfusion circuit (rate of 0.5 mL/min) was established comprising a reservoir (containing Krebs solution under continuous gassing) where the drugs were bath applied throughout the study.

With this setup we firstly tested the two fluorescent probes 6-NBDG and 2-NBDG (30 μM) for their suitability (See results **Section 3.5.1**, **Figure 3.32**) and decided to perform this work with 2-NBDG. All the results that lead to the optimization of this protocol are presented under **Section 3.5.1**. At a glance, the experiment started with the record of the baseline during 3 min, consisting in the record of 6 images to measure the auto-fluorescence of the slice. Then, continuously, the fluorescent glucose analogue (2/6-NBDG; 30 μM) tracer was batch applied to the reservoir of the closed superfusion circuit and the signal recorded for 30 min to determine the linearity of the curve. As within 10 min, the increase of 2/6-NBDG signal reached linearity, a 10-min period was

selected to calculate the prediction curve and determined that the drug would only be applied following the first 10 min of 2/6-NBDG application. This technique allows the real-time monitorization of the glucose probe uptake, crucial to analyse the causal mechanisms for glucose uptake and the associated cellular functions in mammalian cells (Yamada et al., 2007).

Once this method was optimized, we moved to the pharmacological study of the A_{2B} receptor. After recording 6 images for auto-fluorescence (to establish the baseline), 2-(N-(7-nitrobenz-2-oxa-1,3-diazol-4-yl)amino)-2-deoxyglucose (2-NBDG; 30 μM) was applied through the reservoir of the closed superfusion circuit. Since within 10 min, the increase of 2-NBDG signal reached linearity (see results **Section 3.5.1**., **Figure 3.32**), we recorded a 10-min predrug period 10 min after the application of 2-NBDG. At min 20, the slices were challenged with BAY606583 (300 nM) or its vehicle, DMSO (0.1% v/v), and another 10-min period was recorded at every 30 sec. To antagonize A_{2B}R, MRS1754 (200 nM) was applied 3-min before 2-NBDG. All measurements were obtained in duplicate from each animal.

2.3.1.6 $^{14}C_6$-glucose incorporation into glycogen

Experiments were essentially similar to the radioactive glucose uptake assays. Rat or mouse brain slices were treated with adenosine A_{2B}R or cannabinoid CB_1R antagonists during the recovery period according to the study. Upon completion of the 60 min period, $^{14}C_6$-glucose (1 μM) and ^{3}HDG (or in some cases, ^{3}HMG) (2 nM) were added to the maximum three chambers used for 1 animal (to increase protein content per chamber and thus sensitivity) for 30 min, with continuous carboxygenation at 37ºC. From each chamber, 181.8 μL medium was assayed for ^{14}C and ^{3}H counts to determine the radioactivity representing 1 μmole glucose molecules (radioactive and cold). The popular sodium-sulfate procedure for glycogen extraction was performed with slight modifications (Lemos et al, 2012) to the original protocol (Glock, 1936; van Handel, 1965: After the uptake process, the slices were dissolved in 2 mL of NaOH (0.5 M) at 70ºC during 30 min. Then, 100 μL of the dissolved slices was removed to determine protein quantity and ^{14}C and ^{3}H content. The rest of the material received 1 mL 6 % (w/v) Na_2SO_4 at room temperature and then, salts together with glycogen were

precipitated with 7 mL absolute ethanol, and left overnight at 4ºC. Then, the precipitate was centrifuged down at 5600 rpm for 15 min, washed with ethanol again and centrifuged, and the final pellet was dissolved in 1.5 mL distilled water. Both supernatants and the pellet were counted for ^{3}H and ^{14}C. The presence of ^{3}HDG or ^{3}HMG served as an internal control for the purity of the pellet (see **Figure 3.7A**). Data were expressed as both relative and absolute values. Those results are presented in **Sections 3.1.2.2 and 3.5.5**.

2.3.1.7 Cell culture preparation

Neuronal and astrocyte primary cultures were prepared from the neocortex and hippocampi of E18 male and female C57Bl/6 mouse embryos as described before (Matos et al., 2012; Resende et al., 2007). The procedure started with the digestion of the neocortex with 0.125% trypsin (type II-S, from porcine pancreas, Sigma-Aldrich Portugal) for 15 min and 50 µg/mL DNAse (Sigma-Aldrich) in Hank's balanced salt solution without calcium and magnesium (in mM: NaCl 137, KCl 5.36, KH_2PO_4 0.44, $NaHCO_3$ 4.16, Na_2HPO_4 0.34, D-glucose 5, pH 7.2).

After dissociation, astrocytes were grown in plastic Petri dishes (p100) for 14 days in Dulbecco's modified Eagle's medium (DMEM) supplemented with 10% fetal bovine serum, 50 U/mL penicillin (Sigma-Aldrich) and 50 µg/mL streptomycin (Sigma-Aldrich), at 37ºC in an atmosphere of 95%/5% air/CO_2. Half of the medium was replaced after 7 days in culture. The cells were then trypsinized and plated at a cell density of 150,000/cm^2 onto 24-well culture plates, which were previously coated with poly-D-lysine (100 µg/mL, Sigma-Aldrich) and laminin (10 µg/mL, Sigma-Aldrich).

Neuronal cultures were plated at a cell density of 150,000/cm^2 onto 24-well culture plates coated with Poly-D-lysine and laminin, in DMEM supplemented with 10% fetal bovine serum, 50 U/mL penicillin and 50 µg/mL streptomycin. Past 2 h, this medium was replaced with Neurobasal medium supplemented with 2% B27 (GIBCO, Life Technologies), 50 U/mL penicillin, 50 µg/mL streptomycin and 2 mM glutamine (Sigma-Aldrich) and incubated at 37ºC in a 95%/5 % air/CO_2 atmosphere. This medium was replaced (at 40%) every 4 days through the 14 days of the culture growth (37ºC in an atmosphere of 95%/5% air/CO_2). See results, **Section 3.5.3.**

2.3.1.8 ^{3}H-deoxyglucose uptake in neocortical neuron and astrocyte cultures

The cultures were used after 15 days *in vitro*. To perform the experiment, the culture medium was washed twice with Krebs-HEPES, and replaced with 250 µL Krebs-HEPES assay solution (pH 7.4 at 37ºC) containing either the $A_{2B}R$ antagonist, MRS1754 (200 nM) or its vehicle DMSO (0.1%).

The cultures were then incubated for 60 min at 37ºC, and then either the $A_{2B}R$ agonist, BAY656083 (300 nM final concentration) or its vehicle, DMSO together with ^{3}HDG (16.6 nM final concentration) were pipetted gently in the wells in a volume of 250 µL. In 4 wells/plate, the glucose transporter inhibitor, cytochalasin B (CyB; final concentration 10 µM) was also tested – see below.

This incubation was performed for 20 min at 37ºC and then placed into ice to stop the reaction. The exact ^{3}HDG concentration was determined with aliquots of 181.8 µL in each well. The cells were then washed carefully 3 times with 0.5 mL ice-cold Krebs-HEPES and dissolved in 300 µL NaOH (0.5 M).

This protocol was validated by measuring the glucose uptake in the presence of cytochalasin B (CyB; 10 µM), which inhibits some glucose transporters, including GLUT1, in astrocytes (Barros et al., 2009; Klip and Pâquet, 1990. CyB largely inhibited the uptake of glucose in astrocytes ($n = 5$, $P < 0.001$ *vs*. DMSO control; **Figure 3.34)** and as expected, CyB had a much smaller but still significant effect on neuronal glucose transport ($n = 4$, $P < 0.05$; Figure 31), which indicates a gain-of-function for GLUT1 in neuronal culture (Simpson et al., 2007). See results, **Section 3.5.3**.

2.3.2 Measurement of Na^{+}/K^{+}-ATPase activity in rat hippocampal membranes

This assay was optimized following previous studies (Araya et al., 2007; Sarkar, 2002). Pairs of hippocampi of four rats were dissected and homogenized in ice-cold sucrose (0.32 M)-HEPES (10 mM) solution containing protease inhibitor (2 µL/mL, Sigma-Aldrich), then centrifuged for 15 min at 1000 g at 4 ºC. The supernatant was then centrifuged for 15 min at 14000 g. The pellet of the first centrifugation was also resuspended in sucrose solution containing protease-inhibitors, and then pelleted again at 1000 g. The two supernatants were resuspended and pelleted at 14000 g during 15 min. Next, the obtained microsomes were submitted to osmolysis with 1.8 mL in a

solution containing 27 mM Tris/HCl, 3 mM $MgCl_2$, and 100 nM $CaCl_2$ and protease inhibitors, and then were kept on ice until pelleting them again for the ATP assay.

Subsequently, membranes were recovered in the assay solution of the following composition: NaCl 120 mM, KCl 20 mM, $MgCl_2$ 1 mM, Tris/HCl 20 mM and protease inhibitors. An approximately 100 µg of protein in 50 µL was added to 200 µL solutions containing the substances to be tested, *i.e.* the CB_1R inverse agonists, AM251 (500 nM) and rimonabant (500 nM), the CB_1R silent antagonist, O-2050 (500 nM), as well as the pump inhibitor, ouabain (1 mM) alone or in combination or their solvent, DMSO. Next, 50 uL of 12 mM MgATP solution was given to each prewarmed tube, so that the final concentration of ATP became 2 mM, and the tubes were continued to be incubated at 37ºC for more 15 min. At the end of this period, 60 µL of 5 M trichloroacetic acid was pipetted in each tube to stop reactions and precipitate biological material, which was pelleted at 14000 g for 5 min at 4ºC immediately. Next, 96-well plates were filled with 100 uL of decanted (protein free) samples in duplicate (from each of the individual 300 uL aliquots), and an additional 100 µL of a modified Fiske-Subbarow reagent (Fiske and Subbarow, 1925) of the following composition was added to them to determine free phosphate concentrations: 0.8 g Fe_2SO_4, 2 mL H_2SO_4 (1 M), 5 mL ammonium-molibdate adjusted to 10 mL with MQ H_2O. The standard curve consisted of 8 points: distilled water, and 0.25, 0.5, 0.6, 0.7, 0.8, 0.9, 1 mM KH_2PO_4. Plates were read 30 min later at 825 nm. The results obtained with this method are presented in **Section 3.1.2.3**.

2.3.3 *In vitro* measurement of glycogen accumulation and lactate release in brain slices

The experimental layout was essentially the same as for the ^{3}HDG uptake study with slight modifications. Since MRS1754 (100 nM) strongly reduced ^{3}HDG uptake in the bathed slices at 37ºC, we selected this $A_{2B}R$ antagonist to modulate glycogen synthesis and lactate release. The frontal cortex of eight mice and the striata of six mice were selected for this assay, as these target areas provide more tissue and hence, better signal-to-noise ratio. MRS1754 or its vehicle (DMSO) were co-administered in the bath with D-glucose labelled at all six carbon atoms ($^{14}C_6$-D-glucose) at the concentration of 50 nM since the beginning of the 90 min incubation period. This protocol allowed us monitoring the recovery of glycogen stores, which become depleted when sacrificing

the animals (Hutchins and Rogers, 1970). Glycogen was separated from the tissue as described before in **Section 2.3.1.6** (Lemos et al. 2012). Upon completion of the 90 min incubation period, a sample was taken from the bath to determine lactate release. The ^{14}C concentration in the bath, the total ^{14}C retention in the slices and the ^{14}C quantity incorporated in glycogen were counted with the β-counter, while lactate release values were measured with a lactate dehydrogenase kit (Sigma-Aldrich) and nanomole values were expressed in mg protein contents. See **Section 3.5.3** and **Figure 3.36**.

2.3.4 Extracellular electrophysiological recordings in hippocampal slices

Electrophysiological recordings were carried out as previously described for Schaffer fibers (Gonçalves et al., 2015) and for the temporoammonic pathway (Dvorak-Carbone and Schuman, 1999). Rats were decapitated after halothane anesthesia, and the pair of hippocampi were dissected in an ice-cold artificial cerebrospinal fluid (ACSF solution(in mM: 124 NaCl; 3.0 KCl; 1.24 NaH_2PO_4; 10 glucose; 26 $NaHCO_3$; 1.0 $MgSO_4$; 2.0 $CaCl_2$) gassed with 95% O_2 and 5% CO_2. Four hundred μm-thick transversal slices were prepared with a McIllwain tissue chopper and allowed to recover for 30 min at 35 ºC and for 30 min at room temperature in a resting chamber (Harvard Apparatus) with gassed ACSF. For the temporoammonic recordings, cortico-hippocampal slices were prepared using a vibratome and allowed to recover for 1 h at room temperature. Both type of slices come from the same animal hemisphere so it is expected that the adenosinergic tonus is be the same independently of the method used to do the slicing. Individual slices were transferred to a submersion recording chamber of 1 mL capacity, and continuously superfused at a rate of 3 mL/min with gassed ACSF kept at 30.5 ºC. A bipolar concentric electrode was placed either on the Schaffer collateral/commissural pathway or in the *subiculum* to stimulate the temporoammonic pathway and rectangular pulses of 0.1 msec were applied every 20 sec. The orthodromically-evoked field excitatory postsynaptic potentials (fEPSP) were recorded through an extracellular microelectrode pipette filled with 4 M NaCl (2-4 MΩ resistance) and placed in the *stratum radiatum* of the CA1 area for both pathways. We first built an input/output curve to select the intensity of the stimulus to evoke a fEPSP

of about 40% of maximal amplitude. Recordings were obtained with a ISO-80 amplifier (World Precision Instruments, Hertfordshire, UK) and digitized using a ADC-42 board (Pico Technologies, Pelham, NY, USA). Averages of 3 consecutive responses were continuously monitored on a personal computer with the LTP 1.01 software (Anderson and Collingridge, 2001). Long-term potentiation (LTP) was elicited by a high-frequency stimulation protocol (100 Hz, 1 sec duration). The protocol used to induce long-term depression (LTD) was the paired pulse-low frequency stimulation (PP-LFS) (900 paired stimuli, with 200 msec paired pulse interval, 1 Hz inter-pair interval) during 15 min. Changes in synaptic strength were expressed relative to the normalized pre-LTP and PP-LFS and the baseline. Results obtained with this technique are found under **Sections 3.3.2** (for Schaffer fibers) and **3.4.4** (Schaffer fibers and temporoammonic pathway).

2.3.5 Proton HRMAS analysis

The metabolic profiling of the isolated individual hippocampi was determined by proton (^{1}H) high-resolution magic angle spinning (HRMAS) spectroscopy, as previously described (Alves et al., 2015). The spectrometer used was a 800 MHz Bruker NMR (Bruker, UK) equipped with a 4 mm HRMAS Triple H/C/N probe-head, specific for high resolution liquid or semi-solid samples. A 1D Carr–Purcell–Meiboom–Gill (CPMG) NMR sequence was used as previously described (Duarte et al., 2009). The standard acquisition parameters included a 5.45 sec acquisition time, 12 kHz sweep width and a recycle delay of 2 sec. An average of 256 scans were performed to acquire a suitable signal too noise ratio for metabolite quantification. Each FID obtained was multiplied by a 0.5 Hz Lorentzian before the Fourier transformation, to improve the signal to noise ratio. The spectral integration was performed using NUTSpro^{TM} software, allowing metabolite quantification. The results obtained by employing this method are presented in **Sections 3.3.3** (**Figure 3.24)** and **3.4.5** (**Figure 3.27**).

2.3.6 Preparation of total membranes

Conventional SDS-page blotting was performed as described before (Duarte et al., 2007b). Briefly, hippocampal slices of male Wistar rats and frontocortical tissue of 4 month-old male CD-1 mice of sham and STZ-treated groups were collected right during the dissection or after incubation without radioactive tracers. Although during animal

sacrifice some changes in phosphorylation state can occur, we believe that due to the rapidity of the dissection process (20 seconds after decapitation, the brain is put into ice-cold Krebs' solution) it was not significant, thus all changes (upon recovery and treatments) were expressed as % of the phosphorylation of the respective protein in the slices prepared right after decapitation.

The tissues were collected and homogenized in 500 µL of SDS-page buffer containing glycerol (30% v/v), dithiothreitol (0.6 M), Na_3VO_4 (1 mM), SDS (5% w/v) and 375 mM Tris-HCl pH 6.8, boiled at 70 ºC for 5 min and incubated for 2 h at 37ºC. After determining protein quantities the volumes were adjusted to obtain a protein concentration of 1 mg/mL.

2.3.7 Preparation of synaptosomes

The hippocampal synaptosomes were prepared as previously described (Rebola et al., 2003a). The tissue was homogenized in 0.32 M sucrose (pH 7.4) containing 10 mM HEPES and 1 M Tris, with 12 up-down strokes in a Teflon-glass tissue grinder using a motor-driven pestle (700-900 rpm). The mixture was centrifuged (10 min, 3,000 *g*, 4º C) and the consequent supernatant centrifuged once again (14 min, 14,000 *g*, at 4º C). The resulting pellet was then re-suspended into a 45% Percoll solution (v/v of an isotonic physiological solution (in mM: 118 KCl; 1.2 KH_2PO_4, 2.5 HEPES, 5 glucose; 1.2 $MgSO_4$; 25, 114 NaCl; pH 7.4) and then centrifuged (2 min, 14,000 *g*, 4ºC). The top layer, corresponding to the synaptosomal fraction, was carefully re-suspended in isotonic physiological solution and washed by centrifugation (1 min, 7,500 *g*, 4ºC). The protein quantification was done using the bicinchoninic acid (BCA) protein assay reagent kit (Thermo Scientific, Pierce Biotechnology, USA) and read at 570 nm in a spectrophotometer (SPECTRAmax plus 384, with SoftmaxPro software).

2.3.8 Western blot for CB_1R, Akt and GSK3

These blots were carried out in total membranes. Thirty µg of proteins (for blots with CB_1R) or 50 µg of proteins (for Akt and GSK3 blots) were loaded together with the prestained molecular weight markers (Amersham), and subsequently separated by SDS-PAGE (10% with a 4% concentrating gel) under reducing conditions and electro-

transferred to polyvinylidene difluoride membranes (0.45 μm; Amersham). After blocking for 2 hours at room temperature with fatty acid free bovine serum albumin (BSA, 5% w/v; Sigma) in Tris-buffered saline, pH 7.6 containing 0.1% Tween 20 (TBS-T), the membranes were incubated overnight at 4ºC either with rabbit anti-CB_1R C-terminal antibody (Frontiers Institute co, Hokkaido, Japan; 1:1000), or anti-Phospho-Ser473-Akt, rabbit anti-Phospho-Ser21-GSK3α, and rabbit anti-Phospho-Ser21-GSK3α (all at 1:1000; Cell Signal, US). For the reprobing of loaded protein quantities, mouse anti-β-actin (Sigma-Aldrich, Sintra, Portugal; 1:10,000), or the respective rabbit anti-Akt, rabbit anti-GSK3α and rabbit anti-GSK3β antibodies (all at 1:1000; Cell Signal) were employed. After four washing periods for 10 min with TBS-T containing 0.5% BSA, the membranes were incubated with the alkaline phosphatase-conjugated anti-rabbit secondary antibody (at 1:10000; Calbiochem) in TBS-T containing 1% BSA during 90 min at room temperature. After five 10 min-washes in TBS-T with 1% BSA the membranes were incubated with Enhanced Chemi-Fluorescence during 5 min and then analysed with a VersaDoc 3000 (Biorad). Phospoprotein densities were normalized to the respective total protein densities for further comparison. For the results, see **Section 3.1.2.1** and **Figure 3.2**.

2.3.9 Western blot for A_1R

Western blotting of the synaptosomal membranes was performed as previously described (Rebola et al., 2003a). Each sample was normalized to 1 μg/μL by adding SDS-PAGE sample buffer containing 30% (v/v) glycerol, 0.6 M dithiothreitol, 10% (w/v) sodium dodecylsulphate and 375 mM Tris-HCl, pH 6.8, and boiled (95 ºC, 5 min). These diluted samples and the pre-stained molecular weight markers (dual-colour standards from BioRad, Portugal) were loaded into the gel and separated by SDS-PAGE electrophoresis (in 10 % polyacrylamide resolving gels with 4 % polyacrylamide stacking gels, under reducing conditions using a bicine buffered solution (20 mM Tris, 192 mM bicine and 0.1 % SDS, pH 8.3), and then electro-transferred nitrocellulose membranes (from Panreac Química, Barcelona, Spain). The membranes were stained using Poinceau S solution and cut separating the membrane according to the target molecular weight. The membranes with the primary antibodies, were incubated (overnight, 4º C), against A_1R (1: 250; from Sigma, code: s0664) which was diluted in

Tris-buffered saline (in mM: 20 Tris–HCl; 140 mM NaCl, pH 7.6) with 0.1% Tween (TBS-T) and 5% non-fat milk. A mouse or rabbit antibody directed against β-actin (1:2500, from Sigma) was used as loading control. The membranes were incubated (2 h, RT) with horseradish peroxidase-conjugated goat anti-rabbit secondary antibodies (1:5000; Pierce). They were revealed by SuperSignal West Pico Chemiluminescent Substrate (Pierce). The immunoreactivity was detected using an imaging system (VersaDoc3000, Bio-Rad) equipped with the Quantity One software version 4.4.1 (Bio-Rad). The quantification of the protein bands was performed using Image Lab software (version 4.4, Bio-Rad). See results, **Section 3.4.5** and **Figure 3.29.**

2.4 DATA PRESENTATION AND STATISTICS

In this Thesis, all data are presented as mean ±, or +/- S.E.M. Some control *vs*. treatment data type (*e.g.* glucose uptake and metabolism values) were shown as mean +/- S.E.M. of either standalone absolute values (**Figures 3.12A,B**; **3.13A,B**; **3.16A-C**; **3.19A-C**; **3.35**), or of differences from respective control (**Figure 10B,D**), taking into account which representation highlighted better the scientific message.

In many cases, the mean ±, or +/- S.E.M. data were presented normalized (most glucose uptake data, ATP metabolism, some Western blot results, lactate release, glycogen experiments), such as in **Figures 3.1E,F**; **3.3**; **3.4**; **3.5**; **3.6C**; **3.8A**; **3.9**; **3.10A**,**C**; **3.14**; **3.16D**; **3.17B**; **3.18B**; **3.33D**; **3.34A-C**; **3.36**. Normalization was the most suitable manner of data presentation, since a treatment only can be compared to its own vehicle control from the same experiment. The general rule is that if more than one treatment is to be compared to the same control, Repeated Measures ANOVA should be used, unless there are missing data points. Naturally, in the countless experimental days throughout the course of the multiyear experiments, numerous different treatments were in random combinations; therefore, it was not possible to test all the different treatments in each and every experiment. Consequently, there is always missing data points, which does not allow us using Repeated Measures ANOVA. Instead, treatments were normalized to the everyday vehicle. Normalized data sets were tested for normal distribution with the Kolmogorov–Smirnov normality tests. Statistical significance was calculated by one-sample *t*-test against the typical hypothetical values of 100 or 0, where applicable.

For the rest of the data sets, either the text body or the legend to figures indicated the statistical method used, most typically an appropriate *t*-test or a proper combination of ANOVA with a post-hoc test. All tests for the data presented in this Thesis were performed using the GraphPad Prism 5.0 software package.

Chapter 3

Results and Discussion

3 RESULTS AND DISCUSSION

3.1 OPTIMIZATION AND CHARACTERIZATION OF *IN VITRO* GLUCOSE UPTAKE

3.1.1 Optimization of the uptake procedures in acute brain slices

For the optimization of the ^{3}H-2-D-deoxyglucose (^{3}HDG) and $^{14}C_6$-U-D-glucose ($^{14}C_6$-glucose) technique, firstly the slice thickness was established, experimentaly it was observed that 400 μm slice thickness is ideal for both tissue sturdiness and optimal penetration of radiotracers, chemicals and O_2. This optimal thickness was obtained via incubating acute hippocampal slices of three rats at different thicknesses ranging from 300 μm to 1 mm for 60 min in the presence of 1 nM ^{3}HDG. The lowest standard deviation was obtained for the uptake value in case of the 400 and 450 μm-thick slices (data not shown), and we selected the lower thickness for the following assays. Next, optimizing step was the ^{3}HDG and $^{14}C_6$-glucose uptake in both hippocampal and frontocortical slices of the rat, both in terms of recovery period and assay length. Using the dual-label counting protocol of the β-counter available, allowed up to 99.6% efficiency in the separation of ^{3}H and ^{14}C counts in the same samples.

To establish an optimal recovery period the frontocortical and hippocampal slices of 12 rats were divided in 12×10 pools, each pool having 2 cortical and 3 hippocampal slices from one rat, and incubated them for 15 min at 37ºC under carboxygenation in the presence of 1 nM ^{3}HDG and 50 nM ^{14}C-glucose, starting at every fifteen minutes, *i.e.* 0, 15, 30… till 135 min after slice preparation. ^{3}HDG uptake kinetics were fairly stable comparing the different time-points (**Figure 3.1A,B).** One-way ANOVA followed by Bonferroni's *post-hoc* test did not reveal difference in the 15-min ^{3}HDG uptake at the 10 different time-points of the recovery period ($P > 0.05$), but visually, was observed a tendency toward inverse correlation between recovery time and uptake. Virtually, both linear regression and one-phase exponential decay could fairly well represent the ^{3}HDG uptake data in the recovery period in both tissues. Using the extra sum-of-squares F-test as a method of comparison, we determined that the best model is linear regression. Indeed, the dependence of ^{3}HDG uptake on recovery time (τ; min) can be described as $Y = 22.8 + \tau/-17.7$ fmol/(mg protein) uptake for the frontal cortex ($r^2 = 0.82$) and $21.1 + \tau/-27.7$ fmol/(mg protein) for the hippocampus ($r^2 = 0.54$). For both tissues, the slope

was significantly non-zero ($P < 0.05$), confirming that there is a significant effect of the recovery on ^{3}HDG uptake (**Figure 3.1A,B**).

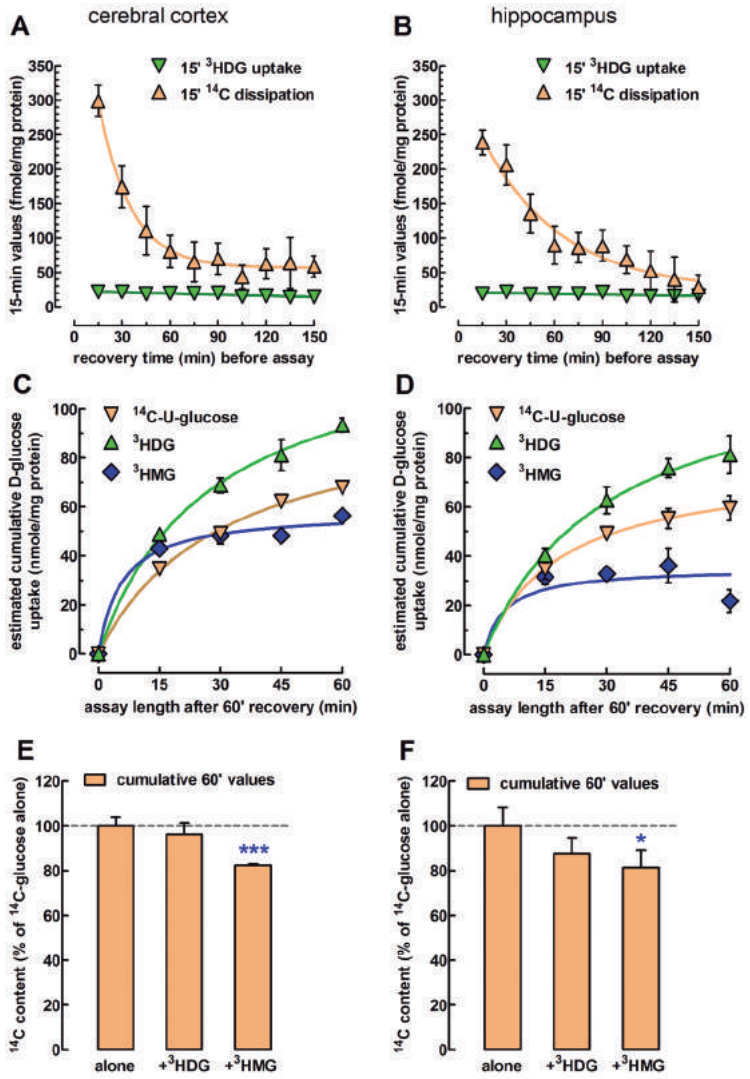

Figure 3.1 – Kinetics of the uptake of radiolabelled glucose analogues in acute frontocortical (A,C,E) and hippocampal (B,D,F) slices of the rat. (A,B) Glucose uptake and metabolism in the recovery period, as assayed with the dual ^{3}HDG/$^{14}C_6$-glucose uptake procedure. The ^{14}C dissipation values reflect 6× the difference between the ^{3}HDG and the ^{14}C contents (for further explanation, see Sections 2.1.1 and 2.1.4). (C,D) Cumulative total D-glucose uptake as estimated from the accumulation of ^{3}H and ^{14}C tracers in 15-min intervals, after 60 min recovery (see also Sections 2.1.2 and 2.1.4). (E,F) A test for the putative interaction between the tracers suggests that ^{3}HMG has a small albeit significant inhibitory action on ^{14}C accumulation after 60 min of incubation. Data points and bars represent the mean ± S.E.M. of n=6 independent observations (rats). *P < 0.05, ***P < 0.001 *vs*. 100%

The ratios of ^{14}C and ^{3}HDG contents of the slices were markedly smaller within the first 45 min of the recovery period compared to the last time-points, which suggests that in the beginning of the recovery, more glucose is metabolized in a dissipative fashion, contributing to greater ^{14}C loss either as $^{14}CO_2$ or ^{14}C-lactate, among others (**Figure 3.1A,B**). The kinetics of ^{14}C dissipation was significantly better modelled with a one-phase exponential decay curve: $Y = (572.0 - 56.7) \times \exp(0.05/\tau) - 56.7$ fmol/(mg protein) for the frontal cortex and $Y = (323.8 - 23.8) \times \exp(0.02/\tau) - 23.8$ fmol/(mg protein) for the hippocampus. The half-life of reaching the bottom plateau of dissipative metabolism was ~14 min recovery for the frontal cortex and ~34 min for the hippocampus. Indeed, between 60 and 90 min of the recovery period, dissipative glucose metabolism became virtually stabilized and exhibited fairly linear kinetics in both tissues (**Figure 3.1A,B**). Hence, it was established that 60 min recovery in a bath at 37ºC under continuous bubbling is sufficient to reach steady-state glucose transport and metabolism in 400 μm-thick acute brain slices of the rat.

Next step was to investigate which tracers and which assay lengths serve best our interest to study glucoregulation in brain slices. Besides 2-deoxy-D-glucose (DG; Kipnis and Cori, 1959), 3-O-methyl-D-glucose (MG) can also be used to monitor glucose transport across cell membranes (Morgan and Park, 1958). In fact, while DG measures both transport and hexokinase activity, it is generally believed that MG uptake only represents the pure transport process, because this hexose is not a substrate of hexokinases (Randle and Morgan, 1964; Rodríguez-Enríquez et al., 2009). This assumption was later challenged because MG is phosphorylated by hexokinases at least in the heart muscle (Gatley et al., 1997).

Here we measured cumulative glucose uptake with the help of the following tracers: $^{14}C_6$-glucose (50 nM) alone or combined with ^{3}HDG (1 nM) or ^{3}H-oxygen-methyl-D-glucose (^{3}HMG; 1 nM). The assays started after 60 min recovery with the bath application of the glucose analogues, and at every 15 min, 5 hippocampal and 2-3 frontocortical slices (~1 mg protein) were removed from the bath to measure accumulated glucose uptake. It was found that the kinetics of specific uptake values were similar to radioligand binding isotherms (**Figure 3.1C,D**), which are derived from the following equation: $Y = U_{max} \times \tau / (\tau_{50} + \tau)$, where U_{max} denotes the theoretical maximum uptake, τ is for time (min) and τ_{50} stands for the time (min) necessary to reach

the half of U_{max} (**Figure 3.1C,D**). In fact, the non-metabolizable analogues accumulate inside the cells until saturating the hexokinases and thus, reach a point where the re-release of the non-metabolizable analogues occur at a faster rate than their phosphorylation that could prevent their re-release. Theoretically, $^{14}C_6$-glucose never should saturate the slice; therefore the saturable kinetics for $^{14}C_6$-glucose uptake may represent the constant metabolism of the tracer leading to equilibrium between the uptake and the loss of ^{14}C. Nevertheless, it is equally possible that the slices gradually slow down (regularize?) their energy metabolism, hence causing a departure from linearity in these cumulative curves.

Last but not least, the reason for measuring $^{14}C_6$-glucose uptake in the absence and presence of ^{3}HDG and ^{3}HMG served as a quality control for the alleged toxicity of nonmetabolizable glucose analogues, even though they would require much higher concentrations for toxic effects (Dringen and Hamprecht, 1993). While the simultaneous presence of the ^{3}H analogues at the marginal 1 nM concentration had no effect on $^{14}C_6$-glucose uptake up to 45 min incubation ($P > 0.05$), with 60 min incubation, ^{3}HMG significantly reduced ^{14}C content in both the frontal cortex and the hippocampus, in comparison with what measured in the absence of ^{3}HMG (**Figure 3.1E,F**). These data certainly can be interpreted either as an increased metabolic efflux of ^{14}C or a result of toxicity, which could be tested by the simultaneous use of ^{14}CDG with ^{3}HMG. Although this side effect can be avoided with shorter incubation times, ^{3}HMG proved little experimental value for additional reasons too: the τ_{50} value for ^{3}HMG (if we represent its kinetics with saturation binding) was 5.7 ± 2.4 min in the cortex (30.5 ± 3.6 min for $^{14}C_6$-glucose and 27.3 ± 3.3 min for ^{3}HDG), and 5.0 ± 3.7 min in the hippocampus (18.1 ± 0.8 for ^{14}C-glucose and 29.8 ± 3.0 min for ^{3}HDG). The U_{max} values are also 2-3 times smaller for ^{3}HMG than for the rest of the tracers. These may be explained by the possibility that ^{3}HMG is indeed not phosphorylated once intracellular. Since we measured so far only the resting glucose uptake, ^{3}HMG uptake kinetics reached equilibrium of entering and leaving the cells already within a few minutes. In line with this, the insulin-stimulated rather than the resting ^{3}HMG transport in the soleus muscle is linear at least for 20 min (Dimitriadis et al., 1998).

Taken that a good signal-to-noise ratio is a prerequisite in the uptake assay, especially when the tissue quantity is minor such as when working with mouse

hippocampal slices, and that appropriate incubation time with receptor ligands as well as good linearity are also key issues, we opted for the τ = 30 min ($\approx \tau_{50}$) to measure ^{3}HDG uptake in the rest of the assays presented in this thesis, combined with 60 min recovery period. To the best of our knowledge, this is the first systematic characterization of *in vitro* glucose uptake in acute brain slices. The chosen 30 min incubation period is well within the maximal 45-60 min period of linearity for *in vivo* ^{3}HDG uptake in the brain (Schmidt et al., 1989), as discussed in the Introduction. So how do this uptake values relate to the values published in the literature? In the book chapter of Magistretti et al. (2002), the global rate of cerebral glucose uptake is assumed between 50-150 µmol / (100 g wet weight × min), based on the difference between arterial and venous glucose content. Using the mean value of 100 µmol glucose and counting roughly with 10 g proteins in 100 g wet tissue, we can establish the following relationship: 10 µmol glucose / (1 g protein × min), that is 10 nmol glucose / (1 mg protein × min). This estimation is close to the range of our resulting observations, since the initial velocity of ^{3}HDG uptake after 60 min recovery was 4.71 nmol/(mg protein) [SD range: 4.01 - 5.60] for the frontal cortex and 4.01 nmol/(mg protein) [SD range: 3.49 - 4.63] in the hippocampus in the first minute of the assay, as calculated from the curves displayed in **Figure 3.1C** and **D**. Additionally, the slices in our experiments were resting, while the global cerebral uptake *in vivo* is a mixed result of ongoing activities.

3.1.2 Characterization of glucose uptake in acute brain slices

Cerebral glucose uptake is expected to be controlled by numerous factors among which the following are thought to have major influence: 1) the Akt-GSK3 pathway; 2) the Na^{+}/K^{+}-ATPases, 3) neuronal activity; and according to our recent publication, 4) the presence of other oxidable substrates (Valente-Silva et al., 2015). As was already described in the Introduction, the endocannabinoid system acting on the cannabinoid CB_1 receptor (CB_1R) plays an important role in activity-dependent neuromodulation besides adenosine. The CB_1R is associated with the Akt-glycogen synthase kinase 3 (GSK3) pathway (Aso et al., 2012; Lemos et al., 2012), which is a major intracellular signalling route for insulin. Moreover, the CB_1R can form heterodimers with the insulin and the insulin-like growth factor 1 receptors (InR and IGF-1R) to inhibit their activation by the peptide hormones (Dalton and Howlett, 2012; Kim et al., 2012). In the

following assays, we aimed at determining the importance and contribution of each factor to glucose uptake in acute slices. The aim was to discover novel ways to enhance cerebral energy metabolism of glucose by the manipulation of either candidate neuromodulator systems or insulin signalling or both.

3.1.2.1 The CB_1R-Akt-GSK3 axis and glycogen synthesis in the acute slice

It is now known that the brain – more specifically, the astrocytes – contain high levels of glycogen, which suddenly drops upon sensory stimulation, ischemia and upon the decapitation of the animal (Cruz and Dienel, 2002b; Lowry et al., 1964). This rapid glycogen clearance explains that early studies did not find significant cerebral amounts of this energy reservoir. The literature prompts a tight association between CB_1Rs and the PI_3K-Akt-GSK3 enzymes in metabolic regulation. Therefore, we mapped the time-course of the phosphorylation of Akt, GSK3α and GSK3β in the freshly prepared hippocampal slices during the recovery period at 37ºC. As **Figure 3.2A** illustrates, Akt phosphorylation at serine-473 dropped in the first 45 min of incubation and remained fairly constant until 150 min. This suggested that an endogenous signal prevented the total dephosphorylation of Akt. The CB_1R-selective agonist, arachidonyl-2'-chloroethylamide (ACEA; 3 μM), which is a non-metabolizable synthetic anandamide analogue (Hillard et al., 1999) did not affect the phosphorylation of Akt between 90 min and 150 min, *i.e.* after the metabolic recovery. In contrast, the CB_1R-selective neutral antagonist O-2050 (1 μM) (Wiley et al., 2011), significantly diminished the Akt phosphorylation by 38.0 ± 8.8% ($n = 6$, $p < 0.05$) when added from min 90 of the recovery period. This suggests that an endogenous tone at the CB_1R helped to stabilize Akt phosphorylation. Notably, at this early stage of our study we used the highest concentrations of the two ligands, which we considered selective (Pertwee et al., 2010). Phospho-Akt phosphorylates (deactivates) GSK3α at serine-21 (Sakamoto et al., 2004). **Figure 3.2B** shows that the P-S21-GSK3α signal also dropped significantly until 45 min, but then returned to a level similar to that measured at 0 min. CB_1R blockade by O-2050 fully prevented the recovery of GSK3α phosphorylation (*i.e.* inhibited the GSK3α phosphorylation by 48.8 ± 8.4%, $P < 0.01$). This bolsters our hypothesis that an emerging endocannabinoid tone helped to reinstate Akt phosphorylation, and in concert with this, the effect of ACEA was endogenously occluded. Albeit phospho-Akt can also

phosphorylate GSK3β at serine-9 (Fang et al., 2000), there was no significant difference ($P > 0.05$) among different time-points and treatments *vs*. control.

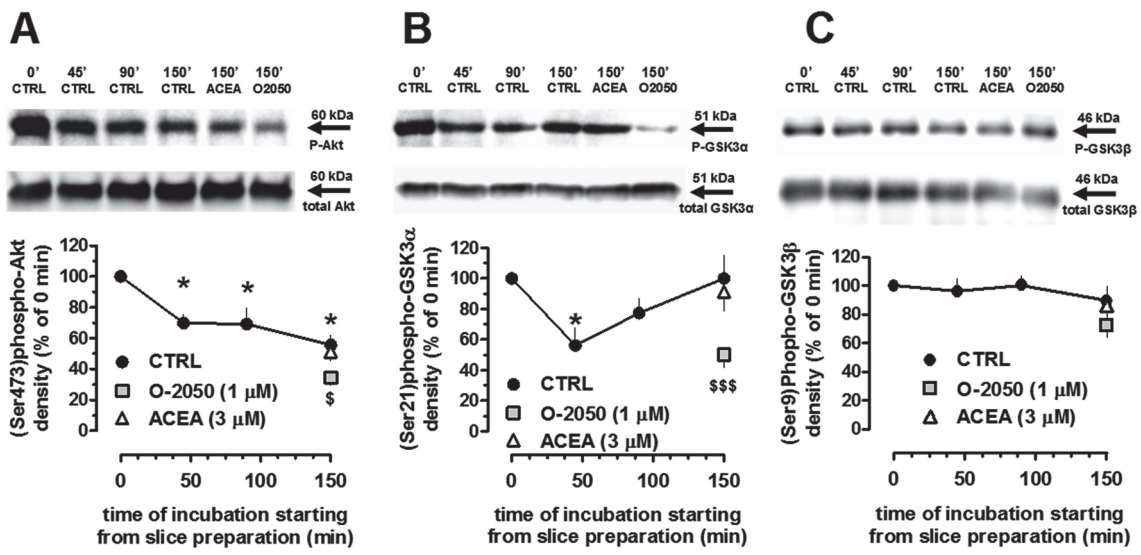

Figure 3.2 – An apparent endocannabinoid tone contributes to the inhibition of GSK3α activity in the acute hippocampal slice. The upper panels exhibit representative blots (A) (Ser473)phospho-Akt (B) (Ser 21)phosphor-GSK3-α and (C) (Ser9)Phospho-GSK3β. The CB_1R agonist, ACEA and the silent (aka neutral) CB_1R antagonist, O-2050 (see later) or their vehicle, DMSO (0.1%) were present since the beginning of the recovery period. The lower panels show the mean ± S.E.M. individual densities obtained from n=6 rats. Phosphorylated proteins were normalized to the bands obtained with the use of total-Akt/GSK3 antibodies upon reprobing. The density ratios of phospho/total proteins were taken as 100% in the tissues that were directly taken from the ice-cold Kreb's solution during dissection, thus more likely representing the *in vivo* level of phosphorylation. Phosphoprotein vs. total protein ratios were first tested for statistical difference with Repeated Measures ANOVA followed by Dunett's post-hoc test comparing the first time-point with later 3 time-points, then the values were normalized to the first time-point and presented accordingly, to enhance differences. $^{\$}P < 0.05$, $^{\$\$\$}P < 0.001$ *vs*. control time point.

Although Akt is one principal enzyme to phosphorylate GSK3β, the multifaceted signalling cascade of the GSK3β isoform also recruits other upstream elements (Grimes and Jope, 2001). In fact, GSK3β dephosphorylation (activation) is restricted in hippocampal neurons by redundant mechanisms to prevent apoptosis (Hetman et al., 2000). These may explain why GSK3β phosphorylation was little affected by the dephosphorylation of Akt in our experiments. Interestingly, GSK3α phosphorylation

started to recover 45 min after slice preparation, and after 90 min, it was already not different from that at the moment of slice preparation. The constant dephosphorylation of Akt was slowed down after 45 min incubation by an apparently emerging endocannabinoid tone (**Figure 3.2A**). This reinstated GSK3α phosphorylation, and the time-course of this process coincided with that for the transition from the metabolic recovery to equilibrium. It is also clear that *in vitro*, one can only work with suboptimal conditions, and we do not even know if the initially increased Akt and GSK3α phosphorylation is the normal physiological or the hyperphosphorylated state. To address this, we investigated if we can modulate glucose uptake and glycogen formation in the resting slices by controlling key elements of the insulin pathway.

3.1.2.2 The Akt-GSK3 axis and glycogen synthesis in the acute slice

It has been clear for decades that the brain is an insulin-sensitive organ. Although insulin has many trophic and homeostatic roles, it is principally known as a hormone to increase glucose transport from the plasma into insulin-sensitive organs (Duarte et al., 2012b; Kleinridders et al., 2014; Kullmann et al., 2015). Thus, it comes as no surprise that carefully planned studies also can detect stimulation of cerebral glucose uptake by insulin *in vivo* (Bingham et al., 2002; Lucignani et al., 1987; McNay et al., 2010). Here we aimed at testing *in vitro* if insulin, given one min before ^{3}HDG application, could increase glucose uptake in both frontocortical and hippocampal slices. Indeed, as **Figure 3.3** demonstrates, insulin (recombinant humulin) increased glucose uptake in the hippocampal slices by above one quarter over the resting level. However, this effect was present only at 30 ($n = 7$, $P < 0.01$) but not at 3 nM ($n = 6$, $P > 0.05$) or 300 nM ($n = 11$, $P > 0.05$) of insulin. The effect of insulin (30 nM) was not affected ($n = 9$, $P > 0.05$) by 9 min pretreatment with the insulin-like growth factor-1 receptor (IGF-1R) antagonist, I-OMe tyrphostin AG-538 (5 μM) (Blum et al., 2000), which also had no effect on glucose uptake *per se* ($n = 9$, $P > 0.05$). These suggest that the likely receptor underlying the effect of insulin was the insulin receptor itself. In contrast to the hippocampus, insulin (3-300 nM) did not stimulate glucose uptake in the frontocortical slices ($n \geq 10$, $P > 0.05$).

The insulin receptor is widely distributed in the mammalian brain (Folli et al., 1994; Pacold and Blackard, 1979; Schulingkamp et al., 2000). Cerebral insulin receptors play

a major role in the regulation of the energy metabolism of the whole body (Brüning et al., 2000; Varela and Horvath, 2012). Insulin receptor activation can also stimulate local and global rates of cerebral glucose metabolism, but only a few studies have documented these findings *in vivo* in humans (Bingham et al., 2002) and rats (McNay et al., 2010). Partly, this is why the brain has long been regarded as an organ that is not dependent on insulin to take up glucose (Biessels et al., 2004).

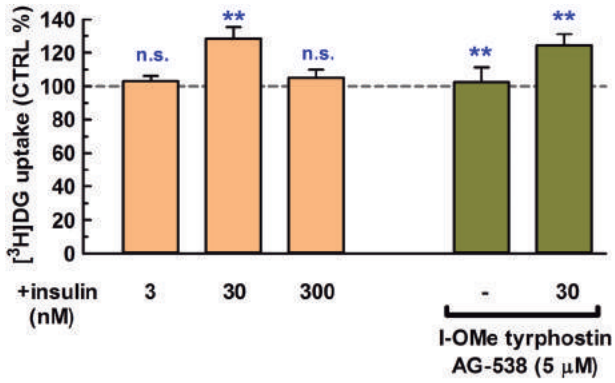

Figure 3.3 – Insulin stimulates glucose uptake with a bell-shaped concentration-response curve, likely via the activation of insulin receptors rather than IGF-1Rs, as concluded by the lack of antagonism by the IGF-1R antagonist tyrphostin. All data are mean + S.E.M. of n = 6-11; **P < 0.01, ***P < 0.001, n.s., not significant *vs*. 100% (control).

The above *in vivo* studies that challenged this dogma are precious as they provide the most complete picture of the studied mechanisms, but they are also inherently confounded by systemic responses. To avoid this, McNay et al. (2010) applied reverse dialysis into the rat hippocampus: insulin rather than IGF-1 facilitated spatial memory with a bell-shaped dose-response curve (such as in our *in vitro* study), and increased the uptake of glucose and its conversion into lactic acid (McNay et al., 2010). Still, it is not clear if changes represent direct effects on glucose transport or indirect effects on neural activity-dependent energy metabolism. In fact, insulin has been shown to stimulate glucose uptake (Clarke et al., 1984; Werner et al., 1989), glycogen synthesis (Hamai et al., 1999), or both (Kum et al., 1992) in cultured astrocytes. In neurons in culture, the picture is more complex. For instance, Werner and colleagues (1989) found no evidence for insulin-stimulated glucose uptake in rat neurons. Another study showed that insulin increases the translocation of the glucose transporter GLUT3 to rat neuronal cell

membranes and an additional depolarization helps to trigger increased glucose transport (Uemura and Greenlee, 2006). Finally, Benomar et al. (2006) reported that insulin stimulates GLUT4 translocation and glucose uptake in a human neuronal cell line. Together, the overall effect of insulin on cerebral glucose uptake is small as compared to the skeletal muscle, and is dependent on small concentration ranges and probably neuromodulators, therefore it is comprehensible that most approaches failed to unveil insulin effect on glucose uptake in brain slices (Abdul-Ghani et al., 2007).

CB_1Rs have been shown to physically complex with insulin and IGF-1Rs both in pancreatic and neuronal cell lines and control the intracellular signalling cascade of insulin and IGF-1 (Dalton and Howlett, 2012; Kim et al., 2012), just like in Chinese hamster ovary (CHO) cells transfected with the human CB_1R (Bouaboula et al., 1997). Based on the findings presented in **Figure 3.2**, it was expected CB_1R ligands to affect glucose uptake and probably, glycogen levels.

To this end, two CB_1R-selective agonists, ACEA (1 μM) and R-methanandamide (1 μM; Abadji et al., 1994), as well as two non-selective synthetic cannabinoids, WIN55212-2 (500 nM; Haycock et al., 1990) and O-2545 (1 μM; Martin et al., 2006) were tested. These agonists were added 5 min before the application of ^{3}HDG (and thus, 4 min before insulin application when co-administered), because we previously showed that 4 min presence of cannabimimetics is enough to achieve CB_1R-mediated inhibition of evoked transmitter release (Bitencourt et al., 2015a). **Figure 3.4** demonstrates that none of these agonists affected the uptake of ^{3}HDG *per se*. This is somewhat surprising taken that CB_1R agonists are capable of transactivating the insulin receptor in the absence of insulin, and to inhibit the autophosphorylation of the receptor in the presence of insulin (Dalton and Howlett, 2012; Kim et al., 2012). Assuming that there was no significant amount of endogenous insulin present in the slice (which nevertheless can be a false assumption taken that insulin is synthesized and released by neurons in the brain (Banks, 2004; Molnár et al., 2014; Santos et al., 1999), the lack of insulinomimetic action of the CB_1R agonists may mean that the CB_1Rs were already active in the slice, and in fact, data in **Figure 3.2** advocates this hypothesis. Also, it may mean that the CB_1Rs are not present in those cells where insulin receptors stimulate glucose uptake.

To test if endogenous or constitutive CB_1R activity had any impact on hippocampal glucose uptake, the slices were incubated with the CB_1R inverse agonists,

AM251 (500 nM; Gatley et al., 1997), rimonabant (500 nM; Rinaldi-Carmona et al., 1994) and PF514273 (500 nM; Dow et al., 2009), and the CB_1R-selective neutral antagonist, O-2050 (500 nM), all added 10 min before ^{3}HDG, *i.e.* 9 min before insulin, at min 50 of the recovery period. Notably, the generally preferred 500 nM concentration reflects the view of our laboratory that the low nanomolar IC_{50} values of these highly potent lipophilic antagonists do not justify risking non-specific (off-target) effects often seen at low micromolar concentrations of these ligands (Köfalvi, 2008). All in all, the three inverse agonists but not the neutral antagonist reduced the resting uptake of glucose to similar but not equal extents, which may reflect the individual inverse agonist efficacy of each antagonist, *i.e.* their capacity of perturb the ligand-free structure of those CB_1Rs that constitutively couples to G proteins (Ledent et al., 1999; Pertwee et al., 2010). We speculate that it was not the prevention of endocannabinoid signalling at CB_1Rs because the CB_1R neutral antagonist O-2050 did not affect glucose uptake. We also noted that the effect of CB_1R inverse agonism was linearly proportional to time: 60 min incubation with AM251 caused the double of reduction in glucose uptake, from -10.4 ± 2.4% to -22.0 ± 4.6% (**Figure 3.4**). Next, we asked if the genetic rather than the chemical ablation of the CB_1R could mimic the effect seen with the inverse agonists. The hippocampal slices of wild-type (WT) mice and their CB_1R KO littermates (Ledent et al., 1999) were co-incubated. Glucose uptake amounted to 70.9 ± 3.4 % (n = 20) in the WT mice (figure not shown). We noticed that glucose uptake was statistically significantly reduced in the slices of CB_1R KO mice as compared to their WT littermates by -17.7 ± 2.8% ($P < 0.001$) during the 30 min uptake period (**Figure 3.4**). Additionally, AM251 also reduced glucose uptake in the WT mice ($P < 0.001$) while having no effect in the CB_1R KO mice ($P > 0.05$), thus confirming the selectivity of AM251. The neutral antagonist, O-2050 did not affect glucose uptake in the WT mice either ($P > 0.05$).

Above we also asked why CB_1R activation is not associated with increased glucose uptake. Our experimental data unequivocally respond this question that a constitutive coupling of a subset of CB_1Rs to undisclosed intracellular pathways guarantees 10-20% of basal glucose uptake in the resting slice. The endogenous coupling obviously occludes exogenous agonists from further stimulating glucose uptake. This may be one reason for why cannabimimetics failed to stimulate glucose uptake. Still, if CB_1Rs were endogenously stimulating the Akt-GSK3 pathways, how

come that insulin was capable of further stimulating glucose uptake? To answer this, we decided to test insulin in the presence of CB_1R ligands. We applied selected agonists and antagonists of the above tested cannabinoids. As **Figure 3.5** depicts, neither CB_1R agonists (ACEA, O-2454 and WIN55212-2) nor antagonists/inverse agonists (O-2050 and rimonabant) enhanced the stimulatory effect of insulin on glucose uptake. On the contrary, while ACEA, rimonabant and O-2545 simply prevented the effect of insulin, WIN55212-2 and O-2050 which *per se* had no effect as we remember, reverted the stimulatory action of insulin into inhibition. Insulin was also combined, at the concentrations of 3 and 300 nM, with the above ligands but the outcome of those experiments was equally disappointing.

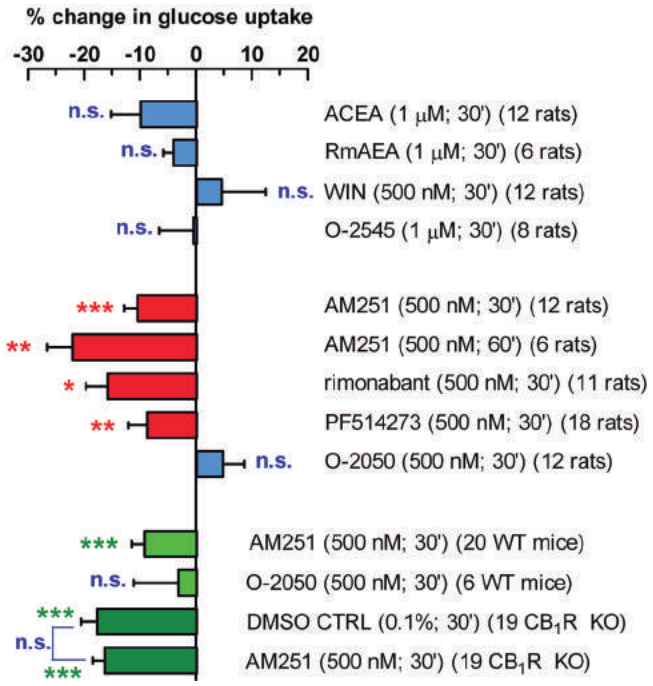

Figure 3.4 – CB_1Rs are constitutively associated with basal glucose uptake in rat and mouse acute hippocampal slices. Blue (non-significant) and red (significant) bars represent data from rat hippocampal slices, while light green (wild-type, WT) and dark green (CB_1R global knockout, KO) bars are from CD-1 mice. All data are mean +/- S.E.M. of n ≥ 6 animals; *P < 0.05, **P < 0.01, ***P < 0.001, n.s., not significant *vs*. no change (0%, control or WT). In order to visually enhance effects, the net change *vs*. control is plotted.

Previous *in vitro* studies were not more successful when dissecting the role of CB_1Rs in insulin signalling. Some studies showed that CB_1R agonists inhibit insulin

signalling in pancreatic β cells (Figler et al., 2011; Kim et al., 2012) and in neuronal cells (Dalton and Howlett, 2012). Nonetheless, others found that the CB_1R inverse agonist, rimonabant also inhibited the signalling pathway of insulin and IGF-1 in CHO cells (Bouaboula et al., 1997), and eventually, rimonabant stimulated glucose uptake in skeletal muscle on its own (Esposito et al., 2008), while it sensitised the skeletal muscle to insulin-induced glucose uptake (Lindborg et al., 2010).

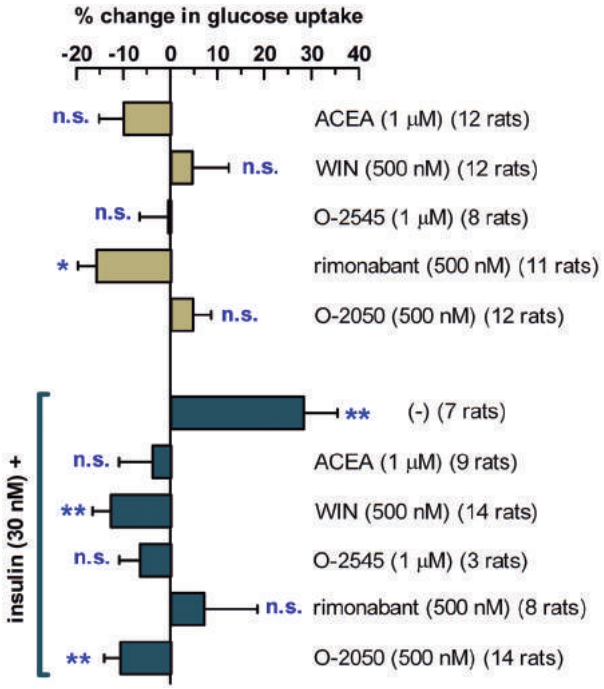

Figure 3.5 – CB_1R ligands impair insulin-induced glucose uptake in acute hippocampal slices. The first 6 bars from the top (cannabinoids and insulin alone) have been presented already in Figures 3.3 and 3.4. We pretreated the slices with either CB_1R antagonists for 9 min or agonists for 4 min before insulin, which was bath-applied for one min before ^{3}HDG, and present thereafter for the 30 min period of incubation (dark blue bars). All data represent mean +/- S.E.M.; *P < 0.05, **P < 0.01, n.s., not significant *vs*. no change (0%, control or WT). In order to visually enhance effects, the net change *vs*. control is plotted.

The lack of conclusive data from both the literature and our study can be a result of the so-called functional selectivity of the ligands, which is also termed as biased agonism and ligand-directed trafficking of responses (Bonhaus et al., 1998; Clarke and Bond, 1998; Makita and Iiri, 2014; Prather, 2008), which is a phenomenon very common for the CB_1R (Mukhopadhyay and Howlett, 2005): most G protein-coupled

receptor (GPCR) ligands have their own intrinsic efficacy in a given system, because when structurally different ligands bind to their cognate receptor they are prone to trigger dissimilar conformational changes. This led to the recent discovery that in a heterodimer that involves a GPCR, an agonist of the GPCR can impede the signalling through the partner receptor in the heterodimer, in part via intercepting the coupling to second messengers. However, antagonists of the same can also alter the conformation of the receptor by simply binding to their orthostatic binding site, and thereby altering the conformation of the partner receptor in the heterodimer, leading to its decreased affinity to either its ligands or the second messengers (Bonaventura et al., 2015).

Another confounding factor from this study is the complexity of the brain parenchyma over cell lines and simple tissues such as the skeletal muscle. Even if one ignores the contribution of microglia and oligodendrocytes to the metabolic responses, which is in fact a common choice, there is difference in the rate of glucose uptake and the process of glucose metabolism in neurons and astrocytes, and these parameters are intricately interdependent on one another and the activity of the circuitry (Hertz et al., 2007; Machler et al.; Pellerin and Magistretti, 2003). Our research group and another published recently that functional CB_1Rs in the mitochondria of astrocytes and neurons inhibit the respiratory chain and consequently, the oxidative metabolism of glucose (Bénard et al., 2012; Duarte et al., 2012c). Additionally, it is well-known that CB_1Rs are present in astrocytes, cholecystokinin-positive interneurons and glutamatergic neurons in the hippocampus, where they modulate the synaptic communication among these elements (Duarte et al., 2012; Katona et al., 1999, 2006; Navarrete and Araque, 2008). Consequently, a bulk assay with ^{3}HDG uptake measurement in the whole slice measures only the sum of a "potpourri" of responses in different cell types or zones in the hippocampus.

To overcome this difficulty, we mapped the putative subregional differences of the uptake of the fluorescent, non-metabolizable deoxyglucose analogue, 6-NBDG (30 μM). 6-NBDG is readily taken up by type-1 glucose transporters (GLUT1) in astrocytes (Barros et al., 2009), and to a smaller extent, probably in neurons, too. The uptake of 6-NBDG was virtually homogenous among the major subregions of the DMSO-treated hippocampus, such as the *Cornu Ammonis* region 1 (CA1), the CA3 and the dentate gyrus (**Figure 3.6A, D**). It was very clear though that 6-NBDG was preferentially taken

up by astrocyte-rich regions, because the *strata pyramidale* and *granulatum* (marked in panel **Figure 3.4D**) appeared much darker in the DMSO-treated slices.

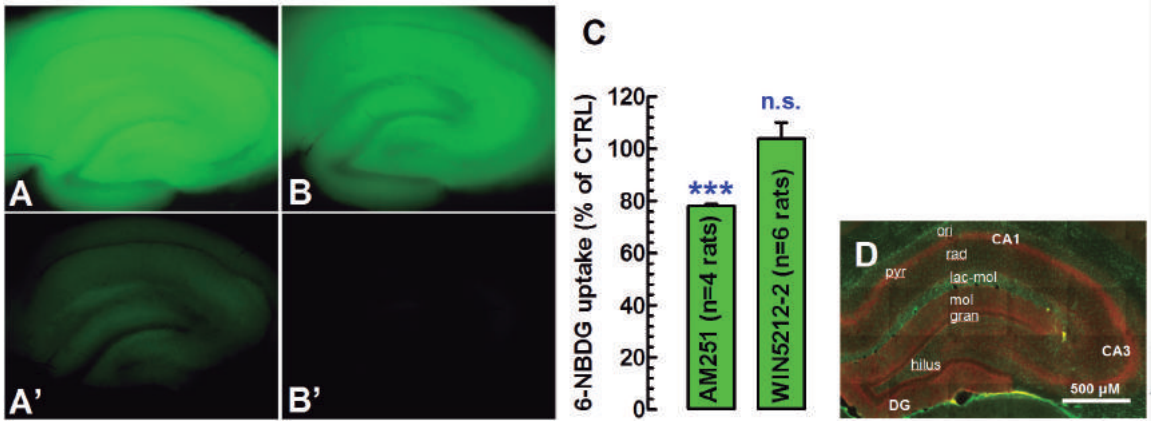

Figure 3.6 – AM251 decreases the uptake of the fluorescent deoxyglucose, 6-NBDG throughout the hippocampal slice. Rat hippocampal slices of 300 µm thickness were incubated at 37ºC for 50 or 55 min, then AM251 (500 nM), WIN55212-2 (500 nM) or their vehicle, DMSO (0.1%) were added in the bath, and at min 60 of the recovery period, 6-NBDG (30 µM) was supplied to the bath of the slices. After 30 min incubation, the slices were washed, transferred to a slide and photographed with an Axiovert 200M microscope. Panels (A) and (B) represent the original photographs of a (A) DMSO-treated (*i.e.*, vehicle control) and a (B) AM251-treated slice from the same animal. (A') and (B') show the residual fluorescence in the DMSO-treated slice, *i.e.* the difference between AM251-treatment and control. (C) Bar graph representing 6-NBDG intensity values of the AM251- and WIN55212-2-treated slices, as normalized to their control. Bars represent mean + S.E.M.; ***P < 0.001, n.s., not significant *vs*. no change (100%, DMSO control). (D) Reproduction of Figure 5A from (Duarte et al., 2012c), representing a low magnification (5×) fluorescent microscope image showing the distribution of fluorescent immunostaining of the astrocytic marker, glial fibrillar acidic protein (GFAP; green) and the CB1R (red) in labelled rat hippocampal subregions: CA1/3, *Cornu Ammonis* 1/3 regions; DG, dentate gyrus; strata: ori, *oriens*; pyr, *pyramidale*, rad, *radiatum*; lac-mol, *lacunosum-moleculare*; mol, moleculare; gran, *granulatum*.

As **Figure 3.4C** summarizes, WIN55212-2 affected the intensity of the 6-NBDG signal neither in the whole slice nor in subregions. This is consistent with what we observed for ^{3}HDG uptake. However, AM251 did decrease the relative fluorescence intensity by 21.9 ± 0.7% (n = 4 rats in triplicate, P < 0.001) in the whole slice. Since that time 6-NBDG uptake on ice was not measure and we also did not have means for quantitative fluorescent analysis, we cannot translate the relative fluorescence scale into

absolute changes. Nevertheless, similar responses to AM251 in the whole slice as with ^{3}HDG uptake were observed. When simultaneously decreasing the brightness of a DMSO- and an AM251-treated slice of the same animal until the AM251-treated slice just become totally black, the possible subregional effects of the treatment may be revealed. However, we found no specific region to be more affected, that is, the effect of CB_1R inverse agonism on glucose uptake virtually affects equally the whole slice (Figure 6A', B'). The zones which remained bright in the DMSO-treated slice (**Figure 3.6A'**) are the ones rich in astrocytes, *i.e.* the *strata oriens*, *radiatum*, *lacunosum-moleculare* and *moleculare*.

Therefore, it is safe to say that AM251 decreases glucose uptake in the astrocytes. Our ultimate aim was to take high-resolution confocal images to compare the fluorescence of different cell types among one another and throughout the treatments. However, we faced a major technical setback: the autofluorescence of (presumably) lipofuscin strongly interfered with 6-NBDG signal at 525 nm emission. Pretreatment with Sudan Black could have quenched autofluorescence but it also obfuscated the slices making it difficult to reliably work with 6-NBDG.

Last but not least, we opted for measuring an obvious endpoint of Akt-GSK3 activity, namely, glycogen levels. Although these data proved negative for CB_1R antagonists, eventually we could discover some interesting features of glucose metabolism during the protocol optimization.

Hippocampal slices of 14 rats were divided in two pools and the experiments were run as previously described in Section 2.1.3. After 50 min of recovery, the slices were treated with either AM251 (500 nM) or O-2050 (500 nM) for 10 min to allow the disengagement of any active coupling of the CB_1R with its intracellular pathways, then 20 times more $^{14}C_6$-glucose (1 μM) was added than normally to increase signal in the glycogen fraction, together with the usual concentration of ^{3}HDG (1 nM). In 6 additional experiments, ^{3}HMG (1 nM) was used to monitor glycogen purity. Our idea with the inclusion of ^{3}HDG was to scrutinize the purification process, as ^{3}HDG is supposed to stay phosphorylated by hexokinases in the form of ^{3}HDG-6-phosphate in the brain cells, thus remaining trapped inside. Unlike glycogen, free glucose and its analogues are highly soluble in ethanol; hence we expected to get rid of the excess ^{14}C labels that are not associated with glycogen after two intensive washing. To make sure

that glycogen was sufficiently washed, ^{3}HDG contamination was also measured in the precipitate to subtract a molar equivalent from the amount of glycogen measured with the ^{14}C label. **Figure 3.7** represents the distribution of the ^{3}H and the ^{14}C labels among the two supernatants and the pellet. The ^{3}H and ^{14}C contents of the supernatants and the pellet (2nd, 3rd and 4th groups of bars) were expressed to the total ^{3}H and ^{14}C contents of the slices, which were determined from the 100 µL aliquot removed from the 2 mL total sample before the precipitation of insoluble materials

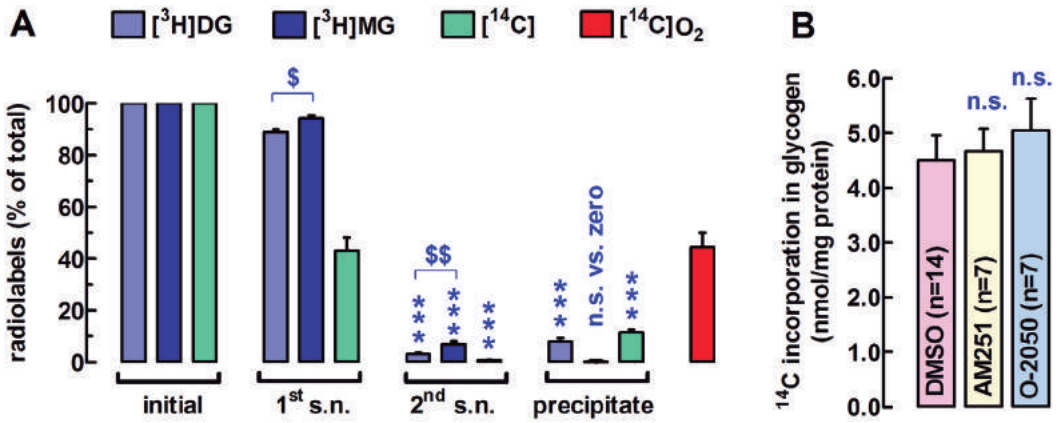

Figure 3.7 – CB_1R blockade does not affect glycogen formation in the hippocampal slice. After 50 min of recovery, the acute slices were treated with either AM251 (500 nM) or O-2050 (500 nM) for 10 min to allow the disengagement of any active coupling of the CB_1R with its intracellular pathways, then 20 times more $^{14}C_6$-glucose (1 µM) was added for the regular uptake assay to increase ^{14}C signal in the glycogen fraction, together with the usual concentration of ^{3}HDG (1 nM). In 6 additional experiments, ^{3}HMG (1 nM) was used to monitor glycogen purity. (A) The relative breakdown of radiolabel distribution among the first and the second supernatant (1st and 2nd s.n.), as well as the pellet (precipitate, aka glycogen), taken the initial label content as 100%. We believe that $^{14}CO_2$ accounts for the missing ^{14}C content after adding up those in the supernatants and the pellet, which disappeared during the washing, and is represented with the last red bar. (B) Absolute amounts of ^{14}C incorporated in glycogen during the incubation period. Bars represent mean + S.E.M.; $^{\$}P < 0.05$, $^{\$\$}P < 0.05$ as determined with Student's paired *t*-test, ***P < 0.001 as determined with one-sample *t*-test against the hypothetical value of 0%, n.s., not significant.

Intriguingly, the 1st supernatant yielded much less ^{14}C content (43.1 ± 5.2% of initial content, n = 14) than what it was expected based on the ^{3}H content (88.9 ± 1.1% of initial content) (**Figure 3.7A**). This difference was maintained for the 2nd supernatant

(3.12 *vs*. 0.84%), but these latter values already suggested that only trace amount of soluble ^{3}H and ^{14}C labels should have remained in the second pellet. Curiously, the ^{14}C content of the second pellet (11.5 ± 1.2 % of initial) did not account for the ^{14}C atoms missing from the supernatant, which allowed us to establish that the unaccounted ^{14}C was presumably a volatile $^{14}CO_2$ fraction that was initially trapped by NaOH in the 2 mL total sample, but likely disappeared during the two-day treatment with Glauber's salt and ethanol. This therefore allows us to calculate that after 30 min incubation with $^{14}C_6$-glucose, 55-56% of the ^{14}C label is associated with non-volatile molecules amidst ~11-12% is ^{14}C-glycogen, and the rest, ~44-45% is incorporated in $^{14}CO_2$.

The most striking data still was the significant (>0%) presence of ^{3}H in the glycogen fraction, which was greater than the ^{3}H content of the 2nd supernatant (8.0 ± 1.3% of initial content, **Figure 3.7A**). This led us to doubt if ^{3}HDG was a non-metabolizable analogue, taken that once phosphorylated by hexokinases, it may be subject to additional metabolism. To test this, glycogen separations were repeated in 6 other rats, and substituted ^{3}HDG with ^{3}HMG, because it is believed that this latter glucose analogue is not a substrate for hexokinases (Randle and Morgan, 1962; Rodríguez-Enríquez et al., 2009). ^{3}H content in the two supernatants were slightly but significantly greater when ^{3}HMG was used instead of ^{3}HDG to monitor glycogen contamination. Accordingly, there was virtually no ^{3}H contamination in the glycogen (pellet) fraction when using ^{3}HMG (0.26 ± 0.25% of initial content, n = 6, P > 0.05 *vs*. 0%). This is a telltale indication that ^{3}HDG readily incorporated into glycogen, and therefore, it is not necessary to subtract a molar equivalent of ^{3}H from ^{14}C-glycogen quantity, especially because there is no evidence for a purported contamination by ethanol-soluble tracers. In fact, there is sporadic evidence in the literature of deoxyglucose incorporation into glycogen: more than 3 decades old neurochemical studies have shown that 1-10% of deoxyglucose incorporates into glycogen in the nervous tissue (Nelson et al., 1984; Pentreath et al., 1982). The underlying mechanism of deoxyglucose incorporation was later addressed for 2-NBDG incorporation (an analogue of 6-NBDG), which allowed the authors to establish the monitorization of fluorescent glycogen synthesis (Louzao et al., 2008). The authors concluded that deoxyglucose-6-phosphate is converted successively into deoxyglucose-1-phosphate by phosphoglucomutase, and then into UPD-2-deoxyglucose by UDP-glucose pyrophosphorylase. Finally, glycogen synthase utilizes UDP-2-deoxyglucose as one

substrate and the non-reducing end of glycogen as another to grow the macromolecule. Nevertheless, neither AM251 nor O-2050 affected glycogen synthesis in the slices significantly (n = 7, P > 0.05) (**Figure 3.7B**).

Taken together, we uncovered that insulin is capable of stimulating glucose uptake in the hippocampal slice via the activation of insulin receptors, and this effect of insulin is dependent on cannabinoid CB_1 receptors. In fact, CB_1Rs appear to be positively coupled to resting glucose uptake, and CB_1R inverse agonists or the genetic deletion of the CB_1R can decrease basal glucose uptake by disrupting this signalling. We also observed that CB_1Rs modulate the Akt-GSK3α pathway (**Figure 3.2A,B**), but without effect on glycogen synthesis. Thus, it is probably GSK3β (**Figure 3.2C**) rather than GSK3α which is chiefly responsible for controlling the activity of glycogen synthase in the astrocytes. To expose the mechanism responsible for the action of CB_1R inverse agonists on glucose uptake, we adventured to the field of Na^+ pump activity.

3.1.2.3 Membrane potential and glucose consumption in the acute slices

Although it is generally believed that the majority of glucose taken up by the brain is spent on Na^+/K^+-ATPases, the supporting evidence is still circumstantial, because studies were carried out mainly either *in vivo* or in cell cultures (Astrup et al., 1981; Attwell and Laughlin, 2001). The major drawback of *in vivo* data is the emergence of systemic confounding factors, while cell cultures lack tissue context. The intermediate solution could be using acute brain slices (or organotypic slices), but slices are not favoured in general for energy metabolism studies, as Dr. Luc Pellerin (Lausanne, Switzerland) explained during a personal communication: the complexity of intercellular metabolic coupling and activity could make it very difficult to disentangle the effects of sodium pumps on glucose uptake. Thus we found here a calling challenge to answer.

There are different Na^+/K^+-ATPases in the brain of varying subunit composition and often dissimilar affinity to ouabain (Juhaszova and Blaustein, 1997). Our group has previously shown that ouabain exerts virtually maximal inhibition of ^{3}H-aspartate uptake into gliosomes (astrocyte-derived microsomes) at the concentration of 1 mM, while at 100 μM, it produces only partial, ~50% inhibition of the total uptake (Matos et

al., 2013). It was therefore expected that ouabain above 100 µM should significantly inhibit resting glucose uptake in the slice. The first concentration tested was an intermediate concentration, 300 µM ouabain. Remarkably, ouabain instead strongly stimulated glucose uptake, as compared with the DMSO control ($P < 0.001$) (**Figure 3.8A**).

This strong stimulation of glucose uptake was not entirely expected. For instance, De Piras and Zadunaisky (1965) found that ouabain (10 µM) prevents high-K^+-induced stimulation of $^{14}CO_2$ production from $^{14}C_6$-glucose in the frog brain. In rat cerebrocortical slices, the same concentration of ouabain also suppressed high-K^+-stimulated brain respiration (Gonda and Quastel, 1962).

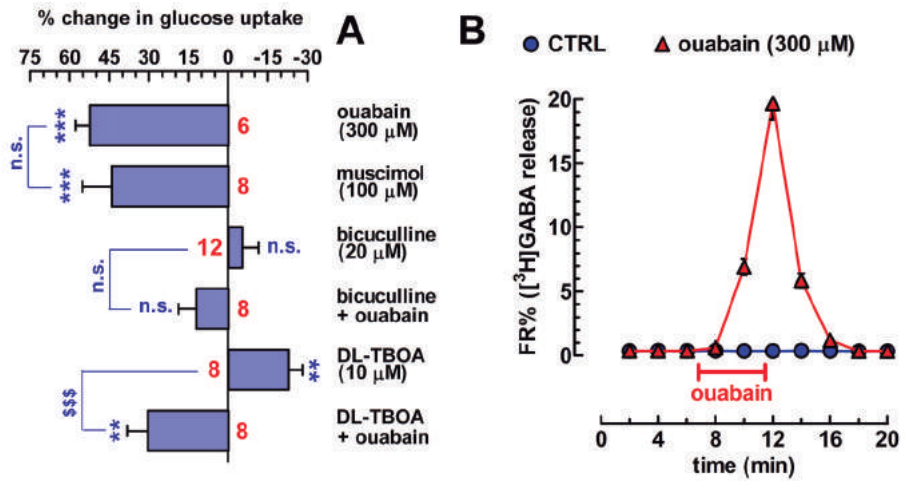

Figure 3.8 – Ouabain massively stimulates glucose uptake in the hippocampal slice, which is a consequence of increased GABA release. (A) Bar graph representing the similar effect of ouabain and the $GABA_A$ receptor agonist, muscimol on ^{3}HDG uptake in the acute hippocampal slices of the rat. Accordingly, the $GABA_A$ antagonist, bicuculline prevented the majority of ouabain-stimulated glucose uptake so that ouabain+bicuculline was no longer significantly different from DMSO control (marked as 0). The glutamate transporter inhibitor, DL-TBOA reduces glucose uptake on its own, which suggest that the ongoing glutamate turnover is responsible for an additional ~23% of resting glucose uptake. Red numbers at the bottom of the bars indicate the number of animals used (n). Bars represent mean ± S.E.M.; **P < 0.01, ***P < 0.001, as determined with one-sample *t*-test against the hypothetical value of 0%, n.s., not significant. (B) A release diagram of preloaded ^{3}HGABA from superfused rat hippocampal slices serves evidence of that a 5-min pulse of ouabain (as marked with the horizontal red bar) can trigger massive amounts of GABA release. FR%, Fractional Relase %. No statistical significance was calculated because the effects are visually compelling.

Very soon, another paper came out which reported findings more helpful for the interpretation of the obtained data. The authors reported that ouabain (up to the tested concentration of 100 μM) stimulated O_2 consumption and lactate release from rabbit cerebrocortical slices under normokalemia (5 mM K^+ in the assay medium), while under high-K^+ depolarization – which in itself strongly stimulated both O_2 consumption and lactate release – ouabain returned these values to the (still) elevated levels seen only with ouabain alone (Ruscák and Whittam, 1967). This latter paper therefore unveiled that albeit ouabain indeed inhibits the stimulation by high-K^+ of brain energy metabolism, in itself, it stimulates glucose metabolism, albeit lesser than high-K^+, and that high-K^+-evoked depolarization can be reverted by the blockade of the Na^+/K^+-ATPase, which normally transports Na^+ outside and K^+ inside (Ruscák and Whittam, 1967). Last but not least, a much more recent study by Veldhuis and colleagues (2003) revealed that ouabain directly injected into the neonatal brain causes excytotoxic cell death by making membrane potentials collapse (by preventing the outward Na^+ entry), leading to massive Na^+ then Ca^{2+} accumulation intracellularly, with a consequent depolarization, and loss of Mg^{2+} block at NMDA channels (Veldhuis et al., 2003).

These studies prompted to test if the effect of ouabain was dependent on the putative increase in glutamate release and reuptake in the highly depolarized slices. The slices pretreated for 10 min with DL-threo-β-benzyloxyaspartic acid (DL-TBOA), which is a competitive, non-transportable blocker of excitatory amino acid transporters, and has an IC_{50} of 3.2-6 μM for all excitatory amino acid transporters (except the EAAT1 at which it has an IC_{50} of 70 μM) (*e.g.* Shigeri et al., 2001). Our group also observed previously that to achieve the maximal inhibition of glutamate uptake in the striatum, one should use more than 100 μM of DL-TBOA, and it displayed a biphasic kinetics with two separate IC_{50} values (Pandolfo et al., 2011). However, extracellular recordings in the hippocampal slices (see later) revealed that above 10 μM, DL-TBOA triggers chaotic excitatory responses. To avoid this, only 10 μM of this inhibitor was used, and as **Figure 3.8A** documents, DL-TBOA readily reduced resting glucose uptake by 22.9 ± 5.2% ($n = 8$, $P < 0.01$) on its own. This finding indirectly confirms the original observation that glutamate reuptake is associated with extra glucose uptake (Magistretti and Pellerin, 1997; Pellerin and Magistretti, 1994), even in the resting slice. However, DL-TBOA failed to modify the effect of ouabain: in pairwise comparison, DL-TBOA+ouabain *vs*. DL-TBOA+DMSO gave the difference of +53.3 ± 6.3 ($n = 8$, P

< 0.001) which equals to the effect of ouabain alone (+52.3 ± 5.5%, n = 8, *vs*. DMSO alone) (see **Figure 3.8A**).

GABAergic signalling and the consequent activation and phosphorylation of $GABA_A$ receptors ($GABA_ARs$) are also associated with highly increased glucose turnover in the hippocampus and elsewhere in the brain (Ackermann et al., 1984; Nudo and Masterton, 1986; Peyron et al., 1994). In accordance with this, the $GABA_AR$ agonist, muscimol (100 μM) also stimulated glucose uptake, comparably to ouabain (by 44.1 ± 11.6, n = 8, P > 0.05 *vs*. ouabain) (**Figure 3.8A**). Moreover, the $GABA_AR$ antagonist, bicuculline (20 μM) prevented ouabain from stimulating glucose uptake, so that ouabain + bicuculline was no longer different from either DMSO control or bicuculline alone (n = 8, P > 0.05). This suggests that the ouabain-induced partial collapse of membrane potential triggered transmitter release, including that of GABA, which in turn massively stimulated glucose uptake via $GABA_AR$ activation. Indeed, this hypothesis was directly tested by measuring ^{3}HGABA release from hippocampal slices, following a protocol modified from our previous publications (Bitencourt et al., 2015b; Köfalvi et al., 2000). The slices were loaded for 10 min with ^{3}HGABA after 60 min recovery, then transferred to release chambers and superfused thereafter. Ouabain (300 nM) triggered an immediate and strong release of the preloaded ^{3}HGABA from the slices as compared to DMSO, which returned soon to baseline as ouabain was removed (**Figure 3.8B**).

Next – albeit predicted by a previous study (Bojorge and de Lores Arnaiz, 1987) – high concentration of insulin (300 nM) did not counteract the stimulator action of ouabain (+55.9 ± 5.5_5% facilitation with ouabain+insulin combined *vs*. DMSO control, n = 6), suggesting that insulin does not likely affect the Na^+/K^+-ATPase in this assay (figure not shown).

Last but not least, rimonabant (500 nM) failed to reduce glucose uptake in the presence of ouabain (+54.9 ± 6.1% facilitation with ouabain+rimonabant combined *vs*. DMSO control, n = 6, figure not shown), although rimonabant *per se* did so (see **Figure 3.4**). The lack of rimonabant action in the presence of ouabain may seem like ouabain preventing CB_1Rs from putatively controlling the Na^+/K^+-ATPase, but it is probably an artefact in a metabolically highly challenged and disturbed slice. As mentioned in the Introduction, CB_1R activation has been shown to stimulate the pump in brain

synaptosomes (Araya et al., 2007), but gramicidin, a Na^+/K^+-ATPase activator alone did not trigger glucose uptake in a previous study (Porras et al., 2008), because an additional Ca^{2+} signal was also required to do that. Thus, CB_1R inverse agonists were not expected either to reduce glucose uptake by deactivating the Na^+/K^+-ATPase, at least not in such an assay where a Na^+/K^+-ATPase inhibitor depolarizes the slice in itself.

Thus, it was important to compare the action of CB_1R antagonists in a direct manner, on free phosphate production from 2 mM ATP in hippocampal membranes, in the presence or absence of ouabain.

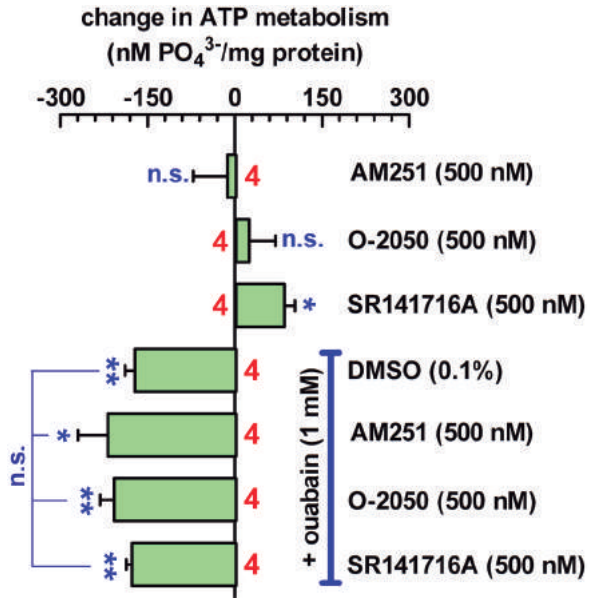

Figure 3.9 – Effect of CB_1R blockade on Na^+/K^+-ATPase activity in permeabilized synaptosome-enriched hippocampal membranes. Ouabain was used at a higher concentration than above, at 1 mM, to maximize Na^+/K^+-ATPase blockade. Red numbers at the bottom of the bars indicate the number of animals used (n). Bars represent mean ± S.E.M.; *P < 0.05, **P < 0.01, n.s., not significant.

We found that neither the neutral antagonist, O-2050 nor the inverse agonist, AM251 affected the activity of Na^+/K^+-ATPases ($P > 0.05$) (**Figure 3.9**). Curiously, rimonabant, which is a structural analogue of AM251, stimulated Na^+/K^+-ATPase-mediated ATP metabolism, because ouabain prevented this effect of rimonabant. It is well-known that cannabinoid ligands sometimes possess additional off-targets besides their cognate receptors (Köfalvi, 2008), which could explain the discrepancy in the

results, but based on the known off-targets of rimonabant, we could not make an educated guess about its mechanism of action on the Na^+ pump. In conclusion, CB_1R ligands did not prove useful to facilitate either glucose uptake or insulin sensitivity in the healthy rodent brains throughout the assays here optimized.

To expand the quest for the possible utility of CB_1R modulators, we decided to move onto a systemic metabolic disease model known to alter CB_1R expression in the hippocampus (Duarte et al., 2007a), namely, the streptozotocin (STZ) -model of T1D. It is a general dogma that diabetes does not affect brain glucose uptake, thus it may be necessary to push to systems to the maximum performance to reveal differences. In this model, we aim at testing the diabetic brain both under resting and strongly stimulated conditions.

To verify which form of chemical stimulation serves best the project interest, 4-aminopyridine (4-AP) was compared with high K^+. Habitually both stimulations to evoke transmitter release from synaptosomes are used (Bitencourt et al., 2015b), and 4-AP is also used to stimulate metabolic fluxes in the hippocampal slices for ^{13}C nuclear magnetic resonance studies (Duarte et al., 2012c; Valente-Silva et al., 2015). Comparing the results obtained through the stimulation by 4-AP and K^+ we observed that the hippocampal slices are resistant to at least 30 mM K^+ stimulation for 30 min, and both K^+ and 4-AP produced a concentration-dependent increase in both ^{3}HDG uptake and ^{14}C loss (*i.e.* glucose metabolism) (**Figure 3.10**).

The EC_{50} of 4-AP was calculated to 102.2 μM and the E_{max} amounted to 119.0% of control, *i.e.* much more potent but way less efficacious than high K^+ to stimulate glucose turnover, hence 4-AP was no longer considered to be included in our experiments. Surprisingly, mouse hippocampal slices did not resist to 30 min treatment with 30 mM K^+ (the cut-off K^+ concentration was 50 mM for the rat slices), meaning that uptake in 30 mM K^+ was even smaller than in the NaCl control, that is, the cells probably shut off and died (figure and data not shown). Mouse slices did respond well to 20 mM K^+ treatment for 30 min (not shown), but to avoid working close to the maximal capacity of the system, it was chosen only a reduced 15 mM K^+ for the mouse slices for the forthcoming experiments.

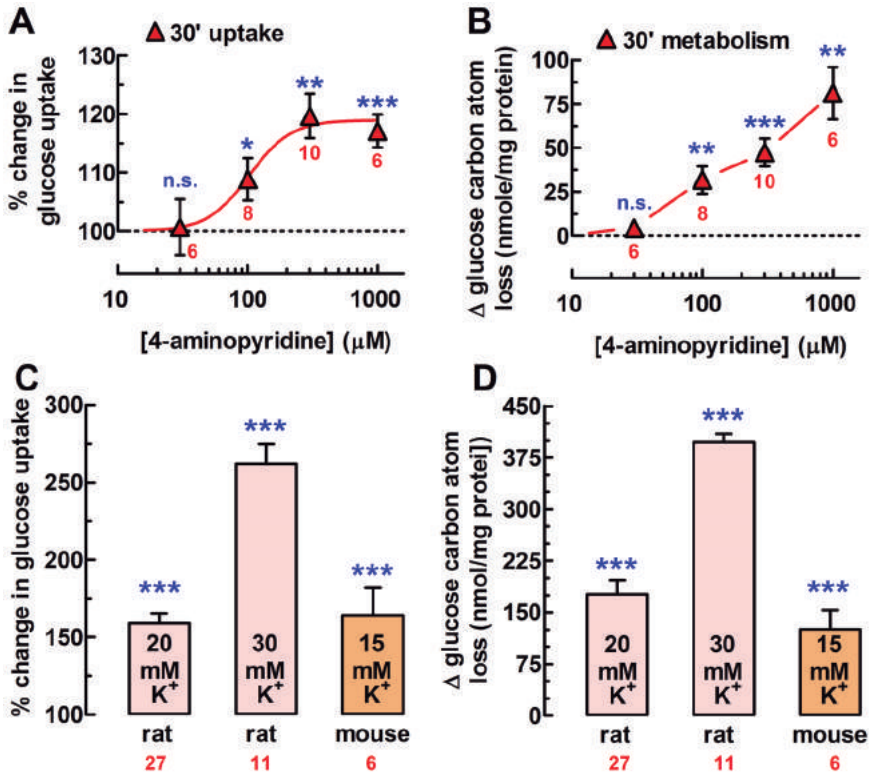

Figure 3.10 – The effect of chemical depolarization on glucose uptake and metabolism in the rat and mouse slices. After 60 min recovery, the slices were treated with either the K^+ channel blocker, 4-aminopyridine or high K^+ concentration in the bath as indicated (where NaCl served as an osmotic control, marked as 100%). Red numbers at the bottom of the bars/symbols indicate the number of animals used. The high animal number for 20 mM K^+ stimulation is due to the inclusion of later data from various studies throughout the years which are not presented elsewhere in the thesis. Bars represent mean + S.E.M.; *P < 0.05, **P < 0.01, ***P < 0.001, n.s., not significant.

3.2 TYPE-1 DIABETES IMPAIRS BRAIN GLUCOSE TURNOVER IN A CB_1R-DEPENDENT FASHION

STZ accumulates in pancreatic β cells after systemic injection, and rapidly kills them, predominantly via DNA alkylation (Bennett and Pegg, 1981). This leads to the strong reduction of circulating insulin levels. Our group previously found that the systemic STZ model of T1D decreases CB_1R expression in the rat hippocampus (Duarte et al., 2007a). As **Figure 3.4** documents, both CB_1R inverse agonists and the genetic deletion of the receptor decrease basal glucose uptake. Hence, we became curious about

how STZ would affect CB_1R density in the mouse brain and if it had any consequence on brain metabolism. Therefore, 16 wild-type (WT) mice and 16 of their CB_1R KO littermates (Ledent et al., 1999) were randomly assigned into four groups of 8, and one of the WT groups as well as one KO group were rendered diabetic, while the other two groups served as control.

3.2.1 Body weight and glycemia

Since there is no available information on the diabetic phenotype differences in the CB_1R KO mice, we monitored body weight and blood glucose levels during the seven weeks post-injection period. The lack of CB_1R receptors visibly influenced the results of untreated T1D on body mass and systemic glucose disposal (**Figure 3.11**), which is in fact new and interesting information, though not surprising taken the roles of CB_1R in systemic metabolism, as discussed in the Introduction (Bermúdez-Silva et al., 2009; Matias et al., 2008b; de Pasquale et al., 1978).

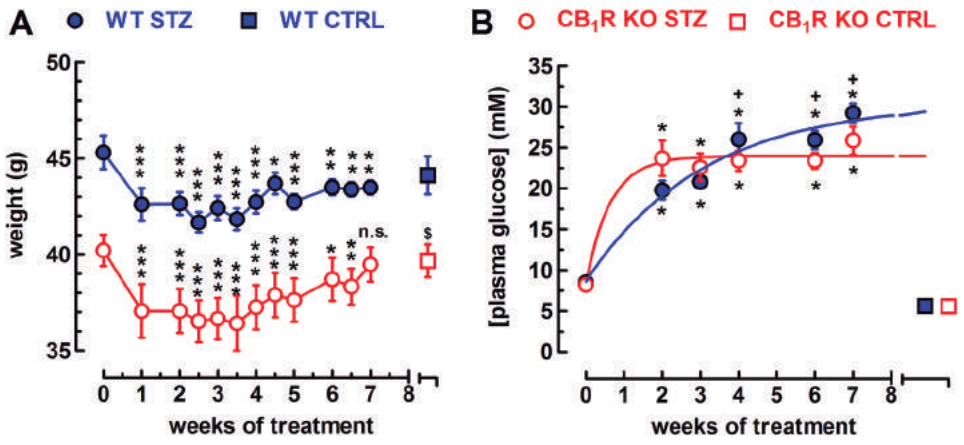

Figure 3.11 – (A) CB_1R KO mice are almost 10% lighter than their WT littermates, and by the 7th week post-injection, they recover their original body weight, unlike their diabetic WT littermates, which are unable to gain mass. B) Blood glucose levels of the diabetic CB_1R KO mice also reach maximum within two weeks, contrasting diabetic WT mice. Symbols represent mean ± S.E.M. of 8 mice; *P < 0.05, **P < 0.01, ***P < 0.001, *vs*. the initial point above 0 weeks, as determined with one way ANOVA followed with Dunnett's multiple comparison *post-hoc* test; $^{+}$P < 0.05, $^{\$}$P < 0.001 between WT and CB_1R KO; n.s., not significant.

As **Figure 3.11A** illustrates, the starting body weight of the total 16 CB_1R KO mice (at 6 weeks age) used in this part of the study was 9.1 ± 1.3% smaller ($P < 0.001$) than their wild-type littermates. After provoking insulinopenia by STZ-injection, diabetic body weight loss at its peak was slightly less severe for the WT mice (25 day post-injection: $-7.6_5 \pm 1.2_5$% of starting body weight, $P < 0.001$ by one-way ANOVA followed by Dunett's multiple comparison test) than in the CB_1R KO mice (at 25 day post-injection: -9.4 ± 3.6%, $P < 0.001$). However, CB_1R KO mice recovered from body weight loss by the 7th week post-injection, having only 1.8 ± 2.2% loss of the original body weight ($P > 0.05$) while the WT mice did not fully recover (-4.0 ± 0.8%, $P < 0.01$) (**Figure 3.11A**). Note that these mice already reached their average adult body weight, thus there was no significant weight gain in the sham animals during the 7 weeks of the treatment period.

Blood glucose levels for the WT mice (5.6 ± 0.1 mM) were not different from those of the CB_1R KO mice (5.6 ± 0.2 mM; $P > 0.05$). However, after STZ-injection, WT glycaemia constantly rose and became significantly different between various time-points (calculated with one-way ANOVA followed by Bonferroni's post-hoc test), with the estimated maximum of 30.6 ± 2.3 mM (mean + S.D.) (**Figure 3.11B**). As for the CB_1R KO mice, blood glucose levels stabilized at the plateau of 23.9 ± 0.8 mM by the 2nd week post-injection (**Figure 3.11B**). These estimates were obtained from fitting one-phase association curves onto the data points.

3.2.2 Diabetes impairs cortical and hippocampal glucose turnover

Upon termination of the treatment period, 1 mouse from each group was sacrificed and used simultaneously, in the same experiment, allowing paired analysis of the uptake parameters. In the resting and the 15 mM K^+-depolarized slices, glucose uptake during the 30 min period was ~25% smaller in the cortex and hippocampus of both diabetic WT mice and the CB_1R KO sham (*vs*. their WT littermates) (n = 8 mice pairs, **Figure 3.12A,B).**

Interestingly, diabetes failed to further compromise resting or stimulated glucose uptake in the cortex and hippocampus of the CB_1R KO mice, thus revealing mutual occlusion between diabetes and genetic deletion of the CB_1R. Although high-K^+-stimulation lost its capacity to trigger equivalent amount of glucose uptake in absolute

terms, in either the diabetic or the CB_1R KO animals (**Figure 3.12A,B**), the relative effect of depolarization when normalized to the respective resting (NaCl) control was similar throughout the groups and brain areas, varying between +53.4% (hippocampus sham WT) and +68.3% (cortex sham CB_1R KO). There was no statistical difference among the absolute amount of K^+-induced glucose uptake throughout the groups despite strong tendencies, probably due to the low statistical power of n = 8 animals.

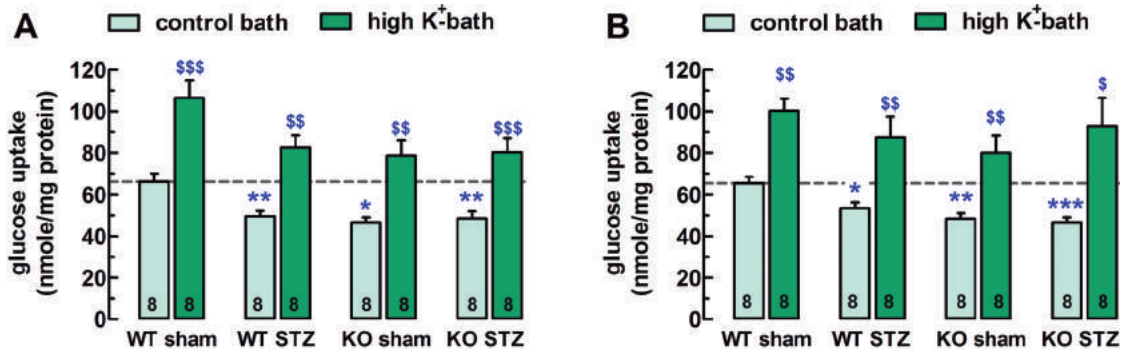

Figure 3.12 – Seven weeks of STZ-induced diabetes and the genetic deletion of the CB_1R cause mutually occlusive impairment on both the resting (with 15 mM extra Na^+) and the 15 mM K^+-depolarization induced uptake of glucose in the cerebral cortex (A) and the hippocampi (B) of male mice of the CD-1 strain. Bars represent mean + S.E.M. of 8 mice; *P < 0.05, **P < 0.01, ***P < 0.001 *vs*. WT sham resting uptake; $^{\$}$P < 0.05, $^{\$\$}$P < 0.01, $^{\$\$\$}$P < 0.001 *vs*. the respective NaCl control of the same animal, as determined with one way ANOVA followed with Dunnett's multiple comparison post-hoc test.

Importantly, $^{14}C_6$-glucose was co-applied with ^{3}HDG in these experiments, and thus measured ^{14}C loss from the slices. As expected, K^+-depolarization significantly increased dissipative glucose carbon atom metabolism, as compared to the NaCl control (**Figure 3.13A,B**). There was no difference in the dissipative glucose metabolism throughout the groups (**Figure 3.13A,B**), with the exception that K^+-depolarization could not significantly increase the resting value in the hippocampi of the diabetic CB_1R KO mice (P > 0.05 *vs*. NaCl control) (**Figure 3.13B**).

The obtained data is thrilling for two reasons. First, it reports for the first time that chronic hyperglycaemia, insulinopenia or both affect brain glucose uptake, and second, that all these are only and exclusively dependent on the CB_1 cannabinoid receptor.

Nonetheless, further studies are required to unveil the underlying link between CB_1R deficiency and lower glucose uptake.

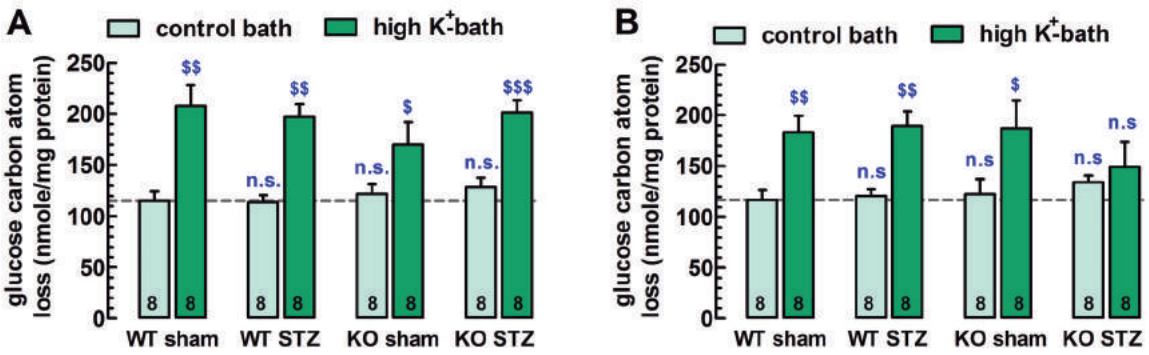

Figure 3.13 – Seven weeks of STZ-induced diabetes and the genetic deletion of the CB_1R did not significantly affect glucose metabolism in acute cerebrocortical (A) and hippocampal (B) slices, except when combined in the hippocampus. Bars represent mean + S.E.M. of 8 mice; $P < 0.05, $$P < 0.01, $$$P < 0.001 *vs*. the respective NaCl control of the same animal, as determined with one way ANOVA followed with Dunnett's multiple comparison post-hoc test.

There are a handful of *in vivo* animal studies tackling the effects of STZ-induced diabetes on brain glucose transport. In one study, the authors concluded that 13 weeks of untreated STZ reduced systemically administered ^{3}HDG accumulation in the frontal cortex of rats (Kainulainen et al., 1993). However, when they normalized the uptake values to the blood glucose levels, essentially no difference was seen in the cerebral uptake between sham and diabetic animals. Diabetes also did not alter the density of glucose transporters 1 and 3 (GLUT1,3) in the brain of the animals. Another *in vivo* study with only 2 weeks of diabetes concluded similar lack of difference in glucose uptake throughout various brain regions of diabetic rats as compared with sham rats, and the authors also found no change in either the vascular-type 55-kDa GLUT1 or in the parenchyma-type 45-kDa GLUT1 or in GLUT3 densities (Simpson et al., 1999). Finally, in rats subjected to 6-8 week of STZ-induced T1D, cerebral rates of glucose uptake was found increased under normoglycemia, which was achieved with systemic insulin injection (Pelligrino et al., 1990).

From these, it is clear that differences in blood glucose, cerebral insulin concentrations, blood-brain barrier permeability and local blood fluxes all affect the

final outcome of *in vivo* experiments, and either the putative impairment in cerebral glucose uptake or the technical approaches were not sufficiently robust to reveal solid conclusions.

The densities of our proteins of interest in the cerebral cortex of the four groups of animals were also analysed. As **Figure 3.14** illustrates, there was a significant drop in CB_1R density in total membranes after 7 weeks of diabetes. Apparently, this drop was sufficient to produce the "CB_1R KO phenotype" on glucose uptake, and this appears to be the funnel where systemic diabetes converged onto glucose uptake. How diabetes affected CB_1R density is unknown to us, but it might be related with the dysregulation of the Akt-mTor pathway, which is typical in the diabetic brain and affects protein synthesis (Duarte et al., 2012a). Nevertheless, there is still no explanation for the decrease in glucose uptake under treatment with CB_1R inverse agonists or upon reduction of CB_1R density. Thus, next we analysed the crucial element of insulin signalling in total membranes of the four groups. Although there were differences in the densities of insulin receptor β-chain, IGF-1Rβ subunits, in the phosphorylation of Akt and GSK3α, we found no repetitive pattern that stood out in all the three protein groups (data not shown). We also found no change in GSK3β phosphorylation, and in GLUT1 or GLUT4 densities (the latter transporter was investigated owing to its sensitivity to insulin) (data not shown).

Interestingly, a previous study did find increased GSK3β phosphorylation in C57bl/6 mouse brain 3 days after a single injection of 150 mg/kg STZ (Clodfelder-Miller et al., 2006). The lack of insulin in fact should have decreased GSK3β phosphorylation, because the authors found a strong tau hyperphosphorylation in the brain of the 3-day-STZ mice, as a consequence of lack of insulin. STZ treatment also increased the phosphorylation of both p38 and JNK, indicating activation of these two kinases. The authors concluded that in comparison with the previously reported modest changes seen in the insulin receptor KO mice, the lack of insulin has much more deleterious effects, which may implicate the involvement of the IGF-1R in the actions of insulin in the brain. Nevertheless, the experimental layout was substantially different from ours thus it does not allow direct comparison of findings.

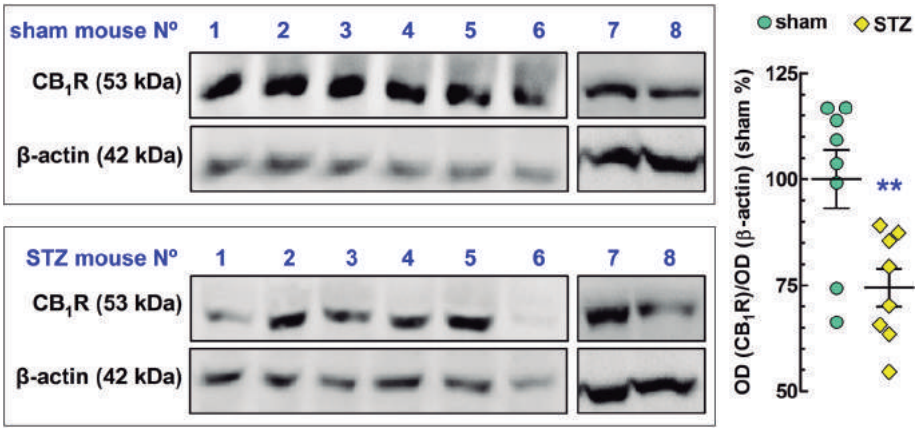

Figure 3.14 – Seven weeks of STZ-induced diabetes decreases CB1R density in cerebrocortical membranes of 13-week old CD-1 male mice. STZ was induced with one intraperitoneal injection of a low STZ dose of 40 mg/kg during five consecutive days. All animals became diabetic, and none suffered major physical disability during the maintenance of diabetes. The proteins were analysed in 3 different gels (two gels with samples from 6 animals and 2 gels with 2×2 samples). Ratios of CB_1R/β-actin densities were averaged and taken as 100%, to which the respective STZ ratios were compared. Points represent mean ± S.E.M **P < 0.01 *vs*. sham ratios.

3.2.3 Metabolic dysregulation in the rat frontal cortex recovers via a CB_1R-dependent mechanism

The above studies in diabetic mice reveal associated deficits in CB_1R densities and glucose metabolism after 7 weeks of diabetes. Next, we asked if STZ-induced diabetes also affects cerebral glucose metabolism in another species, which we assessed with a greater temporal resolution. Thus, brain slices were used from ongoing studies with diabetic rats with 2, 4 and 8 weeks of STZ (*e.g.* Baptista et al., 2011). This study in question found a transient change in major presynaptic markers without major functional consequences in the rat hippocampus with two weeks of diabetes, but these alterations returned to normal level by the 8th week. Furthermore, a new group of animals was included with an intermediate time-point, to allow better resolution for the outcome of the illness. Since the hippocampi of these rats were used for other studies, we studied the frontal cortices. **Figure 3.15** confirms that the STZ-injected rats involved in the study were in fact diabetic. The sham rats showed steadily increasing body weight taken that they had only 12 weeks of age at the beginning of the procedures, while the STZ-injected rats showed reverse tendency. Blood glucose levels were not different among groups of the same treatment, but were highly elevated in the diabetic animals.

Slice experiments were carried out in pairwise manner (slices of one sham and one diabetic animal divided into four or five common chambers). The age of the sham animals (*i.e.* the fact that they were used at different time-points) did not modify the uptake of glucose either in control (+30 mM NaCl) bath or in high-K^+ (30 mM) bath. The control sham glucose uptake in the two-week sham (2W-sham) amounted to 79.4 ± 6.9 nmol/mg protein, n = 14), which was not significantly different from the corresponding value in the mice shown in **Figure 3.12A** (66.3 ± 2.3 nmol/mg protein, n = 8, P > 0.05).

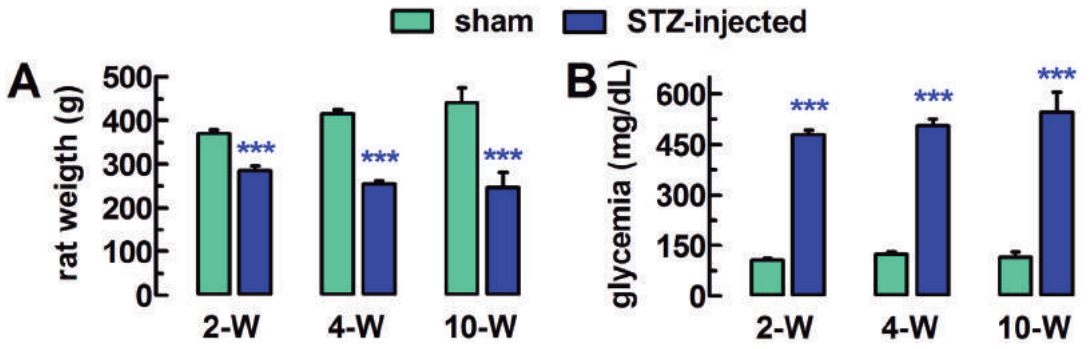

Figure 3.15 – Body weight and blood glucose levels of rats (A). Initial values of the sham and diabetic animals were not significantly different (see Methods), thanked to the randomization. (B) glycemia values for sham and diabetic animals. Bars represent mean + S.E.M. of n = 8-14 rats/group; ***P < 0.001, as determined with two-tailed unpaired Student's *t*-test.

Two-weeks post-STZ injection (2W-STZ), rat cortical slices exhibited 15.2 ± 3.9% decrease in resting glucose uptake (n = 14, P < 0.01) (**Figure 3.16A**), which was normalized by acute treatment of the slices with the synthetic cannabinoid agonist, WIN55212-2 (500 nM; n = 7, P > 0.05 *vs*. DMSO). In contrast, the CB_1R-selective neutral antagonist, O-2050 (500 nM) exacerbated the impairment of glucose uptake to -24.8 ± 7.3% compared to sham (n = 7, P < 0.05) (Figure 16A). Importantly, neither of the tested cannabinoid ligands affected glucose uptake in the sham animals (*P* > 0.05) (**Figure 3.5A**). This suggested that two weeks of insulinopenia rendered the rat frontocortical slices deficient in the CB_1R-mediated basal coupling to glucose uptake, and this time, even the CB_1R neutral antagonist was able to further impair glucose uptake, although this effect of O-2050 was not significantly different from STZ DMSO control (P = 0.06). Nevertheless, these data revealed some indirect effect for CB_1Rs and

hinted a possible gain-of-function of an endocannabinoid-CB_1R signalling pathway to facilitate glucose uptake.

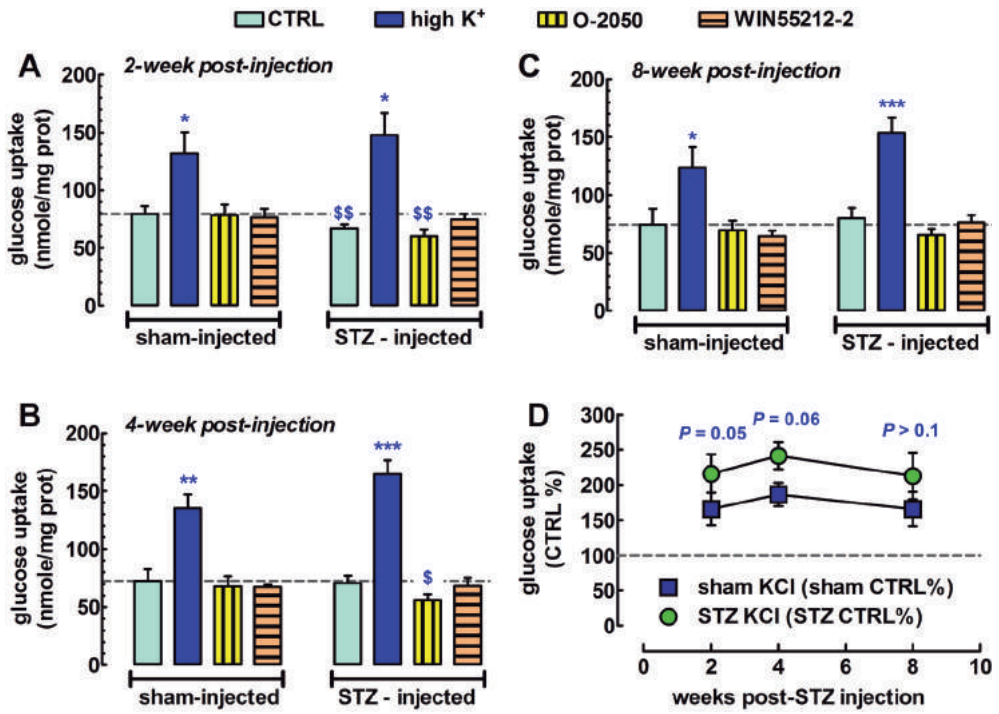

Figure 3.16 – STZ-induced insulinopenia impairs resting glucose uptake in a CB_1R-dependent fashion. A) Two-weeks in STZ-diabetes decreased resting glucose uptake, which is recovered acutely with the synthetic cannabinoid, WIN55212-2 (500 nM). The neutral CB_1R antagonist, O-2050 (500 nM) further decreased glucose uptake, but it was not significantly different from STZ DMSO control. B) After 4 weeks in diabetes, resting glucose uptake normalized, but O-2050 uncovered an impairment, which was likely masked by boosted endocannabinoid signalling. C) After 8 weeks, there was no impairment detected. 30 mM K^+-stimulated glucose uptake was tendentiously greater at the three time-points, but without reaching significance. A-C) All bars and symbols represent mean + or ± S.E.M. of n = 7 - 14 animals; *P < 0.05, **P < 0.01, ***P < 0.001 *vs*. sham DMSO, and $^{\$}P < 0.05$, $^{\$\$}P < 0.01$ *vs*. STZ DMSO control, as obtained with one-way ANOVA following by Bonferroni's post-hoc test. D) The amount of high K^+-stimulated glucose uptake normalized to the appropriate sham or STZ control was tendentiously at the border of significant difference between sham and diabetic animals. Note that all four chambers had identical osmotic condition (achieved with extra NaCl or KCl) and 0.1% DMSO.

Indeed, as **Figure 3.17** reveals, there was a 30.5 ± 5.6% transient decrease in CB_1R density of the sham frontal cortex after 4 weeks in diabetes, which returned to the sham level by the 8th week post-injection. In accordance with this, resting glucose

uptake after 8 weeks in diabetes was not different from that in sham animals, and cannabinoid ligands also left glucose uptake unaffected. This is already in clear contrast with the above findings in mice, taken that after 7 weeks in diabetes, resting glucose uptake remained impaired in the mice, and so did the high-K^+-stimulated glucose uptake (**Figure 3.12A**). This latter phenomenon uncovers an additional layer of difference, because the high-K^+-stimulated glucose uptake tended to be greater in the STZ-treated rats - rather than decreased - throughout the 3 time-points (**Figure 3.16D**).

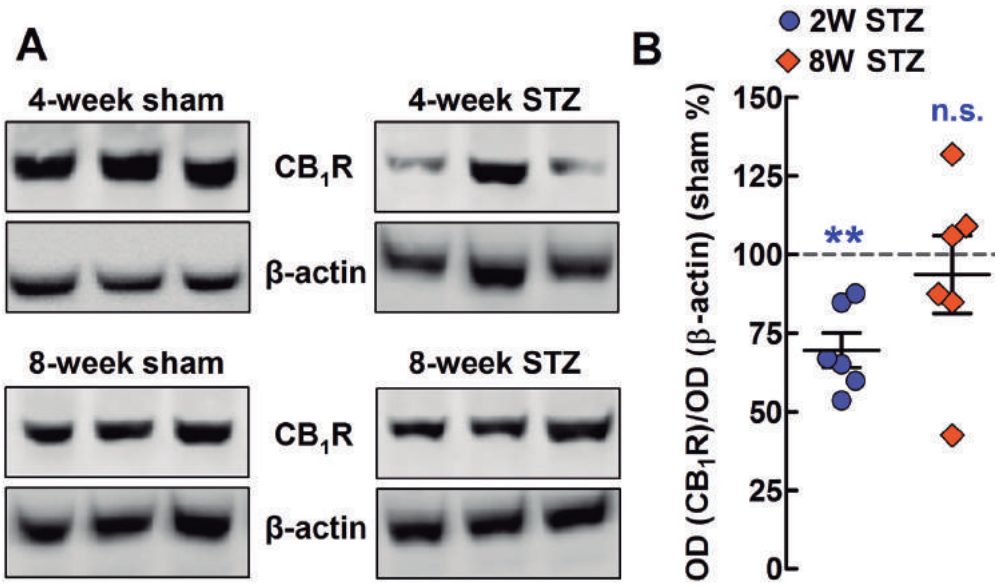

Figure 3.17 – Four weeks of STZ-induced diabetes decreases CB_1R density in frontocortical membranes of 14-week old male Wistar rat, which recovers within the following month. STZ was induced with one single intraperitoneal injection of streptozotocin (STZ). A) The proteins were analysed in 2 different gels (two gels with samples from 6 rats). B) Ratios of CB_1R/β-actin densities of the sham animals were averaged and taken as 100%, to which the respective STZ ratios were compared. All bars and symbols represent mean ± S.E.M, **P < 0.01 *vs*. sham ratios.

Additional analysis of insulin signalling pathways revealed that the density of insulin and IGF-1 receptors as well as the phosphorylation of Akt at Ser473 (figure and data not shown) remained unchanged after 1 or 2 months in diabetes, however, by the end of the first month, phospho-Ser21-GSK3α levels were 17.4 ± 4.1% smaller in the diabetic rats (n = 6, P < 0.01), which was reverted to a small but non-significant

facilitation by the end of the 8-week period, and phospho-S9-GSK3β levels became elevated 19.5 ± 7.2$_5$% (n = 6, P < 0.05) after 8-week in STZ (**Figure 3.18).**

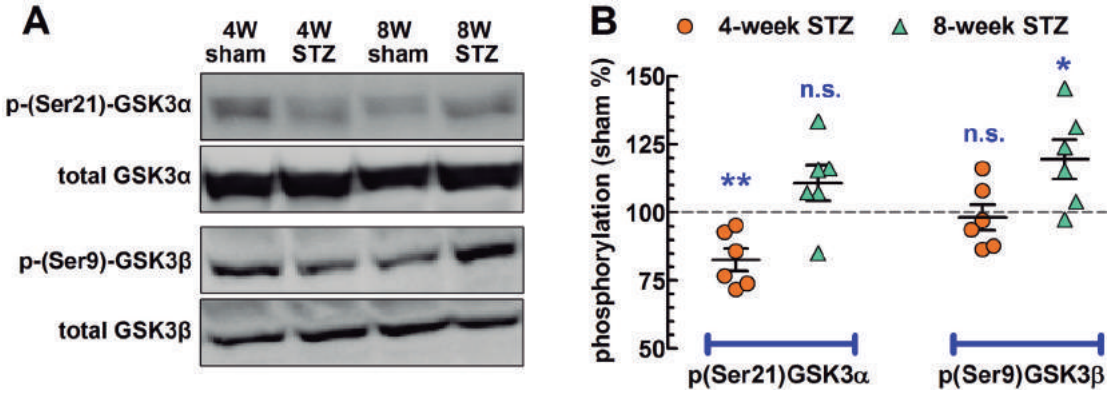

Figure 3.18 – Four weeks of STZ-induced diabetes decreases phospho(Ser21)GSK3α density, while in frontocortical membranes of 14-week old male Wistar rat, which recovers within a month. In contrast, GSK3β phosphorylation at Ser9 becomes significantly elevated by this time. (A) Representative blots. (B) Ratios of phospho-GSK3/total GSK3 densities in the sham animals were averaged and taken as 100%, to which the respective STZ ratios were compared. All symbols represent mean ± S.E.M *P < 0.01, **P < 0.01 *vs*. sham ratios.

As for the resting glucose metabolism, neither diabetes nor cannabinoid ligands altered glucose carbon atom loss in the frontal cortex. Nevertheless, under depolarization by 30 mM K^+, ^{14}C loss from taken up $^{14}C_6$-glucose was very strongly increased in absolute values expressed to protein quantity in both the 2W-STZ rats (by 109.9 ± 42.7 nmol/mg protein, which corresponds to 43.5 ± 16.3% increase, n = 7, P < 0.05) (**Figure 3.19A**) and the 4W-STZ rats (by 147.1 ± 22.0 nmol/mg protein, which corresponds to 39.8 ± 15.2% increase, n = 8, P < 0.001) (**Figure 3.19B**). After 8 weeks of diabetes, however, no significant difference was observed (36.6 ± 15.1% increase, n = 8, P = 0.08) (**Figure 3.19C**).

We recently showed that there are functional CB_1Rs in frontocortical glutamatergic nerve terminals whose activation leads to decreased glutamate release (Bitencourt et al., 2015b). If the decrease in CB_1R density affects glutamatergic terminals too, it would likely allow greater excitatory activity for the circuitry. In fact, some pathological conditions such as juvenile high fever can cause a permanent

decrease in CB_1R density in glutamatergic terminals, thus leading to the development of an epileptic phenotype in the adult (Katona, 2015).

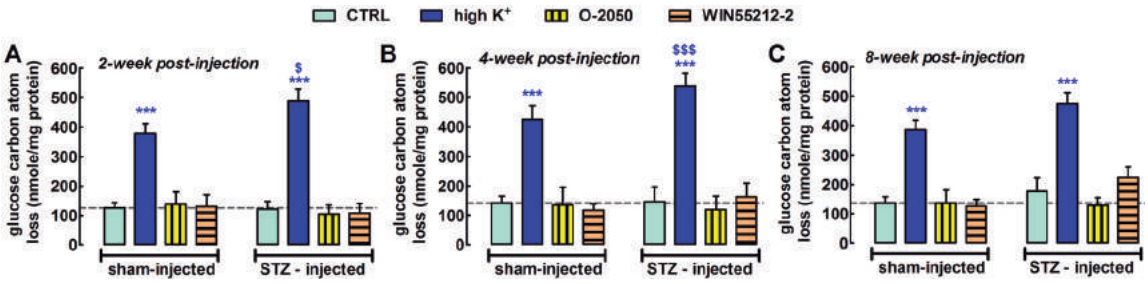

Figure 3.19 – Increased metabolic responsiveness to depolarization in the frontal cortex of STZ-treated rats in the first month of untreated diabetes. (A) 2-weeks post-injection, (B) 4-weeks post injection and (C) 8-weeks post-injection. Note that all four chambers had identical osmotic condition (achieved with extra NaCl or KCl) and 0.1% DMSO. All bars and symbols represent mean + S.E.M. of n = 7 - 14 animals; ***P < 0.001 *vs*. sham DMSO, and $^{\$}$P < 0.05, $^{\$\$\$}$P < 0.001 *vs*. sham KCl, as obtained with one-way ANOVA following by Bonferroni's *post-hoc* test.

The likely explanation for the increased metabolism in terms of absolute values (**Figure 3.18A,B**) can be therefore a result of possible decrease in CB_1R density in glutamatergic nerve terminals which permits a greater excitability in the slice under high K^+-depolarization, and may lead to a greater energy expenditure. Additionally, if CB_1R density drops in the mitochondria, it would allow glucose oxidation to occur at a greater speed (Duarte et al., 2012c).

Altogether, the therapeutic relevance of the systemic STZ-injection model is limited, because apparently, rats and mice are affected differently by untreated T1D, and it is not currently known whether the rat or the mouse model resembles what happens in diabetic patients. Additionally, it is rare but not uncommon that humans endure T1D for a long time without being diagnosed and treated with insulin, at least not in the modern world. The more typical complication of T1D is a result of insulin-induced hypoglycemia – at least in animal models (Sherin et al., 2012), but in diabetic patients, there is limited evidence for recurrent hypoglycemia-induced serious long-term consequences on brain structure and cognitive abilities (Rooijackers et al., 2015). Anyhow, T1D, especially when untreated, is not without deleterious effects to the brain, since it causes damage to the microvasculature and the blood-brain barrier, though the

permeability to glucose from the blood to the brain remains unaffected (Duarte, 2015). Our group and collaborators for instance did not find major neurochemical alterations at the presynaptic level in the hippocampi and the retina of STZ-treated rats after 8 weeks in diabetes (Baptista et al., 2011). Nevertheless, the lack of conclusive data does not contradict other reports that witnessed neurodegeration, deficiency of the principal cells and impaired glutamate clearance by astrocytes (Duarte, 2015), alterations in the density of $GABA_AR$s and cholinergic receptors (Sherin et al., 2012), and impairment in learning and memory and hippocampal NCAM expression (Baydas et al., 2003). Many of these impairments can also lead to epilepsy, and in fact, there is an apparent causal relationship between T1D and focal epilepsy of temporal lobe origin (Keezer et al., 2015). Assuming that the CB_1R has an important role as a circuit breaker, a decrease in CB_1R density (Ludányi et al., 2008) together with the impaired glutamate clearance can surely be the perfect receipt for disaster.

In summary, evidence for the involvement of the CB_1R in the alterations of cerebral glucose metabolism in the T1D models were find, although the data do not point out a clear therapeutic role for this receptor, which is largely due to the lack of conclusive data on the mechanism of action as well as the divergent phenotypes of the diabetic rats and mice. Thus, we decided to move onto other metabolic disease models known to affect the homeostasis of the brain.

3.3 ICV-STZ CAUSES MEMORY IMPAIRMENT RELATED TO METABOLIC CHANGES AND SYNAPTIC DYSFUNCTION

Notably, STZ can be administered intracerebroventricularly (icv), which method was pioneered by Siegfried Hoyer's group (Duelli et al., 1994; Lannert and Hoyer, 1998; Nitsch and Hoyer, 1991). This model causes deregulation at the level of energy substrates and energy metabolism in the brain, and triggers an Alzheimer's disease (AD)-like phenotype. To attempt to further study the relationship between brain metabolic dysfunctions and memory impairment, the icv administration of streptozotocin (STZ) was selected (Correia et al., 2011; Salkovic-Petrisic et al., 2013). The icv-STZ injection has no major known consequence at the peripheral level but does decrease cerebral insulin sensitivity (Grünblatt et al., 2007). The metabolic dysfunction

in the hippocampus is a key event associated with the initiation and/or evolution of memory impairment, therefore strongly resembles Alzheimer's disease (AD).

AD is a common form of progressing dementia of either genetic or sporadic origin, with no cure. The sooner the discovery of the disease the better the chances are to slow its progress (Friedrich, 2013; Reiman and Langbaum, 2009). Neuroimaging including morphometric analysis of cortical thinning along with hippocampal volume reduction, as well as positron emission tomography (PET) evaluation of brain ^{18}F-fluorodeoxyglucose (^{18}FDG) uptake are routinely used to detect preclinical AD (Mistur et al., 2009). As a result of both decreased cellular glucose uptake and regional atrophy, a curtailed ^{1818}FDG-PET signal is a reliable early marker of Alzheimer's-type dementias preceding most other clinical symptoms by many years (Phelps, 2000). Since AD involves both disturbances of glucose homeostasis and cerebral insulin resistance (Correia et al., 2012), AD is also termed as “type-3 diabetes” (Lester-Coll et al., 2006; de la Monte and Wands, 2008) and cerebral glucoregulation may emerges as a novel therapeutic target in AD.

In patients, one of the first identified symptoms of dementia is the progressive loss of the declarative memory (Harrison, 2013; Nestor et al., 2006), which corresponds to the spatial memory in rodents, a hippocampal-dependent type of memory. First, to evaluate the extent of memory impairment in the icv-STZ animal model we performed a battery of behavioural tests.

3.3.1 Icv-STZ induces memory impairment

Firstly, an open field test was performed to access animal locomotion. Icv-STZ treatment did not affect the locomotion: the total distance travelled (22.5 ± 3.7 m, n = 6) was not significantly different when compared to the sham group (26.5 ± 1.2 m, n = 7, P > 0.05), **Figure 3.20**.

The novel object recognition task (NORT), developed by Ennaceur and Delacour (1988), relies in rodent innate exploratory behavior. This task was used to assess nonspatial recognition memory (Griffin et al., 2009b; O’Callaghan et al., 2007) between our animal icv injected with the vehicle (icv-veh) and the icv-STZ-treated ones. This task gives the recognition index score (RI), which quantifies the relation between the

exploration time of the two objects. The RI may vary between -1 and +1, where -1 represents higher exploration of the familiar object, 0 represents no differentiation between them and +1 means higher exploration of the novel object. The icv-STZ animals displayed a RI score (**Figure 3.20B)** with no statistical differences from zero (icv-STZ; – 0.014 ± 0.086, n = 7. P > 0.005), meaning that there was no discrimination between the familiar and novel object. While the icv-veh animals displayed a positive recognition index score (icv-veh, 0.32 ± 0.064, n = 8 P < 0.001), **Figure 3.20B**.

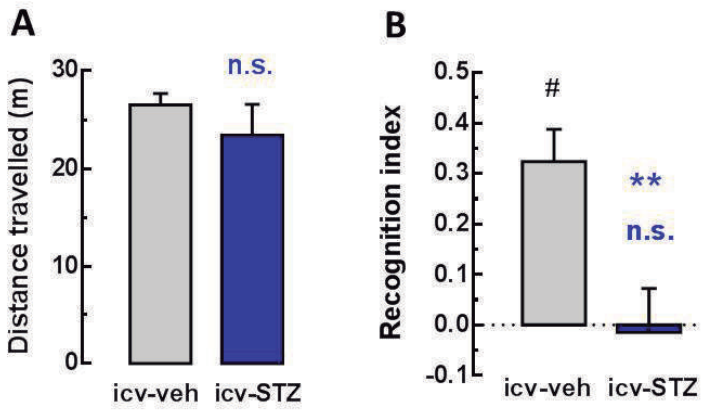

Figure 3.20 - Effect of the icv-STZ treatment in the open field (A) and novel-object recognition task (B). (A) icv-STZ treatment did not modify the distance travelled in the arena (P > 0.05) (B) icv-STZ treatment decreased short-term memory performance in the NORT task. The data are mean + SEM of n = 7-8 rats per group. **P < 0.005 compared to the control group; #P < 0.05 compared to a hypothetical value of 0 in (B).

Note that during the training and testing phases, the total exploration time did not differ between the icv-veh and icv-STZ animals. The fact that the animal recognize the familiar object and distinguish it from the novel one (RI > 0; P < 0.05) means that it formed a memory about the former object (Ennaceur, 2010) and preferentially explores the novel one. This preference for novelty is merely observed when memory is highly accessible – recent memory phase (Antunes and Biala, 2012b; Ennaceur, 2010). This recognition task involves more cognitive skills since the NORT paradigm depends of the influence of both the hippocampus and the perirhinal cortex (Aggleton et al., 2010). Furthermore, the aptitude to gauge a previous item as familiar depends of the integrity of the medial temporal lobe (Hammond et al., 2004). The typical rodent exploratory behaviour was observed in the control animals while the treated ones displayed no

preference between the novel and the familiar object. This impairment observed in the icv-STZ animals corresponds to the same memory domain affected in the early phases of AD (Espinosa et al., 2013b; Selkoe, 2001), because the early neuropathological changes happen in the rhinal cortical region (Braak and Braak, 1985).

The Morris water maze (MWM) task was used then to evaluate the existence of long-term spatial memory deficits. The rats had to learn to escape from the water by finding the submerged platform, which is always in the same quadrant. In this way, the animals are required to create a cognitive map consisting of the associations between the localization of the platform and the environmental cues on the walls of the room or the water maze itself and (Morris et al., 1982; Prediger et al., 2006; Vorhees and Williams, 2006).

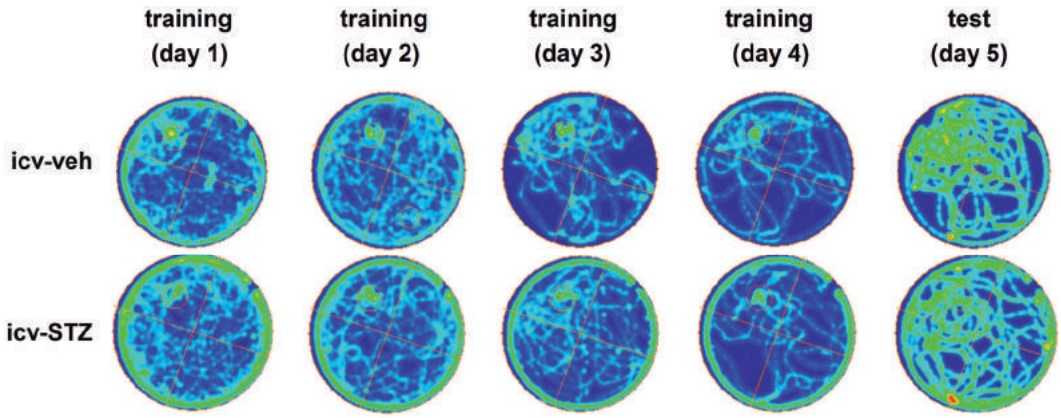

Figure 3.21 – Morris water maze task – spatial version. Average occupation plot of the animal group's centre point representing the pattern of exploration of the icv-veh and icv-STZ during the MWM task. Sham, n=8 and icv-STZ, n = 7. The icv-veh animals present typical explorations were, in the initial trials, the animals show a tendency for *thigmotaxis* behaviour or to perform random searches in the arena (A,B). As expected, in advanced training trials, icv-veh show a gradual change in behaviour, characterized by progressive active quests for the platform, target oriented. As icv-veh animals get acquainted with the environment and paradigm rules, they develop the skill of finding the platform from different starting positions, as shown by the latency to reach the platform. The icv-STZ animal behaviour show a general tendency for *thigmotaxis* behaviour through all the trials with increased incursion (the animal starts moving inwards the platform) and scanning among the trial days with high target scanning behaviour for the last day of trial. During the probe test, the occupation plot show a higher presence of the icv-veh animals in the correct quadrant (where the platform used to be) compared with the icv-STZ animal that present a more random maze exploration.

During the training, all the animals learned to navigate to the platform using spatial mapping (or distal cue) strategy and showed a decrease in escape latency (**Figure 3.21**). Nevertheless, the icv-STZ treated animals showed a lower spatial learning performance and statistical differences were found in the latency times during the training phase after the first day of training ($P < 0.05$) (**Figure 3.22A)**. In the probe trial, statistical difference was observed between the control and icv-STZ animals in their escape latency (icv-veh 18.6 ± 5.8 sec, n = 8; icv-STZ 33.0 ± 8.4, n = 7; $P < 0.05$) (**Figure 3.22B**). Regarding the selectivity of the platform search, the control animals spent more time in the correct quadrant (icv-veh, 23.5 ± 1.9 sec, n = 8; icv-STZ 15.2 ± 1.1 sec n = 8, $P < 0.05$) (**Figure 3.22C**), and also displayed a higher number of crossings of the former location of the removed platform (icv-veh 3.36 ± 0.56 crossings, n = 8; icv-STZ 1.36 ± 0.39 crossings n = 7; $P < 0.05$) (**Figure 3.22D**), serving as a positive control for the probe trial.

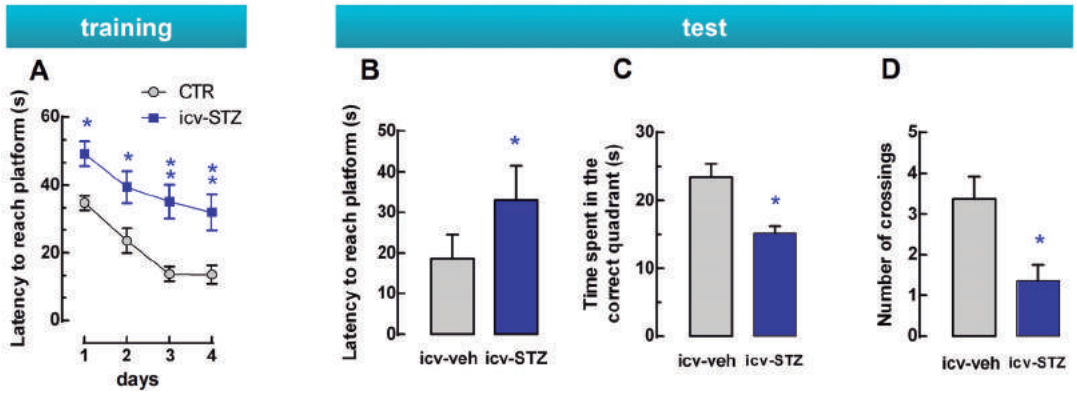

Figure 3.22 – Statistical analysis of the experiments presented in Figure 3.21. (A) Latency to reach the platform during the training (learning phase). (B) Latency to reach platform during the probe trial (s). (C) Time spent in the correct quadrant (s). (D) Number of the former platform crossings. Data represent mean ± or + S.E.M. of n = 8 icv-veh and n = 7 icv-STZ rats. A) *P < 0.05, **P < 0.01, as determined with Repeated Measures two-way ANOVA, (B-D) *P < 0.05, as assessed with two-tailed unpaired Student's *t*-test.

3.3.2 Icv-STZ alters the synaptic plasticity in the hippocampus

Considering the cognitive modifications described above, now we probed for possible underlying neurophysiological alterations in the hippocampal circuitry and synaptic plasticity. First, we aimed at evaluating the effect of icv-STZ treatment on the

recruitability of active fibers with increasing stimulus strength, that is, we carried out an input-output curve (Katz and Miledi, 1970; McLachlan, 1978). The response to the increasing stimulus is saturable, but the maximum density of active synapses and the stimulus strength needed for saturation may differ upon treatment. As **Figure 3.23A** shows, icv-STZ did not significantly affect synaptic density, that is, the circuitry was structurally intact.

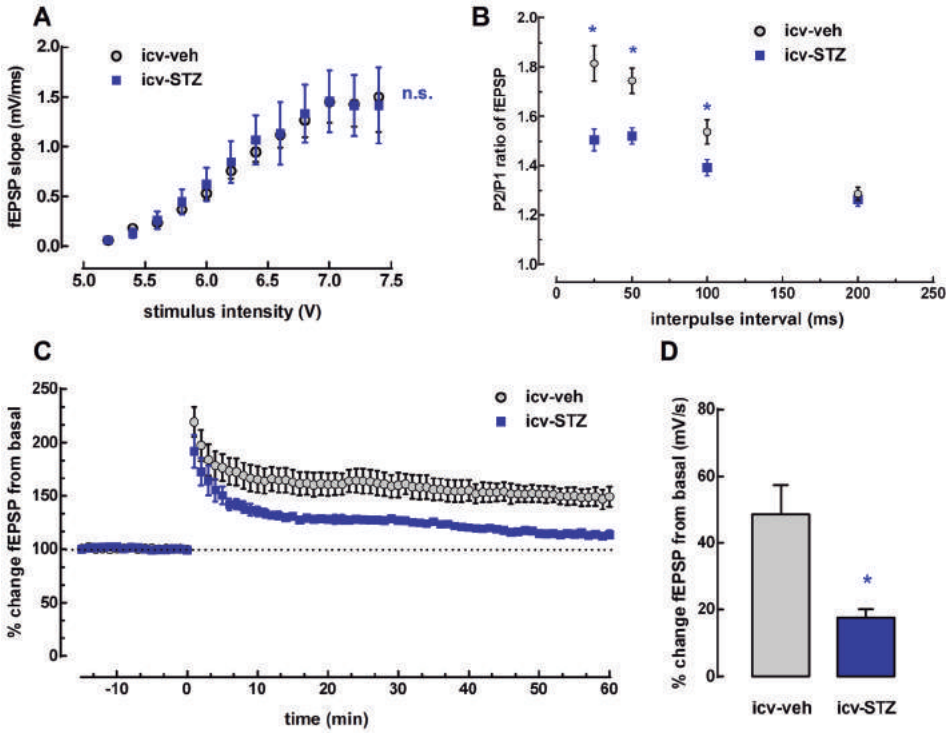

Figure 3.23 – Neurophysiological alterations in the icv-STZ animals, assessed with extracellular recording of the activity of CA3-CA1 (i.e. Schaffer collateral) synapses of 400 µm thick transversal hippocampal slices. (A) Input/output curves show no difference in the density of the density of recruitable synapses and their sensitivity to stimulus. (B) Paired-pulse stimulation protocol reveals presynaptic overactivity of CA3-CA1 synapses. (C) Long-term potentiation protocol confirms presynaptic overactivity ("noisiness"), because the only smaller LTP amplitude could be elicited in the icv-STZ rat hippocampus above basal activity, as compared with icv-sham. *P < 0.05. (D) Statistical comparison of the amplitudes of the recorded last 10 min of LTP seen in panel, while unpaired (C). All data points represent mean ± or + S.E.M. of n = 9 icv-sham and n = 17 icv-STZ slices. *P < 0.05, as assessed with as assessed with two-tailed unpaired Student's *t*-test.

Next, we looked for possible presynaptic modifications in short-term plasticity, as gauged by the paired-pulse ratio (PPR). This means the following: when a neuron is rapidly stimulated twice, the second stimulus-evoked post-synaptic response may differ from the first one. Normally, if this difference is an increase in the PPR, it represents a clear presynaptic deregulation in Ca^{2+} levels, because if the second pulse is delivered within 25-100 ms after the first pulse, there is little chance for the first pulse-evoked post-synaptic responses to feed-back onto the presynaptic release probability, *e.g.* via retrograde release of dopamine or endocannabinoids (Katz and Miledi, 1970; McLachlan, 1978; Gerdeman, 2008). Thus, if the presynaptic boutons were inhibited (aka, Ca^{2+}-deprived), the second depolarization will overimpose its consequent Ca^{2+} entry onto the first stimulus-induced intraterminal Ca^{2+} rise, which will cause a greater transmitter release. Contrariwise, if the second stimulus triggers a smaller than the first response, it usually reflects high intraterminal Ca^{2+} levels, and the second stimulus of the paired pulse occurs when intraterminal Ca^{2+} is being transported outward, leading to a smaller release probability than during the first stimulus.

Our PPR decrease data clearly suggest the second scenario, *i.e.* that the presynaptic terminals were likely harbouring unhealthy amounts of Ca^{2+}, indicating possible impairment in presynaptic plasticity as well. Such condition would mean that above the already elevated basal activity, long-term potentiation protocol can not potentiate synaptic transmission as much as in the icv-sham due to the plafond effect (*i.e.* that synaptic strength can not be of any size). Indeed, LTP protocol (Bliss and Cooke, 2011; Bliss and Lomo, 1973, Sackter, 2008) revealed a large, almost two-third reduction in the LTP amplitude in the hippocampi of icv-STZ animals. Since impaired hippocampal LTP is interpreted as the neurophysiological correlate of cognitive impairment (Bliss and Cooke, 2011; Bliss and Lomo, 1973, Sackter, 2008), our data may explain the hippocampal-dependent cognitive impairments observed in the behavioural studies.

The hippocampus is an extremely plastic structure with a massive synaptic density. Despite that, in some neuropathological conditions the hippocampus assumes maladaptive circuitry conformations leading to a synaptic malfunction even without significant neuronal loss. For instance, Selkoe (2002b) considered that the memory impairment occurring in the initial phase of AD is related to a synaptic failure rather

than synaptic loss. In fact, Aβ is generally believed to be capable of blocking long-term potentiation (LTP) (Paula-Lima et al., 2013), even in acute *in vitro* administrations. In concert with this, icv-STZ has been shown to cause tau hyperphosphorylation (Grünblatt et al., 2006), progressive β-amyloidosis (Salkovic-Petrisic et al., 2011), and synaptic dysfunction (Shonesy et al., 2012). According to the above report, amyloid pathology likely emerges much later (~3 months past STZ injection) than the time-frame we allowed for our model to age, *i.e.* 6-7 weeks post icv-STZ. This allows us to conclude that synaptic dysfunction was prior to the synaptic loss and β-amyloidosis, but coincident with the presence of metabolic dysfunction (lactate/alanine ratio values, meaning oxidative stress - see section below).

3.3.3 Icv-STZ induces oxidative stress

As shown in the representative High Resolution Magic Angle Spinning (HR-MAS) Nuclear Magnetic Resonance (NMR) spectra (**Figure 3.24A** and **B**), the hippocampi of icv-STZ treated animals exhibit a lower lactate/alanine ratio than the control animals, which is an indication of lower glycolytic rate and higher alanine content (Duarte et al., 2012d).

The results obtain for icv-STZ are consistent with an increased oxidative stress (Duarte et al., 2012d). The cognitive impairment of the icv-STZ treated animals observed in the described behavioural tasks (poorer acquisition and retention of memory and deficit in spatial cognition) can be directly related to the damage provoked by the increased oxidative stress.

Indeed, antioxidants such as selenium (Ishrat et al., 2009), S-allyl cysteine (Javed et al., 2011), trans-resveratrol (Sharma and Gupta, 2002), berberin (Bhutada et al., 2011), vinpocetine (Deshmukh et al., 2009) and crocin (Naghizadeh et al., 2013) could prevent the deterioration of the cognitive performance of the icv-STZ treated animals, directly linking brain oxidative stress and cognitive dysfunction. As a short note, oxidative stress can be caused – among others – by insulin resistance (Duarte et al., 2012a), or even iron, zinc and copper supplement (Wong et al., 2014). Oxidative stress precedes the appearance of most hallmarks of AD, hence a causative link may be established (De Felice, 2013; Su et al., 2008; Torrão et al., 2012; Xie et al., 2013).

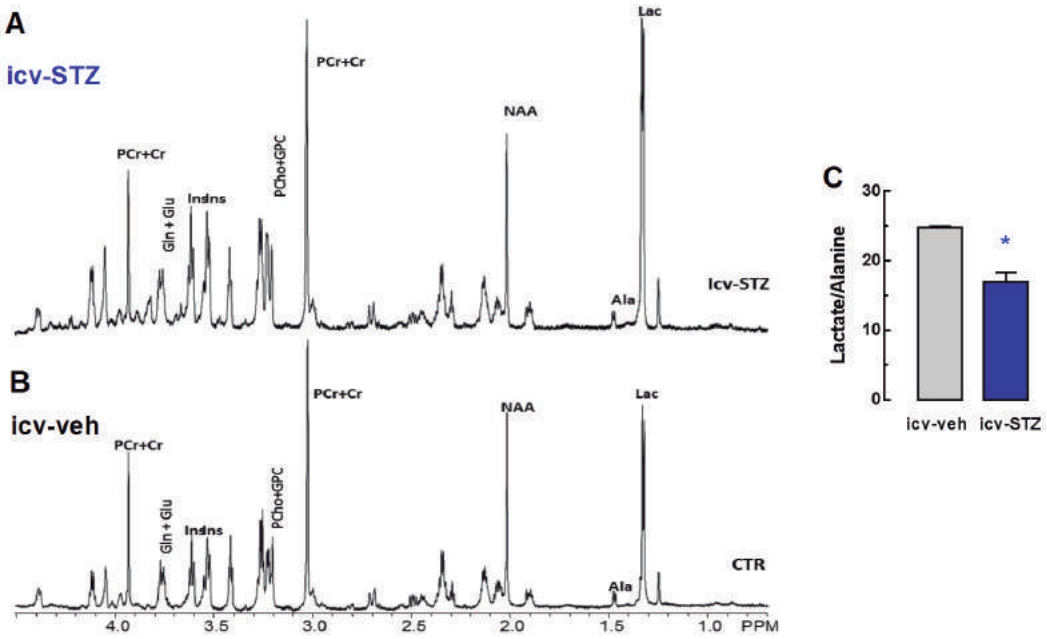

Figure 3.24 – Representative in vivo HR-MAS spectra of hippocampal tissue of (A) icv-STZ and (B) icv-veh rats, expanded from 0.5 to 4.5 ppm. This powerful technique is capable of averaging out the majority of dipole-dipole broadening, resulting in spectra similar to high-resolution NMR spectra in solution. Abbreviations: Ala, alanine; Asc, ascorbate; Asp, aspartate; Cr, creatine; Glc, glucose; Gln, glutamine; Glu, glutamate; Ins, myo-inositol; Lac, lactate; NAA, N-acetylaspartate; PCho, phosphorylcholine; PCr, phosphocreatine; Tau, taurine. (C) Statistical comparison of the effect of icv-STZ treatment on the hippocampus lactate/alanine ratio. Bars represent the mean ± S.E.M. of n = 4 pair of animals. *P < 0.05, as assessed with two-tailed unpaired Student's *t*-test.

3.4 HIGH SUCROSE CONSUMPTION INDUCES MEMORY IMPAIRMENT IN RATS ASSOCIATED WITH ELECTROPHYSIOLOGICAL MODIFICATIONS BUT NOT WITH METABOLIC CHANGES IN THE HIPPOCAMPUS

Intracerebroventricular (icv) injection is one of the most invasive surgical techniques, often leading to lasting neuroinflammation that may affect even the sham brain. So the above findings were repeat in a non-invasive model known of causing cerebral insulin resistance, the high sucrose (HSu) model that we previously developed and characterized (Soares et al., 2013). Because insulin-resistant type 2 diabetes (T2D) is one of the highest risks factors for AD, depression and other neuropsychiatric

disorders, which also involve neurometabolic alterations (Akter et al., 2011a; Anderson et al., 2001; Bystritsky et al.; Carvalho et al., 2012b; Exalto et al., 2012b; Xu et al., 2010b). This Hsu model is a prediabetic rat model and is characterized by fasting normoglycemia, hyperinsulinemia and hypertriglyceridemia in the fed state, and insulin resistance with impaired glucose tolerance (Soares et al., 2013). Regarding the central nervous system, this model is consistent with the assumption that metabolic disturbances can lead to cognitive impairment and memory deficits (Soares et al., 2013).

3.4.1 Impact of high sucrose consumption

The disaccharide sucrose has a monosaccharide glucose conjugated to a fructose, thus high sucrose diet causes recurrent hyperglycemia. Taken that fructose is directly transformed into fatty acids in the liver which is then shipped into body fat, constant fructose intake causes dyslipidemia too, on the long run. The relative contribution of hyperglycemia, dyslipidemia and the hypercaloric diet to the animals' phenotype neither can be disentangled nor is necessary to do so.

During the 11 weeks of treatment, rats drinking *ad libitum* high (35% g/v) sucrose as their only source of liquids, had an average weight similar to that of control rats (**Figure 3.25A**), although they ingested an overall greater amount of calories (control: 3.64 ± 0.13 kJ/2 rats/week, HSu: 4.95 ± 0.19 kJ/2 rats/week, n = 7, $P < 0.05$; assuming that 1 g of sucrose is equivalent with 16.74 J energy and 1 g of chow has 11.72 J) (**Figure 3.25B**): HSu rats tended to consume less chow (control: 310 ± 26 g/2 rats/week *vs*. HSu: 244 ± 21 g/2 rats/week, n = 7 (14 animals), $P = 0.073$) (**Figure 3.25C**), but consumed greater amounts from their sucrose solution (594 ± 29 mL/2 rats/week) than that control rats drank from their drinking water (416 ± 29 mL/2 rats/week, n = 7 cages (2 rats/cage), $P < 0.05$) (**Figure 3.25D**).

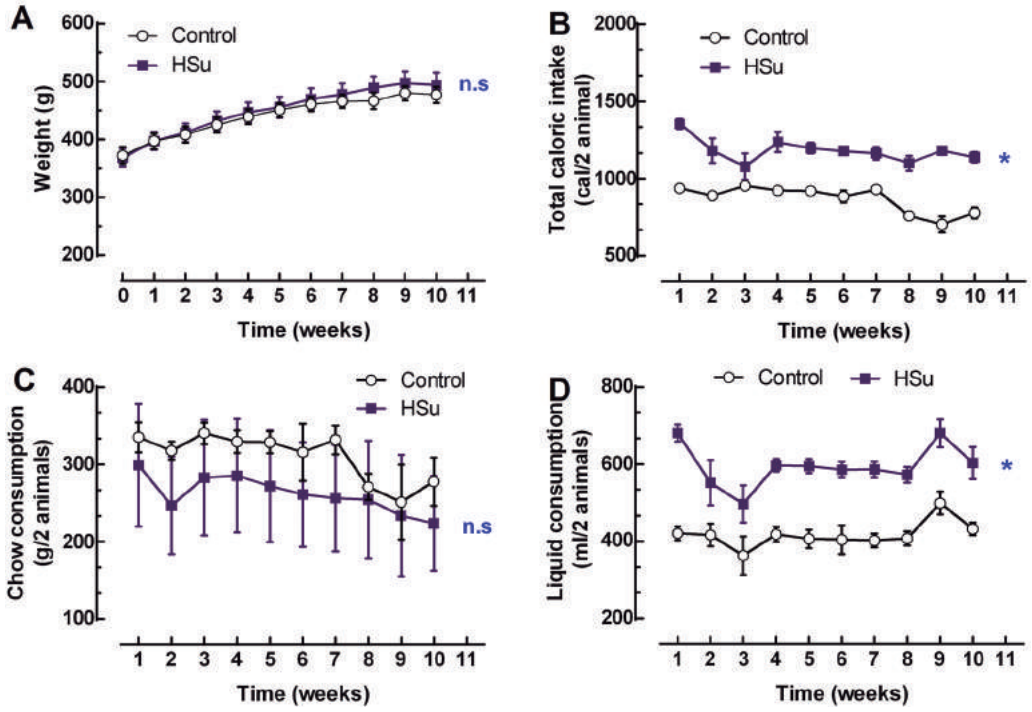

Figure 3.25 – Characterization of rats subject to 11 weeks of high sucrose diet administered in their drinking water. Time course of (A) body weight, (B) total caloric intake, (C) the consumption of standard chow, and finally, (D) liquid consumption of rats drinking 35% sucrose (filled squares) or their control, which drink regular water (open circles). Data points are mean ± SEM of n = 14 in (A) and n = 7 cages (14 rats) per group in (B-C). Unpaired Student's t-test was used to compare the impact of sucrose consumption on the different parameters *P < 0.05 compared to the control group.

3.4.2 High sucrose consumption induces memory and emotional impairment

The analysis of hippocampal-dependent memory using the object displacement (ODT) and novel object recognition (NORT) tests revealed that high sucrose consumption impaired memory performance in both tasks ($P < 0.01$) (**Figure 3.26A,B**), which was not related to changes in the total time exploring the objects in each task (control in ODT: 46.9 ± 7.8 sec, n = 8; HSu in ODT: 50.4 ± 6.8 sec, n = 7, $P > 0.05$; and control in NORT: 35.6 ± 6.6 sec, n = 11; HSu in NORT: 32.3 ± 6.1 sec, n = 12, $P > 0.05$). Moreover, the locomotion of both animal groups was not statistically different ($P > 0.05$), as evaluated by the distance travelled in an open field (**Figure 3.26C**). However, the rats exposed to HSu showed an increased immobility time in the forced swimming test when compared to control rats ($P < 0.01$) (**Figure 3.26D**). The latter test,

which is generally interpreted as a measure of depression-like behavioural despair, is a popular model to evaluate depressive-like phenotype in laboratory rodents (Hales et al., 2014; Porsolt et al., 1977).

As reported in our previous study, we now replicated the observation that rats in a diabetic or a prediabetic condition present memory deficits (Duarte et al., 2009, 2012; Soares et al., 2013; Wang et al., 2014) – a conclusion that was now confirmed with additional behavioural tests. This diabetes-associated memory deficit likely involves an altered information processing through hippocampal circuits, since we observed a disruption of spatial-related memory (**Figure 3.26A** and Soares et al., 2013) and recognition memory (**Figure 3.26B**), which are known to critically depend on hippocampal circuitry (Broadbent et al., 2010; Gril-lo et al., 2015; Pandey et al., 2015).

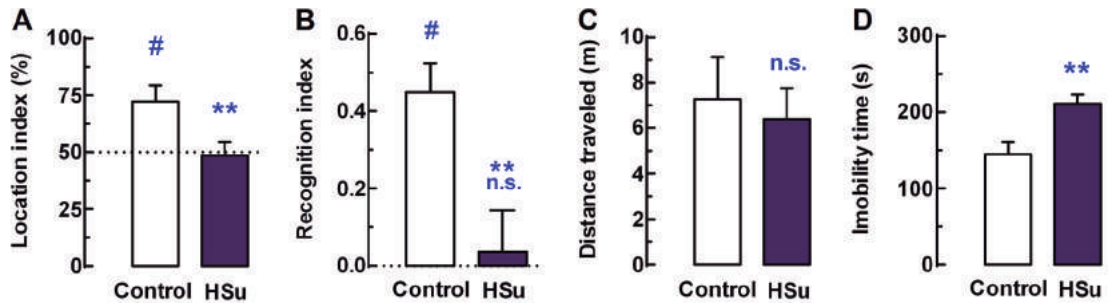

Figure 3.26 – High sucrose consumption (HSu) decreased short-term memory performance in the object displacement test (ODT) (A) and in the novel object recognition tests (NORT) (B), without modifying the locomotor profile in the open field (C) in comparison to controls. Moreover, HSu also increased helpless behaviour in the forced swimming test, indicating depressive-like phenotype (D). The data are mean + SEM of n = 6-8 rats per group. Unpaired Student's *t*-test was used in those tests, **P < 0.01 compared to the control group; To validate the ODT and NORT, the *t*-test was used to compare the location index against a hypothetical value of 50% in the control group in (A) and the recognition index compared to 0 in (B) and the accepted level of significance was $^{\#}$P < 0.05.

The present results are in line with this contention since we have now showed that HSu rats performed poorly in ODT and NORT – two hippocampus-dependent tasks (Assini et al., 2009; Warburton and Brown, 2015). In fact, apart from the hippocampus, the recognition process in rats also has a cortical participation (via the entorhinal cortex and the subiculum), which prompts a seminal role for the temporoammonic pathway in

the recognition tasks in rodents (Agster and Burwell, 2013; Warburton and Brown, 2015).

The relation between diabetes and emotional disturbances such as depression is substantial, as heralded by the fact that insulin resistance by itself (like observed in the pre-diabetic condition) correlates with depressive behaviours including suicidal ideation (Koponen et al., 2015). Furthermore, classical neurochemical features of depression such as a hyposerotoninergic function are also present in insulin resistance-induced depression (Muldoon et al., 2006). Accordingly, it was observed that HSu rats spent more time immobile in the FST, indicating an increased helpless behaviour, often interpreted as a type of depressive-like behaviour in rodents (Porsolt et al., 1977). Although the neurobiological basis for this association between HSu and the increased helpless behaviour still remains to be explored, it is tempting to speculate that it may involve a depression of the temporoammonic pathway, since this was proposed to account for the emotional disturbances associated with chronic stress (Kallarackal et al., 2013). Additionally, it has been also recently published that the insulin pathway (Akt-GSK3β) mediates serotonin's antidepressant action in the subgranular neurons of the dentate gyrus (Papazoglou et al., 2015).

3.4.3 High sucrose consumption does not modify the metabolic profile in the hippocampus

As stated before, from a previous collaboration work (Soares et al., 2013) we know that the HSu animals possess profound alterations of peripheral metabolic parameters. Consequently, it was hypothesized that the consumption of high sucrose might also alter the hippocampal metabolism as a pre-requisite to trigger memory and emotional impairments. The method selected was the HRMAS technique since it enables to obtain a metabolic profile using small amount of tissue.

However, this spectroscopic analysis failed to reveal any evident metabolic impairment in the hippocampus of HSu rats, at the opposite of what was observed in streptozotocin-treated rats using superfused slices (Duarte et al., 2009a). As shown in the representative HR-MAS spectra (**Figure 3.27A,B**), HSu rats displayed a metabolic profile in their hippocampi similar to that found in control rats. Further confirming the lack of major metabolic alterations, the quantification of some metabolites revealed

similar levels in HSu and control rats, namely of n-acetyl-aspartate (NAA) (**Figure 3.27C**), which is an indicator of metabolic stress (Surendran and Bhatnagar, 2011), and of glutamate (**Figure 3.27D**) or GABA (**Figure 3.27E**), the main excitatory and inhibitory neurotransmitters, respectively.

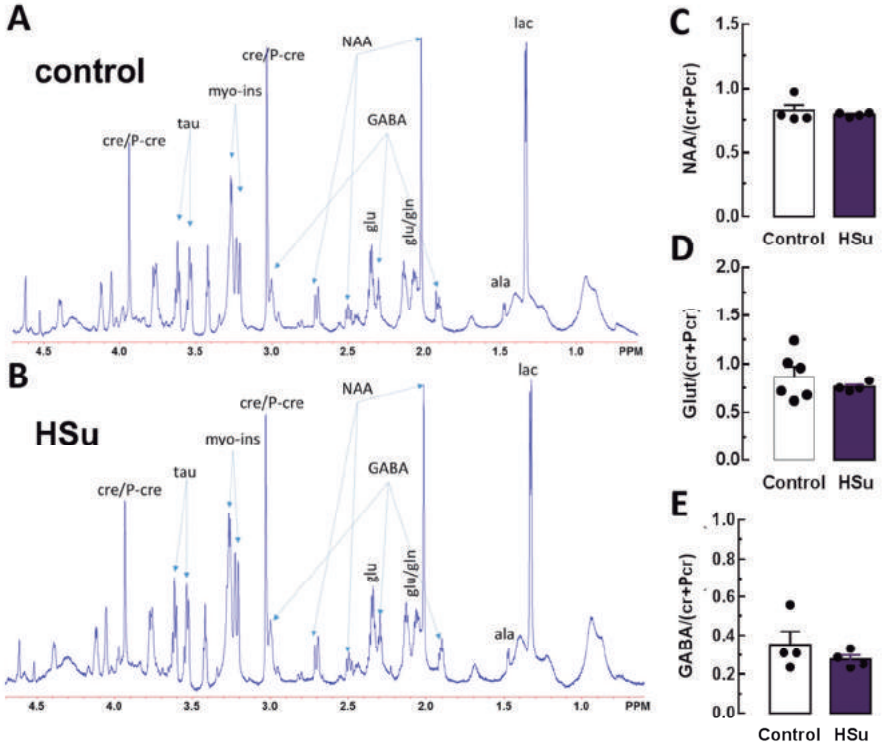

Figure 3.27 – High sucrose consumption (HSu) did not modify the metabolic profile in the hippocampus. The comparison of proton (^{1}H) (HR-MAS) spectra from (A) control and (B) HSu rats revealed a globally superimposable profile. Cre: creatinine; P-cre: phospho-creatinine; tau: taurine; myo-ins: myo-inositol; NAA: N-acetylaspartate; glu: glutamate; ala: alanine; lac: lactate. Accordingly, the levels of C) NAA (an indicator of metabolic stress), (D) glutamate and (E) GABA were similar in HSu and in control rats. The data in (C-E) are mean ± SEM of n = 5 rats per group, n.s., not significant, as assessed with two-tailed unpaired Student's *t*-test.

3.4.4 High sucrose consumption affects synaptic plasticity at temporoammonic pathway-CA1 pyramidal synapses

To better understand the physiological meaning of the results obtained in the behavioural analysis, we teamed up with electrophysiologists to explore the alternative possibility that the memory impairment caused by HSu might result from a hampered

information flow through hippocampal circuits. To this end, we decided to study the different electrophysiological alterations in the hippocampal Schaffer-CA1 and temporoammonic pathways. The rationale behind these experiments is that neuronal communication requires a high amount of energy and is critically dependent on the cellular metabolic state and energy supply (Fusco and Pani, 2013). An imbalance of glucose metabolism affects neuronal circuits and is especially relevant for hippocampal functioning, because this brain structure has the greatest density of excitatory synapses (Harris and Weinberg, 2012) and the activity of these synapses is strictly dependent on glucose availability (Magistretti, 2006). The hippocampus is reciprocally connected to the cerebral cortex, processing and storing information by means of synaptic plasticity mechanisms like LTP and long-term depression (LTD) (Kemp and Manahan-Vaughan, 2004; Martin et al., 2000). The entorhinal cortex projections constitute the main cortical pathways to the hippocampus through two distinct pathways: neurons in layer II of the entorhinal cortex project to dentate gyrus neurons, engaging a tri-synaptic circuit via CA3 neurons and then through the Schaffer fibers to CA1 neurons (Witter et al., 1988); while a distinct pathway links neurons from layer III of the entorhinal cortex directly to the CA1 region via the temporoammonic pathway (Witter et al., 1988). Although both pathways are involved in the acquisition and storage of spatial information (Remondes and Schuman, 2002), their different functional roles are still unclear, in spite of different receptor composition and molecular underpinnings to induce synaptic plasticity present in the Schaffer fibers and the temporoammonic pathways (Magee, 1999, Nolan et al., 2004, Ahmed and Siegelbaum, 2009).

Extracellular electrophysiological recordings at Schaffer collateral–CA1 pyramidal dendrite synapses revealed similar input-output curves in HSu and control rats ($P > 0.05$) (**Figure 3.28A**). Likewise, HSu and control rats displayed similar amplitude of LTP ($t_{2,0.05} = 0.561$) (**Figure 3.28B, C**).

Extracellular electrophysiological recordings in the temporoammonic pathway also showed similar input-output curves in HSu and in control rats ($P > 0.05$) (**Figure 3.28D**). However, temporoammonic pathway synaptic plasticity was hampered in HSu rats, as gauged from the lower amplitude of LTD in HSu compared to control rats ($P < 0.05$) (**Figure 3.28E,F**).

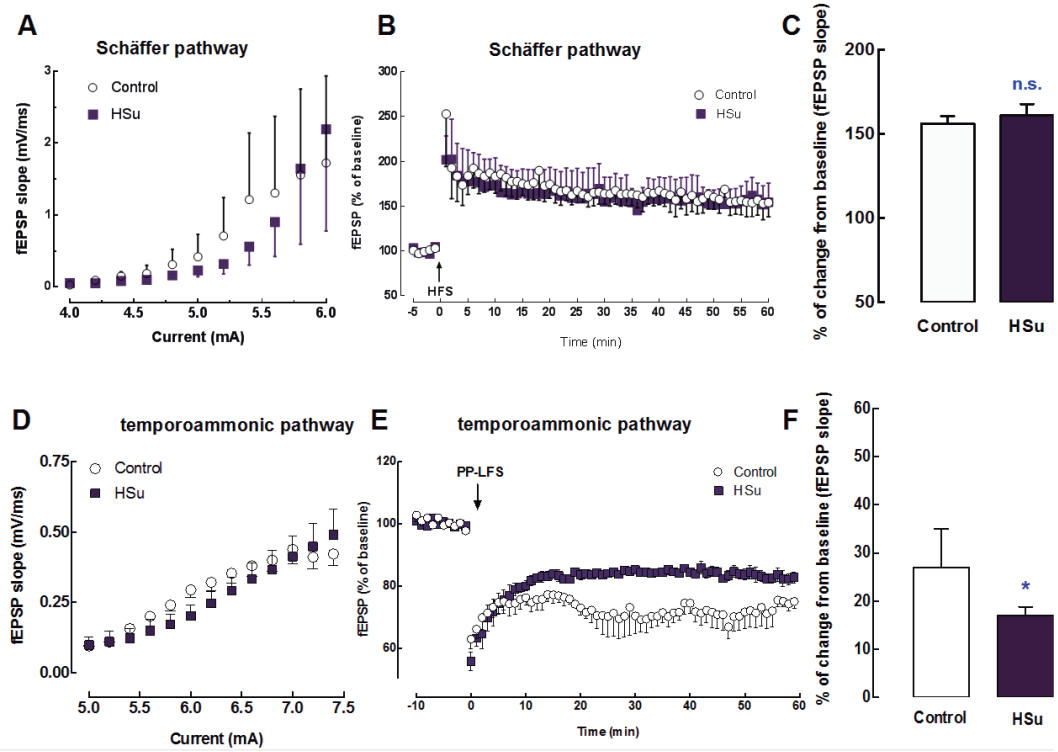

Figure 3.28 – Extracellular recordings in hippocampal slices revealed that high sucrose consumption (HSu) did not modify synaptic transmission either in the Schaffer pathway or in the temporoammonic projections to CA1 pyramidal cells, whereas synaptic plasticity was decreased in the temporoammonic pathway rather than in the Schaffer pathway in HSu compared to control rats. Synaptic transmission, measured as input/output curves, was superimposable in HSu and control rats, both (A) in the Schaffer pathway and in the (D) temporoammonic pathway. (B,C) In the Schaffer pathway, a high-frequency train (HFS: 100 Hz for 1 sec) induced synaptic plasticity, namely LTP induced, which was of similar amplitude in HSu and in control rats, whereas a paired pulse-low frequency stimulation (PP-LFS) composed of 900 paired stimuli (200 msec paired-pulse interval, with a 1 Hz inter-pair interval, during 15 min) induced a LTD in the temporoammonic pathway with a lower amplitude in HSu compared to control rats (E, F). The data are mean + or - SEM of n = 4 rats per group. *P < 0.05 as compared to control, determined with two-tailed unpaired Student's *t*-test.

3.4.5 High sucrose consumption alters the density and neuromodulator efficiency of adenosine A_1 receptors in the hippocampus

Since the adenosine system is a prominent modulator of the neurotransmission in the hippocampus through inhibitory adenosine A_1 receptors (A_1Rs) (Dunwiddie and Masino, 2001), we investigated if HSu consumption might affect the density and function of A_1Rs. Adenosine operating at its most abundant inhibitory A_1R has been

shown to control synaptic plasticity (Hagena and Manahan-Vaughan, 2010; de Mendonça et al., 1997; Rex et al., 2005) and to be affected in diabetic-like conditions (Duarte et al., 2006, 2009b, 2012a; Morrison et al., 1992). Thus, we tested if the exposure to HSu would affect hippocampal A_1Rs. Western blot of hippocampal synaptosomal membranes showed an increase of A_1R density in HSu compared to control rats ($P < 0.05$) (**Figure 3.29A**). Accordingly, the exogenous activation of A_1R with 2-chloroadenosine (Coelho et al., 2006) revealed an increased efficiency to decrease synaptic transmission at Schaffer collateral-CA1 pyramidal synapses in HSu, as compared to control rats at the two higher concentrations tested (**Figure 3.29B**). This increased sensitivity of the exogenous activation of A_1R seems to selectively occur in Schaffer collateral-CA1 pyramidal synapses, since the concentration-dependent inhibition by 2-chloroadenosine of synaptic transmission in the temporoammonic pathway was similar in HSu and control rats (**Figure 3.29D**).

Importantly, we observed that the chronic consumption of high sucrose altered the physiological role of A_1Rs at the Schaffer collateral-CA1 synapses, and left the temporoammonic pathway unaffected. In detail, a supramaximal concentration of the selective A_1R antagonist DPCPX (100 nM) (Sebastião et al., 2000) caused a considerable smaller disinhibition of synaptic transmission in the Schaffer collaterals in the HSu than in control rats ($P < 0.05$) (**Figure 3.29**C), whereas the disinhibition of synaptic transmission by DPCPX (100 nM) in the temporoammonic pathway was similar in HSu and in control rats ($P > 0.05$) (**Figure 3.29E**). This results show an increased A_1R density in hippocampal synapses of the HSu rats, which was the likely cause of the greater efficiency of the A_1R agonist 2-choroadenosine to depress synaptic transmission in Schaffer collateral–CA1 pyramidal cell dendrite synapses of HSu compared to control rats. However, the tonic inhibitory role of A_1R depends both on the density of A_1R as well as on the bioavailability of adenosine in the synaptic cleft (Cunha, 2008). The latter might be limited in the Schaffer fiber synapses in HSu rats, since we observed a reduced disinhibitory effect of the A_1R-selective antagonist, DPCPX.

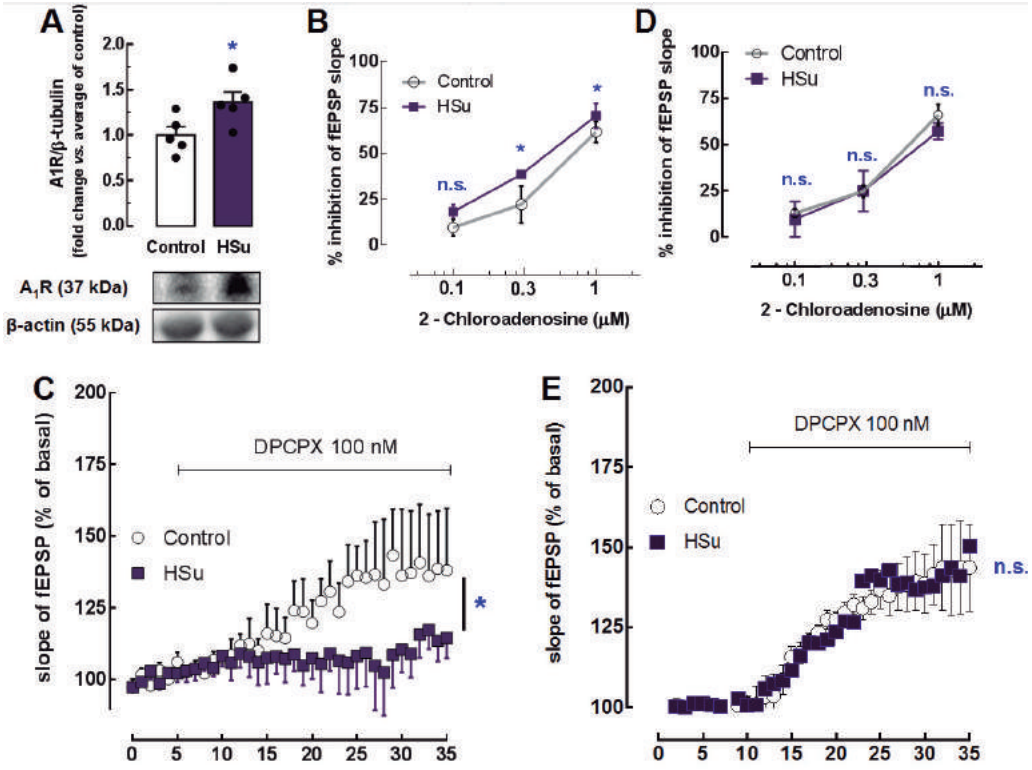

Figure 3.29 – High sucrose consumption (HSu) modified the density of hippocampal adenosine A1 receptors (A1R) and their efficiency to inhibit synaptic transmission in hippocampal slices. (A) Western blot analysis of hippocampal synaptosomal membranes showed that HSu increased the density of synaptic A1R. This was accompanied by an increased efficacy of the A_1R agonist, 2-chloroadenosine to depress synaptic transmission in the (B) Schaffer pathway, rather than in the (D) temporoammonic pathway. Conversely, the blockade of A_1R with a supra-maximal concentration of its selective antagonist, DPCPX (100 nM), showed a loss of endogenous inhibitory tone on the (C) Schaffer-pathway in HSu compared to control rats, while the endogenous tone at the E) temporoammonic-CA1 synapses remained preserved in the HSu compared to control rats. The data are mean + or - SEM of n = 4 rats per group. *P < 0.05, compared to control determined by unpaired Student's *t*-test.

This is tentatively in agreement with the previously reported reduction of the release of ATP and its conversion into extracellular adenosine (Duarte et al., 2007b) and the reduced activity of adenosine transporters in the hippocampus of diabetic rats (Cassar et al., 1998; Morrison et al., 1992). However, our detailed analysis of different CA1 hippocampal circuits revealed that there was no apparent functional modification of the role of A_1R in the temporoammonic pathway, which is the pathway associated with memory and emotional impairments (Remondes and Schuman, 2002) in HSu rats. Therefore, the lack of alteration in A_1R-dependent modulation of synaptic plasticity at

temporoammonic synapses indicates that that HSu affected behavioural performance and hippocampal plasticity in a fashion that was not relied upon A_1Rs. Given that modifications of microglia-associated neuroinflammation seems to be a precocious trigger of diabetes-induced alteration of neuronal function and alterations of microglia impacts synaptic transmission and plasticity (Kettenmann et al., 2013), it is tempting to speculate that HSu consumption might affect glial function as a candidate mechanism to alter synaptic plasticity in the temporoammonic pathway. Certainly, further studies are necessary to elucidate this assumption. Thus, the present findings consolidate the detrimental impact of high sucrose consumption on memory and emotional performance, which appeared independent from an altered metabolic profile in the hippocampus associated with this pre-diabetic model. In contrast, we now observed that the temporoammonic rather than the better characterized Schaffer projections onto CA1 pyramids display deficits of synaptic plasticity that have previously been related to memory and emotional performance. The brain continuously receives sensorial inputs and some of those inputs need to be interpreted by the hippocampus (Biessels and Reagan, 2015). Some of these sensorial inputs use the temporoammonic pathway to reach the CA1 region of the hippocampus (the output of hippocampal signalling). Kinnavane et al. (2015) described the physiological role of the temporoammonic pathway connecting sensorial and cognitive signals in different tasks (e.g., NORT). Those authors explain that when rats explore familiar objects the information pathway starts from the perirhinal cortex to lateral entorhinal cortex, and subsequently to CA1. On the other hand, when the rat is exploring new objects, the pathway starts from perirhinal cortex to lateral entorhinal cortex, then to the dentate gyrus, next to the CA3 and finally CA1 (Kinnavane et al., (2015). It is interesting to note that in both conditions (familiar and novel) the temporoammonic pathway has an active role. Nevertheless, the differences between the two situations are the processing of the information. In humans, CA1 participate in the anchoring of novel sensorial (coming from the temporoammonic pathway) and spatial inputs (from both temporoammonic and CA3) into a pre-existent context (Stokes et al., 2015). Conversely, the Schaffer pathway is not actively engaged in the sensorial acquisition. Its main role is the spatial memory processing after the sensorial input pathway.

Finally, we excluded the possibility that the predominant inhibitory neuromodulation system operated by A_1R might be involved with this HSu-associated

modification of plasticity in the temporoammonic pathway. This prompts the search for other selective modulator of synaptic plasticity of the temporoammonic pathway as possible novel systems to be targeted to correct the memory and emotional deficits associated with HSu consumption.

Therefore, the characterization of HSu model opens a new window of opportunity to explore the relation between metabolic changes, synaptic changes and memory impairment.

3.5 $A_{2B}R$ ACTIVATION ENHANCES GLUCOSE UPTAKE ON A SECOND SCALE IN ACUTE HIPPOCAMPAL SLICES

Next, we investigated the putative glucoregulator role of adenosine in the brain, taken that this neuromodulator is well suited to link metabolic disorders with memory impairment via altered synaptic plasticity, which we also witnessed in the above study. Indeed, the glucose-derived ATP is consumed by numerous energy dependent processes, including glutamatergic signalling and Na^+/K^+-ATPases in the brain (Attwell and Laughlin, 2001). Increased neuronal activity thus triggers a physiological accumulation of extracellular adenosine fed by ATP release (Cunha, 2008) and ATP consumption by the sodium pumps (Sims and Dale, 2014). Hence, when the circuitry is under heavy load and oxidizes more glucose, peaks of extracellular adenosine may serve as a paracrine and/or autocrine adaptive signal to stimulate glucose metabolism via activating one of its membrane-bound metabotropic receptors (Cunha, 2001a). Additionally, pathophysiological conditions including transient cerebral ischemia, were shown to exacerbate ATP conversion into adenosine (Hagberg et al., 1986; Onodera et al., 1986). In fact, the assumption has been toyed with for decades that adenosine generated under energetic crisis protects from cellular damage by restoring energy balance in the brain (Huber et al., 1993; Mori et al., 1992; Newby et al., 1985).

Accordingly, both of the two most abundant adenosine receptors in the brain, the A_1 and A_{2A} subtypes (Fredholm et al., 2011), have been documented to impact on cerebral glucose metabolism besides being important modulators of neuronal activity (Gomes et al., 2011; Nehlig et al., 1994). There are two additional cloned adenosine receptors, the A_{2B} and the A_3 receptors (Fredholm et al., 2011), but their roles have been

less explored in the brain. Notably, A_{2B}Rs have been implicated in peripheral glucose homeostasis (Csóka et al., 2014; Figler et al., 2011; Johnston-Cox et al., 2012; Rüsing et al., 2006) and have been proposed to control astrocytic glycogen metabolism (Allaman et al., 2003; Magistretti et al., 1986). These aspects prompt the attractive hypothesis that A_{2B}R may be associated with cerebral glucoregulation, especially when a metabolic boost is needed. Furthermore, we recently observed that A_{2B}Rs control A_1R-mediated responses in hippocampal glutamatergic synapses (Gonçalves et al., 2015), which may indicate the possible mechanism how high-sucrose diet affected A_1R-dependent plasticity at Schaffer collaterals. Continuing the analysis of the role of adenosine in metabolic modifications, we asked if A_{2B}Rs confer glucoregulation in the hippocampus and what consequences would A_{2B}R have on the animal memory and anxiety-like behaviour.

3.5.1 Behavioural analysis of A_{2B}R KO mice

In those behavioural analyses, it was observed that there was no immediate working memory impairment in the A_{2B}R KO (n = 7) compared to WT animals (n = 7) (**Figure 3.30**) since no difference in alternation was observed between the two groups under the Y-maze test (P > 0.05).

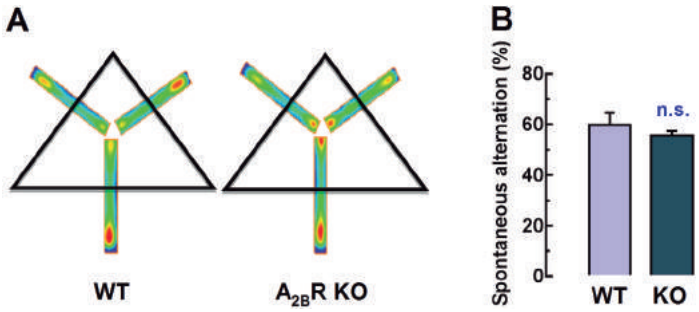

Figure 3.30 – Y-maze test revealing no difference in alternation between the WT and the A_{2B}R KO mice. (A) Average occupation pattern plot showing experimental group's center point in the Y-maze task. The colour gradient from blue (less occupation) to red (more occupation) show that A_{2B}R KO mice group spent more time than control mice group in the central area. (B) Bar graph representing the percentage of time spent in the novel arm. No difference was observed between the WT and the A_{2B}R KO groups (P > 0.05), meaning that A_{2B}R KO mice had no impairment in the immediate working memory. The data are mean ± SEM, of 7 animals in each group. *P < 0.05 compared to control group using an unpaired Student's t-test.

Y-maze "spontaneous alternation" test is a behavioural paradigm that relies on the willingness of rodents to explore new environments, and requires the animal attention and working memory. Rodents typically prefer to investigate a new arm of the maze rather than returning to one that was just previously visited and the result counts the alternations between the three arms, e.g., consecutive entries in each arm without repetition. Many parts of the brain including the hippocampus are involved in this task.

Regarding the anxiety-like behaviour, the classical assessment parameters of the EPM such as the percentage of time spent in the open arm ($n = 7$, $P > 0.05$) or the percentage of entries in the open arms ($n = 7$ A), did not show any difference between $A_{2B}R$ KO and WT animals ($P > 0.05$) (**Figure 3.31**). Curiously, in both the y-maze and EPM test the $A_{2B}R$ KO animals displayed a pattern of exploration different from the WT, i. e., the $A_{2B}R$ KO spent more time exploring the central area (defined as the apparatus area inside the black triangle in **Figure 3.30**) ($P < 0.05$). Further studies are needed to explain this pattern of exploration

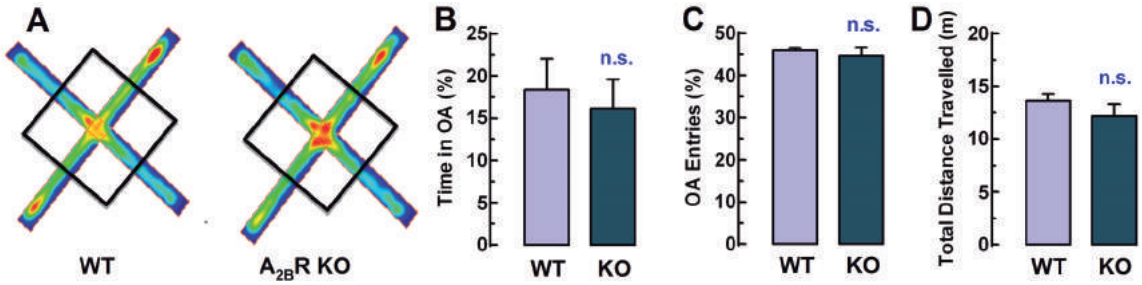

Figure 3.31 – Elevated plus maze test revealing no difference in anxiety for the $A_{2B}R$ KO animals. (A) The colour gradient from blue (less occupation) to red (more occupation) shows the average occupation plot representing the pattern of the animal group's centre point in the EPM task. While WT mice had a similar pattern of exploration for the centre and outside area of the arena, $A_{2B}R$ KO mice spent more time exploring the central part of the arena than the periphery. (B) Bar graph representing the percentage of time spent in the open arm; (C) Percentage of the number of entries in the open arm. (D) Total distance travelled in the elevated plus maze. The data are mean ± SEM, n = 7. P > 0.05 as compared to control group using two-tailed unpaired Student's t-test.

3.5.2 $A_{2B}R$ activation rapidly enhances glucose uptake in hippocampal slices

In **Figure 3.6**, is presented the data with the uptake of the fluorescent deoxyglucose analogue, 6-NBDG. For the actual study, the 6-NBDG uptake was compaired to another commercially available fluorescent deoxyglucose analogue, 2-NBDG, and it was observed that 2-NBDG provides greater glucose uptake signal (see **Figure 3.32**). This is in agreement with a previous finding of another group pioneering 2-NBDG and 6-NBDG uptake in brain slices (Jakoby et al., 2014). They claim, in accordance with Louzao et al. (2008), that 2-NBDG is metabolizable while 6-NBDG is not, hence, its uptake is not likely saturated. We first decided that 2-NBDG would be a more suitable analogue to monitor the spatiotemporal uptake of glucose, because it is more sensitive to changes in energy metabolism and it provides greater signal. Then we analyzed the uptake process and worked out the best mathematical model to model the uptake curve of 2-NBDG. First, the autofluorescence of the slices under the microscope was measured, and this value was then subtracted from all of the following intensity values. Then 2-NBDG (30 μM) was added via an external reservoir where 5 mL of initial perfusion solution was gassed with 95% O_2 and 5% CO_2 and superfused in the chambers in a closed-circuit fashion. According to O'Neil and colleagues (2005), the first couple of minutes of 2-NBDG show a complex oscillation and thus is to be discarded from the calculation.

As **Figure 3.32** shows, data points were discarded in the first 5 min and 30 sec, then the following equation was fitted to the useful data points, up to 20 min:

$$Y = \mathbf{T_{max}} \times \mathbf{X} / (\mathbf{K_d} + \mathbf{X}) + \mathbf{M} \times \mathbf{X} + \boldsymbol{\alpha}$$

where Y stands for the intensity (arbitrary units), X denotes the time (secs), T_{max} represents the maximum number of transporters for 2-NBDG, K_d is the inverse of the affinity of 2-NBDG for its transporters, while M stands for the constant for the "metabolic drain" (as 2-NBDG is slowly metabolizable), which was assumed to be steady for the sake of simplicity, and α (autofluorescence) is the value to be subtracted from the raw data.

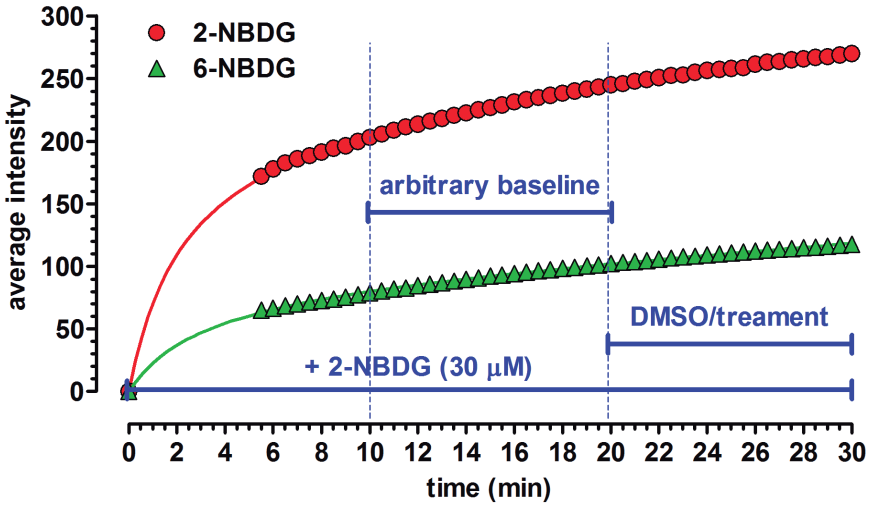

Figure 3.32 – Representative fluorescent uptake traces of 2 or 6-(N-(7-nitrobenz-2-oxa-1,3-diazol-4-yl)amino)-2-deoxyglucose (2/6-NBDG) in hippocampal slices of 300 µm thickness of one young adult C57bl/6 mouse. The slices were mounted in special superfusion chambers made for functional fluorescence microscopy, and superfused with gassed Krebs-HEPES solution at a rate of 0.5 mL/min in a closed circuit, and they were then photographed at every 30 s over the following 30 min, using a 5× Plan Neofluar objective on an inverted Axiovert 200-M fluorescence microscope to allow real-time video imaging. The data were band-pass filtered for excitation (470/40) and emission (525/50). After recording six images for autofluorescence (to establish the baseline), 2 or 6-NBDG) (30 µM) was applied through the reservoir of the closed superfusion circuit. As within 10 min, the increase of 2-NBDG signal reached linearity, we recorded a 10-min predrug period that was used for calculating a "prediction curve", following the first 10 min of 2-NBDG application. Subsequently, at 20 min, the slices were challenged with a drug (this case, BAY656083, 300 nM) or its vehicle, DMSO (0.1%), and we continued recording the changes in fluorescence intensity for more 10 min.

Having optimized 2-NBDG uptake, we proceed to assessed whether $A_{2B}R$ activation affects glucose uptake in superfused hippocampal slices through the monitorization of the rate of 2-NBDG accumulation. To do this, we calculated the departure of the actually measured intensity values, in the presence and absence of the $A_{2B}R$ agonist, BAY656083, from the theoretical curve fitted onto the points up to minute 20. The basal accumulation of 2-NBDG was most evident in astrocyte-rich areas of transverse hippocampal slices, *i.e.* in the *stratum lacunosum*, followed by the *strata radiatum* and *moleculare*, and the smallest signal was found in the *strata pyramidale*

and *granulare* (**Figure 3.33A**), this information is consistent with previous findings (Jakoby et al., 2014).

The next step was to perform a pharmacological study based on the use of BAY606583 and an antagonist $A_{2B}R$, MRS1754, together with $A_{2B}R$ KO mice. The pharmacological activation of $A_{2B}R$ with BAY606583 (300 nM - *i.e.* at a concentration selective for this receptor) rapidly increased the velocity of 2-NBDG accumulation in these hippocampal slices prepared from the wild-type (WT) mice ($n = 7$ in duplicate, $P < 0.05$), as determined by measuring the fluorescence intensity in the whole surface of the transversal slice (**Figure 3.33).** Pretreatment of the slices with the selective $A_{2B}R$ antagonist, MRS1754 (200 nM) for 23 min (*i.e.* starting 3 min before 2-NBDG administration) prevented BAY606583 from stimulating 2-NBDG uptake ($n = 4$, $P > 0.05$; **Figure 3.33D**). Additionally, BAY606583 also failed to stimulate 2-NBDG uptake in the hippocampal slices prepared from $A_{2B}R$ KO mice ($n = 6$, $P > 0.05$; **Figure 3.33D**). Importantly, 2-NBDG accumulation was not statistically different from the WT control neither after pretreatment with MRS1754 ($n = 4$, $P > 0.05$; **Figure 3.33D**) nor in $A_{2B}R$ KO mice ($n = 6$, $P > 0.05$; **Figure 3.33D**), even though the uptake velocity was tendentiously greater in $A_{2B}R$ KO mice ($117.3 \pm 9.8\%$ of WT control, $P > 0.05$). Hence, the lack of effect of BAY606583 either in the presence of MRS1754 or in the absence of $A_{2B}R$ provides compelling evidence for the involvement of $A_{2B}R$ in the action of BAY606583. Interestingly, there was a tendency for increased 2-NBDG influx in the hippocampal slices from $A_{2B}R$ KO mice, which contradicts what one would expect, *i.e.* a decreased glucose uptake in the absence of $A_{2B}R$. However, $A_{2B}R$ KO mice exhibit an apparent systemic metabolic dysregulation (Csóka et al., 2014) that may also have an impact on cerebral glucoregulation – an additional confounding factor to be taken into account when the cerebral glucoregulator role of $A_{2B}R$ is investigated in future studies.

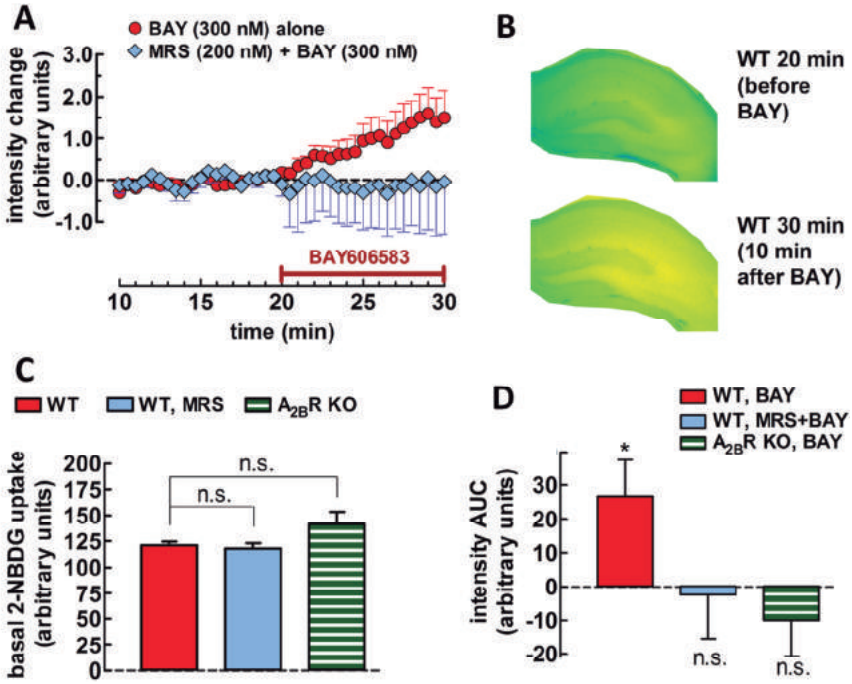

Figure 3.33 – Time-course and regional variation of the effect of $A_{2B}R$ activation on the uptake of the fluorescent glucose analogue, 2-NBDG in 300 µm-thick transversal hippocampal slices of young C57Bl/6j male mice. A) The $A_{2B}R$ agonist BAY606583 (BAY; 300 nM) rapidly increased the accumulation of 2-NBDG throughout the hippocampal slices of the wild-type (WT) mice. The x-axis denotes the time of exposure to 2-NBDG (30 µM), and indicates that BAY606583 was applied 20 min after the addition of the tracer 2-NBDG. The y-axis indicates that the values on the graph are the mean + or - S.E.M. of net changes (n = 7 for BAY606583 alone and n = 4 for BAY606583+MRS1754 (200 nM, an $A_{2B}R$ antagonist)), after the subtraction of the mean intensity values of the respective DMSO controls in each experiment. B) Representative images taken from a WT hippocampal slice immediately before and 10 min after the beginning of BAY606583 superfusion. The false colour scale illustrating the distribution of the fluorescence signal ranges from blue (low signal), through green (moderate signal) up to yellow (strong signal). C) Bar graph summarizing the rate of basal 2-NBDG accumulation, expressed in arbitrary intensity units, under control condition (left, red bar; n = 7) or after ~23 min of preincubation with MRS1754 (middle, light-blue bar; n = 4) in slices from WT mice, and under control condition in slices from $A_{2B}R$ KO (-/-) mice (right, striped green bars; n = 6). Each bar represents the mean + or - S.E.M. of signal intensities in quadruplicates in 4-7 animals at the linear phase, i.e. 19.5 min after the addition of 2-NBDG; *n.s.*, not significant, as assessed with one-way ANOVA followed by Bonferroni's multiple comparison's post-hoc test. D) Effect of drugs normalized to the respective DMSO controls (dashed line crossing the zero value). Values represent the mean + S.E.M. of the individual measurements in duplicates, as obtained with the area under the curve (AUC) method for BAY606583 *vs*. DMSO application in the absence (n = 7) or in the presence of MRS1754 (n = 4) in the WT mice, as well as in the absence of $A_{2B}R$ ($A_{2B}R$ KO; n=6). *P < 0.05.

3.5.1 $A_{2B}R$ activation stimulates glucose transport in cultured astrocytes and neurons

Since the uptake of 2-NBDG underrepresents neuronal glucose transport taken that this substrate is preferentially taken up by astrocytes (Jakoby et al., 2014), we next measured the effect of acute *in vitro* $A_{2B}R$ activation on glucose uptake in primary mouse cortical astrocytes and neurons, using a ^{3}HDG transport assay. Glucose uptake during the 20-min assay amounted to 36.2 ± 5.8 nmol/mg protein in astrocytes (n = 6 in quadruplicates), 25.9 ± 6.6 nmol/mg protein in the cerebrocortical neurons (n = 5 in triplicates) and 10.3 ± 5.5 nmol/mg protein in the hippocampal neurons (n = 4 in triplicates). BAY606583 (300 nM) stimulated the uptake of glucose in astrocytes by 30.4 ± 7.9% (n = 6; $P < 0.05$ *vs*. DMSO control) (**Figure 3.34A**), by 21.8 ± 5.9% in cerebrocortical neurons (n = 5; $P < 0.05$) (**Figure 3.34B**) and by 43.9 ± 10.7% in hippocampal neurons (n = 4; $P < 0.01$ *vs*. DMSO control) (**Figure 3.34C**). The pretreatment with the $A_{2B}R$ antagonist, MRS1754 (200 nM) did not affect the uptake of glucose indicating a lack of endogenous tone in the cultured cells (**Figure 3.34**). However, MRS1754 prevented BAY606583 from stimulating glucose uptake in both cell types (**Figure 3.34**), indicating the involvement of $A_{2B}R$.

The present study provides a direct pharmacological demonstration that the activation of adenosine $A_{2B}Rs$ triggers a rapid and sustained glucose uptake in the mouse brain. This effect appears to occur in both neurons and astrocytes. Hence, $A_{2B}Rs$ may link extracellular adenosine peaks with increased glucose uptake, thus allowing energy metabolism to meet the demands of neural activity. Such mechanism would be essential to avoid hypoenergetic crisis, which can lead to cell death. Indeed, $A_{2B}R$ activation has been linked with increased survival of hippocampal and cortical cells under oxygen-glucose deprivation (Gu et al., 2013; Moidunny et al., 2012; Molz et al., 2015). Hence, $A_{2B}Rs$ seem to generally assist the homeostasis of brain cells.

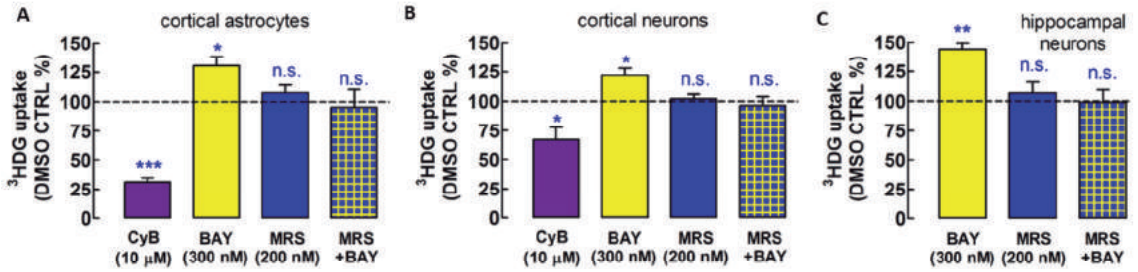

Figure 3.34 – A_{2B}R activation stimulates glucose uptake in cerebrocortical astrocytes as well as in cerebrocortical and hippocampal neurons *in vitro*. The A_{2B}R-selective agonist BAY606583 (BAY; 300 nM; n = 6) stimulated glucose uptake in primary cultures of A) cerebrocortical astrocytes, B) cerebrocortical neurons, and C) hippocampal neurons, obtained from E17-C57Bl/6 mouse embryos, as assessed using the 20 min ^{3}HDG uptake assay. One hour pretreatment with the A_{2B}R-selective antagonist, MRS1754 (MRS; 200 nM; n = 5, astrocytes; n = 4, neurons) prevented the action of the A_{2B}R agonist, while it had no effect on uptake per se (n = 5, astrocytes; n = 4, neurons). D-glucose uptake is calculated according to Lemos et al. (2012), and is expressed in nmol/mg protein, mean + S.E.M of "n" cultures in quadruplicates for the cerebrocortical cultures (4 wells/treatment/culture) and triplicates for the hippocampal cultures. Cytochalasin B (CyB; 10 µM) inhibited the uptake of glucose in 5 astrocytic cultures stronger than in 4 cerebrocortical neuronal cultures, because neuronal glucose uptake is moderately dependent on GLUT1 transporters in culture, while GLUT1 is the primary glucose transporter in astrocytes. CyB was not tested in hippocampal neurons. After 60 min preincubation at 37ºC in the assay medium, ^{3}HDG was co-administered for 20 min with BAY, CyB or their vehicle, DMSO. When used, MRS1754 was present since the beginning of the preincubation period. *P < 0.05 and ***P < 0.001 *vs*. DMSO control; n.s., not significant.

3.5.2 The inhibition of endogenous A_{2B}R activation strongly decreases glucose uptake in brain slices

Next we asked if A_{2B}Rs could also function as endogenous glucoregulators in different brain areas. To this end, acute frontocortical, hippocampal or striatal slices from C57Bl/6 mice were batch-incubated at 37ºC under continuous oxygenation. The control resting glucose uptake in the subsequent 30 min period was not different among the three brain regions investigated (n = 11-14, P > 0.05) (**Figure 3.35**). It was previously observed, in rat hippocampal slices, that the glutamate reuptake inhibitor, DL-TBOA (10 µM) significantly reduces resting ^{3}HDG uptake by 23% in a similar assay (**Figure 3.8**). This of course contributes to extracellular adenosine accumulation. Indeed, one hour pretreatment and 30 min treatment with MRS1754 (100 nM) reduced

glucose uptake in the three brain areas by ~33-41% (n = 6, P < 0.01) as compared to control (**Figure 3.35**). This suggests that extracellular adenosine accumulation in these bathed slices at 37ºC is sufficient to activate A_{2B}Rs. Certainly, the reduction of extracellular adenosine levels with one hour pretreatment and 30 min treatment with adenosine deaminase (3U/mL) similarly diminished glucose uptake by 17-36% in the three types of slices (n = 5-6, P < 0.05) (**Figure 3.35**).

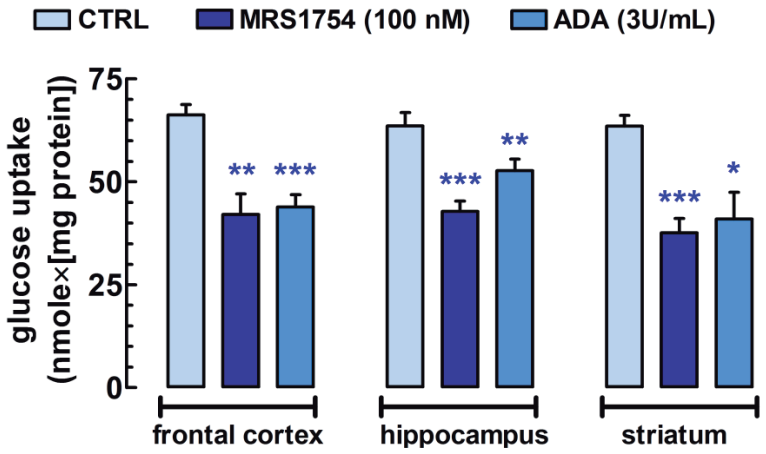

Figure 3.35 – Endogenously active A_{2B}R tonically stimulate glucose uptake in acute 400 µm-thick coronal frontocortical, transversal hippocampal and rostrocaudal striatal slices from C57Bl/6 mice. Brain slices were divided into 4 groups and they were incubated in the assay solution at 37 ºC under continuous gassing with a mixture of 95% O_2 and 5% CO_2. One chamber with a group of slices from the three brain areas was exposed to MRS1754, another group was exposed to adenosine deaminase (ADA; 3U/mL), while the remaining two groups served as control. After 60 min pretreatment, ^{3}HDG (2 nM) was bath-applied to trace the course of glucose uptake for a 30-min period. Total D-glucose uptake (nmol/mg protein) was determined for each group of slices (for further details, see Materials and Methods, and (Lemos et al., 2012). Bars represent the mean + SEM of individual measurements from n = 5-14 mice. *P < 0.05, **P < 0.01, ***P < 0.001 *vs*. control.

3.5.3 The effect of A_{2B}R blockade on glycogen synthesis and lactate release

Concerning the brain, compelling evidence supports glycogen as a major glucose storage with buffer function in astrocytes to mitigate energetic crisis under prolonged intense activity of the circuitry (Hutchins and Rogers, 1970; Pellerin et al., 2007). Importantly, the activation of A_{2B}R can promote Akt phosphorylation (Johnston-Cox et

al., 2012; Schulte and Fredholm, 2003), which in turn can stimulate glycogen synthesis. Furthermore, lactate production can be partly supported by glycogenolysis in astrocytes, and during activity, neurons and thin astrocytic processes in the synapse rely on the oxidation of lactate rather than that of glucose (Pellerin et al., 2007; Pellerin and Magistretti, 2012).

Glycogen levels and lactate release are major parameters reflecting the modulation of glucose metabolism (Brown and Ransom, 2007a; Pellerin et al., 2007). Hence, with the help of the metabolizable glucose analogue $^{14}C_6$-glucose the total glucose uptake and ^{14}C incorporation into glycogen was measured in frontocortical and striatal slices in the 90 min period following slice preparation. Total $^{14}C_6$-glucose retention by the striatal slices during this period (78.8 ± 13.2 nmol/mg protein) was significantly smaller (by 9.2 ± 3.1%, n = 6, $P < 0.05$) in the presence of MRS1754 (100 nM) (**Figure 3.36**), which was a considerably lesser effect amplitude than what we measured with ^{3}HDG after 1 h recovery. Moreover, 20% of the above total retention value represented $^{14}C_6$-glucose incorporation into glycogen (15.4 ± 3.2 nmol/mg protein). As expected, MRS1754 also greatly decreased striatal glycogen levels by 34.9 ± 3.4% ($P < 0.05$) (**Figure 3.36**). Last but not least, lactate loss from the control striatal slices to the medium amounted to 621 ± 78 nmol/mg protein. MRS1754 significantly stimulated lactate release by 24.1 ± 8.9% (n = 6, $P < 0.05$) (**Figure 3.36**).

Frontocortical total ^{14}C retention amounted to 87.9 ± 9.8 % (n = 8). Glycogen synthesis was 18.2 ± 4.0 nmol/mg protein (20.7% of total ^{14}C retention), and lactate loss to the bath was 504 ± 56 nmol/mg protein (n = 8), *i.e.* none of these three parameters were proved statistically different from those in the striatum ($P > 0.05$). $A_{2B}R$ blockade reduced both ^{14}C retention by 12.8 ± 4.0% ($P < 0.05$) and ^{14}C-labelled glycogen content by 38.6 ± 9.9% ($P < 0.05$), but did not affect lactate loss to the medium ($P > 0.05$) (**Figure 3.36**).

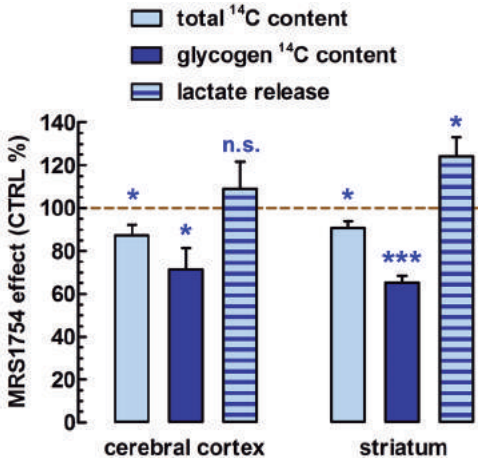

Figure 3.36 – Mapping the role of A_{2B}Rs on glycogen synthesis and lactate release. In acute 400 µm-thick coronal frontocortical and rostrocaudal striatal slices from C57Bl/6 mice. Brain slices were divided into two groups and they were submerged in an assay solution containing the metabolizable glucose analogue, $^{14}C_6$-glucose (50 nM) at 37 ºC under continuous gassing with a mixture of 95% O_2 and 5% CO_2. One chamber with a group of slices from the three brain areas was exposed to MRS1754, the other group was exposed to its vehicle, DMSO (0.1%, control). After 90 min incubation, the slices were washed 3 times in ice-cold assay solution, collected in 2 mL NaOH (0.5 M). After dissolving the slices, 200 µL of these samples was used to count total ^{14}C-retention in the slices and protein quantities, the 1800 µL left were used to precipitate glycogen and count its ^{14}C content as before (Lemos et al., 2012). Lactate content in the bath at the end of the 90 min incubation period was assessed with a lactic acid assay kit. Bars represent the mean ± SEM of individual measurements from n = 6 - 8 mice. *P < 0.05, ***P < 0.001 *vs*. control.

In conclusion, for the studies on the A_{2B}R, we indirectly demonstrated here that A_{2B}R activation is positively linked with glycogen synthesis, but this is accompanied by a reduction in lactate output in the striatum. One likely scenario is thus the following: during strong activity of the circuitry, high extracellular levels of adenosine are generated which in turn will stimulate astrocytic glycogen storage via A_{2B}R activation in the striatum, at the expense of lactate release. This can be a counterregulatory process – a metabolic brake that protects astrocytes from glucose storage depletion and can also dampen extracellular acidification.

That A_{2B}Rs are involved in glucoregulation is not surprising: they can also directly regulate glucose handling by the three major organs involved in peripheral glucoregulation, *i.e.* the liver, the white adipose tissue and the skeletal muscle (Antonioli et al., 2015). Most studies on A_{2B}R in the brain have focused on pathological

conditions (Moidunny et al., 2012; Trincavelli et al., 2004). Studies from Németh et al. (2007) using multiple-low-dose-streptozotocin mice showed that $A_{2B}R$ activation ameliorated T1D reducing hyperglycemia, attenuating proinflammatory mediators and avoiding immune-mediated β-cell destruction. Those authors even suggest $A_{2B}R$ ligands as a possible candidate to help alleviate from some symptoms of T1D (Németh et al., 2007).

There is ample evidence for the presence of $A_{2B}Rs$ in both neurons and astrocytes homogenously distributed in the mammalian brain (Feoktistov and Biaggioni, 1997), thus $A_{2B}Rs$ are well-positioned to modulate glucose metabolism in both cell types. To possibly understand why we did not see changes in lactate loss to the medium in the frontal cortex, we should understand the principal difference between the striatum and the cerebral cortex. The principal neurons of the cerebral cortex are the glutamatergic pyramidal cells, while in the striatum, almost all neurons are GABAergic and there is no evidence for glutamatergic cells whatsoever (Reid and Walsh, 2002). It is not easy to guess whether $A_{2B}R$ activation affects glucose metabolism in GABAergic inhibitory neurons of the striatum, because hippocampal and cerebrocortical cultures at this age contain predominantly excitatory neurons (Banker and Cowan, 1977; de Lima and Voigt, 1997), and in our neuronal cultures, those were the likely candidates which responded with increased glucose uptake to $A_{2A}R$ activation.

$A_{2B}R$ blockade did not significantly affect lactate release in frontocortical slices, contrasting thus the striatal slices. It is possible that $A_{2B}R$ blockade stimulates lactate oxidation in pyramidal cells which would reduce lactate loss to the medium, or the other way around, it would decrease lactate consumption in GABAergic cells of the striatum, hence dumping this energy substrate to the bath. The reason why we believe that this discrepancy is more likely associated to an increase in lactate use by pyramidal cells is because in cerebrocortical neuronal culture, $A_{2B}R$ activation increased glucose uptake. Normally, neurons use either glucose or lactate (Castro et al., 2009), so if $A_{2B}R$ activation increases glucose in pyramidal cells, those neurons would concomitantly use less lactate. And the other way around, in the slice under $A_{2B}R$ blockade one would expect less glucose uptake and more lactate use, on the cost of lactate dumping into the medium for good.

Besides the direct regulation of glucose transport, the modulation of glutamatergic signalling will also affect glucose uptake (Pellerin and Magistretti, 2012). This is because glutamatergic neurotransmission is a costly process, being responsible for the majority of energetic glucose metabolism in the brain (Attwell and Laughlin, 2001). In concert with this, we recently found that $A_{2B}R$ modulate glutamatergic synaptic transmission in the hippocampus (Gonçalves et al., 2015). Not only neurons but also astrocytes are equipped with $A_{2B}R$ (Feoktistov and Biaggioni, 1997; Verkhratsky and Burnstock, 2014), and both cell types are capable of releasing glutamate (Halassa and Haydon, 2010). Therefore, $A_{2B}R$ are well positioned in the tripartite synapse to coordinate glucose uptake according to metabolic demands.

The present pharmacological study is based on the use of a selective $A_{2B}R$ agonist, BAY606583 and an antagonist of this adenosine receptor, MRS1754, together with $A_{2B}R$ KO mice. Hence, the lack of effect of BAY606583 either in the presence of MRS1754 or in the absence of $A_{2B}R$ provides compelling evidence for the involvement of $A_{2B}R$ in the action of BAY606583. Interestingly, there was a tendency for increased 2-NBDG influx in the hippocampal slices from $A_{2B}R$ KO mice, which contradicts what one would expect, *i.e.* a decreased glucose uptake in the absence of $A_{2B}R$. However, $A_{2B}R$ KO mice exhibit an apparent systemic metabolic dysregulation (Csóka et al., 2014) that may also have an impact on cerebral glucoregulation – an additional confounding factor to be taken into account when the cerebral glucoregulator role of $A_{2B}R$ is investigated in future studies.

Glucose availability in the brain regulates cognition and memory in both healthy humans and dementia patients (Branconnier, 1983; Messier, 2004; Watson and Craft, 2004). Although normally metabolic boosters (nootropics) do not mitigate the outcome of neurodegenerative disorders, $A_{2B}R$ agonists eventually possess multiple beneficial actions including boosting cerebral glucose metabolism and increasing cell survival apart from effects on energy metabolism (Gu et al., 2013; Moidunny et al., 2012; Molz et al., 2015). Therefore, further studies are invited to evaluate the clinical potential of $A_{2B}R$ agonists in both animals and man.

Chapter 4

Conclusions

4 CONCLUSIONS

During this thesis work, the basic features of the still ill-defined brain glucose metabolism were studied. The protocols that were optimized allowed characterizing some of the possible mechanisms that directly afford glucoregulation, in the absence of systemic factors and the BBB. For decades, huge efforts have been made worldwide to investigate hot topics in *e.g.* neuroanatomy, neurophysiology, neurodevelopment and neuroprotection, but the energy requirements of these processes are little understood and often ignored. For instance, until recently, it was unclear if the brain availed itself of energy substrates other than glucose. To address this question, we assessed recently how glucose metabolism is affected *in vitro* in the plentiness of lactate, pyruvate and ketone bodies. Intriguingly, we found that ketone bodies can effectively compete with glucose and prevail as energy substrate for acetyl-CoA production (Valente-Silva et al., 2015). Our pioneering study was just scratching the surface and obviously, there is much more to it than meets the eye. The complex network of brain energy flow requires a simple and effective regulatory system. In my opinion, the simplest regulatory mechanism is the fastest and the best, because there is no room for error in the control of energy metabolism of tissues of high oxygen and energy dependence, such as the brain or the heart muscle. Consequently, dysregulated brain glucose metabolism turns the wheel of physiological processes to the direction of pathology, and this path is paved with hypoplasticity, impaired synaptic plasticity, neuroinflammation and neurodegeneration.

It is evident that most, if not all, neuropsychiatric disorders bear specific hallmarks of dysregulation of brain glucose metabolism (Detka et al., 2013; Mosconi, 2005; Teune et al., 2010). There is a paucity of tools that can effectively influence brain glucose metabolism. Our research group is strongly convinced that the stimulation of brain energy metabolism can help to mitigate the outcome of brain disorders. This strategy can hopefully alleviate neurons from energy crisis under dysregulated energy metabolism when the cells are stressed by the energy demand of dealing with protein aggregates. In fact, impaired glucose metabolism shows specific patterns in brain disorders, spatiotemporally coinciding with *e.g.* the density and distribution of misfolded protein aggregates.

The results showing cannabinoid and adenosine receptors involved in glucoregulation came as little surprise. However, the lack of unveil a conclusive mechanisms with regard to CB_1Rs was disappointing. In an ongoing and here not presented investigation, we also found that the CB_2 cannabinoid receptor stimulates glucose uptake in diverse *in vitro* models such as those presented in this thesis. The manuscript of that study is currently past first revision. Whether the two cannabinoid receptors interact in the control of glucose uptake is unknown to us currently, but there is solid published evidence for their heteredimerization in the brain, for instance, in GABAergic cells (Callén et al., 2012). This prompts us to test now if CB_2Rs are somehow involved in the decreased glucose uptake seen under the genetic or chemical ablation of CB_1R. Fortunately, an adenosine receptor subtype that is little studied in the brain proved to be a much more promising target to increase brain glucose uptake and metabolism, and may in fact underlie an important physiological mechanism. Nevertheless, there is still no hard evidence to conclude if these A_{2B}Rs confer a therapeutic target to boost brain metabolism in disease conditions and if so, such an intervention could prevent, halt or revert neuropathology.

To better understand the usefulness of targeting brain metabolism in disease models, the first logical step is to see what goes wrong either with the neuromodulators involved in glucoregulation or the glucoregulation itself, or both. Using different animal models with different approaches of metabolic impairments such as T1D (ip-STZ administration), type-3 diabetes (icv-STZ administration) and prediabetes (high sucrose consumption), numerous hippocampal modifications induced by these metabolic disorders were identified. Both systemic and central impairments of metabolism appeared intertwined with brain dysfunctions, which is in accordance with the literature. The involvement of the neuromodulator and glucoregulator cannabinoid CB_1 and adenosine A_1 and A_{2B} receptors were obviated by our results, hence suggesting that at least the A_{2B}R has proven worth of further attention.

During this PhD study, the potential local central glucoregulator roles of insulin – the hormone widely known as indispensable for peripheral glucoregulation was also dissected. Responsiveness to insulin in hippocampal glucose uptake (**Figure 3.3**) was observed and that this insulin action is somewhat dependent on the CB_1R (**Figure 3.5**). In concert with these, in another revised manuscript we report that glucocorticoids, by

triggering rapid local endocannabinoid synthesis, stimulate CB_1Rs that form physical heterodimers with insulin receptors in the nucleus accumbens, and consequently, impair insulin signalling.

Obviously, the data presented in this thesis – albeit promising – represent only a tiny bit of the tip of the iceberg, and there is a lot ahead to understand about the basics of glucose metabolism in the CNS and the therapeutic targets that would allow physicians in the future to restore or boost declining insulin sensitivity and energy metabolism in the brain both under healthy aging and in diseases.

Chapter 5

References

5 REFERENCES

Abadji, V., Lin, S., Taha, G., Griffin, G., Stevenson, L. A., Pertwee, R. G., et al. (1994). (R)-methanandamide: a chiral novel anandamide possessing higher potency and metabolic stability. *J. Med. Chem.* 37, 1889–1893.

Abbracchio, M. P., Brambilla, R., Ceruti, S., Kim, H. O., von Lubitz, D. K., Jacobson, K. A., et al. (1995). G protein-dependent activation of phospholipase C by adenosine A_3 receptors in rat brain. *Mol. Pharmacol.* 48, 1038–1045.

Abdul-Ghani, M. A., Williams, K., DeFronzo, R. A., and Stern, M. (2007). What is the best predictor of future type 2 diabetes? *Diabetes Care* 30, 1544–1548. doi:10.2337/dc06-1331.

Ackermann, R. F., Finch, D. M., Babb, T. L., and Engel, J. (1984). Increased glucose metabolism during long-duration recurrent inhibition of hippocampal pyramidal cells. *J. Neurosci. Off. J. Soc. Neurosci.* 4, 251–264.

Aggleton, J. P., Albasser, M. M., Aggleton, D. J., Poirier, G. L., and Pearce, J. M. (2010). Lesions of the rat perirhinal cortex spare the acquisition of a complex configural visual discrimination yet impair object recognition. *Behav. Neurosci.* 124, 55–68. doi:10.1037/a0018320.

Akbar, M., Okajima, F., Tomura, H., Shimegi, S., and Kondo, Y. (1994). A single species of A1 adenosine receptor expressed in Chinese hamster ovary cells not only inhibits cAMP accumulation but also stimulates phospholipase C and arachidonate release. *Mol. Pharmacol.* 45, 1036–1042.

Akbarzadeh, A., Norouzian, D., Mehrabi, M. R., Jamshidi, S., Farhangi, A., Verdi, A. A., et al. (2007). Induction of diabetes by Streptozotocin in rats. *Indian J. Clin. Biochem. IJCB* 22, 60–64. doi:10.1007/BF02913315.

Akkerman, S., Blokland, A., Reneerkens, O., van Goethem, N. P., Bollen, E., Gijselaers, H. J. M., et al. (2012). Object recognition testing: methodological considerations on exploration and discrimination measures. *Behav. Brain Res.* 232, 335–347. doi:10.1016/j.bbr.2012.03.022.

Akter, K., Lanza, E. A., Martin, S. A., Myronyuk, N., Rua, M., and Raffa, R. B. (2011a). Diabetes mellitus and Alzheimer's disease: shared pathology and treatment? *Br. J. Clin. Pharmacol.* 71, 365–376. doi:10.1111/j.1365-2125.2010.03830.x.

Akter, K., Lanza, E. A., Martin, S. A., Myronyuk, N., Rua, M., and Raffa, R. B. (2011b). Diabetes mellitus and Alzheimer's disease: shared pathology and treatment?: Diabetes and Alzheimer's disease. *Br. J. Clin. Pharmacol.* 71, 365–376. doi:10.1111/j.1365-2125.2010.03830.x.

Alanko, L., Porkka-Heiskanen, T., and Soinila, S. (2006). Localization of equilibrative nucleoside transporters in the rat brain. *J. Chem. Neuroanat.* 31, 162–168. doi:10.1016/j.jchemneu.2005.12.001.

Alexander, G. E., and Moeller, J. R. (1994). Application of the scaled subprofile model to functional imaging in neuropsychiatric disorders: A principal component approach to modeling brain function in disease. *Hum. Brain Mapp.* 2, 79–94. doi:10.1002/hbm.460020108.

Allaman, I., Lengacher, S., Magistretti, P. J., and Pellerin, L. (2003). A_{2B} receptor activation promotes glycogen synthesis in astrocytes through modulation of gene expression. *Am. J. Physiol. Cell Physiol.* 284, C696–704. doi:10.1152/ajpcell.00202.2002.

Alle, H., Roth, A., and Geiger, J. R. P. (2009). Energy-efficient action potentials in hippocampal mossy fibers. *Science* 325, 1405–1408. doi:10.1126/science.1174331.

Anderson, C. M., Xiong, W., Young, J. D., Cass, C. E., and Parkinson, F. E. (1996). Demonstration of the existence of mRNAs encoding N1/cif and N2/cit sodium/nucleoside cotransporters in rat brain. *Brain Res. Mol. Brain Res.* 42, 358–361.

Anderson, R. J., Freedland, K. E., Clouse, R. E., and Lustman, P. J. (2001). The Prevalence of Comorbid Depression in Adults With Diabetes A meta-analysis. *Diabetes Care* 24, 1069–1078. doi:10.2337/diacare.24.6.1069.

Anderson, W. W., and Collingridge, G. L. (2001). The LTP Program: a data acquisition program for on-line analysis of long-term potentiation and other synaptic events. *J. Neurosci. Methods* 108, 71–83.

Andó, R. D., Bíró, J., Csölle, C., Ledent, C., and Sperlágh, B. (2012). The inhibitory action of exo- and endocannabinoids on [^{3}H]GABA release are mediated by both CB_1 and CB_2 receptors in the mouse hippocampus. *Neurochem. Int.* 60, 145–152. doi:10.1016/j.neuint.2011.11.012.

Antonioli, L., Blandizzi, C., Csóka, B., Pacher, P., and Haskó, G. (2015). Adenosine signalling in diabetes mellitus-pathophysiology and therapeutic considerations. *Nat. Rev. Endocrinol.* 11, 228–241. doi:10.1038/nrendo.2015.10.

Antunes, M., and Biala, G. (2012a). The novel object recognition memory: neurobiology, test procedure, and its modifications. *Cogn. Process.* 13, 93–110. doi:10.1007/s10339-011-0430-z.

Antunes, M., and Biala, G. (2012b). The novel object recognition memory: neurobiology, test procedure, and its modifications. *Cogn. Process.* 13, 93–110. doi:10.1007/s10339-011-0430-z.

Apelt, J., Mehlhorn, G., and Schliebs, R. (1999). Insulin-sensitive GLUT4 glucose transporters are colocalized with GLUT3-expressing cells and demonstrate a chemically distinct neuron-specific localization in rat brain. *J. Neurosci. Res.* 57, 693–705.

Araque, A., Parpura, V., Sanzgiri, R. P., and Haydon, P. G. (1999). Tripartite synapses: glia, the unacknowledged partner. *Trends Neurosci.* 22, 208–215.

Araya, K. A., David Pessoa Mahana, C., and González, L. G. (2007). Role of cannabinoid CB_1 receptors and $G_{i/o}$ protein activation in the modulation of synaptosomal Na^+,K^+-ATPase activity by WIN55,212-2 and delta(9)-THC. *Eur. J. Pharmacol.* 572, 32–39. doi:10.1016/j.ejphar.2007.06.013.

Arendash, G. W., Schleif, W., Rezai-Zadeh, K., Jackson, E. K., Zacharia, L. C., Cracchiolo, J. R., et al. (2006). Caffeine protects Alzheimer's mice against cognitive impairment and reduces brain beta-amyloid production. *Neuroscience* 142, 941–952. doi:10.1016/j.neuroscience.2006.07.021.

Aschner, M. (1998). Astrocytes as mediators of immune and inflammatory responses in the CNS. *Neurotoxicology* 19, 269–281.

Aso, E., Palomer, E., Juvés, S., Maldonado, R., Muñoz, F. J., and Ferrer, I. (2012). CB_1 agonist ACEA protects neurons and reduces the cognitive impairment of AβPP/PS1 mice. *J. Alzheimers Dis. JAD* 30, 439–459. doi:10.3233/JAD-2012-111862.

Assini, F. L., Duzzioni, M., and Takahashi, R. N. (2009). Object location memory in mice: pharmacological validation and further evidence of hippocampal CA1 participation. *Behav. Brain Res.* 204, 206–211. doi:10.1016/j.bbr.2009.06.005.

Astrup, J., Sørensen, P. M., and Sørensen, H. R. (1981). Oxygen and glucose consumption related to Na+-K+ transport in canine brain. *Stroke J. Cereb. Circ.* 12, 726–730.

Attwell, D., and Laughlin, S. B. (2001). An energy budget for signalling in the grey matter of the brain. *J. Cereb. Blood Flow Metab. Off. J. Int. Soc. Cereb. Blood Flow Metab.* 21, 1133–1145. doi:10.1097/00004647-200110000-00001.

Aviles-Olmos, I., Limousin, P., Lees, A., and Foltynie, T. (2013). Parkinson's disease, insulin resistance and novel agents of neuroprotection. *Brain J. Neurol.* 136, 374–384. doi:10.1093/brain/aws009.

Baker, L. D., Cross, D. J., Minoshima, S., Belongia, D., Watson, G. S., and Craft, S. (2011). Insulin resistance and Alzheimer-like reductions in regional cerebral glucose metabolism for cognitively normal adults with prediabetes or early type 2 diabetes. *Arch. Neurol.* 68, 51–57. doi:10.1001/archneurol.2010.225.

Bakirtzi, K., Belfort, G., Lopez-Coviella, I., Kuruppu, D., Cao, L., Abel, E. D., et al. (2009). Cerebellar neurons possess a vesicular compartment structurally and functionally similar to Glut4-storage vesicles from peripheral insulin-sensitive tissues. *J. Neurosci. Off. J. Soc. Neurosci.* 29, 5193–5201. doi:10.1523/JNEUROSCI.0858-09.2009.

Baldwin, S. A., Mackey, J. R., Cass, C. E., and Young, J. D. (1999). Nucleoside transporters: molecular biology and implications for therapeutic development. *Mol. Med. Today* 5, 216–224. doi:10.1016/S1357-4310(99)01459-8.

Ballarín, M., Fredholm, B. B., Ambrosio, S., and Mahy, N. (1991). Extracellular levels of adenosine and its metabolites in the striatum of awake rats: inhibition of

uptake and metabolism. *Acta Physiol. Scand.* 142, 97–103. doi:10.1111/j.1748-1716.1991.tb09133.x.

Banker, G. A., and Cowan, W. M. (1977). Rat hippocampal neurons in dispersed cell culture. *Brain Res.* 126, 397–342.

Banks, W. A. (2004). The source of cerebral insulin. *Eur. J. Pharmacol.* 490, 5–12. doi:10.1016/j.ejphar.2004.02.040.

Banks, W. A., Owen, J. B., and Erickson, M. A. (2012). Insulin in the brain: there and back again. *Pharmacol. Ther.* 136, 82–93. doi:10.1016/j.pharmthera.2012.07.006.

Baptista, F. I., Gaspar, J. M., Cristóvão, A., Santos, P. F., Köfalvi, A., and Ambrósio, A. F. (2011). Diabetes induces early transient changes in the content of vesicular transporters and no major effects in neurotransmitter release in hippocampus and retina. *Brain Res.* 1383, 257–269. doi:10.1016/j.brainres.2011.01.071.

Barros, L. F., Bittner, C. X., Loaiza, A., Ruminot, I., Larenas, V., Moldenhauer, H., et al. (2009). Kinetic validation of 6-NBDG as a probe for the glucose transporter GLUT1 in astrocytes. *J. Neurochem.* 109 Suppl 1, 94–100. doi:10.1111/j.1471-4159.2009.05885.x.

Barros, L. F., and Deitmer, J. W. (2010). Glucose and lactate supply to the synapse. *Brain Res. Rev.* 63, 149–159. doi:10.1016/j.brainresrev.2009.10.002.

Batalha, V. L., Pego, J. M., Fontinha, B. M., Costenla, A. R., Valadas, J. S., Baqi, Y., et al. (2013). Adenosine A_{2A} receptor blockade reverts hippocampal stress-induced deficits and restores corticosterone circadian oscillation. *Mol. Psychiatry* 18, 320–331. doi:10.1038/mp.2012.8.

Baydas, G., Nedzvetskii, V. S., Nerush, P. A., Kirichenko, S. V., and Yoldas, T. (2003). Altered expression of NCAM in hippocampus and cortex may underlie memory and learning deficits in rats with streptozotocin-induced diabetes mellitus. *Life Sci.* 73, 1907–1916.

Bayewitch, M., Avidor-Reiss, T., Levy, R., Barg, J., Mechoulam, R., and Vogel, Z. (1995). The peripheral cannabinoid receptor: adenylate cyclase inhibition and G protein coupling. *FEBS Lett.* 375, 143–147.

Bélanger, A., Lavoie, N., Trudeau, F., Massicotte, G., and Gagnon, S. (2004). Preserved LTP and water maze learning in hyperglycaemic-hyperinsulinemic ZDF rats. *Physiol. Behav.* 83, 483–494. doi:10.1016/j.physbeh.2004.08.031.

Bélanger, M., Allaman, I., and Magistretti, P. J. (2011). Brain energy metabolism: focus on astrocyte-neuron metabolic cooperation. *Cell Metab.* 14, 724–738. doi:10.1016/j.cmet.2011.08.016.

Bélanger, M., and Magistretti, P. J. (2009). The role of astroglia in neuroprotection. *Dialogues Clin. Neurosci.* 11, 281–295.

Belikoff, B. G., Hatfield, S., Georgiev, P., Ohta, A., Lukashev, D., Buras, J. A., et al. (2011). A_{2B} Adenosine Receptor Blockade Enhances Macrophage-Mediated Bacterial Phagocytosis and Improves Polymicrobial Sepsis Survival in Mice. *J. Immunol. Baltim. Md 1950* 186, 2444–2453. doi:10.4049/jimmunol.1001567.

Ben Addi, A., Lefort, A., Hua, X., Libert, F., Communi, D., Ledent, C., et al. (2008). Modulation of murine dendritic cell function by adenine nucleotides and adenosine: involvement of the A_{2B} receptor. *Eur. J. Immunol.* 38, 1610–1620. doi:10.1002/eji.200737781.

Bénard, G., Massa, F., Puente, N., Lourenço, J., Bellocchio, L., Soria-Gómez, E., et al. (2012). Mitochondrial CB_1 receptors regulate neuronal energy metabolism. *Nat. Neurosci.* 15, 558–564. doi:10.1038/nn.3053.

Bennett, R. A., and Pegg, A. E. (1981). Alkylation of DNA in rat tissues following administration of streptozotocin. *Cancer Res.* 41, 2786–2790.

Benomar, Y., Naour, N., Aubourg, A., Bailleux, V., Gertler, A., Djiane, J., et al. (2006). Insulin and leptin induce Glut4 plasma membrane translocation and glucose uptake in a human neuronal cell line by a phosphatidylinositol 3-kinase-dependent mechanism. *Endocrinology* 147, 2550–2556. doi:10.1210/en.2005-1464.

Benowitz, N. L., Jones, R. T., and Lerner, C. B. (1976). Depression of growth hormone and cortisol response to insulin-induced hypoglycemia after prolonged oral delta-9-tetrahydrocannabinol administration in man. *J. Clin. Endocrinol. Metab.* 42, 938–941. doi:10.1210/jcem-42-5-938.

Benton, D. (1990). The impact of increasing blood glucose on psychological functioning. *Biol. Psychol.* 30, 13–19.

Bermúdez-Silva, F. J., Suárez Pérez, J., Nadal, A., and Rodríguez de Fonseca, F. (2009). The role of the pancreatic endocannabinoid system in glucose metabolism. *Best Pract. Res. Clin. Endocrinol. Metab.* 23, 87–102. doi:10.1016/j.beem.2008.10.012.

Bhutada, P., Mundhada, Y., Bansod, K., Tawari, S., Patil, S., Dixit, P., et al. (2011). Protection of cholinergic and antioxidant system contributes to the effect of berberine ameliorating memory dysfunction in rat model of streptozotocin-induced diabetes. *Behav. Brain Res.* 220, 30–41. doi:10.1016/j.bbr.2011.01.022.

Biessels, G. J., Bravenboer, B., and Gispen, W. H. (2004). Glucose, insulin and the brain: modulation of cognition and synaptic plasticity in health and disease: a preface. *Eur. J. Pharmacol.* 490, 1–4. doi:10.1016/j.ejphar.2004.02.057.

Biessels, G. J., and Reagan, L. P. (2015). Hippocampal insulin resistance and cognitive dysfunction. *Nat. Rev. Neurosci.* 16, 660–671. doi:10.1038/nrn4019.

Bingham, E. M., Hopkins, D., Smith, D., Pernet, A., Hallett, W., Reed, L., et al. (2002). The role of insulin in human brain glucose metabolism: an 18fluoro-deoxyglucose positron emission tomography study. *Diabetes* 51, 3384–3390.

Bisogno, T., Melck, D., De Petrocellis, L., and Di Marzo, V. (1999). Phosphatidic acid as the biosynthetic precursor of the endocannabinoid 2-arachidonoylglycerol in intact mouse neuroblastoma cells stimulated with ionomycin. *J. Neurochem.* 72, 2113–2119.

Bitencourt, R. M., Alpár, A., Cinquina, V., Ferreira, S. G., Pinheiro, B. S., Lemos, C., et al. (2015a). Lack of presynaptic interaction between glucocorticoid and CB_1 cannabinoid receptors in GABA- and glutamatergic terminals in the frontal cortex of laboratory rodents. *Neurochem. Int.* doi:10.1016/j.neuint.2015.07.014.

Bitencourt, R. M., Alpár, A., Cinquina, V., Ferreira, S. G., Pinheiro, B. S., Lemos, C., et al. (2015b). Lack of presynaptic interaction between glucocorticoid and CB_1 cannabinoid receptors in GABA- and glutamatergic terminals in the frontal cortex of laboratory rodents. *Neurochem. Int.* doi:10.1016/j.neuint.2015.07.014.

Blaustein, M. P., Juhaszova, M., Golovina, V. A., Church, P. J., and Stanley, E. F. (2002). Na/Ca exchanger and PMCA localization in neurons and astrocytes: functional implications. *Ann. N. Y. Acad. Sci.* 976, 356–366.

Bliss, T. V., and Lomo, T. (1973). Long-lasting potentiation of synaptic transmission in the dentate area of the anaesthetized rabbit following stimulation of the perforant path. *J. Physiol.* 232, 331–356.

Bliss, T. V. P., and Cooke, S. F. (2011). Long-term potentiation and long-term depression: a clinical perspective. *Clinics* 66, 3–17. doi:10.1590/S1807-59322011001300002.

Bloemer, J., Bhattacharya, S., Amin, R., and Suppiramaniam, V. (2014). Impaired insulin signaling and mechanisms of memory loss. *Prog. Mol. Biol. Transl. Sci.* 121, 413–449. doi:10.1016/B978-0-12-800101-1.00013-2.

Bloom, A. S., Tershner, S., Fuller, S. A., and Stein, E. A. (1997). Cannabinoid-induced alterations in regional cerebral blood flow in the rat. *Pharmacol. Biochem. Behav.* 57, 625–631.

Boison, D. (2008). Adenosine as a neuromodulator in neurological diseases. *Curr. Opin. Pharmacol.* 8, 2–7. doi:10.1016/j.coph.2007.09.002.

Boison, D., and Aronica, E. (2015). Comorbidities in Neurology: Is adenosine the common link? *Neuropharmacology* 97, 18–34. doi:10.1016/j.neuropharm.2015.04.031.

Boison, D., Sandau, U. S., Ruskin, D. N., Kawamura, M., and Masino, S. A. (2013). Homeostatic control of brain function – new approaches to understand epileptogenesis. *Front. Cell. Neurosci.* 7. doi:10.3389/fncel.2013.00109.

Bojorge, G., and de Lores Arnaiz, G. R. (1987). Insulin modifies Na^+, K^+-ATPase activity of synaptosomal membranes and whole homogenates prepared from rat cerebral cortex. *Neurochem. Int.* 11, 11–16.

Bonhaus, D. W., Chang, L. K., Kwan, J., and Martin, G. R. (1998). Dual activation and inhibition of adenylyl cyclase by cannabinoid receptor agonists: evidence for agonist-specific trafficking of intracellular responses. *J. Pharmacol. Exp. Ther.* 287, 884–888.

Borea, P. A., Gessi, S., Bar-Yehuda, S., and Fishman, P. (2009). A_3 adenosine receptor: pharmacology and role in disease. *Handb. Exp. Pharmacol.*, 297–327. doi:10.1007/978-3-540-89615-9_10.

Bouaboula, M., Perrachon, S., Milligan, L., Canat, X., Rinaldi-Carmona, M., Portier, M., et al. (1997). A selective inverse agonist for central cannabinoid receptor inhibits mitogen-activated protein kinase activation stimulated by insulin or insulin-like growth factor 1. Evidence for a new model of receptor/ligand interactions. *J. Biol. Chem.* 272, 22330–22339.

Bouaboula, M., Poinot-Chazel, C., Marchand, J., Canat, X., Bourrié, B., Rinaldi-Carmona, M., et al. (1996). Signaling pathway associated with stimulation of CB2 peripheral cannabinoid receptor. Involvement of both mitogen-activated protein kinase and induction of Krox-24 expression. *Eur. J. Biochem. FEBS* 237, 704–711.

Braak, H., and Braak, E. (1985). On areas of transition between entorhinal allocortex and temporal isocortex in the human brain. Normal morphology and lamina-specific pathology in Alzheimer's disease. *Acta Neuropathol. (Berl.)* 68, 325–332. doi:10.1007/BF00690836.

Branconnier, R. J. (1983). The efficacy of the cerebral metabolic enhancers in the treatment of senile dementia. *Psychopharmacol. Bull.* 19, 212–219.

Broadbent, N. J., Gaskin, S., Squire, L. R., and Clark, R. E. (2010). Object recognition memory and the rodent hippocampus. *Learn. Mem.* 17, 5–11. doi:10.1101/lm.1650110.

Broadbent, N. J., Squire, L. R., and Clark, R. E. (2004). Spatial memory, recognition memory, and the hippocampus. *Proc. Natl. Acad. Sci. U. S. A.* 101, 14515–14520. doi:10.1073/pnas.0406344101.

Broch, O. J., and Ueland, P. M. (1980). Regional and subcellular distribution of S-adenosylhomocysteine hydrolase in the adult rat brain. *J. Neurochem.* 35, 484–488.

Broderick, P. A., and Jacoby, J. H. (1989). Central monoamine dysfunction in diabetes: psychotherapeutic implications: electroanalysis by voltammetry. *Acta Physiol. Pharmacol. Latinoam. Organo Asoc. Latinoam. Cienc. Fisiológicas Asoc. Latinoam. Farmacol.* 39, 211–225.

Brown, A. M. (2004). Brain glycogen re-awakened. *J. Neurochem.* 89, 537–552. doi:10.1111/j.1471-4159.2004.02421.x.

Brown, A. M., and Ransom, B. R. (2007). Astrocyte glycogen and brain energy metabolism. *Glia* 55, 1263–1271. doi:10.1002/glia.20557.

Brown, S. M., Wager-Miller, J., and Mackie, K. (2002). Cloning and molecular characterization of the rat CB2 cannabinoid receptor. *Biochim. Biophys. Acta* 1576, 255–264.

Brüning, J. C., Gautam, D., Burks, D. J., Gillette, J., Schubert, M., Orban, P. C., et al. (2000). Role of brain insulin receptor in control of body weight and reproduction. *Science* 289, 2122–2125.

Buckalew, V. M. (2015). Endogenous digitalis-like factors: an overview of the history. *Front. Endocrinol.* 6, 49. doi:10.3389/fendo.2015.00049.

Bystritsky, A., Danial, J., and Kronemyer, D. Interactions Between Diabetes and Anxiety and Depression: Implications for Treatment. *Endocrinol. Metab. Clin. North Am.* doi:10.1016/j.ecl.2013.10.001.

Calabresi, P., Gubellini, P., Picconi, B., Centonze, D., Pisani, A., Bonsi, P., et al. (2001). Inhibition of mitochondrial complex II induces a long-term potentiation of NMDA-mediated synaptic excitation in the striatum requiring endogenous dopamine. *J. Neurosci. Off. J. Soc. Neurosci.* 21, 5110–5120.

Callén, L., Moreno, E., Barroso-Chinea, P., Moreno-Delgado, D., Cortés, A., Mallol, J., et al. (2012). Cannabinoid receptors CB1 and CB2 form functional heteromers in brain. *J. Biol. Chem.* 287, 20851–20865. doi:10.1074/jbc.M111.335273.

Canas, P. M., Porciúncula, L. O., Cunha, G. M. A., Silva, C. G., Machado, N. J., Oliveira, J. M. A., et al. (2009). Adenosine A_{2A} receptor blockade prevents synaptotoxicity and memory dysfunction caused by beta-amyloid peptides via p38 mitogen-activated protein kinase pathway. *J. Neurosci. Off. J. Soc. Neurosci.* 29, 14741–14751. doi:10.1523/JNEUROSCI.3728-09.2009.

Carvalho, C., Cardoso, S., Correia, S. C., Santos, R. X., Santos, M. S., Baldeiras, I., et al. (2012a). Metabolic alterations induced by sucrose intake and Alzheimer's disease promote similar brain mitochondrial abnormalities. *Diabetes* 61, 1234–1242. doi:10.2337/db11-1186.

Carvalho, C., Cardoso, S., Correia, S. C., Santos, R. X., Santos, M. S., Baldeiras, I., et al. (2012b). Metabolic Alterations Induced by Sucrose Intake and Alzheimer's Disease Promote Similar Brain Mitochondrial Abnormalities. *Diabetes* 61, 1234–1242. doi:10.2337/db11-1186.

Cassar, M., Jones, M. G., and Szatkowski, M. (1998). Reduced adenosine uptake accelerates ischaemic block of population spikes in hippocampal slices from streptozotocin-treated diabetic rats. *Eur. J. Neurosci.* 10, 239–245.

Castillo, P. E., Younts, T. J., Chávez, A. E., and Hashimotodani, Y. (2012). Endocannabinoid Signaling and Synaptic Function. *Neuron* 76, 70–81. doi:10.1016/j.neuron.2012.09.020.

Castro, M. A., Beltrán, F. A., Brauchi, S., and Concha, I. I. (2009). A metabolic switch in brain: glucose and lactate metabolism modulation by ascorbic acid. *J. Neurochem.* 110, 423–440. doi:10.1111/j.1471-4159.2009.06151.x.

Cavallucci, V., Ferraina, C., and D'Amelio, M. (2013). Key role of mitochondria in Alzheimer's disease synaptic dysfunction. *Curr. Pharm. Des.* 19, 6440–6450.

Cerami, C., Della Rosa, P. A., Magnani, G., Santangelo, R., Marcone, A., Cappa, S. F., et al. (2015). Brain metabolic maps in Mild Cognitive Impairment predict heterogeneity of progression to dementia. *NeuroImage Clin.* 7, 187–194. doi:10.1016/j.nicl.2014.12.004.

Cheng, A., Hou, Y., and Mattson, M. P. (2010). Mitochondria and neuroplasticity. *ASN NEURO* 2. doi:10.1042/AN20100019.

Chen, J.-F. (2014). Adenosine receptor control of cognition in normal and disease. *Int. Rev. Neurobiol.* 119, 257–307. doi:10.1016/B978-0-12-801022-8.00012-X.

Chen, J.-F., Eltzschig, H. K., and Fredholm, B. B. (2013). Adenosine receptors as drug targets--what are the challenges? *Nat. Rev. Drug Discov.* 12, 265–286. doi:10.1038/nrd3955.

Choi, I. Y., Lee, S. P., Kim, S. G., and Gruetter, R. (2001). In vivo measurements of brain glucose transport using the reversible Michaelis-Menten model and simultaneous measurements of cerebral blood flow changes during hypoglycemia. *J. Cereb. Blood Flow Metab. Off. J. Int. Soc. Cereb. Blood Flow Metab.* 21, 653–663. doi:10.1097/00004647-200106000-00003.

Clarke, D. D., and Sokoloff, L. (1999). Circulation and Energy Metabolism of the Brain. Available at: http://www.ncbi.nlm.nih.gov/books/NBK20413/ [Accessed September 6, 2015].

Clarke, D. W., Boyd, F. T., Kappy, M. S., and Raizada, M. K. (1984). Insulin binds to specific receptors and stimulates 2-deoxy-D-glucose uptake in cultured glial cells from rat brain. *J. Biol. Chem.* 259, 11672–11675.

Clarke, W. P., and Bond, R. A. (1998). The elusive nature of intrinsic efficacy. *Trends Pharmacol. Sci.* 19, 270–276.

Coelho, J. E., Rebola, N., Fragata, I., Ribeiro, J. A., de Mendonça, A., and Cunha, R. A. (2006). Hypoxia-induced desensitization and internalization of adenosine A_1 receptors in the rat hippocampus. *Neuroscience* 138, 1195–1203. doi:10.1016/j.neuroscience.2005.12.012.

Cognato, G. P., Agostinho, P. M., Hockemeyer, J., Müller, C. E., Souza, D. O., and Cunha, R. A. (2010). Caffeine and an adenosine A_{2A} receptor antagonist prevent memory impairment and synaptotoxicity in adult rats triggered by a convulsive episode in early life. *J. Neurochem.* 112, 453–462. doi:10.1111/j.1471-4159.2009.06465.x.

Convit, A., Wolf, O. T., Tarshish, C., and Leon, M. J. de (2003). Reduced glucose tolerance is associated with poor memory performance and hippocampal atrophy among normal elderly. *Proc. Natl. Acad. Sci.* 100, 2019–2022. doi:10.1073/pnas.0336073100.

Correia, J., and Ravasco, P. (2014). Weight changes in Portuguese patients with depression: which factors are involved? *Nutr. J.* 13, 117. doi:10.1186/1475-2891-13-117.

Correia, S. C., Santos, R. X., Carvalho, C., Cardoso, S., Candeias, E., Santos, M. S., et al. (2012). Insulin signaling, glucose metabolism and mitochondria: major players in Alzheimer's disease and diabetes interrelation. *Brain Res.* 1441, 64–78. doi:10.1016/j.brainres.2011.12.063.

Correia, S. C., Santos, R. X., Perry, G., Zhu, X., Moreira, P. I., and Smith, M. A. (2011). Insulin-resistant brain state: the culprit in sporadic Alzheimer's disease? *Ageing Res. Rev.* 10, 264–273. doi:10.1016/j.arr.2011.01.001.

Costenla, A. R., Cunha, R. A., and de Mendonça, A. (2010). Caffeine, adenosine receptors, and synaptic plasticity. *J. Alzheimers Dis. JAD* 20 Suppl 1, S25–34. doi:10.3233/JAD-2010-091384.

Costenla, A. R., Lopes, L. V., de Mendonça, A., and Ribeiro, J. A. (2001). A functional role for adenosine A_3 receptors: modulation of synaptic plasticity in the rat hippocampus. *Neurosci. Lett.* 302, 53–57.

Coulter, D. A., and Eid, T. (2012). Astrocytic regulation of glutamate homeostasis in epilepsy. *Glia* 60, 1215–1226. doi:10.1002/glia.22341.

Crawford, C. R., Patel, D. H., Naeve, C., and Belt, J. A. (1998). Cloning of the human equilibrative, nitrobenzylmercaptopurine riboside (NBMPR)-insensitive nucleoside transporter ei by functional expression in a transport-deficient cell line. *J. Biol. Chem.* 273, 5288–5293.

Crichton, G. E., Elias, M. F., Buckley, J. D., Murphy, K. J., Bryan, J., and Frisardi, V. (2012). Metabolic syndrome, cognitive performance, and dementia. *J. Alzheimers Dis. JAD* 30 Suppl 2, S77–87. doi:10.3233/JAD-2011-111022.

Cruz, N. F., and Dienel, G. A. (2002a). High glycogen levels in brains of rats with minimal environmental stimuli: implications for metabolic contributions of working astrocytes. *J. Cereb. Blood Flow Metab. Off. J. Int. Soc. Cereb. Blood Flow Metab.* 22, 1476–1489. doi:10.1097/00004647-200212000-00008.

Cruz, N. F., and Dienel, G. A. (2002b). High Glycogen Levels in Brains of Rats With Minimal Environmental Stimuli: Implications for Metabolic Contributions of Working Astrocytes. *J. Cereb. Blood Flow Metab.* 22, 1476–1489. doi:10.1097/01.WCB.0000034362.37277.C0.

Csóka, B., Koscsó, B., Töro, G., Kókai, E., Virág, L., Németh, Z. H., et al. (2014). A2B adenosine receptors prevent insulin resistance by inhibiting adipose tissue inflammation via maintaining alternative macrophage activation. *Diabetes* 63, 850–866. doi:10.2337/db13-0573.

Cunha, R. A. (2001a). Adenosine as a neuromodulator and as a homeostatic regulator in the nervous system: different roles, different sources and different receptors. *Neurochem. Int.* 38, 107–125.

Cunha, R. A. (2001b). Regulation of the ecto-nucleotidase pathway in rat hippocampal nerve terminals. *Neurochem. Res.* 26, 979–991.

Cunha, R. A. (2005). Neuroprotection by adenosine in the brain: From A_1 receptor activation to A_{2A} receptor blockade. *Purinergic Signal.* 1, 111–134. doi:10.1007/s11302-005-0649-1.

Cunha, R. A. (2008). Different cellular sources and different roles of adenosine: A_1 receptor-mediated inhibition through astrocytic-driven volume transmission and synapse-restricted A2A receptor-mediated facilitation of plasticity. *Neurochem. Int.* 52, 65–72. doi:10.1016/j.neuint.2007.06.026.

Cunha, R. A., and Agostinho, P. M. (2010). Chronic caffeine consumption prevents memory disturbance in different animal models of memory decline. *J. Alzheimers Dis. JAD* 20 Suppl 1, S95–116. doi:10.3233/JAD-2010-1408.

Cunha, R. A., Vizi, E. S., Ribeiro, J. A., and Sebastião, A. M. (1996). Preferential release of ATP and its extracellular catabolism as a source of adenosine upon high- but not low-frequency stimulation of rat hippocampal slices. *J. Neurochem.* 67, 2180–2187.

Dall'Igna, O. P., Fett, P., Gomes, M. W., Souza, D. O., Cunha, R. A., and Lara, D. R. (2007). Caffeine and adenosine A_{2A} receptor antagonists prevent beta-amyloid (25-35)-induced cognitive deficits in mice. *Exp. Neurol.* 203, 241–245. doi:10.1016/j.expneurol.2006.08.008.

Dalton, G. D., and Howlett, A. C. (2012). Cannabinoid CB1 receptors transactivate multiple receptor tyrosine kinases and regulate serine/threonine kinases to activate ERK in neuronal cells. *Br. J. Pharmacol.* 165, 2497–2511. doi:10.1111/j.1476-5381.2011.01455.x.

Daré, E., Schulte, G., Karovic, O., Hammarberg, C., and Fredholm, B. B. (2007). Modulation of glial cell functions by adenosine receptors. *Physiol. Behav.* 92, 15–20. doi:10.1016/j.physbeh.2007.05.031.

Dawson, G. R., and Tricklebank, M. D. (1995). Use of the elevated plus maze in the search for novel anxiolytic agents. *Trends Pharmacol. Sci.* 16, 33–36.

De Felice, F. G. (2013). Alzheimer's disease and insulin resistance: translating basic science into clinical applications. *J. Clin. Invest.* 123, 531–539. doi:10.1172/JCI64595.

DeFries, J. C., Hegmann, J. P., and Weir, M. W. (1966). Open-field behavior in mice: evidence for a major gene effect mediated by the visual system. *Science* 154, 1577–1579.

De Jong, J. W. (1977). Partial purification and properties of rat-heart adenosine kinase. *Arch. Int. Physiol. Biochim.* 85, 557–569.

de Pasquale, A., Costa, G., and Trovato, A. (1978). The influence of cannabis on glucoregulation. *Bull. Narc.* 30, 33–41.

De Piras, M. M., and Zadunaisky, J. A. (1965). Effect of potassium and oubain on glucose metabolism by frog brain. *J. Neurochem.* 12, 657–661.

den Boon, F. S., Chameau, P., Houthuijs, K., Bolijn, S., Mastrangelo, N., Kruse, C. G., et al. (2014). Endocannabinoids produced upon action potential firing evoke a Cl^- current via type-2 cannabinoid receptors in the medial prefrontal cortex. *Pflüg. Arch. Eur. J. Physiol.* 466, 2257–2268. doi:10.1007/s00424-014-1502-6.

den Boon, F. S., Chameau, P., Schaafsma-Zhao, Q., van Aken, W., Bari, M., Oddi, S., et al. (2012). Excitability of prefrontal cortical pyramidal neurons is modulated by activation of intracellular type-2 cannabinoid receptors. *Proc. Natl. Acad. Sci. U. S. A.* 109, 3534–3539. doi:10.1073/pnas.1118167109.

Deshmukh, R., Sharma, V., Mehan, S., Sharma, N., and Bedi, K. L. (2009). Amelioration of intracerebroventricular streptozotocin induced cognitive dysfunction and oxidative stress by vinpocetine — a PDE1 inhibitor. *Eur. J. Pharmacol.* 620, 49–56. doi:10.1016/j.ejphar.2009.08.027.

Detka, J., Kurek, A., Basta-Kaim, A., Kubera, M., Lasoń, W., and Budziszewska, B. (2013). Neuroendocrine link between stress, depression and diabetes. *Pharmacol. Rep. PR* 65, 1591–1600.

Dias, R. B., Rombo, D. M., Ribeiro, J. A., Henley, J. M., and Sebastião, A. M. (2013). Adenosine: setting the stage for plasticity. *Trends Neurosci.* 36, 248–257. doi:10.1016/j.tins.2012.12.003.

Di Marzo, V., and Fontana, A. (1995). Anandamide, an endogenous cannabinomimetic eicosanoid: "killing two birds with one stone." *Prostaglandins Leukot. Essent. Fatty Acids* 53, 1–11.

Di Marzo, V., Fontana, A., Cadas, H., Schinelli, S., Cimino, G., Schwartz, J. C., et al. (1994). Formation and inactivation of endogenous cannabinoid anandamide in central neurons. *Nature* 372, 686–691. doi:10.1038/372686a0.

Di Marzo, V., Melck, D., Bisogno, T., and De Petrocellis, L. (1998). Endocannabinoids: endogenous cannabinoid receptor ligands with neuromodulatory action. *Trends Neurosci.* 21, 521–528.

Dimitriadis, G., Leighton, B., Parry-Billings, M., Tountas, C., Raptis, S., and Newsholme, E. A. (1998). Furosemide decreases the sensitivity of glucose transport to insulin in skeletal muscle in vitro. *Eur. J. Endocrinol. Eur. Fed. Endocr. Soc.* 139, 118–122.

Dixon, A. K., Gubitz, A. K., Sirinathsinghji, D. J., Richardson, P. J., and Freeman, T. C. (1996). Tissue distribution of adenosine receptor mRNAs in the rat. *Br. J. Pharmacol.* 118, 1461–1468.

Dow, R. L., Carpino, P. A., Hadcock, J. R., Black, S. C., Iredale, P. A., DaSilva-Jardine, P., et al. (2009). Discovery of 2-(2-chlorophenyl)-3-(4-chlorophenyl)-7-(2,2-difluoropropyl)-6,7-dihydro-2H-pyrazolo[3,4-f][1,4]oxazepin-8(5H)-one (PF-

514273), a novel, bicyclic lactam-based cannabinoid-1 receptor antagonist for the treatment of obesity. *J. Med. Chem.* 52, 2652–2655. doi:10.1021/jm900255t.

Drabikowska, A. K., Halec, L., and Shugar, D. (1985). Purification and properties of adenosine kinase from rat liver: separation from deoxyadenosine kinase activity. *Z. Für Naturforschung Sect. C Biosci.* 40, 34–41.

Dringen, R., Bishop, G. M., Koeppe, M., Dang, T. N., and Robinson, S. R. (2007). The pivotal role of astrocytes in the metabolism of iron in the brain. *Neurochem. Res.* 32, 1884–1890. doi:10.1007/s11064-007-9375-0.

Dringen, R., and Hamprecht, B. (1993). Inhibition by 2-deoxyglucose and 1,5-gluconolactone of glycogen mobilization in astroglia-rich primary cultures. *J. Neurochem.* 60, 1498–1504.

Duarte, A. I., Moreira, P. I., and Oliveira, C. R. (2012a). Insulin in central nervous system: more than just a peripheral hormone. *J. Aging Res.* 2012, 384017. doi:10.1155/2012/384017.

Duarte, I. F., Lamego, I., Rocha, C., and Gil, A. M. (2009a). NMR metabonomics for mammalian cell metabolism studies. *Bioanalysis* 1, 1597–1614. doi:10.4155/bio.09.151.

Duarte, J. M. N. (2015). Metabolic Alterations Associated to Brain Dysfunction in Diabetes. *Aging Dis.* 6, 304–321. doi:10.14336/AD.2014.1104.

Duarte, J. M. N., Agostinho, P. M., Carvalho, R. A., and Cunha, R. A. (2012b). Caffeine consumption prevents diabetes-induced memory impairment and synaptotoxicity in the hippocampus of NONcZNO10/LTJ mice. *PloS One* 7, e21899. doi:10.1371/journal.pone.0021899.

Duarte, J. M. N., Carvalho, R. A., Cunha, R. A., and Gruetter, R. (2009b). Caffeine consumption attenuates neurochemical modifications in the hippocampus of streptozotocin-induced diabetic rats. *J. Neurochem.* 111, 368–379. doi:10.1111/j.1471-4159.2009.06349.x.

Duarte, J. M. N., Ferreira, S. G., Carvalho, R. A., Cunha, R. A., and Köfalvi, A. (2012c). CB_1 receptor activation inhibits neuronal and astrocytic intermediary metabolism in the rat hippocampus. *Neurochem. Int.* 60, 1–8. doi:10.1016/j.neuint.2011.10.019.

Duarte, J. M. N., Lei, H., Mlynárik, V., and Gruetter, R. (2012d). The neurochemical profile quantified by in vivo 1H NMR spectroscopy. *NeuroImage* 61, 342–362. doi:10.1016/j.neuroimage.2011.12.038.

Duarte, J. M. N., Nogueira, C., Mackie, K., Oliveira, C. R., Cunha, R. A., and Köfalvi, A. (2007a). Increase of cannabinoid CB_1 receptor density in the hippocampus of streptozotocin-induced diabetic rats. *Exp. Neurol.* 204, 479–484. doi:10.1016/j.expneurol.2006.11.013.

Duarte, J. M. N., Oliveira, C. R., Ambrósio, A. F., and Cunha, R. A. (2006). Modification of adenosine A_1 and A_{2A} receptor density in the hippocampus of streptozotocin-induced diabetic rats. *Neurochem. Int.* 48, 144–150. doi:10.1016/j.neuint.2005.08.008.

Duarte, J. M. N., Oses, J. P., Rodrigues, R. J., and Cunha, R. A. (2007b). Modification of purinergic signaling in the hippocampus of streptozotocin-induced diabetic rats. *Neuroscience* 149, 382–391. doi:10.1016/j.neuroscience.2007.08.005.

Duchen, M. R. (2000). Mitochondria and Ca^{2+} in cell physiology and pathophysiology. *Cell Calcium* 28, 339–348. doi:10.1054/ceca.2000.0170.

Dudai, Y. (2004). The neurobiology of consolidations, or, how stable is the engram? *Annu. Rev. Psychol.* 55, 51–86. doi:10.1146/annurev.psych.55.090902.142050.

Duelli, R., Schröck, H., Kuschinsky, W., and Hoyer, S. (1994). Intracerebroventricular injection of streptozotocin induces discrete local changes in cerebral glucose utilization in rats. *Int. J. Dev. Neurosci. Off. J. Int. Soc. Dev. Neurosci.* 12, 737–743.

Dunwiddie, T. V., and Diao, L. (1994). Extracellular adenosine concentrations in hippocampal brain slices and the tonic inhibitory modulation of evoked excitatory responses. *J. Pharmacol. Exp. Ther.* 268, 537–545.

Dunwiddie, T. V., Diao, L., and Proctor, W. R. (1997). Adenine nucleotides undergo rapid, quantitative conversion to adenosine in the extracellular space in rat hippocampus. *J. Neurosci. Off. J. Soc. Neurosci.* 17, 7673–7682.

Dunwiddie, T. V., and Masino, S. A. (2001). The role and regulation of adenosine in the central nervous system. *Annu. Rev. Neurosci.* 24, 31–55. doi:10.1146/annurev.neuro.24.1.31.

Duran, J., Tevy, M. F., Garcia-Rocha, M., Calbó, J., Milán, M., and Guinovart, J. J. (2012). Deleterious effects of neuronal accumulation of glycogen in flies and mice. *EMBO Mol. Med.* 4, 719–729. doi:10.1002/emmm.201200241.

Dvorak-Carbone, H., and Schuman, E. M. (1999). Long-term depression of temporoammonic-CA1 hippocampal synaptic transmission. *J. Neurophysiol.* 81, 1036–1044.

Dwyer, D. S., Vannucci, S. J., and Simpson, I. A. (2002). Expression, regulation, and functional role of glucose transporters (GLUTs) in brain. *Int. Rev. Neurobiol.* 51, 159–188.

Eckert, T., Tang, C., and Eidelberg, D. (2007). Assessment of the progression of Parkinson's disease: a metabolic network approach. *Lancet Neurol.* 6, 926–932. doi:10.1016/S1474-4422(07)70245-4.

Egertová, M., and Elphick, M. R. (2000). Localisation of cannabinoid receptors in the rat brain using antibodies to the intracellular C-terminal tail of CB. *J. Comp. Neurol.* 422, 159–171.

Eidelberg, D. (2009). Metabolic brain networks in neurodegenerative disorders: a functional imaging approach. *Trends Neurosci.* 32, 548–557. doi:10.1016/j.tins.2009.06.003.

Ennaceur, A. (2010). One-trial object recognition in rats and mice: methodological and theoretical issues. *Behav. Brain Res.* 215, 244–254. doi:10.1016/j.bbr.2009.12.036.

Ennaceur, A., and Delacour, J. (1988). A new one-trial test for neurobiological studies of memory in rats. 1: Behavioral data. *Behav. Brain Res.* 31, 47–59.

Ennaceur, A., Michalikova, S., Bradford, A., and Ahmed, S. (2005). Detailed analysis of the behavior of Lister and Wistar rats in anxiety, object recognition and object location tasks. *Behav. Brain Res.* 159, 247–266. doi:10.1016/j.bbr.2004.11.006.

Espinosa, J., Rocha, A., Nunes, F., Costa, M. S., Schein, V., Kazlauckas, V., et al. (2013a). Caffeine consumption prevents memory impairment, neuronal damage, and adenosine A_{2A} receptors upregulation in the hippocampus of a rat model of sporadic dementia. *J. Alzheimers Dis. JAD* 34, 509–518. doi:10.3233/JAD-111982.

Espinosa, J., Rocha, A., Nunes, F., Costa, M. S., Schein, V., Kazlauckas, V., et al. (2013b). Caffeine Consumption Prevents Memory Impairment, Neuronal Damage, and Adenosine A_{2A} Receptors Upregulation in the Hippocampus of a Rat Model of Sporadic Dementia. *J. Alzheimers Dis.* 34, 509–518. doi:10.3233/JAD-111982.

Esposito, I., Proto, M. C., Gazzerro, P., Laezza, C., Miele, C., Alberobello, A. T., et al. (2008). The cannabinoid CB_1 receptor antagonist rimonabant stimulates 2-deoxyglucose uptake in skeletal muscle cells by regulating the expression of phosphatidylinositol-3-kinase. *Mol. Pharmacol.* 74, 1678–1686. doi:10.1124/mol.108.049205.

Exalto, L. G., Whitmer, R. A., Kappele, L. J., and Biessels, G. J. (2012a). An update on type 2 diabetes, vascular dementia and Alzheimer's disease. *Exp. Gerontol.* 47, 858–864. doi:10.1016/j.exger.2012.07.014.

Exalto, L. G., Whitmer, R. A., Kappele, L. J., and Biessels, G. J. (2012b). An update on type 2 diabetes, vascular dementia and Alzheimer's disease. *Exp. Gerontol.* 47, 858–864. doi:10.1016/j.exger.2012.07.014.

Fang, X., Yu, S. X., Lu, Y., Bast, R. C., Woodgett, J. R., and Mills, G. B. (2000). Phosphorylation and inactivation of glycogen synthase kinase 3 by protein kinase A. *Proc. Natl. Acad. Sci.* 97, 11960–11965. doi:10.1073/pnas.220413597.

Feigin, A., Tang, C., Ma, Y., Mattis, P., Zgaljardic, D., Guttman, M., et al. (2007). Thalamic metabolism and symptom onset in preclinical Huntington's disease. *Brain J. Neurol.* 130, 2858–2867. doi:10.1093/brain/awm217.

Felder, C. C., Joyce, K. E., Briley, E. M., Mansouri, J., Mackie, K., Blond, O., et al. (1995). Comparison of the pharmacology and signal transduction of the human cannabinoid CB1 and CB_2 receptors. *Mol. Pharmacol.* 48, 443–450.

Feoktistov, I., and Biaggioni, I. (1997). Adenosine A_{2B} receptors. *Pharmacol. Rev.* 49, 381–402.

Féraille, E., Carranza, M. L., Gonin, S., Béguin, P., Pedemonte, C., Rousselot, M., et al. (1999). Insulin-induced stimulation of Na^+,K^+-ATPase activity in kidney proximal tubule cells depends on phosphorylation of the alpha-subunit at Tyr-10. *Mol. Biol. Cell* 10, 2847–2859.

Ferreira, S. G., Gonçalves, F. Q., Marques, J. M., Tomé, Â. R., Rodrigues, R. J., Nunes-Correia, I., et al. (2015). Presynaptic adenosine A_{2A} receptors dampen cannabinoid CB_1 receptor-mediated inhibition of corticostriatal glutamatergic transmission. *Br. J. Pharmacol.* 172, 1074–1086. doi:10.1111/bph.12970.

Figler, R. A., Wang, G., Srinivasan, S., Jung, D. Y., Zhang, Z., Pankow, J. S., et al. (2011). Links between insulin resistance, adenosine A_{2B} receptors, and inflammatory markers in mice and humans. *Diabetes* 60, 669–679. doi:10.2337/db10-1070.

Fishman, R. S., and Karnovsky, M. L. (1986). Apparent absence of a translocase in the cerebral glucose-6-phosphatase system. *J. Neurochem.* 46, 371–378.

Flint, R. W., and Riccio, D. C. (1997). Pretest administration of glucose attenuates infantile amnesia for passive avoidance conditioning in rats. *Dev. Psychobiol.* 31, 207–216.

Folli, F., Bonfanti, L., Renard, E., Kahn, C. R., and Merighi, A. (1994). Insulin receptor substrate-1 (IRS-1) distribution in the rat central nervous system. *J. Neurosci. Off. J. Soc. Neurosci.* 14, 6412–6422.

Ford, H., Dai, F., Mu, L., Siddiqui, M. A., Nicklaus, M. C., Anderson, L., et al. (2000). Adenosine deaminase prefers a distinct sugar ring conformation for binding and catalysis: kinetic and structural studies. *Biochemistry (Mosc.)* 39, 2581–2592.

Fox, I. H., and Kelley, W. N. (1978). The role of adenosine and 2'-deoxyadenosine in mammalian cells. *Annu. Rev. Biochem.* 47, 655–686. doi:10.1146/annurev.bi.47.070178.003255.

Fredholm, B. B. (2007). Adenosine, an endogenous distress signal, modulates tissue damage and repair. *Cell Death Differ.* 14, 1315–1323. doi:10.1038/sj.cdd.4402132.

Fredholm, B. B., Bättig, K., Holmén, J., Nehlig, A., and Zvartau, E. E. (1999). Actions of caffeine in the brain with special reference to factors that contribute to its widespread use. *Pharmacol. Rev.* 51, 83–133.

Fredholm, B. B., Chen, J.-F., Cunha, R. A., Svenningsson, P., and Vaugeois, J.-M. (2005). Adenosine and brain function. *Int. Rev. Neurobiol.* 63, 191–270. doi:10.1016/S0074-7742(05)63007-3.

Fredholm, B. B., IJzerman, A. P., Jacobson, K. A., Linden, J., and Müller, C. E. (2011). International Union of Basic and Clinical Pharmacology. LXXXI. Nomenclature and classification of adenosine receptors--an update. *Pharmacol. Rev.* 63, 1–34. doi:10.1124/pr.110.003285.

Fredholm, B. B., Irenius, E., Kull, B., and Schulte, G. (2001). Comparison of the potency of adenosine as an agonist at human adenosine receptors expressed in Chinese hamster ovary cells. *Biochem. Pharmacol.* 61, 443–448.

Freedland, C. S., Whitlow, C. T., Miller, M. D., and Porrino, L. J. (2002). Dose-dependent effects of Delta9-tetrahydrocannabinol on rates of local cerebral glucose utilization in rat. *Synap. N. Y. N* 45, 134–142. doi:10.1002/syn.10089.

Friedrich, M. J. (2013). Studies suggest potential approaches for early detection of Alzheimer disease. *JAMA* 309, 18–19. doi:10.1001/jama.2012.105106.

Galiègue, S., Mary, S., Marchand, J., Dussossoy, D., Carrière, D., Carayon, P., et al. (1995). Expression of central and peripheral cannabinoid receptors in human immune tissues and leukocyte subpopulations. *Eur. J. Biochem. FEBS* 232, 54–61.

Galve-Roperh, I., Rueda, D., Gómez del Pulgar, T., Velasco, G., and Guzmán, M. (2002). Mechanism of extracellular signal-regulated kinase activation by the CB(1) cannabinoid receptor. *Mol. Pharmacol.* 62, 1385–1392.

Gao, Y., Vasilyev, D. V., Goncalves, M. B., Howell, F. V., Hobbs, C., Reisenberg, M., et al. (2010). Loss of retrograde endocannabinoid signaling and reduced adult neurogenesis in diacylglycerol lipase knock-out mice. *J. Neurosci. Off. J. Soc. Neurosci.* 30, 2017–2024. doi:10.1523/JNEUROSCI.5693-09.2010.

Gatley, S. J., Lan, R., Pyatt, B., Gifford, A. N., Volkow, N. D., and Makriyannis, A. (1997). Binding of the non-classical cannabinoid CP 55,940, and the diarylpyrazole AM251 to rodent brain cannabinoid receptors. *Life Sci.* 61, PL 191–197.

Gazzerro, P., Caruso, M. G., Notarnicola, M., Misciagna, G., Guerra, V., Laezza, C., et al. (2007). Association between cannabinoid type-1 receptor polymorphism and body mass index in a southern Italian population. *Int. J. Obes. 2005* 31, 908–912. doi:10.1038/sj.ijo.0803510.

Geiger, J. D., and Fyda, D. M. (1991). "ADENOSINE TRANSPORT IN NERVOUS SYSTEM TISSUES," in *Adenosine in the Nervous System* (Elsevier), 1–23. Available at: http://linkinghub.elsevier.com/retrieve/pii/B9780126726404500078 [Accessed September 12, 2015].

Gérard, C. M., Mollereau, C., Vassart, G., and Parmentier, M. (1991). Molecular cloning of a human cannabinoid receptor which is also expressed in testis. *Biochem. J.* 279 (Pt 1), 129–134.

Gérard, C., Mollereau, C., Vassart, G., and Parmentier, M. (1990). Nucleotide sequence of a human cannabinoid receptor cDNA. *Nucleic Acids Res.* 18, 7142.

Gevaerd, M. S., Takahashi, R. N., Silveira, R., and Da Cunha, C. (2001). Caffeine reverses the memory disruption induced by intra-nigral MPTP-injection in rats. *Brain Res. Bull.* 55, 101–106.

Ghasemi, R., Haeri, A., Dargahi, L., Mohamed, Z., and Ahmadiani, A. (2013). Insulin in the brain: sources, localization and functions. *Mol. Neurobiol.* 47, 145–171. doi:10.1007/s12035-012-8339-9.

Ghosh, A., Cheung, Y. Y., Mansfield, B. C., and Chou, J. Y. (2005). Brain contains a functional glucose-6-phosphatase complex capable of endogenous glucose production. *J. Biol. Chem.* 280, 11114–11119. doi:10.1074/jbc.M410894200.

Gibbs, M. E., Hutchinson, D., and Hertz, L. (2008). Astrocytic involvement in learning and memory consolidation. *Neurosci. Biobehav. Rev.* 32, 927–944. doi:10.1016/j.neubiorev.2008.02.001.

Giménez-Llort, L., Fernández-Teruel, A., Escorihuela, R. M., Fredholm, B. B., Tobeña, A., Pekny, M., et al. (2002). Mice lacking the adenosine A1 receptor are anxious and aggressive, but are normal learners with reduced muscle strength and survival rate. *Eur. J. Neurosci.* 16, 547–550.

Giménez-Llort, L., Masino, S. A., Diao, L., Fernández-Teruel, A., Tobeña, A., Halldner, L., et al. (2005). Mice lacking the adenosine A1 receptor have normal spatial learning and plasticity in the CA1 region of the hippocampus, but they habituate more slowly. *Synap. N. Y. N* 57, 8–16. doi:10.1002/syn.20146.

Giove, F., Mangia, S., Bianciardi, M., Garreffa, G., Di Salle, F., Morrone, R., et al. (2003). The physiology and metabolism of neuronal activation: in vivo studies by NMR and other methods. *Magn. Reson. Imaging* 21, 1283–1293.

Gjedde, A., and Marrett, S. (2001). Glycolysis in neurons, not astrocytes, delays oxidative metabolism of human visual cortex during sustained checkerboard stimulation in vivo. *J. Cereb. Blood Flow Metab. Off. J. Int. Soc. Cereb. Blood Flow Metab.* 21, 1384–1392. doi:10.1097/00004647-200112000-00002.

Gladden, L. B. (2004). Lactate metabolism: a new paradigm for the third millennium. *J. Physiol.* 558, 5–30. doi:10.1113/jphysiol.2003.058701.

Goldman, H., Dagirmanjian, R., Drew, W. G., and Murphy, S. (1975). delta9-tetrahydrocannabinol alters flow of blood to subcortical areas of the conscious rat brain. *Life Sci.* 17, 477–482.

Gomes, C. V., Kaster, M. P., Tomé, A. R., Agostinho, P. M., and Cunha, R. A. (2011). Adenosine receptors and brain diseases: neuroprotection and neurodegeneration. *Biochim. Biophys. Acta* 1808, 1380–1399. doi:10.1016/j.bbamem.2010.12.001.

Gómez del Pulgar, T., Velasco, G., and Guzmán, M. (2000). The CB_1 cannabinoid receptor is coupled to the activation of protein kinase B/Akt. *Biochem. J.* 347, 369–373.

Gonçalves, F. Q., Pires, J., Pliassova, A., Beleza, R., Lemos, C., Marques, J. M., et al. (2015). Adenosine A2b receptors control A1 receptor-mediated inhibition of synaptic transmission in the mouse hippocampus. *Eur. J. Neurosci.* 41, 876–886. doi:10.1111/ejn.12851.

Gonda, O., and Quastel, J. H. (1962). Effects of ouabain on cerebral metabolism and transport mechanisms in vitro. *Biochem. J.* 84, 394–406.

Gray, J. H., Owen, R. P., and Giacomini, K. M. (2004). The concentrative nucleoside transporter family, SLC28. *Pflüg. Arch. Eur. J. Physiol.* 447, 728–734. doi:10.1007/s00424-003-1107-y.

Griffin, E. W., Bechara, R. G., Birch, A. M., and Kelly, A. M. (2009a). Exercise enhances hippocampal-dependent learning in the rat: evidence for a BDNF-related mechanism. *Hippocampus* 19, 973–980. doi:10.1002/hipo.20631.

Griffin, E. W., Bechara, R. G., Birch, A. M., and Kelly, A. M. (2009b). Exercise enhances hippocampal-dependent learning in the rat: evidence for a BDNF-related mechanism. *Hippocampus* 19, 973–980. doi:10.1002/hipo.20631.

Grillo, C. A., Piroli, G. G., Hendry, R. M., and Reagan, L. P. (2009). Insulin-stimulated translocation of GLUT4 to the plasma membrane in rat hippocampus is PI3-kinase dependent. *Brain Res.* 1296, 35–45. doi:10.1016/j.brainres.2009.08.005.

Grillo, C. A., Piroli, G. G., Lawrence, R. C., Wrighten, S. A., Green, A. J., Wilson, S. P., et al. (2015). Hippocampal Insulin Resistance Impairs Spatial Learning and Synaptic Plasticity. *Diabetes*. doi:10.2337/db15-0596.

Grimes, C. A., and Jope, R. S. (2001). The multifaceted roles of glycogen synthase kinase 3beta in cellular signaling. *Prog. Neurobiol.* 65, 391–426.

Gruetter, R. (2002). In vivo ^{13}C NMR studies of compartmentalized cerebral carbohydrate metabolism. *Neurochem. Int.* 41, 143–154.

Gruetter, R. (2003). Glycogen: the forgotten cerebral energy store. *J. Neurosci. Res.* 74, 179–183. doi:10.1002/jnr.10785.

Gruetter, R., Ugurbil, K., and Seaquist, E. R. (1998). Steady-state cerebral glucose concentrations and transport in the human brain. *J. Neurochem.* 70, 397–408.

Grünblatt, E., Koutsilieri, E., Hoyer, S., and Riederer, P. (2006). Gene expression alterations in brain areas of intracerebroventricular streptozotocin treated rat. *J. Alzheimers Dis. JAD* 9, 261–271.

Grünblatt, E., Salkovic-Petrisic, M., Osmanovic, J., Riederer, P., and Hoyer, S. (2007). Brain insulin system dysfunction in streptozotocin intracerebroventricularly treated rats generates hyperphosphorylated tau protein. *J. Neurochem.* 101, 757–770. doi:10.1111/j.1471-4159.2006.04368.x.

Gu, L., Huang, B., Shen, W., Gao, L., Ding, Z., Wu, H., et al. (2013). Early activation of nSMase2/ceramide pathway in astrocytes is involved in ischemia-associated neuronal damage via inflammation in rat hippocampi. *J. Neuroinflammation* 10, 109. doi:10.1186/1742-2094-10-109.

Guzmán, M., Galve-Roperh, I., and Sánchez, C. (2001). Ceramide: a new second messenger of cannabinoid action. *Trends Pharmacol. Sci.* 22, 19–22.

Habeck, C., Foster, N. L., Perneczky, R., Kurz, A., Alexopoulos, P., Koeppe, R. A., et al. (2008). Multivariate and univariate neuroimaging biomarkers of Alzheimer's disease. *NeuroImage* 40, 1503–1515. doi:10.1016/j.neuroimage.2008.01.056.

Hack, S. P., and Christie, M. J. (2003). Adaptations in adenosine signaling in drug dependence: therapeutic implications. *Crit. Rev. Neurobiol.* 15, 235–274.

Hagberg, H., Andersson, P., Butcher, S., Sandberg, M., Lehmann, A., and Hamberger, A. (1986). Blockade of N-methyl-D-aspartate-sensitive acidic amino acid receptors inhibits ischemia-induced accumulation of purine catabolites in the rat striatum. *Neurosci. Lett.* 68, 311–316.

Hagena, H., and Manahan-Vaughan, D. (2010). Frequency facilitation at mossy fiber-CA3 synapses of freely behaving rats contributes to the induction of persistent LTD via an adenosine-A1 receptor-regulated mechanism. *Cereb. Cortex N. Y. N 1991* 20, 1121–1130. doi:10.1093/cercor/bhp184.

Halassa, M. M., Fellin, T., and Haydon, P. G. (2009). Tripartite synapses: roles for astrocytic purines in the control of synaptic physiology and behavior. *Neuropharmacology* 57, 343–346. doi:10.1016/j.neuropharm.2009.06.031.

Halassa, M. M., and Haydon, P. G. (2010). Integrated brain circuits: astrocytic networks modulate neuronal activity and behavior. *Annu. Rev. Physiol.* 72, 335–355. doi:10.1146/annurev-physiol-021909-135843.

Hales, C. A., Stuart, S. A., Anderson, M. H., and Robinson, E. S. J. (2014). Modelling cognitive affective biases in major depressive disorder using rodents. *Br. J. Pharmacol.* 171, 4524–4538. doi:10.1111/bph.12603.

Hamai, M., Minokoshi, Y., and Shimazu, T. (1999). L-Glutamate and insulin enhance glycogen synthesis in cultured astrocytes from the rat brain through different intracellular mechanisms. *J. Neurochem.* 73, 400–407.

Hammond, R. S., Tull, L. E., and Stackman, R. W. (2004). On the delay-dependent involvement of the hippocampus in object recognition memory. *Neurobiol. Learn. Mem.* 82, 26–34. doi:10.1016/j.nlm.2004.03.005.

Hansson, E., Eriksson, P., and Nilsson, M. (1985). Amino acid and monoamine transport in primary astroglial cultures from defined brain regions. *Neurochem. Res.* 10, 1335–1341.

Harkany, T., Guzmán, M., Galve-Roperh, I., Berghuis, P., Devi, L. A., and Mackie, K. (2007). The emerging functions of endocannabinoid signaling during CNS development. *Trends Pharmacol. Sci.* 28, 83–92. doi:10.1016/j.tips.2006.12.004.

Harrison, J. (2013). Cognitive approaches to early Alzheimer's disease diagnosis. *Med. Clin. North Am.* 97, 425–438. doi:10.1016/j.mcna.2012.12.014.

Harrold, J. A., Elliott, J. C., King, P. J., Widdowson, P. S., and Williams, G. (2002). Down-regulation of cannabinoid-1 (CB_1) receptors in specific extrahypothalamic regions of rats with dietary obesity: a role for endogenous cannabinoids in driving appetite for palatable food? *Brain Res.* 952, 232–238.

Haskó, G., Pacher, P., Vizi, E. S., and Illes, P. (2005). Adenosine receptor signaling in the brain immune system. *Trends Pharmacol. Sci.* 26, 511–516. doi:10.1016/j.tips.2005.08.004.

Haycock, D. A., Kuster, J. E., Stevenson, J. I., Ward, S. J., and D'Ambra, T. (1990). Characterization of aminoalkylindole binding: selective displacement by cannabinoids. *NIDA Res. Monogr.* 105, 304–305.

Henderson, G. B., and Strauss, B. P. (1991). Evidence for cAMP and cholate extrusion in C6 rat glioma cells by a common anion efflux pump. *J. Biol. Chem.* 266, 1641–1645.

Herkenham, M., Lynn, A. B., Little, M. D., Johnson, M. R., Melvin, L. S., de Costa, B. R., et al. (1990). Cannabinoid receptor localization in brain. *Proc. Natl. Acad. Sci. U. S. A.* 87, 1932–1936.

Herrera, B., Carracedo, A., Diez-Zaera, M., Gómez del Pulgar, T., Guzmán, M., and Velasco, G. (2006). The CB_2 cannabinoid receptor signals apoptosis via ceramide-dependent activation of the mitochondrial intrinsic pathway. *Exp. Cell Res.* 312, 2121–2131. doi:10.1016/j.yexcr.2006.03.009.

Hertz, L. (2008). Bioenergetics of cerebral ischemia: a cellular perspective. *Neuropharmacology* 55, 289–309. doi:10.1016/j.neuropharm.2008.05.023.

Hertz, L., and Dienel, G. A. (2002). Energy metabolism in the brain. *Int. Rev. Neurobiol.* 51, 1–102.

Hertz, L., Peng, L., and Dienel, G. A. (2007). Energy metabolism in astrocytes: high rate of oxidative metabolism and spatiotemporal dependence on glycolysis/glycogenolysis. *J. Cereb. Blood Flow Metab. Off. J. Int. Soc. Cereb. Blood Flow Metab.* 27, 219–249. doi:10.1038/sj.jcbfm.9600343.

Hetman, M., Cavanaugh, J. E., Kimelman, D., and Xia, Z. (2000). Role of glycogen synthase kinase-3beta in neuronal apoptosis induced by trophic withdrawal. *J. Neurosci. Off. J. Soc. Neurosci.* 20, 2567–2574.

Hillard, C. J., Manna, S., Greenberg, M. J., DiCamelli, R., Ross, R. A., Stevenson, L. A., et al. (1999). Synthesis and characterization of potent and selective agonists of the neuronal cannabinoid receptor (CB1). *J. Pharmacol. Exp. Ther.* 289, 1427–1433.

Hof, P. R., Trapp, B. D., De Vellis, J., Claudio, L., and Colman, D. R. (2004). "Chapter 1 - Cellular Components of Nervous Tissue," in *From Molecules to Networks*, ed. J. H. B. L. Roberts (Burlington: Academic Press), 1–29. Available at: http://www.sciencedirect.com/science/article/pii/B9780121486600500020 [Accessed October 8, 2015].

Hollister, L. E. (1986). Health aspects of cannabis. *Pharmacol. Rev.* 38, 1–20.

Howarth, C. (2014). The contribution of astrocytes to the regulation of cerebral blood flow. *Brain Imaging Methods* 8, 103. doi:10.3389/fnins.2014.00103.

Howlett, A. C. (1995). Pharmacology of cannabinoid receptors. *Annu. Rev. Pharmacol. Toxicol.* 35, 607–634. doi:10.1146/annurev.pa.35.040195.003135.

Howlett, A. C., Breivogel, C. S., Childers, S. R., Deadwyler, S. A., Hampson, R. E., and Porrino, L. J. (2004). Cannabinoid physiology and pharmacology: 30 years of progress. *Neuropharmacology* 47 Suppl 1, 345–358. doi:10.1016/j.neuropharm.2004.07.030.

Howlett, A. C., and Mukhopadhyay, S. (2000). Cellular signal transduction by anandamide and 2-arachidonoylglycerol. *Chem. Phys. Lipids* 108, 53–70.

Huber, M., Kittner, B., Hojer, C., Fink, G. R., Neveling, M., and Heiss, W. D. (1993). Effect of propentofylline on regional cerebral glucose metabolism in acute ischemic stroke. *J. Cereb. Blood Flow Metab. Off. J. Int. Soc. Cereb. Blood Flow Metab.* 13, 526–530. doi:10.1038/jcbfm.1993.68.

Hughes, R. N. (2002). Sex-related glucose effects on responsiveness to brightness change in middle-aged rats. *Pharmacol. Biochem. Behav.* 73, 485–490.

Hughes, R. N. (2003). Effects of glucose on responsiveness to change in young adult and middle-aged rats. *Physiol. Behav.* 78, 529–534.

Hutchins, D. A., and Rogers, K. J. (1970). Physiological and drug-induced changes in the glycogen content of mouse brain. *Br. J. Pharmacol.* 39, 9–25.

Hyder, F., Patel, A. B., Gjedde, A., Rothman, D. L., Behar, K. L., and Shulman, R. G. (2006). Neuronal-glial glucose oxidation and glutamatergic-GABAergic function. *J. Cereb. Blood Flow Metab. Off. J. Int. Soc. Cereb. Blood Flow Metab.* 26, 865–877. doi:10.1038/sj.jcbfm.9600263.

Inoue, K., Kato, F., and Tsuda, M. (2010). The Modulation of Synaptic Transmission by the Glial Purinergic System. *Open Neurosci. J.* 4, 84–92. doi:10.2174/1874082001004010084.

Irving, A. J., McDonald, N. A., and Harkany, T. (2008). "CB1 Cannabinoid Receptors: Molecular Biology, Second Messenger Coupling and Polarized Trafficking in Neurons," in *Cannabinoids and the Brain*, ed. A. Köfalvi (Springer US), 59–73. Available at: http://link.springer.com/chapter/10.1007/978-0-387-74349-3_5 [Accessed December 26, 2015].

Ishrat, T., Parveen, K., Khan, M. M., Khuwaja, G., Khan, M. B., Yousuf, S., et al. (2009). Selenium prevents cognitive decline and oxidative damage in rat model of streptozotocin-induced experimental dementia of Alzheimer's type. *Brain Res.* 1281, 117–127. doi:10.1016/j.brainres.2009.04.010.

Ivanov, A. I., Malkov, A. E., Waseem, T., Mukhtarov, M., Buldakova, S., Gubkina, O., et al. (2014). Glycolysis and oxidative phosphorylation in neurons and astrocytes during network activity in hippocampal slices. *J. Cereb. Blood Flow Metab. Off. J. Int. Soc. Cereb. Blood Flow Metab.* 34, 397–407. doi:10.1038/jcbfm.2013.222.

Izquierdo, I., Medina, J. H., Vianna, M. R., Izquierdo, L. A., and Barros, D. M. (1999). Separate mechanisms for short- and long-term memory. *Behav. Brain Res.* 103, 1–11.

Jacobson, K. A., von Lubitz, D. K., Daly, J. W., and Fredholm, B. B. (1996). Adenosine receptor ligands: differences with acute versus chronic treatment. *Trends Pharmacol. Sci.* 17, 108–113.

Jakoby, P., Schmidt, E., Ruminot, I., Gutiérrez, R., Barros, L. F., and Deitmer, J. W. (2014). Higher transport and metabolism of glucose in astrocytes compared with neurons: a multiphoton study of hippocampal and cerebellar tissue slices. *Cereb. Cortex N. Y. N 1991* 24, 222–231. doi:10.1093/cercor/bhs309.

Javed, H., Khan, M. M., Khan, A., Vaibhav, K., Ahmad, A., Khuwaja, G., et al. (2011). S-allyl cysteine attenuates oxidative stress associated cognitive impairment and neurodegeneration in mouse model of streptozotocin-induced experimental dementia of Alzheimer's type. *Brain Res.* 1389, 133–142. doi:10.1016/j.brainres.2011.02.072.

Jiménez, A. I., Castro, E., Mirabet, M., Franco, R., Delicado, E. G., and Miras-Portugal, M. T. (1999). Potentiation of ATP calcium responses by A_{2B} receptor stimulation and other signals coupled to Gs proteins in type-1 cerebellar astrocytes. *Glia* 26, 119–128.

Jockers, R., Linder, M. E., Hohenegger, M., Nanoff, C., Bertin, B., Strosberg, A. D., et al. (1994). Species difference in the G protein selectivity of the human and bovine A1-adenosine receptor. *J. Biol. Chem.* 269, 32077–32084.

Johansson, B., Halldner, L., Dunwiddie, T. V., Masino, S. A., Poelchen, W., Giménez-Llort, L., et al. (2001). Hyperalgesia, anxiety, and decreased hypoxic neuroprotection in mice lacking the adenosine A_1 receptor. *Proc. Natl. Acad. Sci. U. S. A.* 98, 9407–9412. doi:10.1073/pnas.161292398.

Johnston-Cox, H., Koupenova, M., Yang, D., Corkey, B., Gokce, N., Farb, M. G., et al. (2012). The A_{2B} adenosine receptor modulates glucose homeostasis and obesity. *PloS One* 7, e40584. doi:10.1371/journal.pone.0040584.

Juhaszova, M., and Blaustein, M. P. (1997). Na^+ pump low and high ouabain affinity alpha subunit isoforms are differently distributed in cells. *Proc. Natl. Acad. Sci. U. S. A.* 94, 1800–1805.

Jurcovicova, J. (2014). Glucose transport in brain – effect of inflammation. *Endocr. Regul.* 48, 35–48.

Kacem, K., Lacombe, P., Seylaz, J., and Bonvento, G. (1998). Structural organization of the perivascular astrocyte endfeet and their relationship with the endothelial glucose transporter: a confocal microscopy study. *Glia* 23, 1–10.

Kainulainen, H., Schürmann, A., Vilja, P., and Joost, H. G. (1993). In-vivo glucose uptake and glucose transporter proteins GLUT1 and GLUT3 in brain tissue from streptozotocin-diabetic rats. *Acta Physiol. Scand.* 149, 221–225. doi:10.1111/j.1748-1716.1993.tb09615.x.

Kallarackal, A. J., Kvarta, M. D., Cammarata, E., Jaberi, L., Cai, X., Bailey, A. M., et al. (2013). Chronic stress induces a selective decrease in AMPA receptor-mediated synaptic excitation at hippocampal temporoammonic-CA1 synapses. *J. Neurosci. Off. J. Soc. Neurosci.* 33, 15669–15674. doi:10.1523/JNEUROSCI.2588-13.2013.

Kaminski, N. E., Koh, W. S., Yang, K. H., Lee, M., and Kessler, F. K. (1994). Suppression of the humoral immune response by cannabinoids is partially mediated through inhibition of adenylate cyclase by a pertussis toxin-sensitive G-protein coupled mechanism. *Biochem. Pharmacol.* 48, 1899–1908.

Kandel, E. R. (2001). The molecular biology of memory storage: a dialogue between genes and synapses. *Science* 294, 1030–1038. doi:10.1126/science.1067020.

Katona, I. (2015). Cannabis and Endocannabinoid Signaling in Epilepsy. *Handb. Exp. Pharmacol.* 231, 285–316. doi:10.1007/978-3-319-20825-1_10.

Katona, I., and Freund, T. F. (2012). Multiple functions of endocannabinoid signaling in the brain. *Annu. Rev. Neurosci.* 35, 529–558. doi:10.1146/annurev-neuro-062111-150420.

Katona, I., Sperlágh, B., Sík, A., Käfalvi, A., Vizi, E. S., Mackie, K., et al. (1999). Presynaptically located CB_1 cannabinoid receptors regulate GABA release from axon terminals of specific hippocampal interneurons. *J. Neurosci. Off. J. Soc. Neurosci.* 19, 4544–4558.

Katona, I., Urbán, G. M., Wallace, M., Ledent, C., Jung, K.-M., Piomelli, D., et al. (2006). Molecular composition of the endocannabinoid system at glutamatergic synapses. *J. Neurosci. Off. J. Soc. Neurosci.* 26, 5628–5637. doi:10.1523/JNEUROSCI.0309-06.2006.

Katz, B., and Miledi, R. (1970). Further study of the role of calcium in synaptic transmission. *J. Physiol.* 207, 789–801.

Keezer, M. R., Novy, J., and Sander, J. W. (2015). Type 1 diabetes mellitus in people with pharmacoresistant epilepsy: Prevalence and clinical characteristics. *Epilepsy Res.* 115, 55–57. doi:10.1016/j.eplepsyres.2015.05.008.

Kettenmann, H., Kirchhoff, F., and Verkhratsky, A. (2013). Microglia: new roles for the synaptic stripper. *Neuron* 77, 10–18. doi:10.1016/j.neuron.2012.12.023.

Kim, K., Oh, C.-M., Ohara-Imaizumi, M., Park, S., Namkung, J., Yadav, V. K., et al. (2015). Functional role of serotonin in insulin secretion in a diet-induced insulin-resistant state. *Endocrinology* 156, 444–452. doi:10.1210/en.2014-1687.

Kim, W., Lao, Q., Shin, Y.-K., Carlson, O. D., Lee, E. K., Gorospe, M., et al. (2012). Cannabinoids induce pancreatic β-cell death by directly inhibiting insulin receptor activation. *Sci. Signal.* 5, ra23. doi:10.1126/scisignal.2002519.

Kinnavane, L., Albasser, M. M., and Aggleton, J. P. (2015). Advances in the behavioural testing and network imaging of rodent recognition memory. *Behav. Brain Res.* 285, 67–78. doi:10.1016/j.bbr.2014.07.049.

Klann, E., and Sweatt, J. D. (2008). Altered protein synthesis is a trigger for long-term memory formation. *Neurobiol. Learn. Mem.* 89, 247–259. doi:10.1016/j.nlm.2007.08.009.

Kleinridders, A., Ferris, H. A., Cai, W., and Kahn, C. R. (2014). Insulin action in brain regulates systemic metabolism and brain function. *Diabetes* 63, 2232–2243. doi:10.2337/db14-0568.

Kletzien, R. F., Harris, P. K., and Foellmi, L. A. (1994). Glucose-6-phosphate dehydrogenase: a "housekeeping" enzyme subject to tissue-specific regulation by hormones, nutrients, and oxidant stress. *FASEB J. Off. Publ. Fed. Am. Soc. Exp. Biol.* 8, 174–181.

Köfalvi, A. (2008). "Alternative Interacting Sites and Novel Receptors for Cannabinoid Ligands," in *Cannabinoids and the Brain*, ed. A. Köfalvi (Springer US), 131–160. Available at: http://link.springer.com/chapter/10.1007/978-0-387-74349-3_9 [Accessed March 23, 2015].

Köfalvi, A., Sperlágh, B., Zelles, T., and Vizi, E. S. (2000). Long-lasting facilitation of 4-amino-n-[2,3-(3)H]butyric acid ([(3)H]GABA) release from rat hippocampal slices by nicotinic receptor activation. *J. Pharmacol. Exp. Ther.* 295, 453–462.

Kopf, S. R., and Baratti, C. M. (1995). The impairment of retention induced by insulin in mice may be mediated by a reduction in central cholinergic activity. *Neurobiol. Learn. Mem.* 63, 220–228. doi:10.1006/nlme.1995.1026.

Kressin, K., Kuprijanova, E., Jabs, R., Seifert, G., and Steinhäuser, C. (1995). Developmental regulation of Na^+ and K^+ conductances in glial cells of mouse hippocampal brain slices. *Glia* 15, 173–187. doi:10.1002/glia.440150210.

Kull, B., Svenningsson, P., and Fredholm, B. B. (2000). Adenosine A_{2A} receptors are colocalized with and activate G_{olf} in rat striatum. *Mol. Pharmacol.* 58, 771–777.

Kullmann, S., Heni, M., Fritsche, A., and Preissl, H. (2015). Insulin action in the human brain: evidence from neuroimaging studies. *J. Neuroendocrinol.* 27, 419–423. doi:10.1111/jne.12254.

Kum, W., Zhu, S. Q., Ho, S. K., Young, J. D., and Cockram, C. S. (1992). Effect of insulin on glucose and glycogen metabolism and leucine incorporation into protein in cultured mouse astrocytes. *Glia* 6, 264–268. doi:10.1002/glia.440060404.

Kunos, G., Osei-Hyiaman, D., Liu, J., Godlewski, G., and Bátkai, S. (2008). Endocannabinoids and the control of energy homeostasis. *J. Biol. Chem.* 283, 33021–33025. doi:10.1074/jbc.R800012200.

Lalonde, R. (2002). The neurobiological basis of spontaneous alternation. *Neurosci. Biobehav. Rev.* 26, 91–104.

Lang, U. E., and Borgwardt, S. (2013). Molecular mechanisms of depression: perspectives on new treatment strategies. *Cell. Physiol. Biochem. Int. J. Exp. Cell. Physiol. Biochem. Pharmacol.* 31, 761–777. doi:10.1159/000350094.

Lang, U. E., Lang, F., Richter, K., Vallon, V., Lipp, H.-P., Schnermann, J., et al. (2003). Emotional instability but intact spatial cognition in adenosine receptor 1 knock out mice. *Behav. Brain Res.* 145, 179–188.

Lannert, H., and Hoyer, S. (1998). Intracerebroventricular administration of streptozotocin causes long-term diminutions in learning and memory abilities and in cerebral energy metabolism in adult rats. *Behav. Neurosci.* 112, 1199–1208.

Lara, D. R. (2010). Caffeine, mental health, and psychiatric disorders. *J. Alzheimers Dis. JAD* 20 Suppl 1, S239–248. doi:10.3233/JAD-2010-1378.

Latini, L., Bisicchia, E., Sasso, V., Chiurchiù, V., Cavallucci, V., Molinari, M., et al. (2014). Cannabinoid CB_2 receptor CB_2R stimulation delays rubrospinal mitochondrial-dependent degeneration and improves functional recovery after spinal cord hemisection by ERK1/2 inactivation. *Cell Death Dis.* 5, e1404. doi:10.1038/cddis.2014.364.

Latini, S., and Pedata, F. (2001). Adenosine in the central nervous system: release mechanisms and extracellular concentrations. *J. Neurochem.* 79, 463–484.

Ledent, C., Valverde, O., Cossu, G., Petitet, F., Aubert, J. F., Beslot, F., et al. (1999). Unresponsiveness to cannabinoids and reduced addictive effects of opiates in CB1 receptor knockout mice. *Science* 283, 401–404.

Lee, I., Hunsaker, M. R., and Kesner, R. P. (2005). The role of hippocampal subregions in detecting spatial novelty. *Behav. Neurosci.* 119, 145–153. doi:10.1037/0735-7044.119.1.145.

Lee, M. K., Graham, S. N., and Gold, P. E. (1988). Memory enhancement with posttraining intraventricular glucose injections in rats. *Behav. Neurosci.* 102, 591–595.

Lemos, C., Valério-Fernandes, A., Ghisleni, G. C., Ferreira, S. G., Ledent, C., de Ceballos, M. L., et al. (2012). Impaired hippocampal glucoregulation in the cannabinoid CB_1 receptor knockout mice as revealed by an optimized in vitro experimental approach. *J. Neurosci. Methods* 204, 366–373. doi:10.1016/j.jneumeth.2011.11.028.

de Leon, M. J., Mosconi, L., Blennow, K., DeSanti, S., Zinkowski, R., Mehta, P. D., et al. (2007). Imaging and CSF studies in the preclinical diagnosis of Alzheimer's disease. *Ann. N. Y. Acad. Sci.* 1097, 114–145. doi:10.1196/annals.1379.012.

Lester-Coll, N., Rivera, E. J., Soscia, S. J., Doiron, K., Wands, J. R., and de la Monte, S. M. (2006). Intracerebral streptozotocin model of type 3 diabetes: relevance to sporadic Alzheimer's disease. *J. Alzheimers Dis. JAD* 9, 13–33.

Leybaert, L., De Bock, M., Van Moorhem, M., Decrock, E., and De Vuyst, E. (2007). Neurobarrier coupling in the brain: adjusting glucose entry with demand. *J. Neurosci. Res.* 85, 3213–3220. doi:10.1002/jnr.21189.

de Lima, A. D., and Voigt, T. (1997). Identification of two distinct populations of gamma-aminobutyric acidergic neurons in cultures of the rat cerebral cortex. *J. Comp. Neurol.* 388, 526–540.

Lindborg, K. A., Teachey, M. K., Jacob, S., and Henriksen, E. J. (2010). Effects of in vitro antagonism of endocannabinoid-1 receptors on the glucose transport system in normal and insulin-resistant rat skeletal muscle. *Diabetes Obes. Metab.* 12, 722–730. doi:10.1111/j.1463-1326.2010.01227.x.

Li, P., Rial, D., Canas, P. M., Yoo, J.-H., Li, W., Zhou, X., et al. (2015). Optogenetic activation of intracellular adenosine A_{2A} receptor signaling in the hippocampus is sufficient to trigger CREB phosphorylation and impair memory. *Mol. Psychiatry*. doi:10.1038/mp.2014.182.

Lister, R. G. (1987). The use of a plus-maze to measure anxiety in the mouse. *Psychopharmacology (Berl.)* 92, 180–185.

Liu, L., Zhao, X., Pierre, S. V., and Askari, A. (2007). Association of PI3K-Akt signaling pathway with digitalis-induced hypertrophy of cardiac myocytes. *Am. J. Physiol. Cell Physiol.* 293, C1489–1497. doi:10.1152/ajpcell.00158.2007.

Li, Y., and Kim, J. (2015). Neuronal expression of CB_2 cannabinoid receptor mRNAs in the mouse hippocampus. *Neuroscience* 311, 253–267. doi:10.1016/j.neuroscience.2015.10.041.

Li, Z., Jo, J., Jia, J.-M., Lo, S.-C., Whitcomb, D. J., Jiao, S., et al. (2010). Caspase-3 activation via mitochondria is required for long-term depression and AMPA receptor internalization. *Cell* 141, 859–871. doi:10.1016/j.cell.2010.03.053.

Lodish, H., Berk, A., Zipursky, S. L., Matsudaira, P., Baltimore, D., and Darnell, J. (2000). Overview of Neuron Structure and Function. Available at: http://www.ncbi.nlm.nih.gov/books/NBK21535/ [Accessed October 8, 2015].

Londos, C., Cooper, D. M., and Wolff, J. (1980). Subclasses of external adenosine receptors. *Proc. Natl. Acad. Sci. U. S. A.* 77, 2551–2554.

Long, J. S., Schoonen, P. M., Graczyk, D., O'Prey, J., and Ryan, K. M. (2015). p73 engages A_{2B} receptor signalling to prime cancer cells to chemotherapy-induced death. *Oncogene*. doi:10.1038/onc.2014.436.

Lopes, L. V., Sebastião, A. M., and Ribeiro, J. A. (2011). Adenosine and related drugs in brain diseases: present and future in clinical trials. *Curr. Top. Med. Chem.* 11, 1087–1101.

Louzao, M. C., Espiña, B., Vieytes, M. R., Vega, F. V., Rubiolo, J. A., Baba, O., et al. (2008). "Fluorescent glycogen" formation with sensibility for in vivo and in vitro detection. *Glycoconj. J.* 25, 503–510. doi:10.1007/s10719-007-9075-7.

Lowry, O. H., and Passonneau, J. V. (1964). The relationships between substrates and enzymes of glycolysis in brain. *J. Biol. Chem.* 239, 31–42.

Lowry, O. H., Passonneau, J. V., Hasselberger, F. X., and Schulz, D. W. (1964). Effect of Ischemia on Known Substrates and Cofactors of the Glycolytic Pathway in Brain. *J. Biol. Chem.* 239, 18–30.

Lozovaya, N., Min, R., Tsintsadze, V., and Burnashev, N. (2009). Dual modulation of CNS voltage-gated calcium channels by cannabinoids: Focus on CB_1 receptor-independent effects. *Cell Calcium* 46, 154–162. doi:10.1016/j.ceca.2009.07.007.

Luchsinger, J. A., Reitz, C., Patel, B., Tang, M.-X., Manly, J. J., and Mayeux, R. (2007). Relation of diabetes to mild cognitive impairment. *Arch. Neurol.* 64, 570–575. doi:10.1001/archneur.64.4.570.

Lucignani, G., Namba, H., Nehlig, A., Porrino, L. J., Kennedy, C., and Sokoloff, L. (1987). Effects of insulin on local cerebral glucose utilization in the rat. *J. Cereb. Blood Flow Metab. Off. J. Int. Soc. Cereb. Blood Flow Metab.* 7, 309–314. doi:10.1038/jcbfm.1987.65.

Ludányi, A., Eross, L., Czirják, S., Vajda, J., Halász, P., Watanabe, M., et al. (2008). Downregulation of the CB_1 cannabinoid receptor and related molecular elements of the endocannabinoid system in epileptic human hippocampus. *J. Neurosci. Off. J. Soc. Neurosci.* 28, 2976–2990. doi:10.1523/JNEUROSCI.4465-07.2008.

Lu, G., Zhou, Q.-X., Kang, S., Li, Q.-L., Zhao, L.-C., Chen, J.-D., et al. (2010). Chronic morphine treatment impaired hippocampal long-term potentiation and spatial memory via accumulation of extracellular adenosine acting on adenosine A1 receptors. *J. Neurosci. Off. J. Soc. Neurosci.* 30, 5058–5070. doi:10.1523/JNEUROSCI.0148-10.2010.

Lund-Andersen, H. (1979). Transport of glucose from blood to brain. *Physiol. Rev.* 59, 305–352.

Lundgaard, I., Li, B., Xie, L., Kang, H., Sanggaard, S., Haswell, J. D. R., et al. (2015). Direct neuronal glucose uptake Heralds activity-dependent increases in cerebral metabolism. *Nat. Commun.* 6, 6807. doi:10.1038/ncomms7807.

Mächler, P., Wyss, M. T., Elsayed, M., Stobart, J., Gutierrez, R., von Faber-Castell, A., et al. (2016). In Vivo Evidence for a Lactate Gradient from Astrocytes to Neurons. *Cell Metab.* doi:10.1016/j.cmet.2015.10.010.

Mächler, P., Wyss, M. T., Elsayed, M., Stobart, J., Gutierrez, R., von Faber-Castell, A., et al. In Vivo Evidence for a Lactate Gradient from Astrocytes to Neurons. *Cell Metab.* 0. doi:10.1016/j.cmet.2015.10.010.

Mackie, K. (2005). Distribution of cannabinoid receptors in the central and peripheral nervous system. *Handb. Exp. Pharmacol.*, 299–325.

Mackie, K., and Hille, B. (1992). Cannabinoids inhibit N-type calcium channels in neuroblastoma-glioma cells. *Proc. Natl. Acad. Sci. U. S. A.* 89, 3825–3829.

Mackie, K., Lai, Y., Westenbroek, R., and Mitchell, R. (1995). Cannabinoids activate an inwardly rectifying potassium conductance and inhibit Q-type calcium currents in AtT20 cells transfected with rat brain cannabinoid receptor. *J. Neurosci. Off. J. Soc. Neurosci.* 15, 6552–6561.

Maejima, T., Oka, S., Hashimotodani, Y., Ohno-Shosaku, T., Aiba, A., Wu, D., et al. (2005). Synaptically driven endocannabinoid release requires Ca^{2+}-assisted metabotropic glutamate receptor subtype 1 to phospholipase Cbeta4 signaling cascade in the cerebellum. *J. Neurosci. Off. J. Soc. Neurosci.* 25, 6826–6835. doi:10.1523/JNEUROSCI.0945-05.2005.

Maggi, L., Trettel, F., Scianni, M., Bertollini, C., Eusebi, F., Fredholm, B. B., et al. (2009). LTP impairment by fractalkine/CX3CL1 in mouse hippocampus is mediated through the activity of adenosine receptor type 3 (A_3R). *J. Neuroimmunol.* 215, 36–42. doi:10.1016/j.jneuroim.2009.07.016.

Magistretti, J., Ma, L., Shalinsky, M. H., Lin, W., Klink, R., and Alonso, A. (2004). Spike patterning by Ca^{2+}-dependent regulation of a muscarinic cation current in entorhinal cortex layer II neurons. *J. Neurophysiol.* 92, 1644–1657. doi:10.1152/jn.00036.2004.

Magistretti, P. J. (2004). "Chapter 3 - Brain Energy Metabolism," in *From Molecules to Networks*, ed. J. H. B. L. Roberts (Burlington: Academic Press), 67–89. Available at: http://www.sciencedirect.com/science/article/pii/B9780121486600500044 [Accessed September 8, 2015].

Magistretti, P. J. (2006). Neuron-glia metabolic coupling and plasticity. *J. Exp. Biol.* 209, 2304–2311. doi:10.1242/jeb.02208.

Magistretti, P. J., and Allaman, I. (2007). Glycogen: a Trojan horse for neurons. *Nat. Neurosci.* 10, 1341–1342. doi:10.1038/nn1107-1341.

Magistretti, P. J., and Allaman, I. (2015). A cellular perspective on brain energy metabolism and functional imaging. *Neuron* 86, 883–901. doi:10.1016/j.neuron.2015.03.035.

Magistretti, P. J., Hof, P. R., and Martin, J. L. (1986). Adenosine stimulates glycogenolysis in mouse cerebral cortex: a possible coupling mechanism between neuronal activity and energy metabolism. *J. Neurosci. Off. J. Soc. Neurosci.* 6, 2558–2562.

Magistretti, P. J., and Pellerin, L. (1997). Metabolic coupling during activation. A cellular view. *Adv. Exp. Med. Biol.* 413, 161–166.

Magistretti, P. J., and Pellerin, L. (1999). Astrocytes Couple Synaptic Activity to Glucose Utilization in the Brain. *News Physiol. Sci. Int. J. Physiol. Prod. Jointly Int. Union Physiol. Sci. Am. Physiol. Soc.* 14, 177–182.

Magistretti, P. J., Pellerin, L., and Martin, J.-L. (2002). Brain energy metabolism : an integrated cellular perspective. *Psychopharmacol. Fourth Gener. Prog.*, 657–670.

Magistretti, P. J., Sorg, O., and Martin, J.-L. (1993). Regulation of glycogen metabolism in astrocytes: physiological, pharmacological and pathological aspects. *Astrocytes Pharmacol. Funct.*, 243–265.

Maher, F., Vannucci, S. J., and Simpson, I. A. (1994). Glucose transporter proteins in brain. *FASEB J. Off. Publ. Fed. Am. Soc. Exp. Biol.* 8, 1003–1011.

Mahfouz, M., Makar, A. B., Ghoneim, M. T., and Mikhail, M. M. (1975). Effect of hashish on brain gamma aminobutyric acid system, blood fibrinolytic activity and glucose and some serum enzymes in the rat. *Pharm.* 30, 772–774.

Mailleux, P., and Vanderhaeghen, J. J. (1992). Distribution of neuronal cannabinoid receptor in the adult rat brain: a comparative receptor binding radioautography and in situ hybridization histochemistry. *Neuroscience* 48, 655–668.

Makita, N., and Iiri, T. (2014). Biased agonism: a novel paradigm in G protein-coupled receptor signaling observed in acquired hypocalciuric hypercalcemia. *Endocr. J.* 61, 303–309.

Mangia, S., DiNuzzo, M., Giove, F., Carruthers, A., Simpson, I. A., and Vannucci, S. J. (2011). Response to “comment on recent modeling studies of astrocyte-neuron metabolic interactions”: much ado about nothing. *J. Cereb. Blood Flow Metab. Off. J. Int. Soc. Cereb. Blood Flow Metab.* 31, 1346–1353. doi:10.1038/jcbfm.2011.29.

Mangia, S., Simpson, I. A., Vannucci, S. J., and Carruthers, A. (2009). The in vivo neuron-to-astrocyte lactate shuttle in human brain: evidence from modeling of

measured lactate levels during visual stimulation. *J. Neurochem.* 109 Suppl 1, 55–62. doi:10.1111/j.1471-4159.2009.06003.x.

Margulies, J. E., and Hammer, R. P. (1991). Delta 9-tetrahydrocannabinol alters cerebral metabolism in a biphasic, dose-dependent manner in rat brain. *Eur. J. Pharmacol.* 202, 373–378.

Marsicano, G., and Lutz, B. (1999). Expression of the cannabinoid receptor CB_1 in distinct neuronal subpopulations in the adult mouse forebrain. *Eur. J. Neurosci.* 11, 4213–4225.

Martin, B. R., Wiley, J. L., Beletskaya, I., Sim-Selley, L. J., Smith, F. L., Dewey, W. L., et al. (2006). Pharmacological characterization of novel water-soluble cannabinoids. *J. Pharmacol. Exp. Ther.* 318, 1230–1239. doi:10.1124/jpet.106.104109.

Matheus, F. C., Rial, D., Real, J. I., Lemos, C., Takahashi, R. N., Bertoglio, L. J., et al. (2015). Temporal Dissociation of Striatum and Prefrontal Cortex Uncouples Anhedonia and Defense Behaviors Relevant to Depression in 6-OHDA-Lesioned Rats. *Mol. Neurobiol.* doi:10.1007/s12035-015-9330-z.

Matias, I., Marzo, V. D., and Köfalvi, A. (2008a). "Endocannabinoids in Energy Homeostasis and Metabolic Disorders," in *Cannabinoids and the Brain*, ed. A. Köfalvi (Springer US), 277–316. Available at: http://link.springer.com/chapter/10.1007/978-0-387-74349-3_14 [Accessed June 18, 2015].

Matias, I., Marzo, V. D., and Köfalvi, A. (2008b). "Endocannabinoids in Energy Homeostasis and Metabolic Disorders," in *Cannabinoids and the Brain*, ed. A. Köfalvi (Springer US), 277–316. Available at: http://link.springer.com/chapter/10.1007/978-0-387-74349-3_14 [Accessed August 15, 2015].

Matos, M., Augusto, E., Agostinho, P., Cunha, R. A., and Chen, J.-F. (2013). Antagonistic interaction between adenosine A_{2A} receptors and Na+/K+-ATPase-α2 controlling glutamate uptake in astrocytes. *J. Neurosci. Off. J. Soc. Neurosci.* 33, 18492–18502. doi:10.1523/JNEUROSCI.1828-13.2013.

Matos, M., Augusto, E., Santos-Rodrigues, A. D., Schwarzschild, M. A., Chen, J.-F., Cunha, R. A., et al. (2012). Adenosine A_{2A} receptors modulate glutamate uptake in cultured astrocytes and gliosomes. *Glia* 60, 702–716. doi:10.1002/glia.22290.

Matsuda, L. A., Bonner, T. I., and Lolait, S. J. (1993). Localization of cannabinoid receptor mRNA in rat brain. *J. Comp. Neurol.* 327, 535–550. doi:10.1002/cne.903270406.

Matsuda, L. A., Lolait, S. J., Brownstein, M. J., Young, A. C., and Bonner, T. I. (1990). Structure of a cannabinoid receptor and functional expression of the cloned cDNA. *Nature* 346, 561–564. doi:10.1038/346561a0.

McAllister, S. D., Griffin, G., Satin, L. S., and Abood, M. E. (1999). Cannabinoid receptors can activate and inhibit G protein-coupled inwardly rectifying potassium channels in a xenopus oocyte expression system. *J. Pharmacol. Exp. Ther.* 291, 618–626.

McIlwain, K. L., Merriweather, M. Y., Yuva-Paylor, L. A., and Paylor, R. (2001). The use of behavioral test batteries: effects of training history. *Physiol. Behav.* 73, 705–717.

McKenna, M. C., Dienel, G. A., Sonnewald, U., Waagepetersen, H. S., and Schousboe, A. (2012). "Energy Metabolism of the Brain," in *Basic Neurochemistry* (Elsevier), 200–231. Available at: http://linkinghub.elsevier.com/retrieve/pii/B9780123749475000110 [Accessed June 19, 2015].

McLachlan, E. M. (1978). The statistics of transmitter release at chemical synapses. *Int. Rev. Physiol.* 17, 49–117.

McNay, E. C., Ong, C. T., McCrimmon, R. J., Cresswell, J., Bogan, J. S., and Sherwin, R. S. (2010). Hippocampal memory processes are modulated by insulin and high-fat-induced insulin resistance. *Neurobiol. Learn. Mem.* 93, 546–553. doi:10.1016/j.nlm.2010.02.002.

McNay, E. C., and Recknagel, A. K. (2011). Brain insulin signaling: a key component of cognitive processes and a potential basis for cognitive impairment in type 2 diabetes. *Neurobiol. Learn. Mem.* 96, 432–442. doi:10.1016/j.nlm.2011.08.005.

Mechoulam, R., Hanuš, L. O., Pertwee, R., and Howlett, A. C. (2014). Early phytocannabinoid chemistry to endocannabinoids and beyond. *Nat. Rev. Neurosci.* 15, 757–764. doi:10.1038/nrn3811.

Meghji, P., and Newby, A. C. (1990). Sites of adenosine formation, action and inactivation in the brain. *Neurochem. Int.* 16, 227–232.

de Mendonça, A., Almeida, T., Bashir, Z. I., and Ribeiro, J. A. (1997). Endogenous adenosine attenuates long-term depression and depotentiation in the CA1 region of the rat hippocampus. *Neuropharmacology* 36, 161–167.

de Mendonça, A., and Ribeiro, J. A. (2001). Adenosine and synaptic plasticity. *Drug Dev. Res.* 52, 283–290. doi:10.1002/ddr.1125.

Messier, C. (2004). Glucose improvement of memory: a review. *Eur. J. Pharmacol.* 490, 33–57. doi:10.1016/j.ejphar.2004.02.043.

Messier, C., Pierre, J., Desrochers, A., and Gravel, M. (1998). Dose-dependent action of glucose on memory processes in women: effect on serial position and recall priority. *Brain Res. Cogn. Brain Res.* 7, 221–233.

Metzger, M. M. (2000). Glucose enhancement of a facial recognition task in young adults. *Physiol. Behav.* 68, 549–553.

Meye, F. J., Ramakers, G. M. J., and Adan, R. a. H. (2014). The vital role of constitutive GPCR activity in the mesolimbic dopamine system. *Transl. Psychiatry* 4, e361. doi:10.1038/tp.2013.130.

Meye, F. J., Trezza, V., Vanderschuren, L. J. M. J., Ramakers, G. M. J., and Adan, R. a. H. (2013). Neutral antagonism at the cannabinoid 1 receptor: a safer treatment for obesity. *Mol. Psychiatry* 18, 1294–1301. doi:10.1038/mp.2012.145.

Miller, K. E., and Sheetz, M. P. (2004). Axonal mitochondrial transport and potential are correlated. *J. Cell Sci.* 117, 2791–2804. doi:10.1242/jcs.01130.

Mistur, R., Mosconi, L., Santi, S. D., Guzman, M., Li, Y., Tsui, W., et al. (2009). Current Challenges for the Early Detection of Alzheimer's Disease: Brain Imaging and CSF Studies. *J. Clin. Neurol. Seoul Korea* 5, 153–166. doi:10.3988/jcn.2009.5.4.153.

Miyata, S., Yamada, N., Hirano, S., Tanaka, S., and Kamei, J. (2007). Diabetes attenuates psychological stress-elicited 5-HT secretion in the prefrontal cortex but not in the amygdala of mice. *Brain Res.* 1147, 233–239. doi:10.1016/j.brainres.2007.02.001.

Moidunny, S., Vinet, J., Wesseling, E., Bijzet, J., Shieh, C.-H., van Ijzendoorn, S. C. D., et al. (2012). Adenosine A_{2B} receptor-mediated leukemia inhibitory factor release from astrocytes protects cortical neurons against excitotoxicity. *J. Neuroinflammation* 9, 198. doi:10.1186/1742-2094-9-198.

Molina-Holgado, E., Vela, J. M., Arévalo-Martín, A., Almazán, G., Molina-Holgado, F., Borrell, J., et al. (2002). Cannabinoids promote oligodendrocyte progenitor survival: involvement of cannabinoid receptors and phosphatidylinositol-3 kinase/Akt signaling. *J. Neurosci. Off. J. Soc. Neurosci.* 22, 9742–9753.

Molina-Holgado, F., Pinteaux, E., Heenan, L., Moore, J. D., Rothwell, N. J., and Gibson, R. M. (2005). Neuroprotective effects of the synthetic cannabinoid HU-210 in primary cortical neurons are mediated by phosphatidylinositol 3-kinase/AKT signaling. *Mol. Cell. Neurosci.* 28, 189–194. doi:10.1016/j.mcn.2004.09.004.

Molnár, G., Faragó, N., Kocsis, Á. K., Rózsa, M., Lovas, S., Boldog, E., et al. (2014). GABAergic neurogliaform cells represent local sources of insulin in the cerebral cortex. *J. Neurosci. Off. J. Soc. Neurosci.* 34, 1133–1137. doi:10.1523/JNEUROSCI.4082-13.2014.

Molz, S., Olescowicz, G., Kraus, J. R., Ludka, F. K., and Tasca, C. I. (2015). Purine receptors are required for DHA-mediated neuroprotection against oxygen and glucose deprivation in hippocampal slices. *Purinergic Signal.* 11, 117–126. doi:10.1007/s11302-014-9438-z.

de la Monte, S. M., and Wands, J. R. (2008). Alzheimer's Disease Is Type 3 Diabetes–Evidence Reviewed. *J. Diabetes Sci. Technol. Online* 2, 1101–1113.

Moreira, P. I., Cardoso, S. M., Santos, M. S., and Oliveira, C. R. (2006). The key role of mitochondria in Alzheimer's disease. *J. Alzheimers Dis. JAD* 9, 101–110.

Morgan, N. H., Stanford, I. M., and Woodhall, G. L. (2009). Functional CB_2 type cannabinoid receptors at CNS synapses. *Neuropharmacology* 57, 356–368. doi:10.1016/j.neuropharm.2009.07.017.

Morgenthaler, F. D., van Heeswijk, R. B., Xin, L., Laus, S., Frenkel, H., Lei, H., et al. (2008). Non-invasive quantification of brain glycogen absolute concentration. *J. Neurochem.* 107, 1414–1423.

Mori, M., Nishizaki, T., and Okada, Y. (1992). Protective effect of adenosine on the anoxic damage of hippocampal slice. *Neuroscience* 46, 301–307.

Morrison, P. D., Mackinnon, M. W., Bartrup, J. T., Skett, P. G., and Stone, T. W. (1992). Changes in adenosine sensitivity in the hippocampus of rats with streptozotocin-induced diabetes. *Br. J. Pharmacol.* 105, 1004–1008.

Morris, R. G., Garrud, P., Rawlins, J. N., and O'Keefe, J. (1982). Place navigation impaired in rats with hippocampal lesions. *Nature* 297, 681–683.

Morris, R. G. M., Moser, E. I., Riedel, G., Martin, S. J., Sandin, J., Day, M., et al. (2003). Elements of a neurobiological theory of the hippocampus: the role of activity-dependent synaptic plasticity in memory. *Philos. Trans. R. Soc. Lond. B. Biol. Sci.* 358, 773–786. doi:10.1098/rstb.2002.1264.

Mosconi, L. (2005). Brain glucose metabolism in the early and specific diagnosis of Alzheimer's disease. FDG-PET studies in MCI and AD. *Eur. J. Nucl. Med. Mol. Imaging* 32, 486–510. doi:10.1007/s00259-005-1762-7.

Mueckler, M. M. (1992). The molecular biology of mammalian glucose transporters. *Curr. Opin. Nephrol. Hypertens.* 1, 12–20.

Mukhopadhyay, S., and Howlett, A. C. (2005). Chemically distinct ligands promote differential CB_1 cannabinoid receptor-Gi protein interactions. *Mol. Pharmacol.* 67, 2016–2024. doi:10.1124/mol.104.003558.

Munro, S., Thomas, K. L., and Abu-Shaar, M. (1993). Molecular characterization of a peripheral receptor for cannabinoids. *Nature* 365, 61–65. doi:10.1038/365061a0.

Murai, T., Okuda, S., Tanaka, T., and Ohta, H. (2007). Characteristics of object location memory in mice: Behavioral and pharmacological studies. *Physiol. Behav.* 90, 116–124. doi:10.1016/j.physbeh.2006.09.013.

Myhrer, T. (2003). Neurotransmitter systems involved in learning and memory in the rat: a meta-analysis based on studies of four behavioral tasks. *Brain Res. Brain Res. Rev.* 41, 268–287.

Nabavi, S., Fox, R., Proulx, C. D., Lin, J. Y., Tsien, R. Y., and Malinow, R. (2014). Engineering a memory with LTD and LTP. *Nature* advance online publication. doi:10.1038/nature13294.

Naghizadeh, B., Mansouri, M. T., Ghorbanzadeh, B., Farbood, Y., and Sarkaki, A. (2013). Protective effects of oral crocin against intracerebroventricular

streptozotocin-induced spatial memory deficit and oxidative stress in rats. *Phytomedicine Int. J. Phytother. Phytopharm.* 20, 537–542. doi:10.1016/j.phymed.2012.12.019.

Navarrete, M., and Araque, A. (2008). Endocannabinoids mediate neuron-astrocyte communication. *Neuron* 57, 883–893. doi:10.1016/j.neuron.2008.01.029.

Nedergaard, M., Ransom, B., and Goldman, S. A. (2003). New roles for astrocytes: redefining the functional architecture of the brain. *Trends Neurosci.* 26, 523–530. doi:10.1016/j.tins.2003.08.008.

Nehlig, A., Daval, J. L., and Boyet, S. (1994). Effects of selective adenosine A1 and A2 receptor agonists and antagonists on local rates of energy metabolism in the rat brain. *Eur. J. Pharmacol.* 258, 57–66.

Nehlig, A., Wittendorp-Rechenmann, E., and Lam, C. D. (2004). Selective uptake of [14C]2-deoxyglucose by neurons and astrocytes: high-resolution microautoradiographic imaging by cellular ^{14}C-trajectography combined with immunohistochemistry. *J. Cereb. Blood Flow Metab. Off. J. Int. Soc. Cereb. Blood Flow Metab.* 24, 1004–1014. doi:10.1097/01.WCB.0000128533.84196.D8.

Nelson, T. J., Sun, M.-K., Hongpaisan, J., and Alkon, D. L. (2008). Insulin, PKC signaling pathways and synaptic remodeling during memory storage and neuronal repair. *Eur. J. Pharmacol.* 585, 76–87. doi:10.1016/j.ejphar.2008.01.051.

Nelson, T., Kaufman, E. E., and Sokoloff, L. (1984). 2-Deoxyglucose incorporation into rat brain glycogen during measurement of local cerebral glucose utilization by the 2-deoxyglucose method. *J. Neurochem.* 43, 949–956.

Németh, Z. H., Bleich, D., Csóka, B., Pacher, P., Mabley, J. G., Himer, L., et al. (2007). Adenosine receptor activation ameliorates type 1 diabetes. *FASEB J. Off. Publ. Fed. Am. Soc. Exp. Biol.* 21, 2379–2388. doi:10.1096/fj.07-8213com.

Nestor, P. J., Fryer, T. D., and Hodges, J. R. (2006). Declarative memory impairments in Alzheimer's disease and semantic dementia. *NeuroImage* 30, 1010–1020. doi:10.1016/j.neuroimage.2005.10.008.

Neves, G., Cooke, S. F., and Bliss, T. V. P. (2008). Synaptic plasticity, memory and the hippocampus: a neural network approach to causality. *Nat. Rev. Neurosci.* 9, 65–75. doi:10.1038/nrn2303.

Newby, A. C., Worku, Y., and Holmquist, C. A. (1985). Adenosine formation. Evidence for a direct biochemical link with energy metabolism. *Adv. Myocardiol.* 6, 273–284.

Nicholls, D. G., and Budd, S. L. (2000). Mitochondria and neuronal survival. *Physiol. Rev.* 80, 315–360.

Nitsch, R., and Hoyer, S. (1991). Local action of the diabetogenic drug, streptozotocin, on glucose and energy metabolism in rat brain cortex. *Neurosci. Lett.* 128, 199–202.

Novitskiy, S. V., Ryzhov, S., Zaynagetdinov, R., Goldstein, A. E., Huang, Y., Tikhomirov, O. Y., et al. (2008). Adenosine receptors in regulation of dendritic cell differentiation and function. *Blood* 112, 1822–1831. doi:10.1182/blood-2008-02-136325.

Nudo, R. J., and Masterton, R. B. (1986). Stimulation-induced [14C]2-deoxyglucose labeling of synaptic activity in the central auditory system. *J. Comp. Neurol.* 245, 553–565. doi:10.1002/cne.902450410.

O'Callaghan, R. M., Ohle, R., and Kelly, Á. M. (2007). The effects of forced exercise on hippocampal plasticity in the rat: A comparison of LTP, spatial- and non-spatial learning. *Behav. Brain Res.* 176, 362–366. doi:10.1016/j.bbr.2006.10.018.

Ohno, M., and Watanabe, S. (1996). Working memory failure by stimulation of hippocampal adenosine A1 receptors in rats. *Neuroreport* 7, 3013–3016.

Olah, M. E. (1997). Identification of A_{2A} adenosine receptor domains involved in selective coupling to Gs. Analysis of chimeric A_1/A_{2A} adenosine receptors. *J. Biol. Chem.* 272, 337–344.

O'Neil, R. G., Wu, L., and Mullani, N. (2005). Uptake of a fluorescent deoxyglucose analog (2-NBDG) in tumor cells. *Mol. Imaging Biol. MIB Off. Publ. Acad. Mol. Imaging* 7, 388–392. doi:10.1007/s11307-005-0011-6.

Onodera, H., Iijima, K., and Kogure, K. (1986). Mononucleotide metabolism in the rat brain after transient ischemia. *J. Neurochem.* 46, 1704–1710.

Orr, A. G., Hsiao, E. C., Wang, M. M., Ho, K., Kim, D. H., Wang, X., et al. (2015a). Astrocytic adenosine receptor A_{2A} and Gs-coupled signaling regulate memory. *Nat. Neurosci.* 18, 423–434. doi:10.1038/nn.3930.

Orr, A. G., Hsiao, E. C., Wang, M. M., Ho, K., Kim, D. H., Wang, X., et al. (2015b). Astrocytic adenosine receptor A_{2A} and Gs-coupled signaling regulate memory. *Nat. Neurosci.* 18, 423–434. doi:10.1038/nn.3930.

Pacold, S. T., and Blackard, W. G. (1979). Central nervous system insulin receptors in normal and diabetic rats. *Endocrinology* 105, 1452–1457. doi:10.1210/endo-105-6-1452.

Pagnussat, N., Almeida, A. S., Marques, D. M., Nunes, F., Chenet, G. C., Botton, P. H. S., et al. (2015). Adenosine A_{2A} receptors are necessary and sufficient to trigger memory impairment in adult mice. *Br. J. Pharmacol.* 172, 3831–3845. doi:10.1111/bph.13180.

Palizgir, M., Bakhtiari, M., and Esteghamati, A. (2013). Association of depression and anxiety with diabetes mellitus type 2 concerning some sociological factors. *Iran. Red Crescent Med. J.* 15, 644–648. doi:10.5812/ircmj.12107.

Pandey, S. P., Singh, H. K., and Prasad, S. (2015). Alterations in Hippocampal Oxidative Stress, Expression of AMPA Receptor GluR2 Subunit and Associated Spatial Memory Loss by Bacopa monnieri Extract (CDRI-08) in Streptozotocin-Induced Diabetes Mellitus Type 2 Mice. *PloS One* 10, e0131862. doi:10.1371/journal.pone.0131862.

Pandolfo, P., Machado, N. J., Köfalvi, A., Takahashi, R. N., and Cunha, R. A. (2013). Caffeine regulates frontocorticostriatal dopamine transporter density and improves attention and cognitive deficits in an animal model of attention deficit hyperactivity disorder. *Eur. Neuropsychopharmacol. J. Eur. Coll. Neuropsychopharmacol.* 23, 317–328. doi:10.1016/j.euroneuro.2012.04.011.

Pandolfo, P., Silveirinha, V., dos Santos-Rodrigues, A., Venance, L., Ledent, C., Takahashi, R. N., et al. (2011). Cannabinoids inhibit the synaptic uptake of adenosine and dopamine in the rat and mouse striatum. *Eur. J. Pharmacol.* 655, 38–45. doi:10.1016/j.ejphar.2011.01.013.

Panza, F., Frisardi, V., Capurso, C., Imbimbo, B. P., Vendemiale, G., Santamato, A., et al. (2010). Metabolic syndrome and cognitive impairment: current epidemiology and possible underlying mechanisms. *J. Alzheimers Dis. JAD* 21, 691–724. doi:10.3233/JAD-2010-091669.

Papazoglou, I. K., Jean, A., Gertler, A., Taouis, M., and Vacher, C.-M. (2015). Hippocampal GSK3β as a Molecular Link Between Obesity and Depression. *Mol. Neurobiol.* 52, 363–374. doi:10.1007/s12035-014-8863-x.

Pappenheimer, J. R., and Setchell, B. P. (1973). Cerebral glucose transport and oxygen consumption in sheep and rabbits. *J. Physiol.* 233, 529–551.

Pascual, O., Casper, K. B., Kubera, C., Zhang, J., Revilla-Sanchez, R., Sul, J.-Y., et al. (2005). Astrocytic purinergic signaling coordinates synaptic networks. *Science* 310, 113–116. doi:10.1126/science.1116916.

Patel, A. B., Lai, J. C. K., Chowdhury, G. M. I., Hyder, F., Rothman, D. L., Shulman, R. G., et al. (2014). Direct evidence for activity-dependent glucose phosphorylation in neurons with implications for the astrocyte-to-neuron lactate shuttle. *Proc. Natl. Acad. Sci. U. S. A.* 111, 5385–5390. doi:10.1073/pnas.1403576111.

Patel, M. S., and Korotchkina, L. G. (2001). Regulation of mammalian pyruvate dehydrogenase complex by phosphorylation: complexity of multiple phosphorylation sites and kinases. *Exp. Mol. Med.* 33, 191–197. doi:10.1038/emm.2001.32.

Paula-Lima, A. C., Brito-Moreira, J., and Ferreira, S. T. (2013). Deregulation of excitatory neurotransmission underlying synapse failure in Alzheimer's disease. *J. Neurochem.* 126, 191–202. doi:10.1111/jnc.12304.

Paylor, R., Spencer, C. M., Yuva-Paylor, L. A., and Pieke-Dahl, S. (2006). The use of behavioral test batteries, II: effect of test interval. *Physiol. Behav.* 87, 95–102. doi:10.1016/j.physbeh.2005.09.002.

Peakman, M. C., and Hill, S. J. (1994). Adenosine A_{2B}-receptor-mediated cyclic AMP accumulation in primary rat astrocytes. *Br. J. Pharmacol.* 111, 191–198.

Peleli, M., Hezel, M., Zollbrecht, C., Persson, A. E. G., Lundberg, J. O., Weitzberg, E., et al. (2015). In adenosine A_{2B} knockouts acute treatment with inorganic nitrate improves glucose disposal, oxidative stress, and AMPK signaling in the liver. *Front. Physiol.* 6, 222. doi:10.3389/fphys.2015.00222.

Pellerin, L., Bouzier-Sore, A.-K., Aubert, A., Serres, S., Merle, M., Costalat, R., et al. (2007). Activity-dependent regulation of energy metabolism by astrocytes: an update. *Glia* 55, 1251–1262. doi:10.1002/glia.20528.

Pellerin, L., and Magistretti, P. J. (1994). Glutamate uptake into astrocytes stimulates aerobic glycolysis: a mechanism coupling neuronal activity to glucose utilization. *Proc. Natl. Acad. Sci. U. S. A.* 91, 10625–10629.

Pellerin, L., and Magistretti, P. J. (2003). Food for thought: challenging the dogmas. *J. Cereb. Blood Flow Metab. Off. J. Int. Soc. Cereb. Blood Flow Metab.* 23, 1282–1286. doi:10.1097/01.WCB.0000096064.12129.3D.

Pellerin, L., and Magistretti, P. J. (2012). Sweet sixteen for ANLS. *J. Cereb. Blood Flow Metab. Off. J. Int. Soc. Cereb. Blood Flow Metab.* 32, 1152–1166. doi:10.1038/jcbfm.2011.149.

Pelligrino, D. A., Lipa, M. D., and Albrecht, R. F. (1990). Regional blood-brain glucose transfer and glucose utilization in chronically hyperglycemic, diabetic rats following acute glycemic normalization. *J. Cereb. Blood Flow Metab. Off. J. Int. Soc. Cereb. Blood Flow Metab.* 10, 774–780. doi:10.1038/jcbfm.1990.135.

Peng, L., Huang, R., Yu, A. C. H., Fung, K. Y., Rathbone, M. P., and Hertz, L. (2005). Nucleoside transporter expression and function in cultured mouse astrocytes. *Glia* 52, 25–35. doi:10.1002/glia.20216.

Pentreath, V. W., Seal, L. H., and Kai-Kai, M. A. (1982). Incorporation of [^{3}H]2-deoxyglucose into glycogen in nervous tissues. *Neuroscience* 7, 759–767.

Perea, G., Navarrete, M., and Araque, A. (2009). Tripartite synapses: astrocytes process and control synaptic information. *Trends Neurosci.* 32, 421–431. doi:10.1016/j.tins.2009.05.001.

Perea, G., Sur, M., and Araque, A. (2014). Neuron-glia networks: integral gear of brain function. *Front. Cell. Neurosci.* 8, 378. doi:10.3389/fncel.2014.00378.

Perez-Buira, S., Barrachina, M., Rodriguez, A., Albasanz, J. L., Martín, M., and Ferrer, I. (2007). Expression levels of adenosine receptors in hippocampus and frontal cortex in argyrophilic grain disease. *Neurosci. Lett.* 423, 194–199. doi:10.1016/j.neulet.2007.06.049.

Pertwee, R. G. (2005). Inverse agonism and neutral antagonism at cannabinoid CB_1 receptors. *Life Sci.* 76, 1307–1324. doi:10.1016/j.lfs.2004.10.025.

Pertwee, R. G., Howlett, A. C., Abood, M. E., Alexander, S. P. H., Di Marzo, V., Elphick, M. R., et al. (2010). International Union of Basic and Clinical Pharmacology. LXXIX. Cannabinoid receptors and their ligands: beyond CB_1 and CB_2. *Pharmacol. Rev.* 62, 588–631. doi:10.1124/pr.110.003004.

Peyron, R., Le Bars, D., Cinotti, L., Garcia-Larrea, L., Galy, G., Landais, P., et al. (1994). Effects of GABAA receptors activation on brain glucose metabolism in normal subjects and temporal lobe epilepsy (TLE) patients. A positron emission tomography (PET) study. Part I: Brain glucose metabolism is increased after GABAA receptors activation. *Epilepsy Res.* 19, 45–54.

Phelps, M. E. (2000). PET: the merging of biology and imaging into molecular imaging. *J. Nucl. Med. Off. Publ. Soc. Nucl. Med.* 41, 661–681.

Phillips, E., and Newsholme, E. A. (1979). Maximum activities, properties and distribution of 5' nucleotidase, adenosine kinase and adenosine deaminase in rat and human brain. *J. Neurochem.* 33, 553–558.

Pilitsis, J. G., and Kimelberg, H. K. (1998). Adenosine receptor mediated stimulation of intracellular calcium in acutely isolated astrocytes. *Brain Res.* 798, 294–303.

Piomelli, D. (2003). The molecular logic of endocannabinoid signalling. *Nat. Rev. Neurosci.* 4, 873–884. doi:10.1038/nrn1247.

Placzek, E. A., Okamoto, Y., Ueda, N., and Barker, E. L. (2008). Membrane microdomains and metabolic pathways that define anandamide and 2-arachidonyl glycerol biosynthesis and breakdown. *Neuropharmacology* 55, 1095–1104. doi:10.1016/j.neuropharm.2008.07.047.

Ponce-Lopez, T., Liy-Salmeron, G., Hong, E., and Meneses, A. (2011). Lithium, phenserine, memantine and pioglitazone reverse memory deficit and restore phospho-GSK3β decreased in hippocampus in intracerebroventricular streptozotocin induced memory deficit model. *Brain Res.* 1426, 73–85. doi:10.1016/j.brainres.2011.09.056.

Pontieri, F. E., Conti, G., Zocchi, A., Fieschi, C., and Orzi, F. (1999). Metabolic mapping of the effects of WIN 55212-2 intravenous administration in the rat. *Neuropsychopharmacol. Off. Publ. Am. Coll. Neuropsychopharmacol.* 21, 773–776. doi:10.1016/S0893-133X(99)00064-0.

Porras, O. H., Ruminot, I., Loaiza, A., and Barros, L. F. (2008). Na^+-Ca^{2+} cosignaling in the stimulation of the glucose transporter GLUT1 in cultured astrocytes. *Glia* 56, 59–68. doi:10.1002/glia.20589.

Porsolt, R. D., Le Pichon, M., and Jalfre, M. (1977). Depression: a new animal model sensitive to antidepressant treatments. *Nature* 266, 730–732.

Poston, K. L., and Eidelberg, D. (2010). FDG PET in the Evaluation of Parkinson's Disease. *PET Clin.* 5, 55–64. doi:10.1016/j.cpet.2009.12.004.

Prather, P. L. (2008). "CB_2 Cannabinoid Receptors: Molecular, Signaling, and Trafficking Properties," in *Cannabinoids and the Brain*, ed. A. Köfalvi (Springer US), 75–90. Available at: http://link.springer.com/chapter/10.1007/978-0-387-74349-3_6 [Accessed December 22, 2015].

Prediger, R. D. S., Batista, L. C., Medeiros, R., Pandolfo, P., Florio, J. C., and Takahashi, R. N. (2006). The risk is in the air: Intranasal administration of MPTP to rats reproducing clinical features of Parkinson's disease. *Exp. Neurol.* 202, 391–403. doi:10.1016/j.expneurol.2006.07.001.

Prediger, R. D. S., Batista, L. C., and Takahashi, R. N. (2005a). Caffeine reverses age-related deficits in olfactory discrimination and social recognition memory in rats. Involvement of adenosine A_1 and A_{2A} receptors. *Neurobiol. Aging* 26, 957–964. doi:10.1016/j.neurobiolaging.2004.08.012.

Prediger, R. D. S., Fernandes, D., and Takahashi, R. N. (2005b). Blockade of adenosine A_{2A} receptors reverses short-term social memory impairments in spontaneously hypertensive rats. *Behav. Brain Res.* 159, 197–205. doi:10.1016/j.bbr.2004.10.017.

Prediger, R. D. S., Pamplona, F. A., Fernandes, D., and Takahashi, R. N. (2005c). Caffeine improves spatial learning deficits in an animal model of attention deficit hyperactivity disorder (ADHD) -- the spontaneously hypertensive rat (SHR). *Int. J. Neuropsychopharmacol. Off. Sci. J. Coll. Int. Neuropsychopharmacol. CINP* 8, 583–594. doi:10.1017/S1461145705005341.

Ragozzino, M. E., Unick, K. E., and Gold, P. E. (1996). Hippocampal acetylcholine release during memory testing in rats: augmentation by glucose. *Proc. Natl. Acad. Sci. U. S. A.* 93, 4693–4698.

Raichle, M. E., and Mintun, M. A. (2006). Brain work and brain imaging. *Annu. Rev. Neurosci.* 29, 449–476. doi:10.1146/annurev.neuro.29.051605.112819.

Raizada, M. K. (1983). Localization of insulin-like immunoreactivity in the neurons from primary cultures of rat brain. *Exp. Cell Res.* 143, 351–357.

Randle, P., and Morgan, H. E. (1964). "Regulation of glucose uptake by muscle," in *Vitamins and Hormones*, 199–249.

Ransom, B., Behar, T., and Nedergaard, M. (2003). New roles for astrocytes (stars at last). *Trends Neurosci.* 26, 520–522. doi:10.1016/j.tins.2003.08.006.

Ravinet Trillou, C., Delgorge, C., Menet, C., Arnone, M., and Soubrié, P. (2004). CB_1 cannabinoid receptor knockout in mice leads to leanness, resistance to diet-induced obesity and enhanced leptin sensitivity. *Int. J. Obes. Relat. Metab. Disord. J. Int. Assoc. Study Obes.* 28, 640–648. doi:10.1038/sj.ijo.0802583.

Ravona-Springer, R., Moshier, E., Schmeidler, J., Godbold, J., Akrivos, J., Rapp, M., et al. (2012). Changes in glycemic control are associated with changes in cognition

in non-diabetic elderly. *J. Alzheimers Dis. JAD* 30, 299–309. doi:10.3233/JAD-2012-120106.

Rebola, N., Pinheiro, P. C., Oliveira, C. R., Malva, J. O., and Cunha, R. A. (2003a). Subcellular localization of adenosine A_1 receptors in nerve terminals and synapses of the rat hippocampus. *Brain Res.* 987, 49–58.

Rebola, N., Sebastião, A. M., de Mendonca, A., Oliveira, C. R., Ribeiro, J. A., and Cunha, R. A. (2003b). Enhanced adenosine A_{2A} receptor facilitation of synaptic transmission in the hippocampus of aged rats. *J. Neurophysiol.* 90, 1295–1303. doi:10.1152/jn.00896.2002.

Reddington, M., and Pusch, R. (1983). Adenosine metabolism in a rat hippocampal slice preparation: incorporation into S-adenosylhomocysteine. *J. Neurochem.* 40, 285–290.

Rees, D. A., and Alcolado, J. C. (2005). Animal models of diabetes mellitus. *Diabet. Med. J. Br. Diabet. Assoc.* 22, 359–370. doi:10.1111/j.1464-5491.2005.01499.x.

Reid, C. B., and Walsh, C. A. (2002). Evidence of common progenitors and patterns of dispersion in rat striatum and cerebral cortex. *J. Neurosci. Off. J. Soc. Neurosci.* 22, 4002–4014. doi:20026368.

Reiman, E. M., and Langbaum, J. B. S. (2009). "Brain Imaging in the Evaluation of Putative Alzheimer's Disease-Slowing, Risk-Reducing and Prevention Therapies," in *Imaging the Aging Brain*, eds. W. Jagust and M. D'Esposito (Oxford University Press), 319–350. Available at: http://www.oxfordscholarship.com/view/10.1093/acprof:oso/9780195328875.001.0001/acprof-9780195328875-chapter-20 [Accessed December 22, 2015].

Remondes, M., and Schuman, E. M. (2002). Direct cortical input modulates plasticity and spiking in CA1 pyramidal neurons. *Nature* 416, 736–740. doi:10.1038/416736a.

Resende, R., Pereira, C., Agostinho, P., Vieira, A. P., Malva, J. O., and Oliveira, C. R. (2007). Susceptibility of hippocampal neurons to Abeta peptide toxicity is associated with perturbation of Ca^{2+} homeostasis. *Brain Res.* 1143, 11–21. doi:10.1016/j.brainres.2007.01.071.

Rex, C. S., Kramár, E. A., Colgin, L. L., Lin, B., Gall, C. M., and Lynch, G. (2005). Long-term potentiation is impaired in middle-aged rats: regional specificity and reversal by adenosine receptor antagonists. *J. Neurosci. Off. J. Soc. Neurosci.* 25, 5956–5966. doi:10.1523/JNEUROSCI.0880-05.2005.

Rial, D., Lara, D. R., and Cunha, R. A. (2014). The adenosine neuromodulation system in schizophrenia. *Int. Rev. Neurobiol.* 119, 395–449. doi:10.1016/B978-0-12-801022-8.00016-7.

Ribeiro, J. A., and Sebastião, A. M. (2010). Caffeine and adenosine. *J. Alzheimers Dis. JAD* 20 Suppl 1, S3–15. doi:10.3233/JAD-2010-1379.

Rimonabant: depression and suicide (2009). *Prescrire Int.* 18, 24.

Rinaldi-Carmona, M., Barth, F., Héaulme, M., Shire, D., Calandra, B., Congy, C., et al. (1994). SR141716A, a potent and selective antagonist of the brain cannabinoid receptor. *FEBS Lett.* 350, 240–244.

Roche, J. P., Bounds, S., Brown, S., and Mackie, K. (1999). A mutation in the second transmembrane region of the CB_1 receptor selectively disrupts G protein signaling and prevents receptor internalization. *Mol. Pharmacol.* 56, 611–618.

Rodríguez-Enríquez, S., Marín-Hernández, A., Gallardo-Pérez, J. C., and Moreno-Sánchez, R. (2009). Kinetics of transport and phosphorylation of glucose in cancer cells. *J. Cell. Physiol.* 221, 552–559. doi:10.1002/jcp.21885.

Rogers, P. J., and Dernoncourt, C. (1998). Regular caffeine consumption: a balance of adverse and beneficial effects for mood and psychomotor performance. *Pharmacol. Biochem. Behav.* 59, 1039–1045.

Rombo, D. M., Newton, K., Nissen, W., Badurek, S., Horn, J. M., Minichiello, L., et al. (2015). Synaptic mechanisms of adenosine A_{2A} receptor-mediated hyperexcitability in the hippocampus. *Hippocampus* 25, 566–580. doi:10.1002/hipo.22392.

Romero-Zerbo, S. Y., and Bermúdez-Silva, F. J. (2014). Cannabinoids, eating behaviour, and energy homeostasis. *Drug Test. Anal.* 6, 52–58. doi:10.1002/dta.1594.

Rooijackers, H. M. M., Wiegers, E. C., Tack, C. J., van der Graaf, M., and de Galan, B. E. (2015). Brain glucose metabolism during hypoglycemia in type 1 diabetes: insights from functional and metabolic neuroimaging studies. *Cell. Mol. Life Sci. CMLS*. doi:10.1007/s00018-015-2079-8.

Rossi, D. (2015). Astrocyte physiopathology: At the crossroads of intercellular networking, inflammation and cell death. *Prog. Neurobiol.* 130, 86–120. doi:10.1016/j.pneurobio.2015.04.003.

Rossini, A. A., Like, A. A., Chick, W. L., Appel, M. C., and Cahill, G. F. (1977). Studies of streptozotocin-induced insulitis and diabetes. *Proc. Natl. Acad. Sci. U. S. A.* 74, 2485–2489.

Rudolphi, K. A., and Schubert, P. (1997). Modulation of neuronal and glial cell function by adenosine and neuroprotection in vascular dementia. *Behav. Brain Res.* 83, 123–128.

Rueda, D., Galve-Roperh, I., Haro, A., and Guzmán, M. (2000). The CB_1 cannabinoid receptor is coupled to the activation of c-Jun N-terminal kinase. *Mol. Pharmacol.* 58, 814–820.

Ruiu, S., Pinna, G. A., Marchese, G., Mussinu, J.-M., Saba, P., Tambaro, S., et al. (2003). Synthesis and characterization of NESS 0327: a novel putative

antagonist of the CB_1 cannabinoid receptor. *J. Pharmacol. Exp. Ther.* 306, 363–370. doi:10.1124/jpet.103.049924.

Ruscák, M., and Whittam, R. (1967). The metabolic response of brain slices to agents affecting the sodium pump. J. Physiol. 190, 595–610.

Rüsing, D., Müller, C. E., and Verspohl, E. J. (2006). The impact of adenosine and A_{2B} receptors on glucose homoeostasis. *J. Pharm. Pharmacol.* 58, 1639–1645. doi:10.1211/jpp.58.12.0011.

Ryzhov, S., Zaynagetdinov, R., Goldstein, A. E., Novitskiy, S. V., Blackburn, M. R., Biaggioni, I., et al. (2008). Effect of A_{2B} adenosine receptor gene ablation on adenosine-dependent regulation of proinflammatory cytokines. *J. Pharmacol. Exp. Ther.* 324, 694–700. doi:10.1124/jpet.107.131540.

Sakamoto, K., Arnolds, D. E. W., Ekberg, I., Thorell, A., and Goodyear, L. J. (2004). Exercise regulates Akt and glycogen synthase kinase-3 activities in human skeletal muscle. *Biochem. Biophys. Res. Commun.* 319, 419–425. doi:10.1016/j.bbrc.2004.05.020.

Salkovic-Petrisic, M., Knezovic, A., Hoyer, S., and Riederer, P. (2013). What have we learned from the streptozotocin-induced animal model of sporadic Alzheimer's disease, about the therapeutic strategies in Alzheimer's research. *J. Neural Transm. Vienna Austria 1996* 120, 233–252. doi:10.1007/s00702-012-0877-9.

Salkovic-Petrisic, M., Osmanovic-Barilar, J., Brückner, M. K., Hoyer, S., Arendt, T., and Riederer, P. (2011). Cerebral amyloid angiopathy in streptozotocin rat model of sporadic Alzheimer's disease: a long-term follow up study. *J. Neural Transm. Vienna Austria 1996* 118, 765–772. doi:10.1007/s00702-011-0651-4.

Sánchez, C., de Ceballos, M. L., Gomez del Pulgar, T., Rueda, D., Corbacho, C., Velasco, G., et al. (2001). Inhibition of glioma growth in vivo by selective activation of the CB_2 cannabinoid receptor. *Cancer Res.* 61, 5784–5789.

Sánchez, C., Galve-Roperh, I., Rueda, D., and Guzmán, M. (1998). Involvement of sphingomyelin hydrolysis and the mitogen-activated protein kinase cascade in the Delta9-tetrahydrocannabinol-induced stimulation of glucose metabolism in primary astrocytes. *Mol. Pharmacol.* 54, 834–843.

Santos, M. S., Pereira, E. M., and Carvaho, A. P. (1999). Stimulation of immunoreactive insulin release by glucose in rat brain synaptosomes. *Neurochem. Res.* 24, 33–36.

Sarkar, P. K. (2002). A quick assay for Na^+-K^+-AtPase specific activity. *Z. Für Naturforschung C J. Biosci.* 57, 562–564.

Savonenko, A. V., Melnikova, T., Wang, Y., Ravert, H., Gao, Y., Koppel, J., et al. (2015). Cannabinoid CB2 Receptors in a Mouse Model of Aβ Amyloidosis: Immunohistochemical Analysis and Suitability as a PET Biomarker of Neuroinflammation. *PloS One* 10, e0129618. doi:10.1371/journal.pone.0129618.

Schmidt, K., Lucignani, G., Mori, K., Jay, T., Palombo, E., Nelson, T., et al. (1989). Refinement of the kinetic model of the 2-[^{14}C]deoxyglucose method to incorporate effects of intracellular compartmentation in brain. *J. Cereb. Blood Flow Metab. Off. J. Int. Soc. Cereb. Blood Flow Metab.* 9, 290–303. doi:10.1038/jcbfm.1989.47.

Scholey, A. B., and Fowles, K. A. (2002). Retrograde enhancement of kinesthetic memory by alcohol and by glucose. *Neurobiol. Learn. Mem.* 78, 477–483.

Schubert, D. (2005). Glucose metabolism and Alzheimer's disease. *Ageing Res. Rev.* 4, 240–257. doi:10.1016/j.arr.2005.02.003.

Schulingkamp, R. J., Pagano, T. C., Hung, D., and Raffa, R. B. (2000). Insulin receptors and insulin action in the brain: review and clinical implications. *Neurosci. Biobehav. Rev.* 24, 855–872.

Schulte, G., and Fredholm, B. B. (2003). The Gs-coupled adenosine A_{2B} receptor recruits divergent pathways to regulate ERK1/2 and p38. *Exp. Cell Res.* 290, 168–176.

Sebastião, A. M., Cunha, R. A., de Mendonça, A., and Ribeiro, J. A. (2000). Modification of adenosine modulation of synaptic transmission in the hippocampus of aged rats. *Br. J. Pharmacol.* 131, 1629–1634. doi:10.1038/sj.bjp.0703736.

Sebastião, A. M., and Ribeiro, J. A. (1996). Adenosine A_2 receptor-mediated excitatory actions on the nervous system. *Prog. Neurobiol.* 48, 167–189.

Sebastião, A. M., and Ribeiro, J. A. (2000). Fine-tuning neuromodulation by adenosine. *Trends Pharmacol. Sci.* 21, 341–346.

Sebastião, A. M., Stone, T. W., and Ribeiro, J. A. (1990). The inhibitory adenosine receptor at the neuromuscular junction and hippocampus of the rat: antagonism by 1,3,8-substituted xanthines. *Br. J. Pharmacol.* 101, 453–459.

Selkoe, D. J. (2001). Alzheimer's disease: genes, proteins, and therapy. *Physiol. Rev.* 81, 741–766.

Selkoe, D. J. (2002a). Alzheimer's disease is a synaptic failure. *Science* 298, 789–791. doi:10.1126/science.1074069.

Selkoe, D. J. (2002b). Alzheimer's disease is a synaptic failure. *Science* 298, 789–791. doi:10.1126/science.1074069.

Shah, K., Desilva, S., and Abbruscato, T. (2012). The role of glucose transporters in brain disease: diabetes and Alzheimer's Disease. *Int. J. Mol. Sci.* 13, 12629–12655. doi:10.3390/ijms131012629.

Sharma, M., and Gupta, Y. K. (2002). Chronic treatment with trans resveratrol prevents intracerebroventricular streptozotocin induced cognitive impairment and oxidative stress in rats. *Life Sci.* 71, 2489–2498.

Sheehan, J. P., Swerdlow, R. H., Miller, S. W., Davis, R. E., Parks, J. K., Parker, W. D., et al. (1997). Calcium homeostasis and reactive oxygen species production in cells transformed by mitochondria from individuals with sporadic Alzheimer's disease. *J. Neurosci. Off. J. Soc. Neurosci.* 17, 4612–4622.

Sherin, A., Anu, J., Peeyush, K. T., Smijin, S., Anitha, M., Roshni, B. T., et al. (2012). Cholinergic and GABAergic receptor functional deficit in the hippocampus of insulin-induced hypoglycemic and streptozotocin-induced diabetic rats. *Neuroscience* 202, 69–76. doi:10.1016/j.neuroscience.2011.11.058.

Shigeri, Y., Shimamoto, K., Yasuda-Kamatani, Y., Seal, R. P., Yumoto, N., Nakajima, T., et al. (2001). Effects of threo-beta-hydroxyaspartate derivatives on excitatory amino acid transporters (EAAT4 and EAAT5). *J. Neurochem.* 79, 297–302.

Shoemaker, J. L., Ruckle, M. B., Mayeux, P. R., and Prather, P. L. (2005). Agonist-directed trafficking of response by endocannabinoids acting at CB_2 receptors. *J. Pharmacol. Exp. Ther.* 315, 828–838. doi:10.1124/jpet.105.089474.

Shonesy, B. C., Thiruchelvam, K., Parameshwaran, K., Rahman, E. A., Karuppagounder, S. S., Huggins, K. W., et al. (2012). Central insulin resistance and synaptic dysfunction in intracerebroventricular-streptozotocin injected rodents. *Neurobiol. Aging* 33, 430.e5–18. doi:10.1016/j.neurobiolaging.2010.12.002.

Simpson, I. A., Appel, N. M., Hokari, M., Oki, J., Holman, G. D., Maher, F., et al. (1999). Blood-brain barrier glucose transporter: effects of hypo- and hyperglycemia revisited. *J. Neurochem.* 72, 238–247.

Simpson, I. A., Carruthers, A., and Vannucci, S. J. (2007). Supply and demand in cerebral energy metabolism: the role of nutrient transporters. *J. Cereb. Blood Flow Metab. Off. J. Int. Soc. Cereb. Blood Flow Metab.* 27, 1766–1791. doi:10.1038/sj.jcbfm.9600521.

Simpson, I. A., Dwyer, D., Malide, D., Moley, K. H., Travis, A., and Vannucci, S. J. (2008). The facilitative glucose transporter GLUT3: 20 years of distinction. *Am. J. Physiol. - Endocrinol. Metab.* 295, E242–E253. doi:10.1152/ajpendo.90388.2008.

Sims, R. E., and Dale, N. (2014). Activity-Dependent Adenosine Release May Be Linked to Activation of Na^+-K^+ ATPase: An In Vitro Rat Study. *PLoS ONE* 9. doi:10.1371/journal.pone.0087481.

Singh, L. S., and Sharma, R. (2000). Purification and characterization of intestinal adenosine deaminase from mice. *Mol. Cell. Biochem.* 204, 127–134.

Slipetz, D. M., O'Neill, G. P., Favreau, L., Dufresne, C., Gallant, M., Gareau, Y., et al. (1995). Activation of the human peripheral cannabinoid receptor results in inhibition of adenylyl cyclase. *Mol. Pharmacol.* 48, 352–361.

Snel, J., and Lorist, M. M. (2011). Effects of caffeine on sleep and cognition. *Prog. Brain Res.* 190, 105–117. doi:10.1016/B978-0-444-53817-8.00006-2.

Soares, E., Prediger, R. D., Nunes, S., Castro, A. A., Viana, S. D., Lemos, C., et al. (2013). Spatial memory impairments in a prediabetic rat model. *Neuroscience* 250, 565–577. doi:10.1016/j.neuroscience.2013.07.055.

Sobrero, R., May-Collado, L. J., Agnarsson, I., and Hernández, C. E. (2011). Expensive brains: "brainy" rodents have higher metabolic rate. *Front. Evol. Neurosci.* 3, 2. doi:10.3389/fnevo.2011.00002.

Sokoloff, L. (1977). Relation between physiological function and energy metabolism in the central nervous system. *J. Neurochem.* 29, 13–26.

Sokoloff, L. (2004). "Energy Metabolism in Neural Tissues in vivo at Rest and in Functionally Altered States," in *Brain Energetics and Neuronal Activity*, eds. R. G. Shulman and D. L. Rothman (John Wiley & Sons, Ltd), 11–30. Available at: http://onlinelibrary.wiley.com/doi/10.1002/0470020520.ch2/summary [Accessed September 6, 2015].

Sokoloff, L., Reivich, M., Kennedy, C., Des Rosiers, M. H., Patlak, C. S., Pettigrew, K. D., et al. (1977). The [14C]deoxyglucose method for the measurement of local cerebral glucose utilization: theory, procedure, and normal values in the conscious and anesthetized albino rat. *J. Neurochem.* 28, 897–916.

el-Sourogy, M., Malek, A. Y., Ibrahim, H. H., Farag, A., and el-Shihy, A. (1966). The effect of Cannabis indica on carbohydrate metabolism in rabbits. *J. Egypt. Med. Assoc.* 49, 626–628.

Sousa, V. C., Assaife-Lopes, N., Ribeiro, J. A., Pratt, J. A., Brett, R. R., and Sebastião, A. M. (2011). Regulation of hippocampal cannabinoid CB_1 receptor actions by adenosine A1 receptors and chronic caffeine administration: implications for the effects of Δ9-tetrahydrocannabinol on spatial memory. *Neuropsychopharmacol. Off. Publ. Am. Coll. Neuropsychopharmacol.* 36, 472–487. doi:10.1038/npp.2010.179.

S Roriz-Filho, J., Sá-Roriz, T. M., Rosset, I., Camozzato, A. L., Santos, A. C., Chaves, M. L. F., et al. (2009). (Pre)diabetes, brain aging, and cognition. *Biochim. Biophys. Acta* 1792, 432–443. doi:10.1016/j.bbadis.2008.12.003.

Stephenson, P. E. (1977). Physiologic and psychotropic effects of caffeine on man. A review. *J. Am. Diet. Assoc.* 71, 240–247.

Stern, J. E., and Filosa, J. A. (2013). Bidirectional neuro-glial signaling modalities in the hypothalamus: role in neurohumoral regulation. *Auton. Neurosci. Basic Clin.* 175, 51–60. doi:10.1016/j.autneu.2012.12.009.

Stokes, J., Kyle, C., and Ekstrom, A. D. (2015). Complementary roles of human hippocampal subfields in differentiation and integration of spatial context. *J. Cogn. Neurosci.* 27, 546–559. doi:10.1162/jocn_a_00736.

Strachan, M. W., Deary, I. J., Ewing, F. M., and Frier, B. M. (1997). Is type II diabetes associated with an increased risk of cognitive dysfunction? A critical review of published studies. *Diabetes Care* 20, 438–445.

Su, B., Wang, X., Nunomura, A., Moreira, P. I., Lee, H., Perry, G., et al. (2008). Oxidative stress signaling in Alzheimer's disease. *Curr. Alzheimer Res.* 5, 525–532.

Sugiura, T. (2008). "Biosynthesis of Anandamide and 2-Arachidonoylglycerol," in *Cannabinoids and the Brain*, ed. A. Köfalvi (Springer US), 15–30. Available at: http://link.springer.com/chapter/10.1007/978-0-387-74349-3_2 [Accessed December 26, 2015].

Sugiura, T., Kondo, S., Kishimoto, S., Miyashita, T., Nakane, S., Kodaka, T., et al. (2000). Evidence that 2-arachidonoylglycerol but not N-palmitoylethanolamine or anandamide is the physiological ligand for the cannabinoid CB_2 receptor. Comparison of the agonistic activities of various cannabinoid receptor ligands in HL-60 cells. *J. Biol. Chem.* 275, 605–612.

Su, L., Cai, Y., Xu, Y., Dutt, A., Shi, S., and Bramon, E. (2014). Cerebral metabolism in major depressive disorder: a voxel-based meta-analysis of positron emission tomography studies. *BMC Psychiatry* 14, 321. doi:10.1186/s12888-014-0321-9.

Sünram-Lea, S. I., Foster, J. K., Durlach, P., and Perez, C. (2001). Glucose facilitation of cognitive performance in healthy young adults: examination of the influence of fast-duration, time of day and pre-consumption plasma glucose levels. *Psychopharmacology (Berl.)* 157, 46–54.

Suzuki, A., Stern, S. A., Bozdagi, O., Huntley, G. W., Walker, R. H., Magistretti, P. J., et al. (2011). Astrocyte-neuron lactate transport is required for long-term memory formation. *Cell* 144, 810–823. doi:10.1016/j.cell.2011.02.018.

Szkudelski, T. (2001). The mechanism of alloxan and streptozotocin action in B cells of the rat pancreas. *Physiol. Res. Acad. Sci. Bohemoslov.* 50, 537–546.

Tabák, A. G., Herder, C., Rathmann, W., Brunner, E. J., and Kivimäki, M. (2012). Prediabetes: a high-risk state for diabetes development. *Lancet Lond. Engl.* 379, 2279–2290. doi:10.1016/S0140-6736(12)60283-9.

Takahashi, R. N., Pamplona, F. A., and Prediger, R. D. S. (2008). Adenosine receptor antagonists for cognitive dysfunction: a review of animal studies. *Front. Biosci. J. Virtual Libr.* 13, 2614–2632.

Tam, J., Vemuri, V. K., Liu, J., Bátkai, S., Mukhopadhyay, B., Godlewski, G., et al. (2010). Peripheral CB_1 cannabinoid receptor blockade improves cardiometabolic risk in mouse models of obesity. *J. Clin. Invest.* 120, 2953–2966. doi:10.1172/JCI42551.

Tanimura, A., Yamazaki, M., Hashimotodani, Y., Uchigashima, M., Kawata, S., Abe, M., et al. (2010). The endocannabinoid 2-arachidonoylglycerol produced by diacylglycerol lipase alpha mediates retrograde suppression of synaptic transmission. *Neuron* 65, 320–327. doi:10.1016/j.neuron.2010.01.021.

Teune, L. K., Bartels, A. L., de Jong, B. M., Willemsen, A. T. M., Eshuis, S. A., de Vries, J. J., et al. (2010). Typical cerebral metabolic patterns in

neurodegenerative brain diseases. *Mov. Disord. Off. J. Mov. Disord. Soc.* 25, 2395–2404. doi:10.1002/mds.23291.

Thorn, J. A., and Jarvis, S. M. (1996). Adenosine transporters. *Gen. Pharmacol.* 27, 613–620.

Tiwari, V., Kuhad, A., Bishnoi, M., and Chopra, K. (2009). Chronic treatment with tocotrienol, an isoform of vitamin E, prevents intracerebroventricular streptozotocin-induced cognitive impairment and oxidative-nitrosative stress in rats. *Pharmacol. Biochem. Behav.* 93, 183–189. doi:10.1016/j.pbb.2009.05.009.

Toescu, E. C. (2000). Mitochondria and Ca(2+) signaling. *J. Cell. Mol. Med.* 4, 164–175.

Topol, E. J., Bousser, M.-G., Fox, K. A. A., Creager, M. A., Despres, J.-P., Easton, J. D., et al. (2010). Rimonabant for prevention of cardiovascular events (CRESCENDO): a randomised, multicentre, placebo-controlled trial. *Lancet Lond. Engl.* 376, 517–523. doi:10.1016/S0140-6736(10)60935-X.

Torrão, A. S., Café-Mendes, C. C., Real, C. C., Hernandes, M. S., Ferreira, A. F. B., Santos, T. O., et al. (2012). Different approaches, one target: understanding cellular mechanisms of Parkinson's and Alzheimer's diseases. *Rev. Bras. Psiquiatr. São Paulo Braz. 1999* 34 Suppl 2, S194–205.

Torres, F. V., Hansen, F., and Locks-Coelho, L. D. (2013). Increase of extracellular glutamate concentration increases its oxidation and diminishes glucose oxidation in isolated mouse hippocampus: reversible by TFB-TBOA. *J. Neurosci. Res.* 91, 1059–1065. doi:10.1002/jnr.23187.

Trincavelli, M. L., Marroni, M., Tuscano, D., Ceruti, S., Mazzola, A., Mitro, N., et al. (2004). Regulation of A2B adenosine receptor functioning by tumour necrosis factor a in human astroglial cells. *J. Neurochem.* 91, 1180–1190. doi:10.1111/j.1471-4159.2004.02793.x.

Tsacopoulos, M., and Magistretti, P. J. (1996). Metabolic coupling between glia and neurons. *J. Neurosci. Off. J. Soc. Neurosci.* 16, 877–885.

Tsou, K., Brown, S., Sañudo-Peña, M. C., Mackie, K., and Walker, J. M. (1998). Immunohistochemical distribution of cannabinoid CB_1 receptors in the rat central nervous system. *Neuroscience* 83, 393–411.

Uemura, E., and Greenlee, H. W. (2006). Insulin regulates neuronal glucose uptake by promoting translocation of glucose transporter GLUT3. *Exp. Neurol.* 198, 48–53. doi:10.1016/j.expneurol.2005.10.035.

Valente-Silva, P., Lemos, C., Köfalvi, A., Cunha, R. A., and Jones, J. G. (2015). Ketone bodies effectively compete with glucose for neuronal acetyl-CoA generation in rat hippocampal slices. *NMR Biomed.* doi:10.1002/nbm.3355.

van Calker, D., Müller, M., and Hamprecht, B. (1978). Adenosine inhibits the accumulation of cyclic AMP in cultured brain cells. *Nature* 276, 839–841.

van Calker, D., Müller, M., and Hamprecht, B. (1979). Adenosine regulates via two different types of receptors, the accumulation of cyclic AMP in cultured brain cells. *J. Neurochem.* 33, 999–1005.

Vannucci, S. J., Maher, F., and Simpson, I. A. (1997). Glucose transporter proteins in brain: delivery of glucose to neurons and glia. *Glia* 21, 2–21.

Varela, L., and Horvath, T. L. (2012). Leptin and insulin pathways in POMC and AgRP neurons that modulate energy balance and glucose homeostasis. *EMBO Rep.* 13, 1079–1086. doi:10.1038/embor.2012.174.

Veldhuis, W. B., van der Stelt, M., Delmas, F., Gillet, B., Veldink, G. A., Vliegenthart, J. F. G., et al. (2003). In vivo excitotoxicity induced by ouabain, a Na+/K+-ATPase inhibitor. *J. Cereb. Blood Flow Metab. Off. J. Int. Soc. Cereb. Blood Flow Metab.* 23, 62–74.

Ventura-Sobrevilla, J., Boone-Villa, V. D., Aguilar, C. N., Román-Ramos, R., Vega-Avila, E., Campos-Sepúlveda, E., et al. (2011). Effect of varying dose and administration of streptozotocin on blood sugar in male CD1 mice. *Proc. West. Pharmacol. Soc.* 54, 5–9.

Verkhratsky, A., and Burnstock, G. (2014). Purinergic and glutamatergic receptors on astroglia. *Adv. Neurobiol.* 11, 55–79. doi:10.1007/978-3-319-08894-5_4.

Vilchez, D., Ros, S., Cifuentes, D., Pujadas, L., Vallès, J., García-Fojeda, B., et al. (2007). Mechanism suppressing glycogen synthesis in neurons and its demise in progressive myoclonus epilepsy. *Nat. Neurosci.* 10, 1407–1413. doi:10.1038/nn1998.

Viscomi, M. T., Oddi, S., Latini, L., Pasquariello, N., Florenzano, F., Bernardi, G., et al. (2009). Selective CB_2 receptor agonism protects central neurons from remote axotomy-induced apoptosis through the PI3K/Akt pathway. *J. Neurosci. Off. J. Soc. Neurosci.* 29, 4564–4570. doi:10.1523/JNEUROSCI.0786-09.2009.

Viswanathan, A., and Freeman, R. D. (2007). Neurometabolic coupling in cerebral cortex reflects synaptic more than spiking activity. *Nat. Neurosci.* 10, 1308–1312. doi:10.1038/nn1977.

Voet, D., and Voet, J. G. (1995). *Biochemistry*. J. Wiley & Sons.

Volkow, N. D., Gillespie, H., Mullani, N., Tancredi, L., Grant, C., Ivanovic, M., et al. (1991). Cerebellar metabolic activation by delta-9-tetrahydro-cannabinol in human brain: a study with positron emission tomography and 18F-2-fluoro-2-deoxyglucose. *Psychiatry Res.* 40, 69–78.

Von Lubitz, D. K., Lin, R. C., Boyd, M., Bischofberger, N., and Jacobson, K. A. (1999). Chronic administration of adenosine A3 receptor agonist and cerebral ischemia: neuronal and glial effects. *Eur. J. Pharmacol.* 367, 157–163.

Von Lubitz, D. K., Lin, R. C., Popik, P., Carter, M. F., and Jacobson, K. A. (1994). Adenosine A3 receptor stimulation and cerebral ischemia. *Eur. J. Pharmacol.* 263, 59–67.

Vorhees, C. V., and Williams, M. T. (2006). Morris water maze: procedures for assessing spatial and related forms of learning and memory. *Nat. Protoc.* 1, 848–858. doi:10.1038/nprot.2006.116.

Vyska, K., Magloire, J. R., Freundlieb, C., Höck, A., Becker, V., Schmid, A., et al. (1985). In vivo determination of the kinetic parameters of glucose transport in the human brain using 11C-methyl-D-glucose (CMG) and dynamic positron emission tomography (dPET). *Eur. J. Nucl. Med.* 11, 97–106.

Walf, A. A., and Frye, C. A. (2007). The use of the elevated plus maze as an assay of anxiety-related behavior in rodents. *Nat. Protoc.* 2, 322–328. doi:10.1038/nprot.2007.44.

Watson, G. S., and Craft, S. (2004). Modulation of memory by insulin and glucose: neuropsychological observations in Alzheimer's disease. *Eur. J. Pharmacol.* 490, 97–113. doi:10.1016/j.ejphar.2004.02.048.

Wei, C. J., Li, W., and Chen, J.-F. (2011). Normal and abnormal functions of adenosine receptors in the central nervous system revealed by genetic knockout studies. *Biochim. Biophys. Acta BBA - Biomembr.* 1808, 1358–1379. doi:10.1016/j.bbamem.2010.12.018.

Werner, H., Raizada, M. K., Mudd, L. M., Foyt, H. L., Simpson, I. A., Roberts, C. T., et al. (1989). Regulation of rat brain/HepG2 glucose transporter gene expression by insulin and insulin-like growth factor-I in primary cultures of neuronal and glial cells. *Endocrinology* 125, 314–320. doi:10.1210/endo-125-1-314.

Whitlow, C. T., Freedland, C. S., and Porrino, L. J. (2002). Metabolic mapping of the time-dependent effects of delta 9-tetrahydrocannabinol administration in the rat. *Psychopharmacology (Berl.)* 161, 129–136. doi:10.1007/s00213-002-1001-x.

Wiesinger, H., Hamprecht, B., and Dringen, R. (1997). Metabolic pathways for glucose in astrocytes. *Glia* 21, 22–34.

Wiley, J. L., Breivogel, C. S., Mahadevan, A., Pertwee, R. G., Cascio, M. G., Bolognini, D., et al. (2011). Structural and pharmacological analysis of O-2050, a putative neutral cannabinoid CB_1 receptor antagonist. *Eur. J. Pharmacol.* 651, 96–105. doi:10.1016/j.ejphar.2010.10.085.

Williams, J. M., Thompson, V. L., Mason-Parker, S. E., Abraham, W. C., and Tate, W. P. (1998). Synaptic activity-dependent modulation of mitochondrial gene expression in the rat hippocampus. *Brain Res. Mol. Brain Res.* 60, 50–56.

Winocur, G., and Gagnon, S. (1998). Glucose treatment attenuates spatial learning and memory deficits of aged rats on tests of hippocampal function. *Neurobiol. Aging* 19, 233–241.

Winocur, G., and Greenwood, C. E. (2005). Studies of the effects of high fat diets on cognitive function in a rat model. *Neurobiol. Aging* 26 Suppl 1, 46–49. doi:10.1016/j.neurobiolaging.2005.09.003.

Winocur, G., Greenwood, C. E., Piroli, G. G., Grillo, C. A., Reznikov, L. R., Reagan, L. P., et al. (2005). Memory impairment in obese Zucker rats: an investigation of cognitive function in an animal model of insulin resistance and obesity. *Behav. Neurosci.* 119, 1389–1395. doi:10.1037/0735-7044.119.5.1389.

Wong, B. X., Hung, Y. H., Bush, A. I., and Duce, J. A. (2014). Metals and cholesterol: two sides of the same coin in Alzheimer's disease pathology. *Front. Aging Neurosci.* 6, 91. doi:10.3389/fnagi.2014.00091.

Wu, J., Bie, B., Yang, H., Xu, J. J., Brown, D. L., and Naguib, M. (2013). Activation of the CB_2 receptor system reverses amyloid-induced memory deficiency. *Neurobiol. Aging* 34, 791–804. doi:10.1016/j.neurobiolaging.2012.06.011.

Wyss, M. T., Jolivet, R., Buck, A., Magistretti, P. J., and Weber, B. (2011). In vivo evidence for lactate as a neuronal energy source. *J. Neurosci. Off. J. Soc. Neurosci.* 31, 7477–7485. doi:10.1523/JNEUROSCI.0415-11.2011.

Xie, H., Hou, S., Jiang, J., Sekutowicz, M., Kelly, J., and Bacskai, B. J. (2013). Rapid cell death is preceded by amyloid plaque-mediated oxidative stress. *Proc. Natl. Acad. Sci.* doi:10.1073/pnas.1217938110.

Xu, W., Caracciolo, B., Wang, H.-X., Winblad, B., Backman, L., Qiu, C., et al. (2010a). Accelerated Progression From Mild Cognitive Impairment to Dementia in People With Diabetes. *Diabetes* 59, 2928–2935. doi:10.2337/db10-0539.

Xu, W., Caracciolo, B., Wang, H.-X., Winblad, B., Bäckman, L., Qiu, C., et al. (2010b). Accelerated progression from mild cognitive impairment to dementia in people with diabetes. *Diabetes* 59, 2928–2935. doi:10.2337/db10-0539.

Yamada, K., Saito, M., Matsuoka, H., and Inagaki, N. (2007). A real-time method of imaging glucose uptake in single, living mammalian cells. *Nat. Protoc.* 2, 753–762. doi:10.1038/nprot.2007.76.

Yamagata, K., Hakata, K., Maeda, A., Mochizuki, C., Matsufuji, H., Chino, M., et al. (2007). Adenosine induces expression of glial cell line-derived neurotrophic factor (GDNF) in primary rat astrocytes. *Neurosci. Res.* 59, 467–474. doi:10.1016/j.neures.2007.08.016.

Yang, D., Koupenova, M., McCrann, D. J., Kopeikina, K. J., Kagan, H. M., Schreiber, B. M., et al. (2008). The A2b adenosine receptor protects against vascular injury. *Proc. Natl. Acad. Sci. U. S. A.* 105, 792–796. doi:10.1073/pnas.0705563105.

Yao, S. Y. M., Ng, A. M. L., Vickers, M. F., Sundaram, M., Cass, C. E., Baldwin, S. A., et al. (2002). Functional and molecular characterization of nucleobase transport by recombinant human and rat equilibrative nucleoside transporters 1 and 2. Chimeric constructs reveal a role for the ENT2 helix 5-6 region in nucleobase translocation. *J. Biol. Chem.* 277, 24938–24948. doi:10.1074/jbc.M200966200.

Zhang, P., Bannon, N. M., Ilin, V., Volgushev, M., and Chistiakova, M. (2015). Adenosine effects on inhibitory synaptic transmission and excitation-inhibition balance in the rat neocortex. *J. Physiol.* 593, 825–841. doi:10.1113/jphysiol.2014.279901.

Zhou, A.-M., Li, W.-B., Li, Q.-J., Liu, H.-Q., Feng, R.-F., and Zhao, H.-G. (2004). A short cerebral ischemic preconditioning up-regulates adenosine receptors in the hippocampal CA1 region of rats. *Neurosci. Res.* 48, 397–404. doi:10.1016/j.neures.2003.12.010.

Zimmermann, H. (1996). Biochemistry, localization and functional roles of ecto-nucleotidases in the nervous system. *Prog. Neurobiol.* 49, 589–618.